The Institute of Paper Chemistry

Appleton, Wisconsin

Doctor's Dissertation

Scale of Flocculation for Fully Developed Turbulent Tube Flow of Dilute Fiber Suspensions

W. Harvey Persinger, Jr.

June, 1974

SCALE OF FLOCCULATION FOR FULLY DEVELOPED TURBULENT TUBE FLOW OF DILUTE FIBER SUSPENSIONS

A thesis submitted by

W. Harvey Persinger, Jr.

B.S.Ch.E. 1966, Purdue University

M.S. 1971, Lawrence University

in partial fulfillment of the requirements
of The Institute of Paper Chemistry
for the degree of Doctor of Philosophy
from Lawrence University,
Appleton, Wisconsin

June, 1974

"We can rejoice, too, when we run into problems and trials for we know that they are good for us — they help us learn to be patient."

Romans 5:3

TABLE OF CONTENTS

SUMMARY

An experimental investigation of dilute rayon fiber suspensions (0.05 to 0.24 g/100 ml) in turbulent tube flow is described. A discussion of background material pertinent to the study is also presented.

The object of this study was to develop a technique to measure statistical indicators of local time-average floc (fiber network) sizes and to use this technique to study the effect of mean fiber consistency and Reynolds number on the distribution of average floc sizes. Specially designed fiber optic light guide probes were employed to measure local time-dependent signals in a flowing suspension. These fluctuating signals were related to consistency variations through a separate calibration procedure. Measurements were made primarily in the damped turbulent flow regime of fiber suspension flow. Digitized data representing recorded fluctuating signals were analyzed using statistical definitions commonly applied in turbulent research (correlation and scale functions) and local time-average scales of flocculation were determined for the longitudinal (or tube axis) direction. These scales were considered to be a measure of local time-average floc lengths. Attempts were also made to determine average radial floc dimensions using crosscorrelation analyses, but the results of this part of the program did not produce results that could be translated into average dimensions.

In general, the time-average longitudinal floc lengths were found to be dependent on radial position; increasing in magnitude in going from the tube wall to the center line. They were also found to be directly dependent on the average suspension consistency and inversely dependent on the local velocity.

Results of this study indicate that the fiber optic probe can be used to collect fluctuating consistency signals which, when analyzed in terms of autocorrelation and scale, produce meaningful indicators of local time-average floc

lengths. This technique could prove quite useful in studying the effects of the different variables on flocculation.

The equations derived by Sanders and Meyer to predict consistency and velocity distributions for water-fiber systems fitted the consistency and velocity profile data determined in this study quite well. This investigation indicates also that the von Karman constant is a function of both average consistency and flow rate, decreasing with increasing consistency and increasing with increasing flow rate. Consistency distribution profiles were also found to be dependent on average consistency and flow rate and tended to become more uniform with increasing flow rate and decreasing average consistency.

INTRODUCTION

The mechanism of fiber network formation and its influence on the flow properties of pulp fiber suspension is a central problem in papermaking. This problem is probably most accentuated at the wet end of a paper machine, where it is now generally recognized that the quality of the paper web formation is decisively dependent on the state of turbulence in the pulp suspension stream that flows through the slice and onto the wire. The state of turbulence in the slice jet, as characterized by intensity and scale of secondary velocity fluctuations, is responsible for the properties of the flocculation spectrum of the suspension which in turn determine the macroscopic basis weight distribution of the sheet and, consequently, its appearance. The importance of turbulence and flocculation in papermaking cannot be overemphasized.

In view of this, it is not surprising that the flow characteristics of fiber suspensions have been widely studied (1-36). In addition, much of the effort in the last 25 years has been centered on gaining a better understanding of the basic underlying principles involved.

An extensive survey of the literature will not be presented here. Rather, a few of the more important studies relevant to hydrodynamic flocculation will be discussed. For more comprehensive reviews on the subject, the reader is referred to publications such as Daily and Bugliarello, et al. (32-34), Parker (35), and Meyer (36).

FIBER SUSPENSION FLOW

When a suspension of fibers is made to flow, the resulting velocity gradients cause the fibers to move relative to one another, and undergo rotations which are believed to be of considerable importance in the mechanism

of flocculation. The shearing motion provides a flow condition whereby the fibers can interact with one another and form, depending on the flow regime, coherent networks or network fragments called flocs. In turbulent flow, flocculation is of a dynamic nature. The shearing and normal stresses change the contact between individual fibers or fiber groups, favor the entanglement of free fibers and simultaneously redisperse previously formed networks.

FLOW REGIMES

Prior work (26) indicates that in tube flow of fiber suspensions four regimes may be distinguished. The first regime occurs at very low flow rates and is termed laminar plug flow. In this flow, the core is a coherent network of fibers and the velocity gradient is confined to an essentially fiber-free water annulus near the wall. The water annulus thickness increases with increasing flow rate and varies with fiber properties and consistency (33).

Next is the plug turbulence regime. As the flow rate is increased beyond the laminar plug flow regime, there is a certain state where the flow in the water annulus becomes unstable and an increasingly turbulent water layer forms around the plug. Additional increases in the flow rate produce turbulent stresses in excess of the yield stress of the fiber network. This causes progressive disintegration of the plug until it disappears. This is the onset of the third regime, damped turbulence, in which the flow is turbulent across the entire cross section except for the boundary layer. At higher flow rates the Newtonian turbulence regime is encountered. In this last regime, the velocity and pressure drop-flow correlations are indistinguishable from those of water alone.

FRICTION FACTOR-REYNOLDS NUMBER CORRELATION

It is a common engineering practice to present flow data on a friction factor *versus* Reynolds number plot such as shown in Fig. 1. For fibrous suspensions, the friction factor f is a function of Reynolds number Re, pipe diameter D, temperature T, consistency c, and fiber type[1]. For smooth pipes, $f = f(Re, D, T, c, \text{fiber type})$ which is defined as

$$f = 2(u_*/\langle\bar{u}\rangle)^2 = D\Delta P/(2L\rho\langle\bar{u}\rangle^2). \tag{1}$$

In Fig. 1, laminar flow of a Newtonian fluid is represented by the straight line described by the formula $f = 16/Re$. Newtonian turbulent flow is represented by Prandtl's universal friction law (37,38).

$$1/\sqrt{f} = 4 \log(Re\sqrt{f}) - 0.40. \tag{2}$$

Referring to Fig. 1, laminar plug flow for an arbitrary consistency has pressure losses in pipe flow greater than for water at comparable flow rates. In the plug turbulence regime, the pressure loss for pipe flow gradually becomes less than that for water.

In the damped turbulent region the friction factor is practically constant over a considerable range of velocities. It is also lower than that for water and, as a consequence, less power is required for pumping stock than for water. Finally, in the Newtonian turbulent regime the suspension curve joins the water curve.

The degrees to which the fiber suspensions deviate from Newtonian behavior and the flow rate at which the different regimes are encountered depend on the consistency, fiber properties, and pipe diameter.

---

[1] Definitions of all symbols may be found in the Nomenclature section.

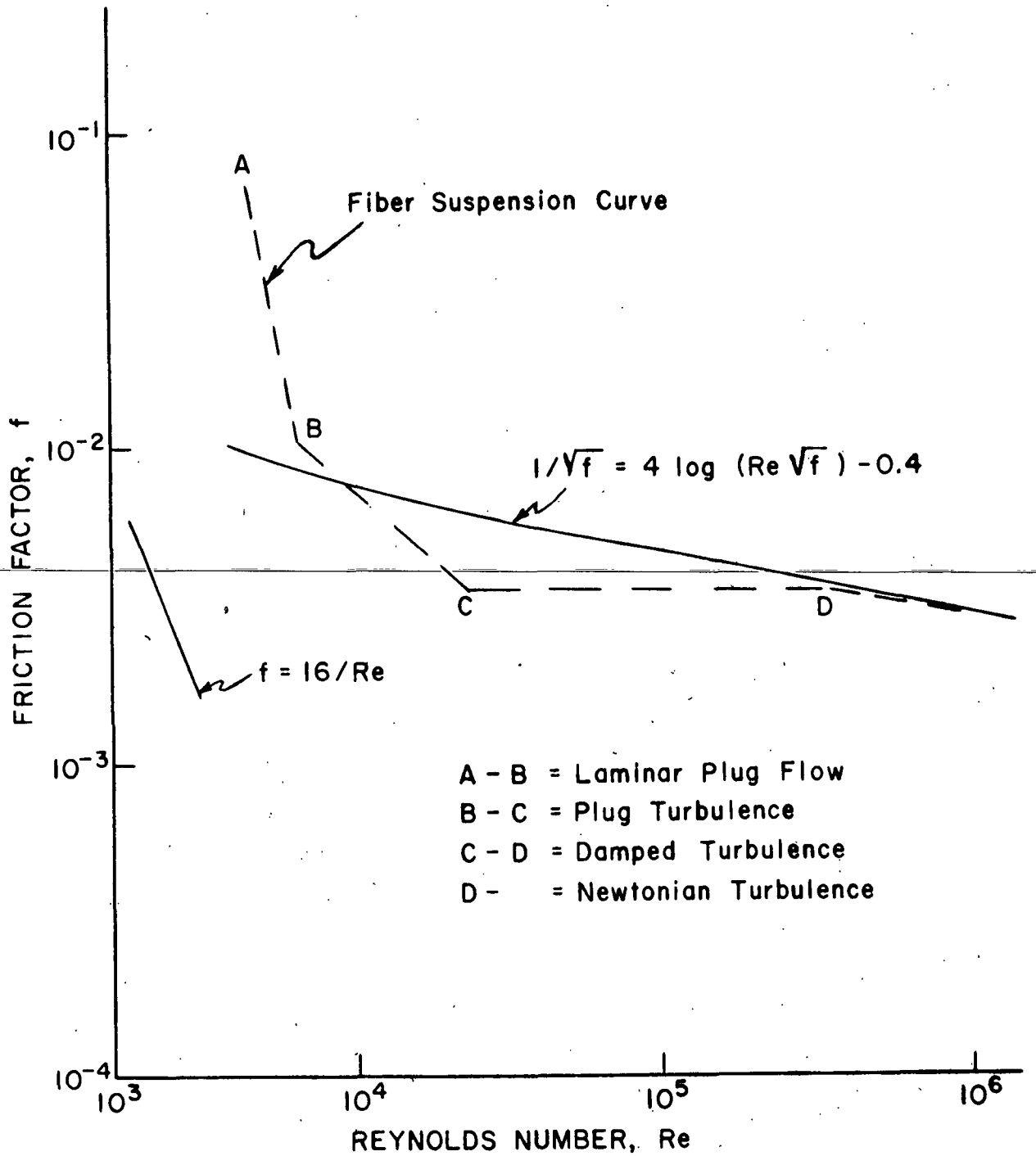

Figure 1. Typical Friction-Factor vs. Reynolds Number Curve for Fiber Suspension Flow

TWO-PHASE SYSTEM

Fiber suspensions are characterized by the presence of two distinct phases — water and solid fibers — and, therefore, the flow of such suspensions cannot be represented by modified Newtonian or non-Newtonian equations which are applicable to single phase or homogeneous suspensions. To develop a quantitative description of turbulent suspension flow, a knowledge of the coupled behavior of the water and the solid phase is necessary.

Sanders and Meyer (27,31,36) approached the problem of describing turbulent fiber suspension flow by treating it as a two-phase system in which it was assumed that both water and fiber can be treated as quasi-continua and that, in general, the fibers and water move at different velocities. The development of these equations will not be repeated here since the aforementioned literature discusses them well.

In Sanders' work (27,31), use of the two-phase approach allowed development of equations which predicted the forms of the consistency and velocity distributions in steady-state pipe flow.

The two-phase equations of motion for the z-direction were solved and Equation (3) was derived to describe the velocity distribution of fiber suspensions in the turbulent core.

$$\frac{du^+}{d \ln s^+} = \frac{\sqrt{\bar{\varepsilon}}}{\kappa}\left(1 - \frac{\mu \bar{a}\bar{\varepsilon}\bar{u}_{rz} R}{\rho u_*^2}\right)^{1/2} = \frac{1}{\kappa_*} . \qquad (3)$$

This equation predicted a logarithmic velocity distribution for turbulent fiber suspensions and an apparent von Karman constant κ_* for suspensions different from the von Karman constant κ for Newtonian fluids. Seely's results (26) were in agreement with this observation. It was deduced from

experimental evidence of Seely (26) and Sanders (27) that the relative velocity term $\underline{u}_{\underline{rz}}$ in Equation (3) was negative. This is equivalent to stating that the time-average fiber velocity was greater than the water velocity. The apparent von Karman constant for suspensions was found to decrease with increased consistency and to increase with increased flow rate. Also, κ_* was found to approach the water value at high flow rates.

Starting with the equation of continuity for the water phase and using an extension of Prandtl's mixing length hypothesis, a consistency distribution equation of the following form was derived.

$$\ln\left(\frac{1 - \bar{c}_v}{1 - \bar{c}_{vo}}\right) = \frac{- C'_w \kappa_*}{\kappa_\varepsilon \kappa_w u_*} (\ln s - \ln s_o). \qquad (4)$$

The term $(1 - \bar{c}_{vo})$ was taken as unity since the volume fraction of fibers at the laminar sublayer c_{vo} is very small. The resulting equation predicted that $\ln (1 - \bar{c}_v)$ was a linear function of $\ln s$ with the slope being a function of the velocity profile as characterized by the apparent von Karman constant κ_* and a void fraction exchange term characterized by $C'_w/\kappa_\varepsilon \kappa_w$.

The equation fitted Sanders' data very well (27). In addition, he found, by using experimental values of κ_* and the friction velocity u_* and slopes from Equation (4), that $C'_w/\kappa_\varepsilon \kappa_w$ decreased with increased flow rate and increased with increased consistency. It was suggested that this mass exchange term may be useful as an index of the overall scale of flocculation for a turbulent suspension (27).

The very good agreement between Sanders' experimental data and the predictions of the two-phase equation adds validity to this approach to describing turbulent flow of fiber suspensions.

FACTORS AFFECTING FLOCCULATION

The problem of fiber flocculation is of a very complex nature. Broadly speaking, the flocculation of fibers in a suspension is a result of fiber motion, collisions, and mechanical entanglement under the influence of a number of forces. The forces arise from mechanical, electrostatic, and molecular origins. Among the numerous factors affecting flocculation of fibers are (22,23,39):

1. Properties of the fibers
    a. length
    b. width and thickness
    c. flexural rigidity
    d. surface conditions
2. Fiber concentration
3. Fluid variables
    a. viscosity of the suspending medium
    b. the state of turbulence
    c. rate of shear (in the vicinity of solid walls)
    d. temperature
4. Ionic environment
    a. pH
    b. presence of additives

FIBER PROPERTIES

It is generally agreed that greater fiber length, greater flexibility, and higher consistency increases flocculation tendencies. Mechanical entanglement is believed to be the predominant mechanism in explaining the

experimental observations of physical effects. Fiber flexibility depends on the fiber length and its rigidity. The ratio l/d is commonly used as a measure of the tendency of the fibers to interlock and form networks. Everything else being equal, the tendency to flocculate appears to be directly proportional to fiber length.

As the degree of beating increases, without appreciable fiber shortening, the degree of flocculation increases. As more fibrils are brushed out of the fiber surface there is a greater tendency for the "hooks" to interact and tangle as the fibers collide. At the same time, more shearing force is required to separate the entangled fibers. Beating also increases wood pulp fiber flexibility and thereby results in an increase in flocculation tendency.

FIBER CONCENTRATION

The consistency of the fiber suspension has a major effect upon the degree of flocculation. Above a certain critical consistency, fibers do not have sufficient space for unimpeded rotations, etc., and therefore increasing the consistency further causes more fiber-fiber interactions and thus an increase in the flocculation tendency.

FLUID VARIABLES

Shear has a great effect on fiber flocculation. At ordinary consistencies shear is a factor that brings fibers together to form flocs and at the same time disperses previously formed networks. This concept of a "dynamic equilibrium" during which the formation and the disruption of flocs are balanced over a period of time was described by Hubley, et al. (13). Robertson and Mason (18), using an optical transmission technique to measure flocculation, have shown that as the shear rate increases, for example due to an increase

in stock velocity, the average floc size decreases while the number of flocs per unit volume increases. This is in agreement with present thoughts on flocculation.

The effect of increasing the temperature is to decrease the viscosity of a fluid system, which results in a decrease in the shearing stress at a solid wall. Beasley (16) found that the time required to flocculate fibers in a Wollwage flocculation tester (40) increased when temperature of the suspension was decreased. He noted that, of the variables he studied, consistency and temperature had the greatest effect on flocculation.

PRESENCE OF ADDITIVES

The role of additives in determining the flocculation properties of a pulp is not fully understood, but the experimental observations are normally explained by the electrokinetic or zeta potential of the fiber. A colloidal substance, when adsorbed onto a fiber surface, will impart to the fiber surface the electrokinetic properties of the colloid itself. The principal effect of additives is to alter the chemical or electrochemical nature of the fiber surface.

While there is general agreement regarding the effect of physical parameters such as length, flexibility, and consistency on fiber flocculation, there appears to be considerable disagreement about the effects of many colloidal factors upon fiber flocculation. This disagreement probably stems from the widely different methods and conditions that have been employed for study. In most cases flow conditions, an important set of variables, were ill defined.

The effect of air in the stock is thought to increase flocculation by the attachment of bubbles simultaneously to two or more fibers (17).

PREVIOUS FLOCCULATION STUDIES

Several methods have been used to study fiber flocculation and to investigate the factors determining the flocculation tendency of fibers. Among them were measurement of time required to flocculate a dispersed fiber suspension (40), measurement of the equilibrium state of flocculation in a dilute sheared suspension by optical means (13), direct tensile strength measurement of fiber flocs at papermaking consistencies (20), measurement of the equilibrium state of flocculation in turbulently flowing suspensions (18), measurement of formation of standard handsheets (41), and performance of frequency analysis on consistency signals detected by fiber optic light guides (29).

Wollwage (40) investigated the effects of consistency, beating, and additives by using a flocculation meter consisting of a long, vertical tube down which a previously dispersed suspension filling the tube was caused to flow. This work was verified by Erspamer (41) who also studied the variation in sheet formation caused by fiber networks by making sheets and examining them on the Thwing Davis formation tester. The work of Wollwage (40), Erspamer (41), and also Beasley (16) showed that ionic effects alter the flocculation rates of fibers under conditions of low consistency and low shear rate.

The work by Mason, et al. (13,18), however, indicates that ionic effects are appreciable only at very low rates of shear and low consistency. They studied fiber suspension flocculation by measuring the time-average light transmission across the flow in a Couette viscometer. Fluctuations in the transmitted light were used to compute the degree of flocculation. A flocculation index σ/N_o was proposed on the basis of statistical theory. The index was a function of both the number and size of the aggregations. σ was the

root mean square or standard deviation of the fluctuations and was regarded as a statistical measure of the size of the particle aggregates, and $\underline{N}_o$ was related to the average number of particles per unit volume. Both σ and $\underline{N}_o$ were obtained by using pulse counting methods where a count was registered each time the photocell output crossed a predetermined level in a particular direction.

Andersson (24) measured flocculation using the root mean square of optical density variations and utilized stereophotography and dyed fibers to investigate the structure of the fiber suspensions. He found that the flocs were irregular in shape, the smaller flocs tending to be oblong or string shaped. The fiber aggregates showed complicated motion in addition to deformation and rupture, and the motion of the fibers relative to the mean flow rate was irregular. His dyed fiber studies indicated the turbulent mixing of flocs rather than of individual fibers.

Robertson and Mason (18) in a study of flocculation in flowing pulp suspensions, observed two transition regions in flocculation behavior as the flow velocity was increased. These changes appeared to be related to plug, mixed, and turbulent flow regimes. Above the first transition they observed a decrease in flocculation with increased velocity and decreased concentration. In a later publication (19) they presented more details, including a measure of the number of optical transmission fluctuations per unit length of flowing suspension. These fluctuations, however, were an integral of the fluctuations across the whole tube flow cross section, not the fluctuations at a particular point in the flow.

The most recent work in this area was performed at the Swedish Forest Products Laboratory (29,30). A two-branch fiber optic light guide was used to

study flocculation in the slice of a headbox. The fluctuating light output from the light guide was converted to a voltage and a frequency analysis of the signal was then performed. The frequency spectrum was converted to a wavelength spectrum which served as an indication of the flocculation of the pulp at the measuring conditions. Wavelengths ranging from around one up to several hundred millimeters were reported.

DISCUSSION OF THE PROBLEM

The importance of fiber flocculation in papermaking processes has prompted many investigations to achieve a better understanding of the mechanism of flocculation and the effect of the many different variables on it. Many of these investigations, particularly the ones studying the effects of additives, pH, and temperature, were performed in unique systems where flow variables were not well defined. As brought out by Mason and coworkers (11-15,18-20), flow variables are quite important in fiber flocculation. For this reason, even studies concerning the effects of additives, etc., should be performed in a system where flow variables can be defined and controlled.

Investigations involving photographic or photoelectric techniques have shed considerable insight on fiber flocculation, but they are limited to quite dilute suspensions and they do not measure conditions at distinct points in the cross section of flow.

A technique for measuring flocculation at various locations in a field of flow is needed. This would afford a means for more direct evaluation of the effects of different variables on flocculation. As information is gathered, a better understanding of the mechanism of flocculation can be developed.

The object of this thesis is to develop such a technique. It is felt that the fiber optical probe used by Sanders (27) to measure time-mean consistency variations across a tube is an instrument with considerable potential for measuring characteristic parameters of local flocculation. Although Sanders used a time-mean value signal from the light probe in his work, prior to time-smoothing, the signal exhibited fluctuations which, in spite of the inertia of his graphical recorder, were probably due to consistency variations.

The current work at the Swedish Forest Products Laboratory (30) substantiates this.

This thesis centers around the use of fiber optic light guides to obtain fluctuating consistency signals from a fiber suspension flow and relating these signals to time-average local floc sizes using definitions commonly applied in turbulence research. Whereas the work being done in Sweden results in a flocculation spectrum with characteristic lengths of up to several hundred millimeters, this study will yield average lengths particular to a set of flocculation variables and to a distinct location in the cross section of flow. A radial distribution of floc lengths is thus possible.

The system chosen for developing and studying this flocculation-measuring technique was a vertical pipe loop designed to produce fully developed turbulent flow conditions at the measuring station. This type of system is one in which the geometry is well defined and also one in which many studies have been conducted because similarity is easily achieved. Figure 2 shows the coordinates and a few definitions for tube flow.

For an initial study, it was decided not to investigate the effect of additives, pH, and colloidal factors that may affect flocculation. Rather, this study is concerned with developing a measuring technique and studying the distribution of flocculation as a function of local velocity and mean fiber consistency. A brief background discussion pertinent to the statistical definitions used in this study follows.

The definition of turbulent motion as "... an irregular condition of flow in which the various quantities show a random variation with time and space coordinates so that statistically distinct average values can be

discerned," offered by Hinze (42) is a good starting point. This point of view was anticipated in 1935 by G. I. Taylor (43) who proposed the use of the theory of a continuous random variable and opened, under the special assumption that turbulence is homogeneous and isotropic, a new approach to the problem of turbulent flow. This condition is of practical importance for the wake flow behind grids used in wind channels, and experimental work (44) has confirmed Taylor's predictions. This approach has also afforded many workers the stimulus and means to attack other problems.

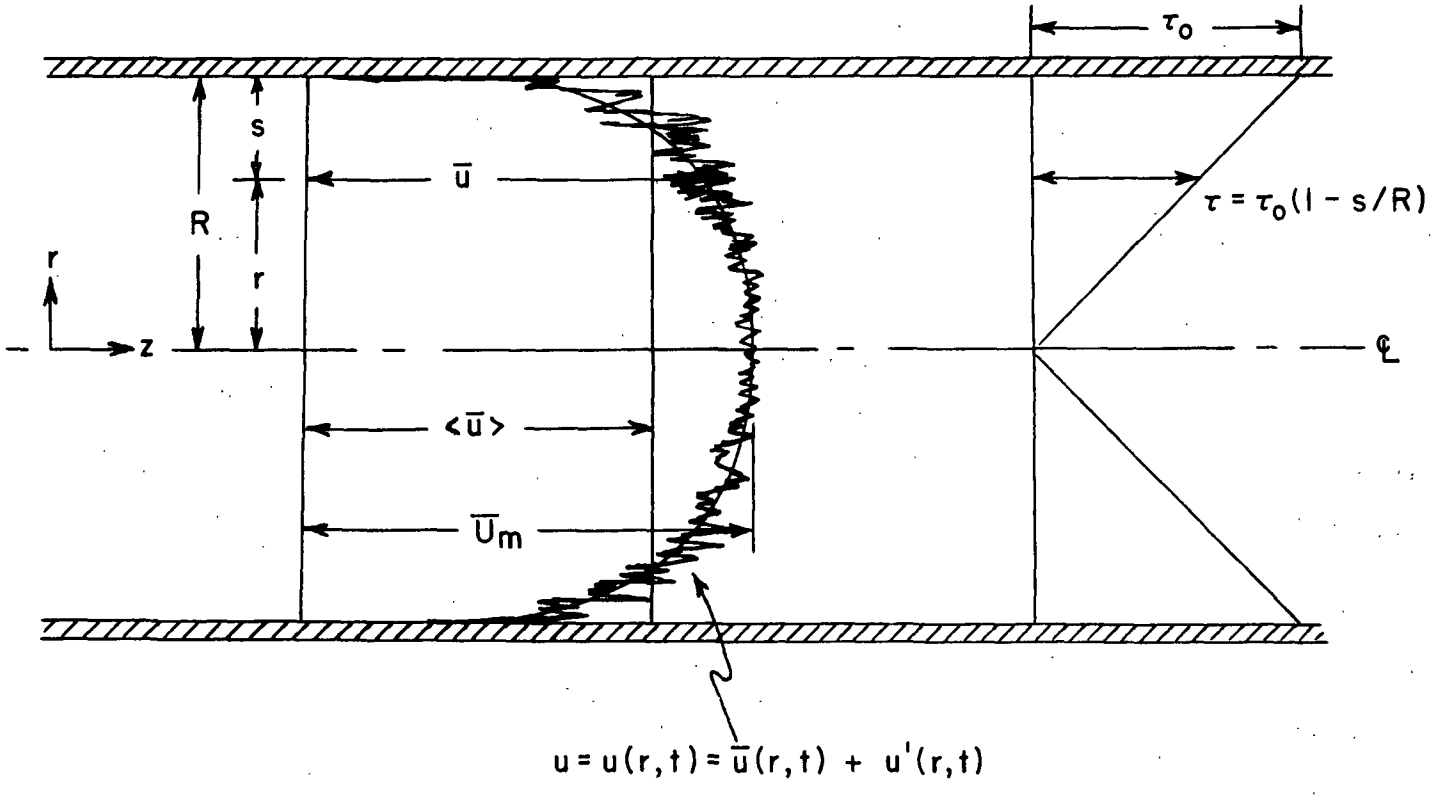

Figure 2. Coordinates and Definitions for Tube Flow

When a physical phenomenon such as turbulent flow is considered in terms of a random process, its properties can be determined by computing time-averages over sample functions. If the properties are statistically steady, not a function of time, the process is referred to as being stationary. In addition, if the properties do not differ when they are computed over different sample functions, the

random process is said to be ergodic (45). Random data representing stationary physical phenomena are generally ergodic and, for this reason, the properties of stationary random phenomena can usually be measured properly from a single observed time-history record (45).

The mean value μ_x and autocorrelation R_x are two important properties of random processes that can be determined. For a stationary random process, the mean value is a constant and the autocorrelation function is dependent only upon a time displacement τ. They are defined as follows:

$$\mu_x = \lim_{T\to\infty} \frac{1}{T} \int_0^T x(t)\, dt, \tag{5}$$

$$R_x(\tau) = \frac{\int_0^T x(t) \cdot x(t+\tau)\, dt}{\int_0^T x(t)^2\, dt}. \tag{6}$$

Correlation is a measure of the similarity between two waveforms. With reference to the fluctuating velocity depicted in Fig. 2, two types of correlation functions can be described. A temporal correlation or autocorrelation coefficient is where the fluctuations are separated by a distance in time. A spatial correlation or crosscorrelation coefficient can be defined for fluctuations separated, for example, by a radial distance r. These definitions are

$$R_z(r,\tau) = \frac{\int_0^T \overline{u'(r,t) \cdot u'(r,t+\tau)}\, dt}{\int_0^T \overline{u'^2(r,t)}\, dt}, \tag{7}$$

$$R_r(r,\Delta r) = \frac{\int_0^T \overline{u'(r,t) \cdot u'(r+\Delta r,t)}\, dt}{\int_0^T \left[\overline{u'^2(r,t)} \cdot \overline{u'^2(r+\Delta r,t)}\right]^{1/2} dt} \quad . \tag{8}$$

Taylor defined a length, or scale, of turbulence $\underline{\ell}$ based on such correlations, which can be considered a possible definition of the "average size of the eddies" (43). This length was defined as

$$\ell = \int_0^\infty R_y\, dy = \int_0^Y R_y\, dy \tag{9}$$

where $\underline{Y}$ is the distance where $R_{\underline{y}}$ becomes zero. $R_{\underline{y}}$ is the correlation between two velocities measured at two points separated by a distance $\underline{y}$.

A temporal and a spatial scale of turbulence may be defined for the correlation coefficients defined by Equations (10) and (11), respectively, as

$$L_z(r) = \bar{u}(r) \int_0^{T'} R_z(r,\tau)\, d\tau, \tag{10}$$

$$L_r(r) = \int_0^{\Delta r'} R_r(r,\Delta r)\, d\Delta r. \tag{11}$$

These scales may then be considered as average dimensions of eddies in the $\underline{z}$- and $\underline{r}$-directions, respectively.

Two characteristic lengths, $L_{\underline{z}}$ and $L_{\underline{r}}$, which may be referred to as scales of flocculation in the $\underline{z}$- and $\underline{r}$-directions, respectively, have been chosen as indicators of the time-average local floc size. In turbulence theory, scale factors describe sizes of fluid entities (eddies) whereas in flocculation these scale factors can be used to describe sizes of local mass variations. Analogous to Taylor's definitions, these flocculation scales are obtained by integrating

the appropriate correlation coefficient over the range of importance and are defined also by Equations (10) and (11). The two correlation coefficients from which these scales can be obtained are

$$R_z(r,\tau) = \frac{\int_0^T c_1(r,t) \cdot c_1(r,t+\tau)\,dt}{\int_0^T c_1^2(r,t)\,dt}, \tag{12}$$

$$R_r(r,\Delta r) = \frac{\int_0^T c_1(r,t) \cdot c_2(r+\Delta r,t)\,dt}{\int_0^T \left[c_1^2(r,t) \cdot c_2^2(r+\Delta r,t)\right]^{1/2} dt}, \tag{13}$$

where L_z and L_r are scales of flocculation in the z- and r-directions

R_z is an autocorrelation of a consistency signal

R_r is a crosscorrelation between two signals

$\bar{u}(r)$ is a local time-mean velocity of the fiber suspension

t is real time

τ is a delay time varied between 0 and τ' (the time at which time coherence of a signal with itself apparently ceases to exist)

T is a length of time large enough to ensure the time-mean consistency's becoming stationary

r is the position of fiber optic Probe No. 1

Δr is the separation of Probe No. 2 from Probe No. 1; varying from 0 to $\Delta r'$ (the distance at which any coherence between c_1 and c_2, or their respective light intensities of reflection, apparently ceases to exist)

c_1 and c_2 are consistencies of fiber suspensions at Points 1 and 2, respectively.

EXPERIMENTAL

The experimental program consisted primarily of four major parts. First, verification was needed that the vertical pipe loop was hydraulically smooth and functioning properly. Next, flow rate — pressure drop correlations and velocity profiles for fiber suspension flow had to be determined in order to establish flow rate and consistency ranges and also to tabulate velocities needed in the calculation of the axial-direction scale of flocculation. A third subprogram was a study and the calibration of both of the two-branch fiber optic light guides used for consistency measurements.

Upon completion of the first three parts, a well-defined system was established in which the final and most important part of the study could be performed. This was the actual measurement, recording and analysis of time-varying signals representing local consistency variations in fully developed turbulent tube flow.

A fiber having a fairly high length-to-diameter ratio was desired so that network formation due to mechanical entanglement would be enhanced. Therefore, the fiber used for this study was undyed 3.0-denier (approximately 17-μm diameter) rayon, which was cut to uniform 1/8-inch length by Cellusuede Products, Incorporated of Rockford, Illinois. These dimensions yielded an l/d of approximately 187 which is about three times the value for a typical softwood pulp fiber.

The consistency range was 0.05 to 0.25 g/100 ml and the Reynolds number range was 6.0×10^4 to 1.60×10^5, based on the water density and viscosity. These ranges were established by the physical limitations of the system and also by the desire to perform the investigations in the damped turbulent to

Newtonian turbulent flow regimes. Most of the flow was in the damped turbulent regime.

The first, second, and fourth portions were performed in a 2.852-inch inside diameter vertical pipe loop, whereas the calibration studies were performed primarily in a smaller loop system.

EQUIPMENT

THE PIPE LOOP

The pipe loop system used to collect fiber suspension flow data is shown in Fig. 3 and 4. The pressure instrumentation for the loop is shown in Fig. 5. The loop was mounted vertically to minimize gravitational effects on uniformity of consistency distribution and it was equipped with a 90° crossover section between the upleg and the downleg for good mixing and thus to avoid any residual secondary flow patterns. The major elements of the loop are identified in Fig. 3 and 4. The vertical portion of the loop was constructed of electropolished seamless stainless steel tubing. The upleg had a 1.865-inch inside diameter and the downleg had a 2.852-inch inside diameter. The adjoining sections were carefully mated and aligned to prevent flow disturbances at these points. Auxillary piping and valving was of two- or three-inch PVC, copper, or brass.

Test fluid was circulated through the loop by a Gould's Model 3157 centrifugal pump (A) having a 6 1/4-inch impeller. The pump was driven through a Speed-Selector variable speed system by a 5-hp electric motor. A two-inch Foxboro Dynalog magnetic flowmeter (B) was used to measure flow rates and a calibrated discharge tank (C) was used for flow measurement checks. A recycle

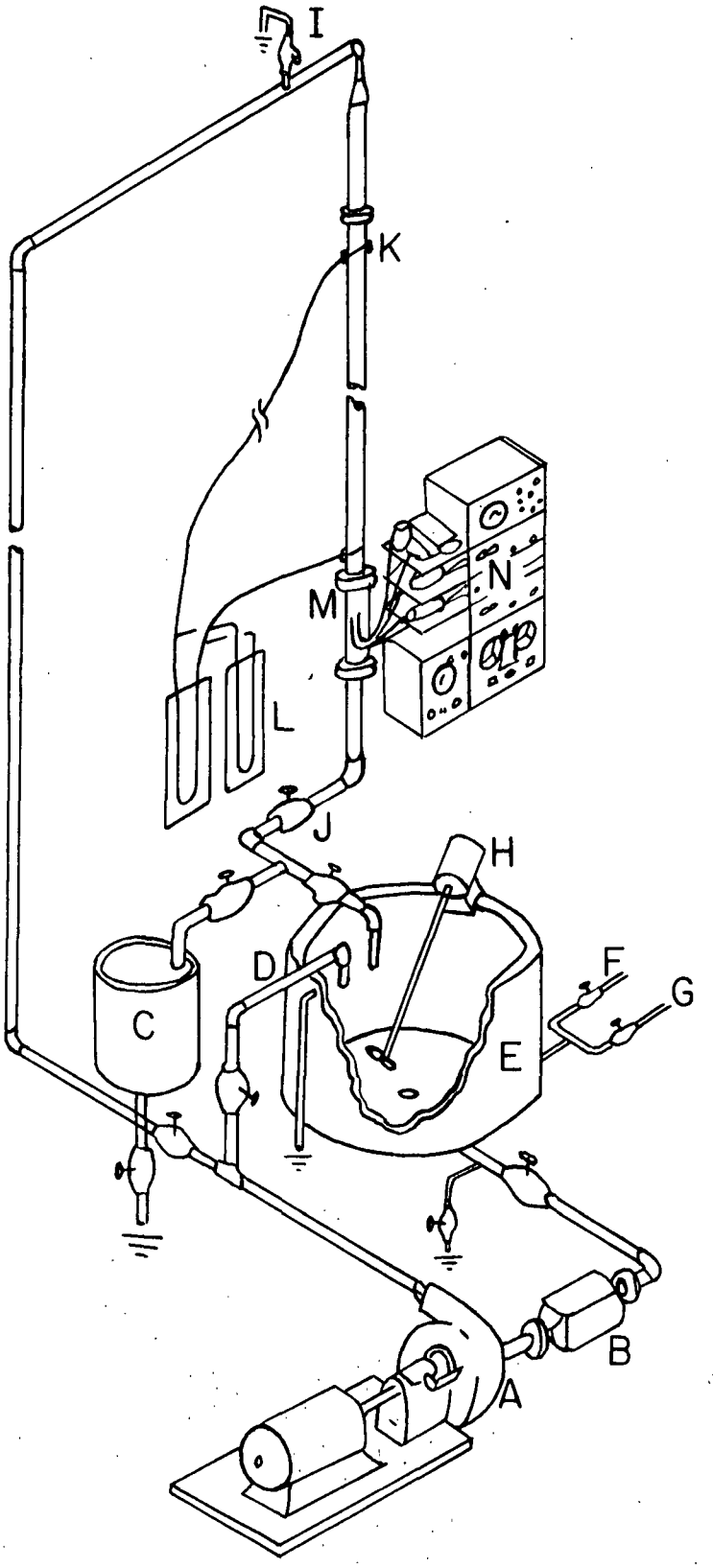

Figure 3. Sketch of Vertical Flow Loop.
A. Centrifugal Pump — Gould's Model 3157, driven through a Speed Selector Variable Speed Drive; B. Magnetic Flowmeter — Foxboro, 2 inch; C. Volumetric Discharge Tank — 65 gal.; D. Recycle Line; E. Jacketed Stock Tank — 200 gal.; F. Cooling Water; G. Steam; H. Electric Mixer — Álsop, 1/4 hp; I. Air Bleed Valve; J. Diaphragm Throttling Valve — Hills-McCanna, 3 inch; K. Pressure Taps; L. Manometer; M. Lucite Test Section; N. Instruments

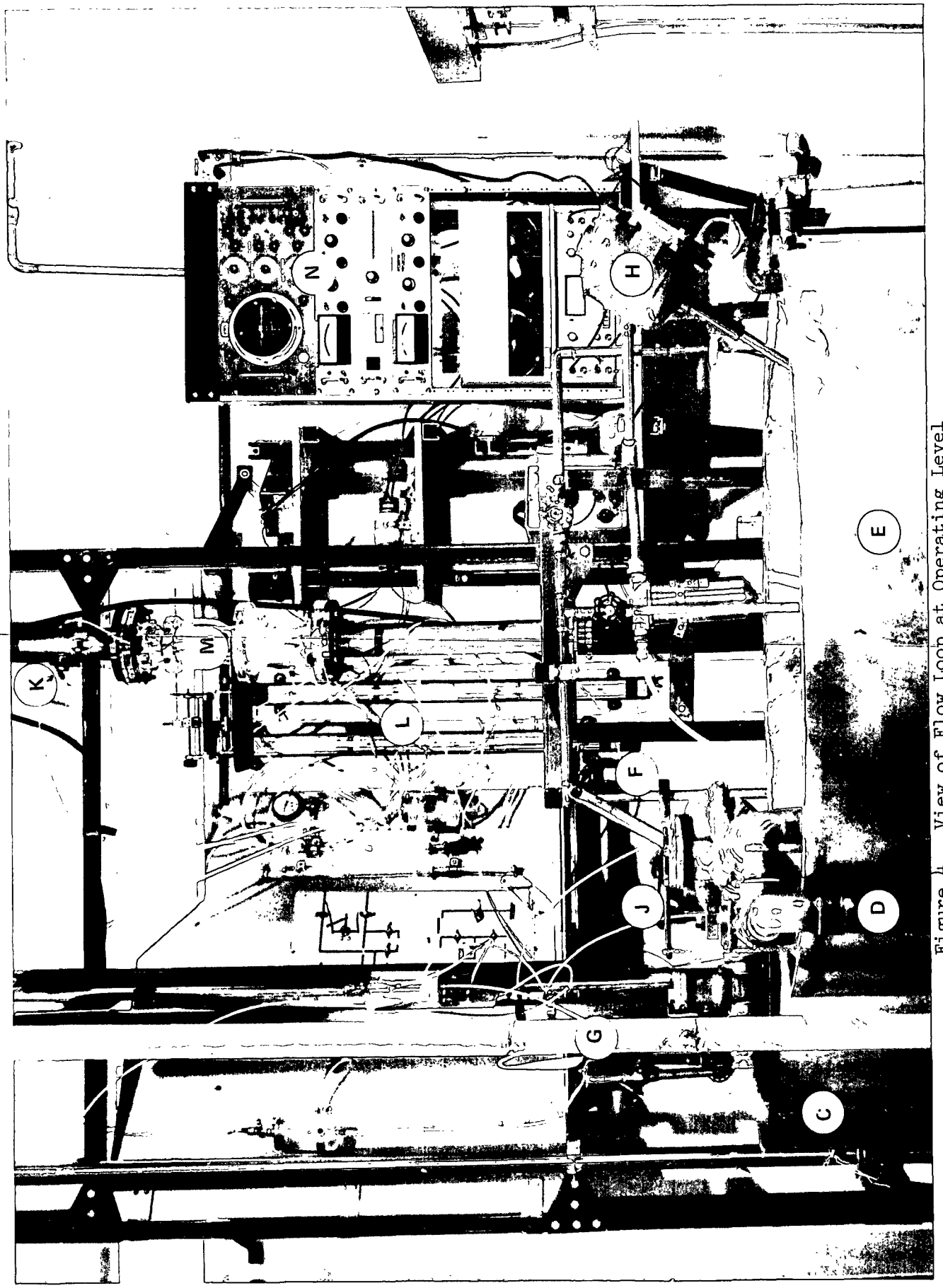

Figure 4. View of Flow Loop at Operating Level

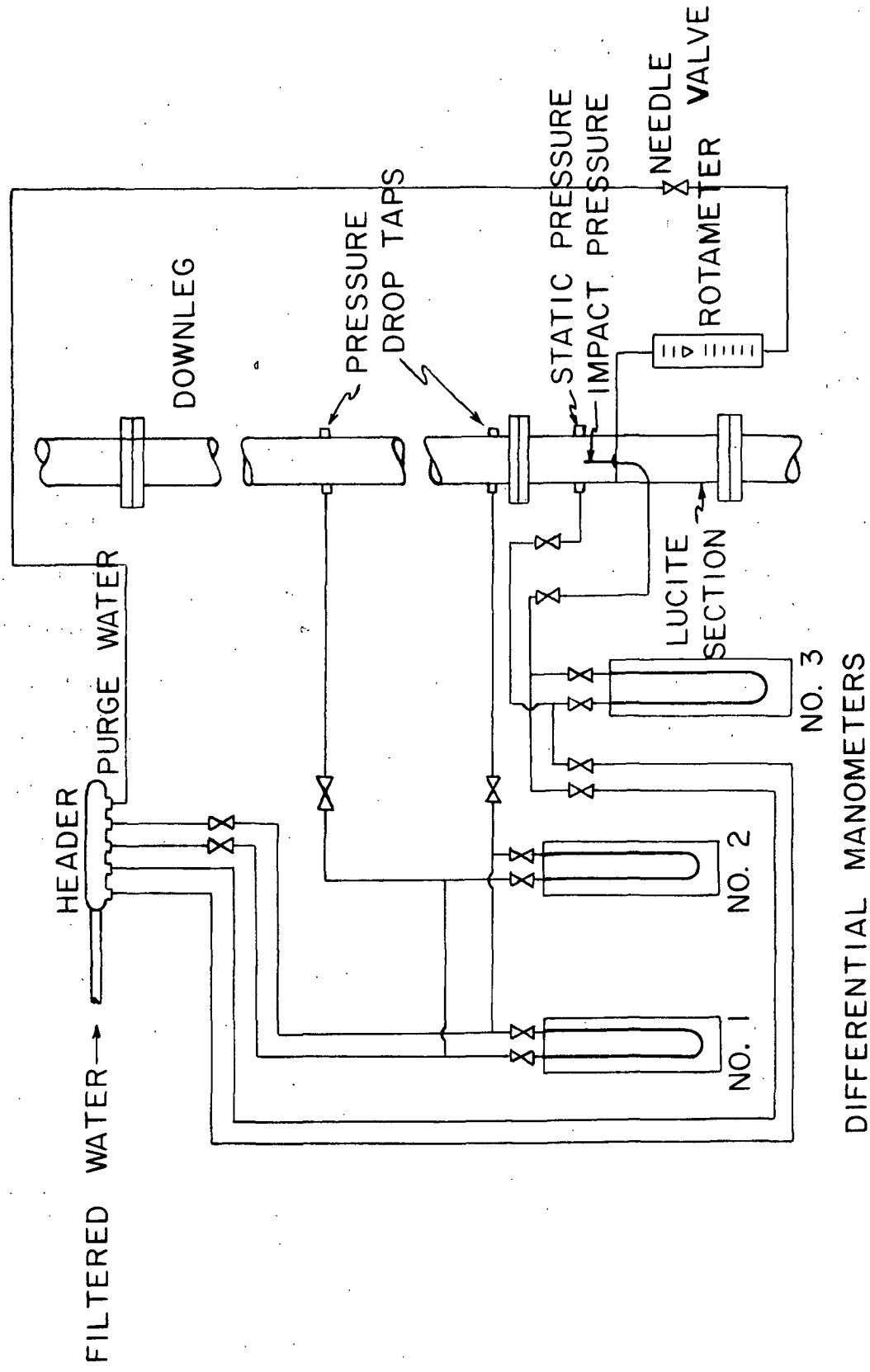

Figure 5. Pressure Instrumentation for Vertical Flow Loop

line (D) to the stock tank (E) was used for start-up ease and for straining the fibers from the suspension upon shutdown.

The stock tank was constructed of stainless steel and had a capacity of approximately 250 gallons. It was equipped with a jacket for temperature control. Manual control of either cooling water (F) or steam feeds (G) to the jacket allowed the temperature to be controlled at 25 ± 0.2°C. The stock tank was also equipped with a 1/4-hp Alsop electric mixer (H) to maintain a good dispersion of the fiber suspension, and an overflow vacuum siphon to continually bleed water from the system to compensate for purge water addition.

An air bleed valve (I) at the top of the loop allowed the loop to be purged of air. A three-inch diaphragm valve (J) on the discharge side of the loop permitted control of the static pressure in the loop, while a pressure tap at the top of the loop, connected to a pressure gage on the operating level, allowed the pressure level at the top of the loop to be monitored and thereby controlled to a positive value. This kept air from being drawn into the loop. Pressure differentials between the two static pressure taps (K) were measured with liquid-liquid manometers (L) (Fig. 5).

The test section (M) was located near the bottom of the loop downleg and was preceded by a length of three-inch pipe equal to 107 pipe diameters. This entrance length was greater than the critical lengths of 25 to 45 equivalent pipe diameters found necessary by Nikuradse (37) and Deissler (46) to achieve fully developed turbulent flow. Either one of two Lucite sections, both having an inside diameter bored to match that of the stainless steel tubing, could be installed in the loop system. One Lucite section contained an annular-purge impact probe for velocity measurements, and the other housed the two light

guides for floc measurements. Instruments (N) were mounted adjacent to the loop.

ANNULAR-PURGE IMPACT PROBE

An ordinary pitot tube would plug in fiber suspension flow so a probe with a purge jacket was employed. This type probe was developed and first used at the Beloit Corporation (25). Seely (26), Sanders (27), and Walseth (28) all used this type probe successfully in their work. The velocity sensing probe used in this study was of an annular-purge design and is shown in Fig. 6.

The probe consisted of a conventional impact probe surrounded by an annular jacket through which purge water flowed. The tip of the sensing element, inner tube, projected about 1/32 inch beyond the outer tube and was effectively kept free from fiber stapling by the purge water. The impact tube was water-filled and was connected to one side of a liquid-liquid differential manometer.

The outside tube used in this investigation had a 0.095-inch diameter and extended 1.65-inches upstream of the diametrical support bar. The probe was mounted in a Lucite test section on the diametrical support bar as illustrated in Fig. 7. Connected externally to the support bar was an assembly consisting essentially of a lead screw unit and a scale. This made it possible to move the probe across the tube diameter and determine the probe position via direct reading.

TWO-BRANCH LIGHT GUIDES

The consistency sensing elements used in this study were fiber optic light guides specially constructed by Americal Optical Corporation. The fiber

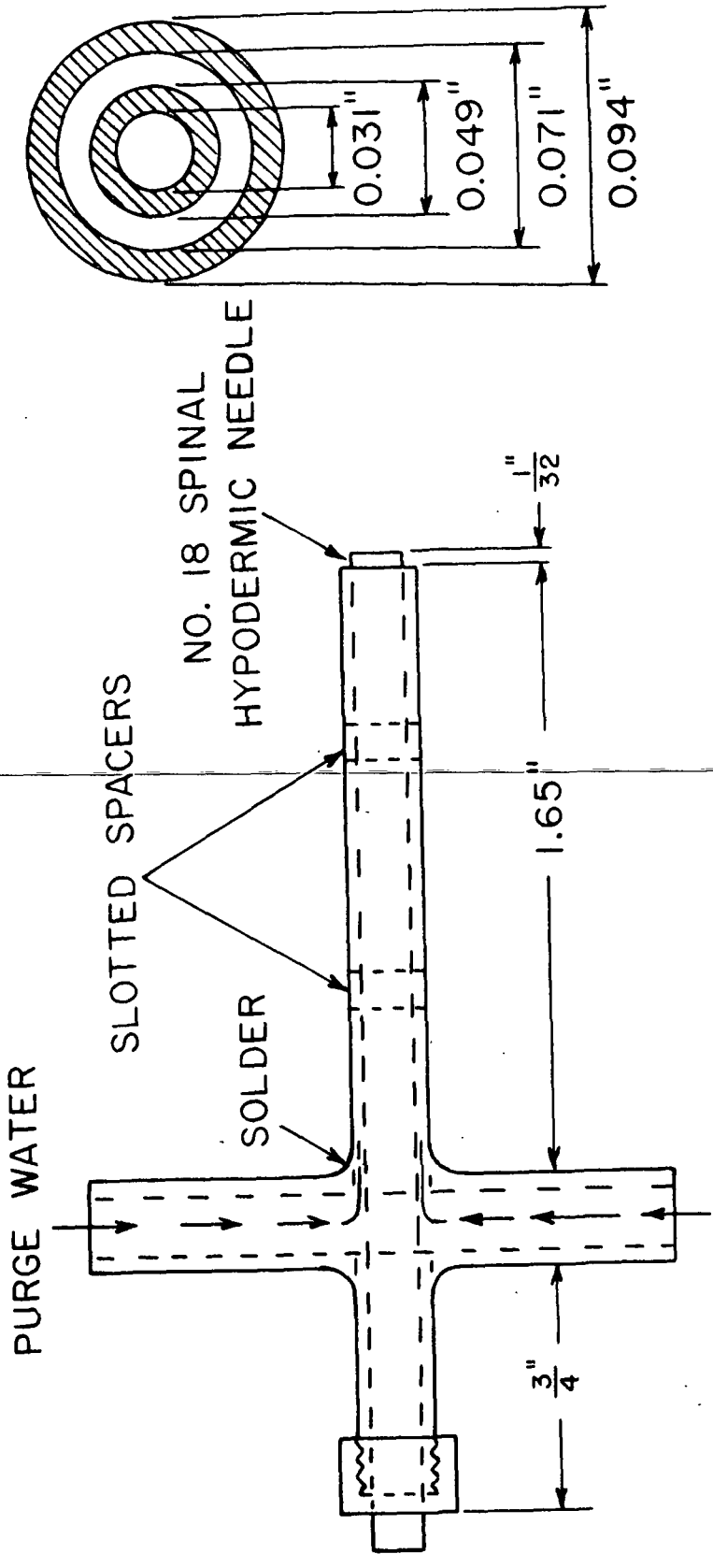

Figure 6. Annular Purge Impact Probe

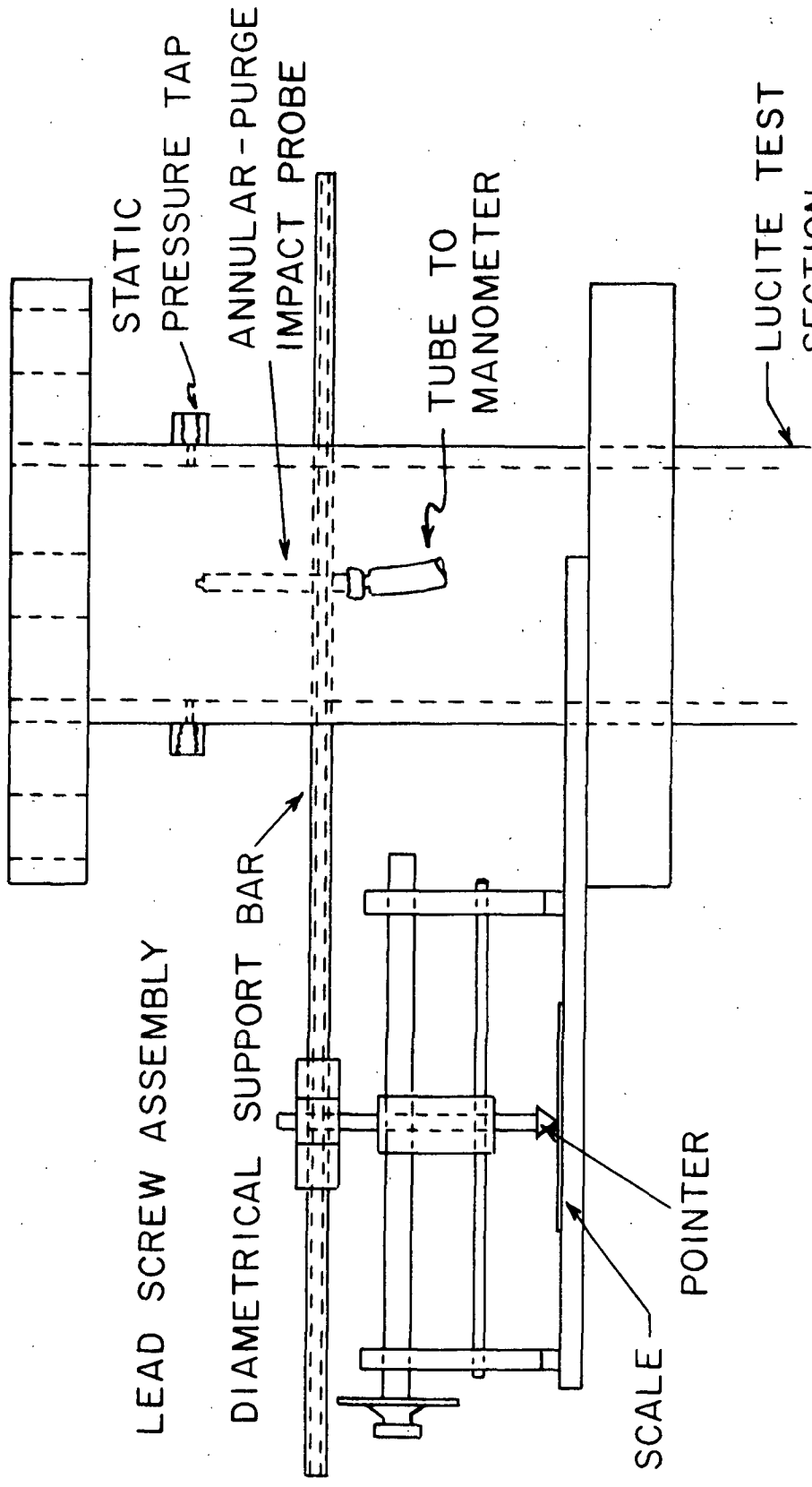

Figure 7. Traversing Mechanism for Annular-Purge Impact Probe

optic probe was used in fiber suspension studies at the Beloit Corporation (27) and also at The Institute of Paper Chemistry (27,28). One of similar design was also used by workers at the Swedish Forest Products Laboratory (29).

In this study, two-branch light guides, with the glass threads from each branch arranged in a random mix in the common probe tip, were employed. The glass threads were 0.003 inch in diameter and consisted of a core glass (refractive index = 1.62) and a protective plastic coating (refractive index = 1.52). Two such probes were required. Figures 8 and 9 show these light guides and their dimensions. One probe had to have the probe tip offset 1/2 inch from the main body so that, when it was mounted in the Lucite test section, it could be moved adjacent to the other light guide. Since, in the experimental procedure, it was desired to have the two light guide tips come into virtual contact at times, the annular-purge jacket design used by Sanders (27) could not be used. Specially constructed purge tubes having a crescent-shaped discharge area were used to keep fibers from effectively stapling over the probe tip. Figures 8 and 9 also show the crescent purge tubes mounted alongside the light guides.

Both probes were mounted inside a Lucite test section on diametrical support bars. The positioning of the two probes was affected by two lead screw mechanisms mounted externally in a "piggy back" fashion. The dual unit mechansim is illustrated in Fig. 10.

ELECTRONICS

The electronic equipment necessary to gather and record the fluctuating consistency signals from the suspension is shown in Fig. 11 and 12. Figure 11

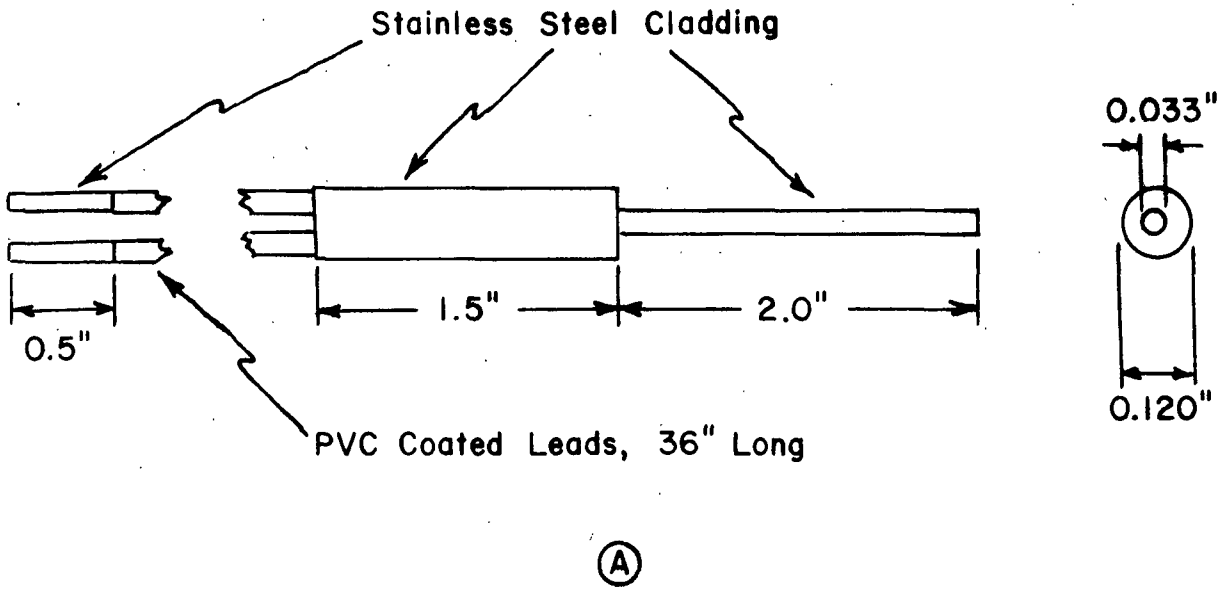

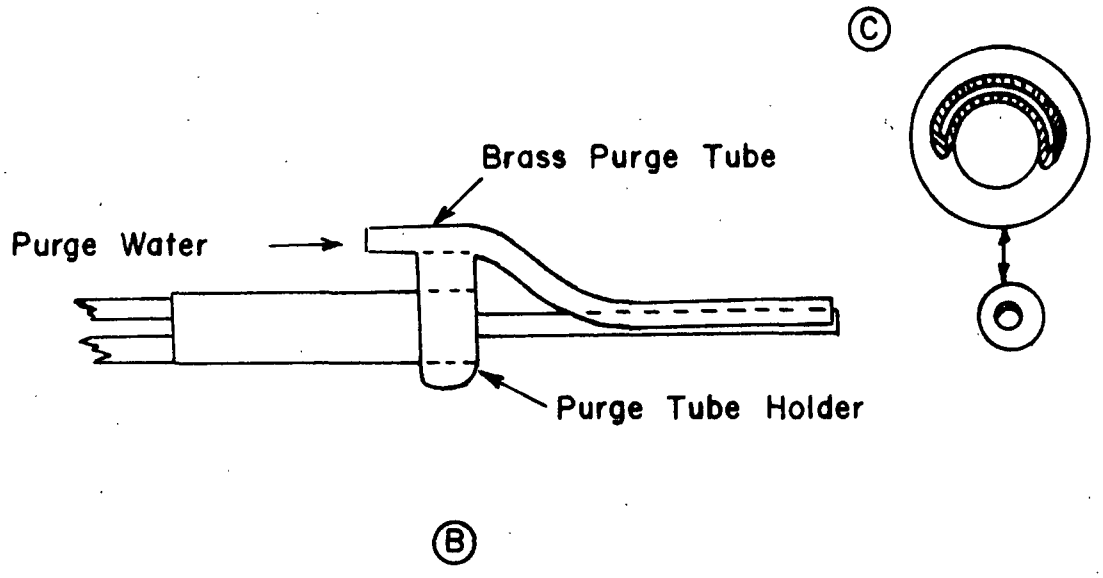

Figure 8. Straight Light Guide: A) Dimensions, B) Purge Tube Attached, C) Enlarged View of Probe Tip

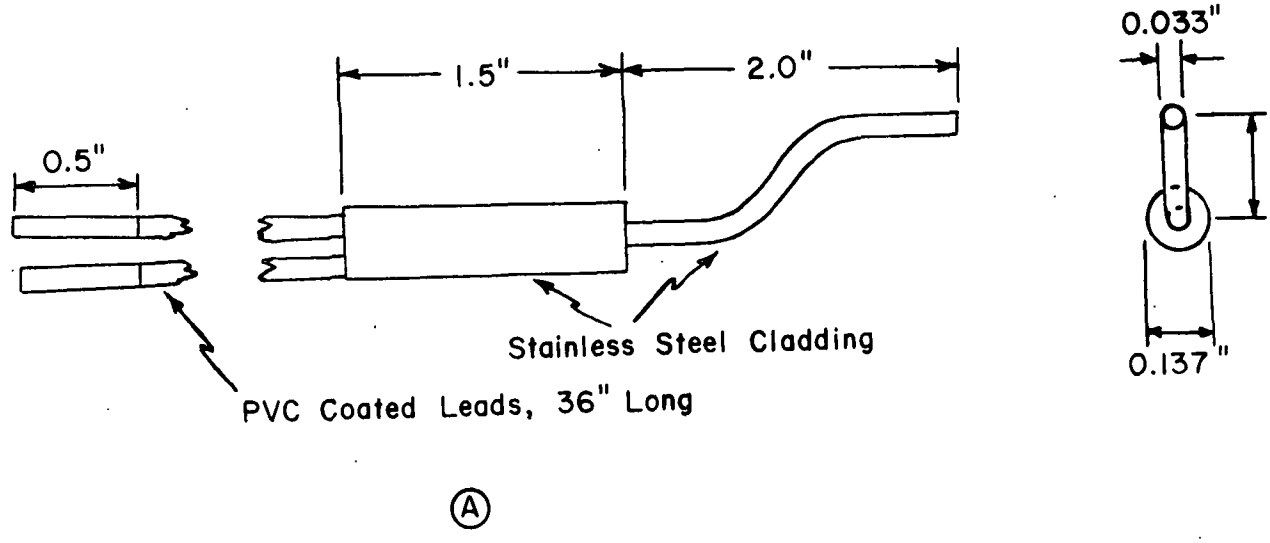

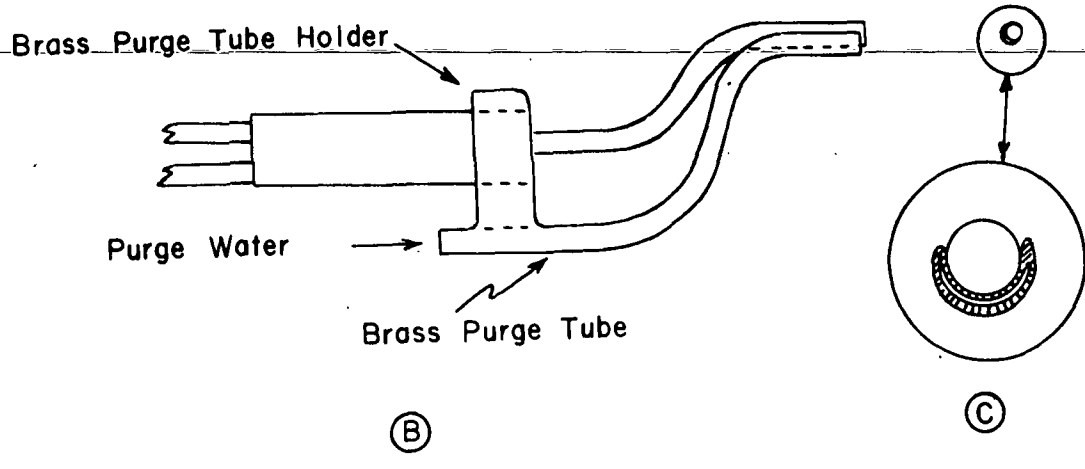

Figure 9. Offset Light Guide: A) Dimensions, B) Purge Tube Attached, C) Enlarged View of Probe Tip

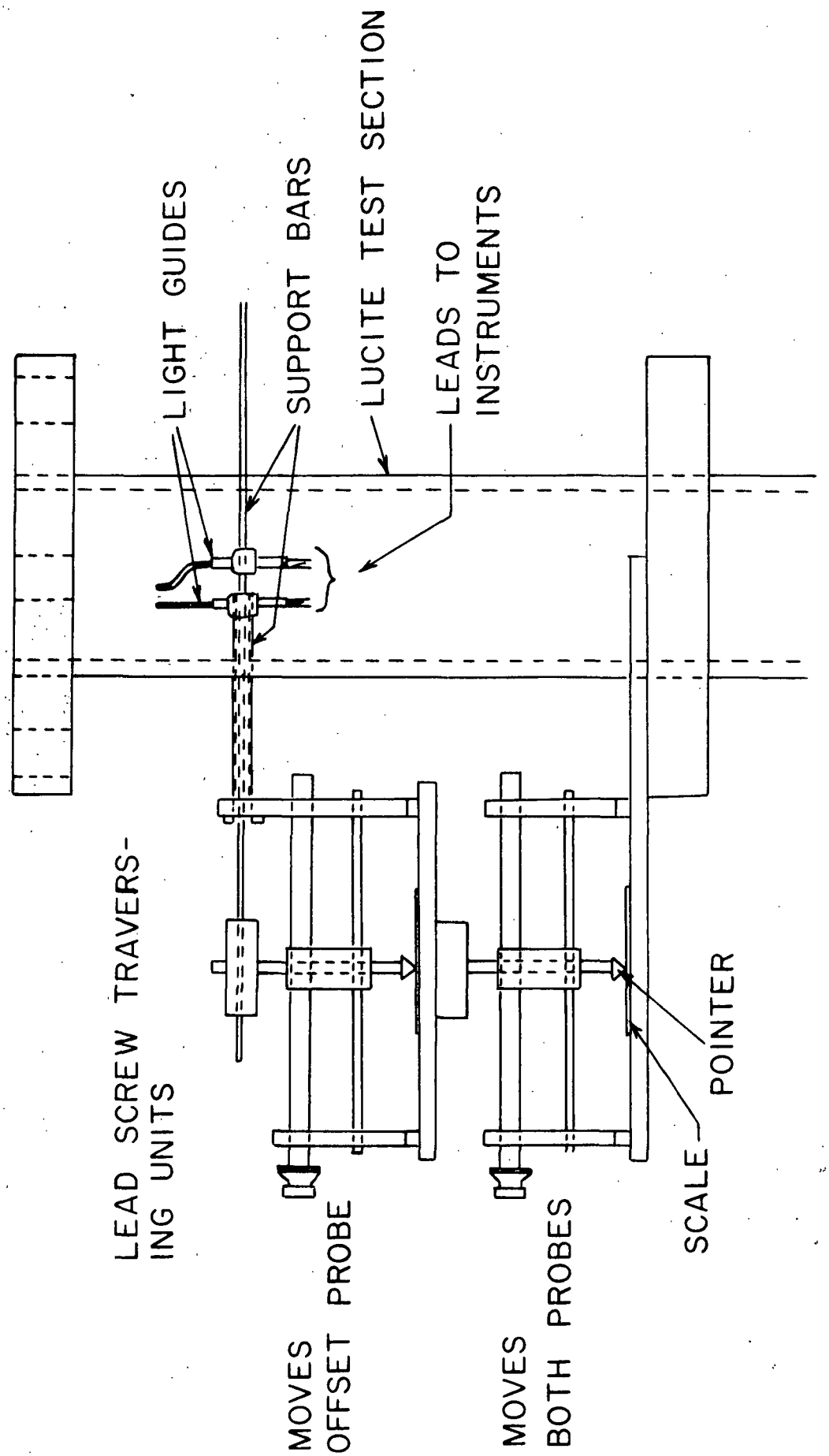

Figure 10. Dual Unit Traversing Mechanism for Light Guides

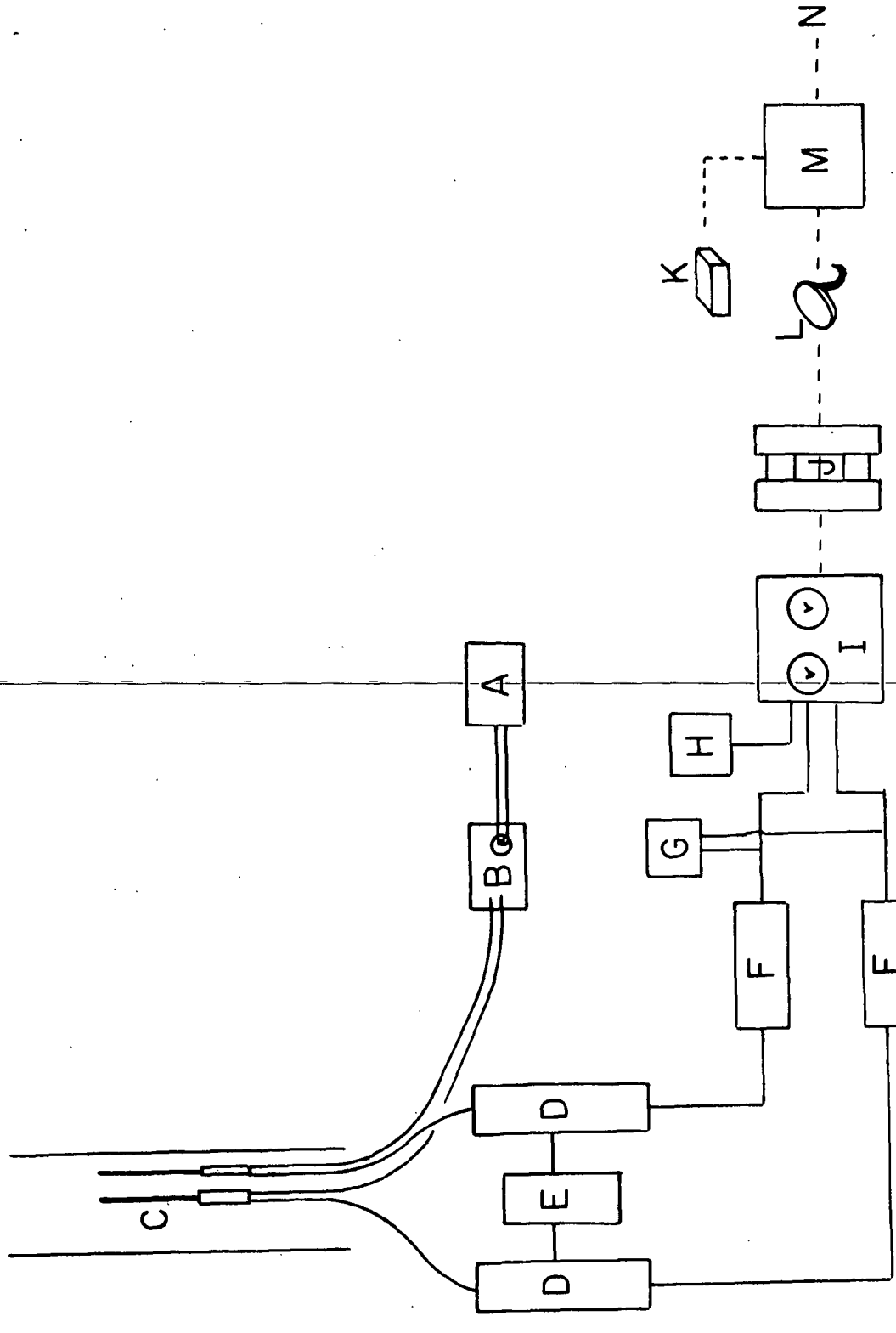

Figure 11. Schematic of Consistency Signal Collection and Analysis.

A. Kepco Model PRM 6.3-8 dc Power Supply; B. Quartz-Iodide Lamp; C. Fiber Optic Light Guides in Lucite Section; D. EMI Phototube and Photomultiplier Housing; E. Brandenburg Photomultiplier Power Supply; F. EMI Picoammeter; G. Signal Monitor (DuMont 403R Oscilliscope or Esterline Angus Model E 1101S Strip Chart Recorder); H. Hewlett-Packard Model 200AB Audio-oscillator; I. Hewlett-Packard Model 3960B Analog Recorder; J. Analog-to-Digital Converter; K. Program and Other Data; L. Digital Data; M. IBM 360 Digital Computer; N. Computer Output

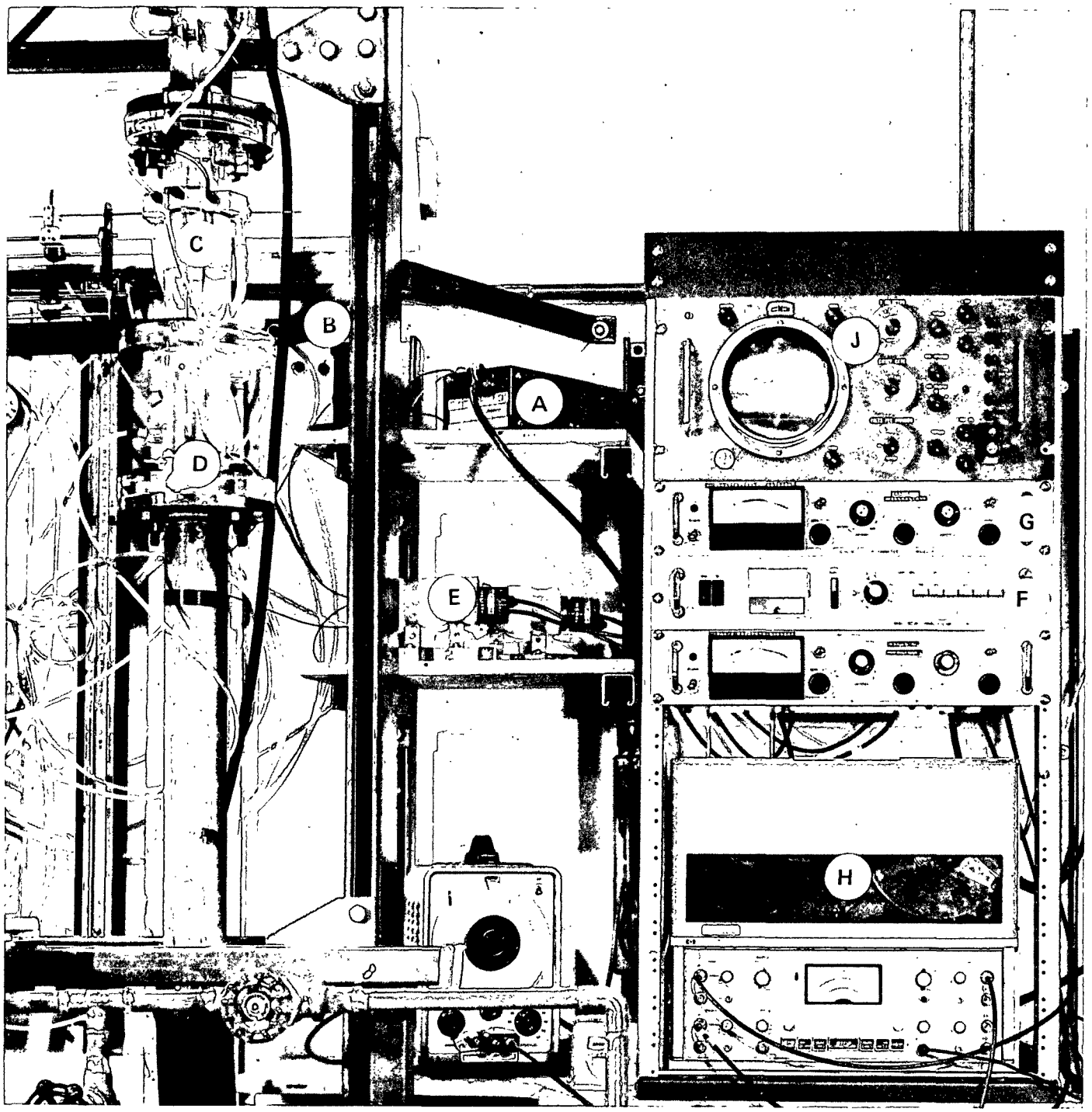

Figure 12. Photograph Showing Instrument Setup for Collecting and Recording Fluctuating Consistency Signals: (A) dc Power Supply, (B) Quartz-Iodide Lamp, (C) Light Guides, (D) Lucite Test Section, (E) Photomultiplier, (F) Photomultiplier Power Supply, (G) Picoammeter, (H) Analog Instrumentation Recorder, (I) Audio-oscillator, and (J) Oscilliscope

is a schematic showing where the various items fit in the instrument train[2] and Fig. 12 is a photograph of the equipment setup next to the pipe loop.

A Kepco PRM 6.3-8 modular power supply (A) having multiple output regulated dc voltages, was used to operate a quartz-iodide lamp (B) at 6 volts. The lamp was mounted in a housing which had fittings to hold one lead tip from each of the two light guides (C) mounted in the Lucite section (D).

The other branch of each of the light guides was connected to a photomultiplier unit (E) by an adapter constructed to hold the probe lead securely in a constant position with respect to the photomultiplier. Two photomultipliers were required. Each had an EMI Type 9524-B, 11 box and grid dynodes, phototube mounted in an EMI Type T 124/B11M phototube housing. Each housing had a potentiometer in series with the high voltage for adjustment in balancing the gain for the two tubes.

The photomultipliers were powered by a Brendenburg Type 472 R photomultiplier power supply (F) capable of supplying 10 to 2100 volts (bipolar) at a 5-ma maximum.

Two EMI Type 1012 picoammeters (G) were used to amplify the signal from the photomultipliers to a level sufficient for recording.

The amplified samples were recorded on two FM channels of a four-channel Hewlett-Packard Model 3960-B analog instrumentation recorder (H). The other two channels were direct, with channel four having capabilities for voice recording. Tape speeds were 15, 3 3/4, or 15/16 inches per second. 3M Type 801-1/4-1800PR instrumentation tape was used for recordings.

---

[2] Specifications for these instruments can be found in Appendix I.

A Hewlett-Packard Model 200 AB Audio-oscillator (I) was used to supply an oscillatory signal that was used as a data valid signal and recorded on Channel three of the recorder.

THE CALIBRATION LOOP

The small loop system used to calibrate the light guides is shown schematically in Fig. 13 and in the photograph in Fig. 14. The main components of the system are listed in both figures.

Stock was pumped from the Lucite mix tank around the 1 1/2-inch loop by a Tri-Clover centrifugal pump driven at a constant speed by a 1/2-hp electric motor. Flow rates were measured by the same Foxboro Dynalog magnetic flowmeter used in the vertical flow loop. A flow nozzle and probe support unit, Fig. 15, was mounted on the end of the loop downleg and extended into the mix tank. The nozzle was a 3/4-inch bore through a solid piece of PVC that was also threaded to fit on the end of the 1 1/2-inch PVC downleg tubing. A 1 1/2-inch diaphragm valve was used to regulate the flow rate through the loop. The capacity of the loop system was about 26 liters.

The electronic system previously described was also used for calibration studies. However, an Esterline Angus strip chart recorder with a low pass filter ahead of it replaced the magnetic recorder so that mean signal traces could be viewed.

PROCEDURES AND DATA

ESTABLISHING THAT THE FLOW LOOP FUNCTIONED PROPERLY

The flow loop was first tested with water as the test fluid to establish that the system was hydraulically smooth and functioning properly.

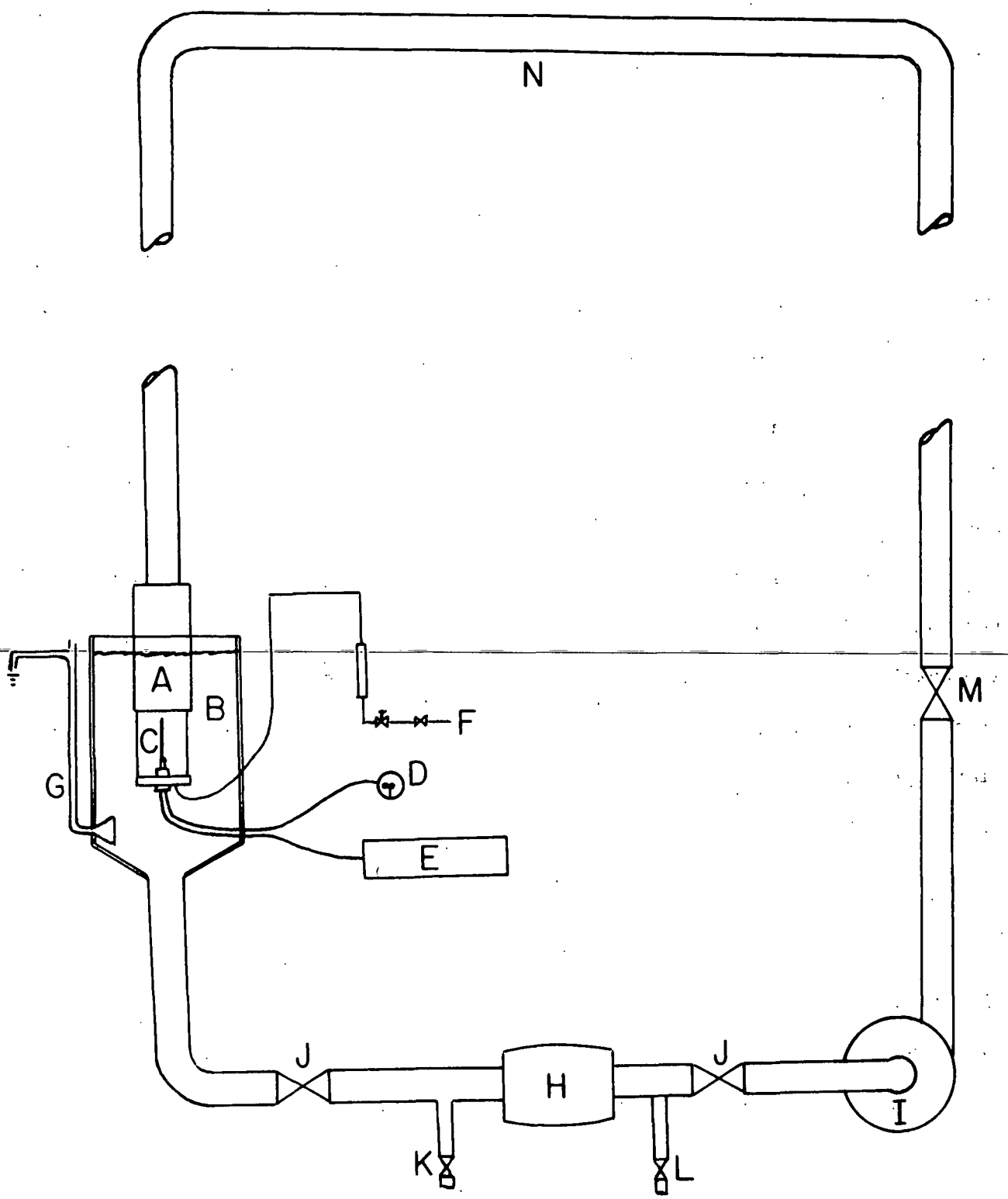

Figure 13. Calibration Loop System Consisting of:

(A) Nozzle and Support (Fig. 15); (B) Lucite Mix Tank; (C) Light Guides; (D) Lamp; (E) Instruments (Fig. 14); (F) Purge Water; (G) Constant Level Overflow; (H) Magnetic Flowmeter; (I) Constant Speed Centrifugal Pump; (J) Gate-Type Shut-Off Valves; (K) Water Supply; (L) Drain; (M) 1 1/2-Inch Diaphragm Valve, and (N) PVC Pipe Loop

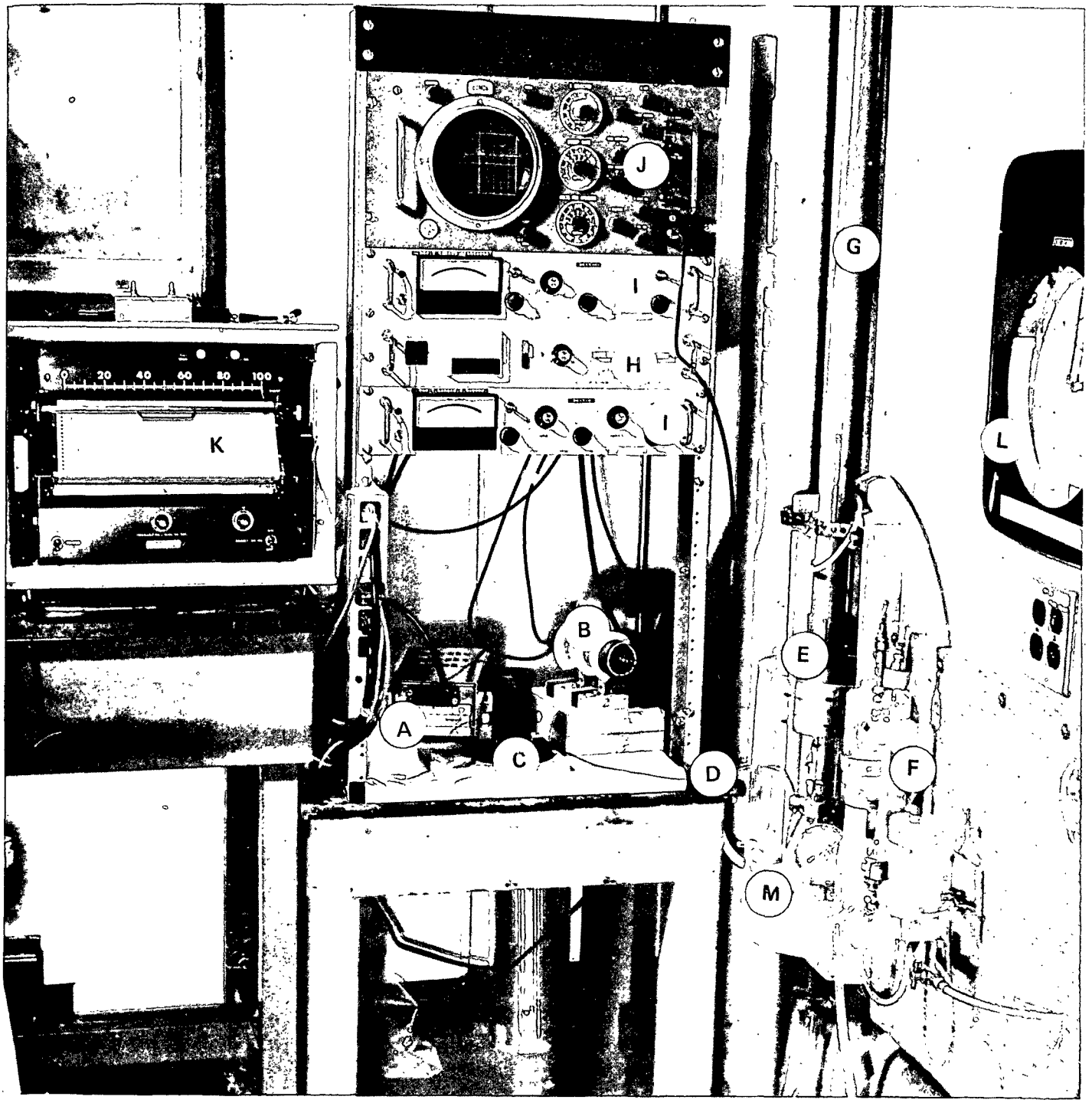

Figure 14. Calibration Loop Setup: (A) dc Power Pac, (B) Photomultiplier, (C) Lamp, (D) Light Guide, (E) Nozzle-Probe Support, (F) Purge Water System, (G) Calibration Loop Downleg, (H) Photomultiplier Power Supply, (I) Picoammeter, (J) Oscilliscope, (K) Strip Chart Recorder, (L) Magnetic Flowmeter Recorder, and (M) Lucite Mix Tank

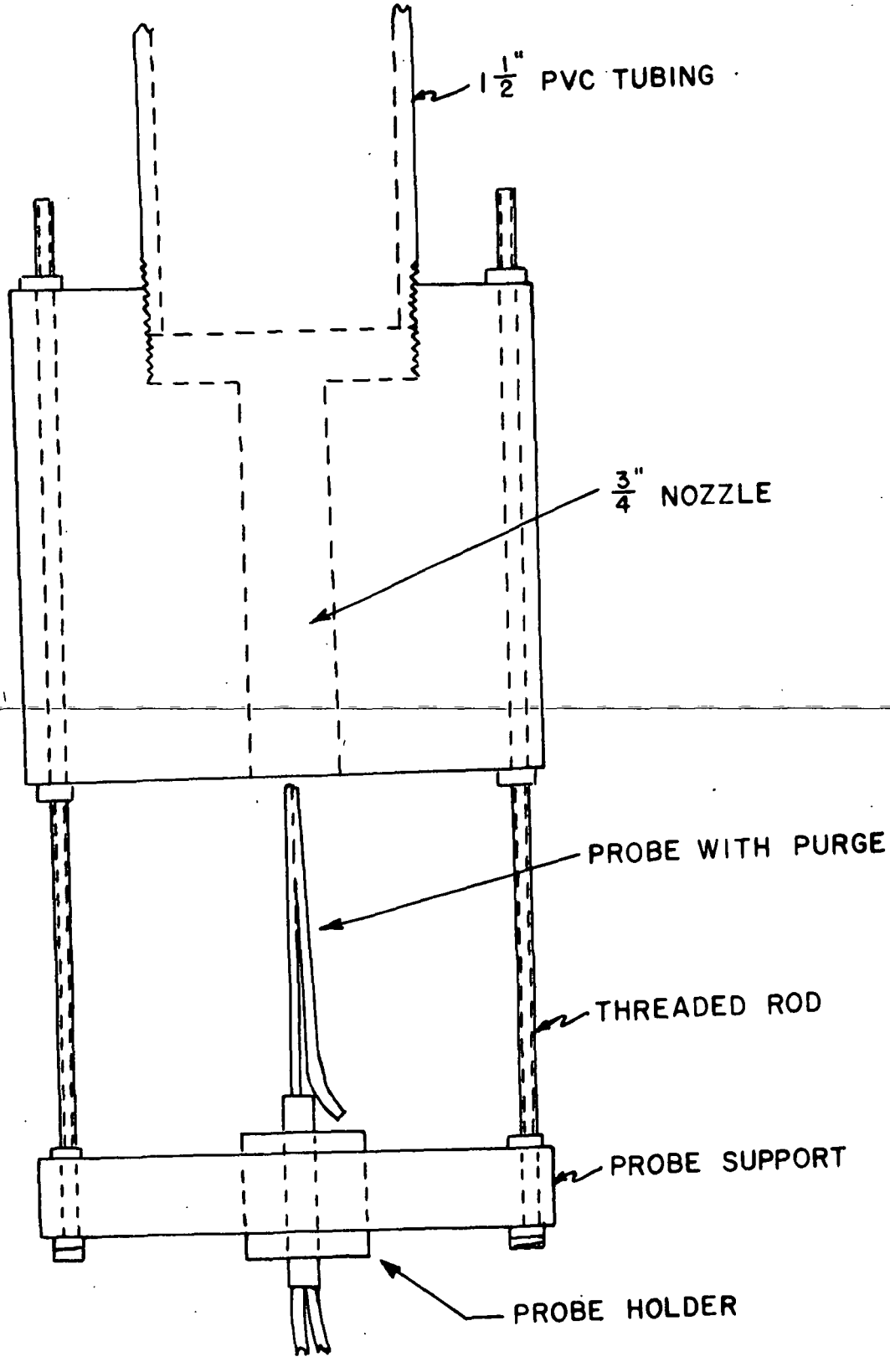

Figure 15. Nozzle and Probe Support

Pressure Drop-Flow Rate

To establish whether or not the loop was hydraulically smooth, flow rates and pressure drop data were collected. Using water as the test fluid, the loop was operated at flow rates corresponding to Reynolds numbers from 1.3×10^4 to 1.60×10^5. The 3-inch diaphragm valve and the variable speed pump drive were used to regulate the flow rate which was then read from the magnetic flowmeter recorder chart.

Pressure drops were measured on the downleg of the loop. The pressure tap locations were separated by 41 pipe diameters with the upstream tap being about 64 pipe diameters downstream of the top elbow and the downstream tap about 4 to 5 pipe diameters upstream from the tips of the probes mounted in the Lucite test section. Each of the tap locations consisted of two taps into the pipe wall opposite each other. Figure 5 illustrates the pressure instrumentation for the loop. Pressure differentials were measured on liquid-liquid differential manometers. Both carbon tetrachloride (CCl_4), with a specific gravity of 1.58, and chlorobenzene (CB), with a specific gravity of 1.10, were used as manometer fluids.

Connections from the pressure taps to the manometers and water supply header were made with 1/8 × 1/4-inch Polyflo tubing and Imperial Eastman fittings. Valves were 1/8-inch Circle seal type.

The pressure drop and flow rate data were converted to Fanning friction factor f and Reynolds number Re data. Figure 16 shows the correlation of these data for water at 20 and 25°C. The agreement between these data and the established correlation (38) indicated that the loop was smooth and was functioning properly.

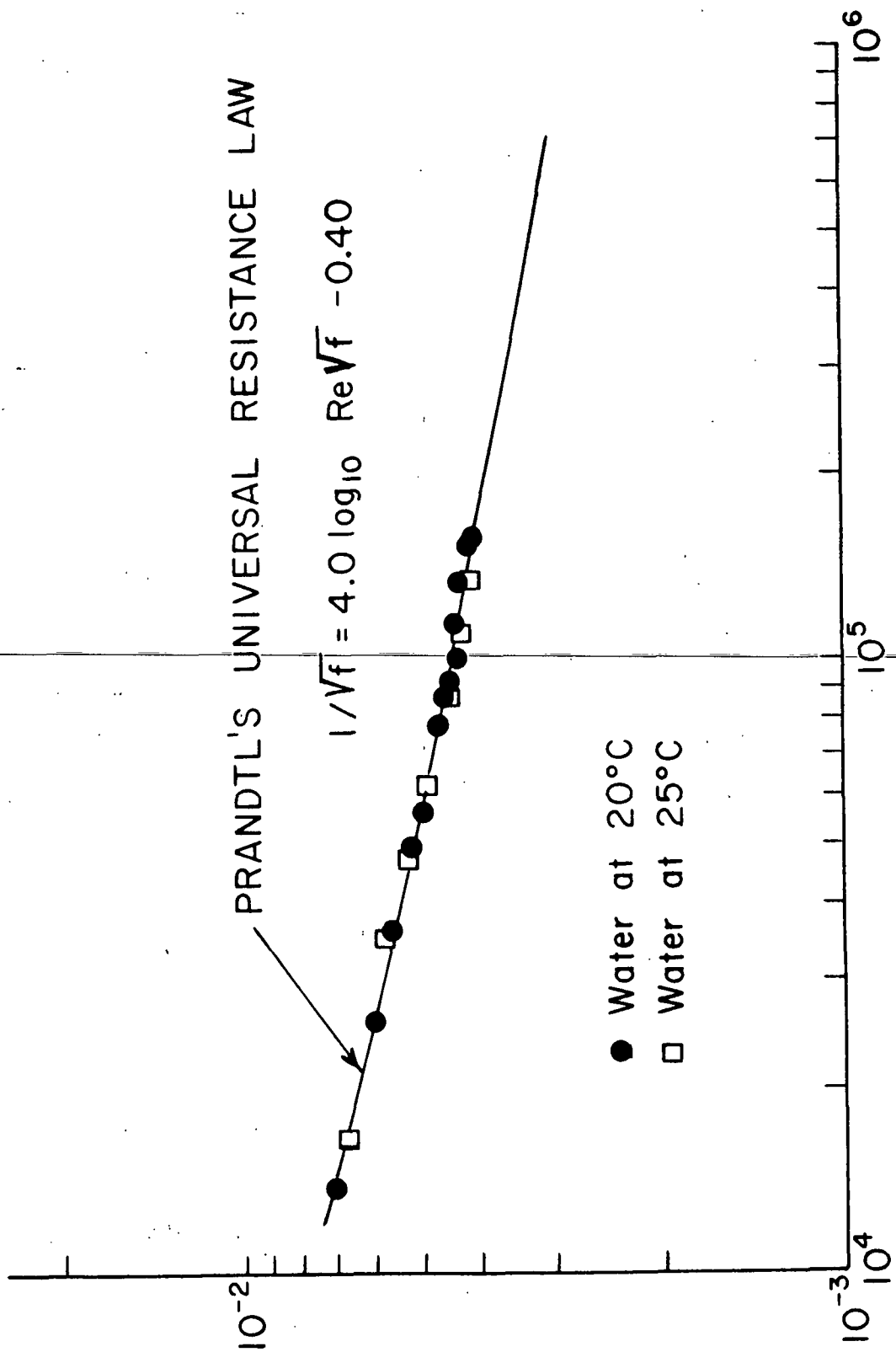

Figure 16. Friction Factor vs. Reynolds Number Correlation for Water

Velocity Profiles

Velocity profile measurements were made with an annular-purge impact probe. The impact portion of the probe was water-filled and was connected to one side of a water-CCl_4 differential manometer. The other side of the manometer was connected to static pressure taps located on the Lucite test section, in the plane of the probe tip but perpendicular to the plane of the diametrical support bar.

The annular-purge probe functioned as described by others (25-27). For purge water flow rates less than a critical value, a plateau region of constant impact pressure was obtained for a constant suspension flow rate. At purge rates greater than the critical value, the impact pressure suddenly swung negative, evidently from the purge jet's dragging the sensing volume in front of the probe.

Water velocity profiles, as measured over a flow range of 0.102 to 0.247 ft^3/sec were symmetrical about the pipe axis whether measured in the plane of or perpendicular to the plane of the top crossover section of the flow loop. Representative profiles are shown in Fig. 17.

The water profile data were also plotted in the form of dimensionless velocity versus the logarithm of dimensionless position with the resulting correlation shown in Fig. 18.

Operation of the impact probe was also checked by comparing the integrated velocity profiles to volumetric discharge rates as measured with the calibrated magnetic flowmeter. The comparison is shown in Table I and the agreement can be seen to be very good.

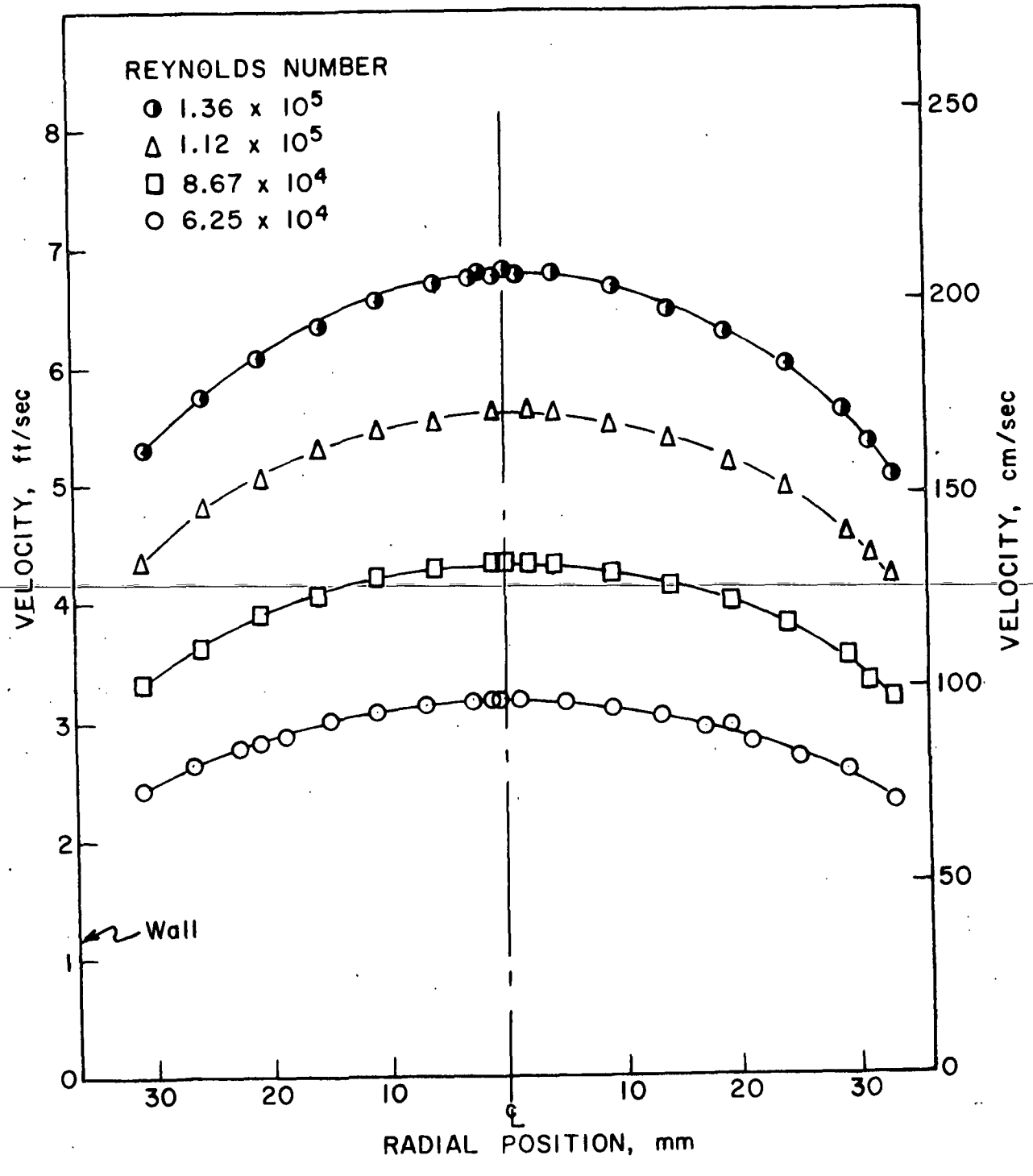

Figure 17. Representative Water Velocity Profiles

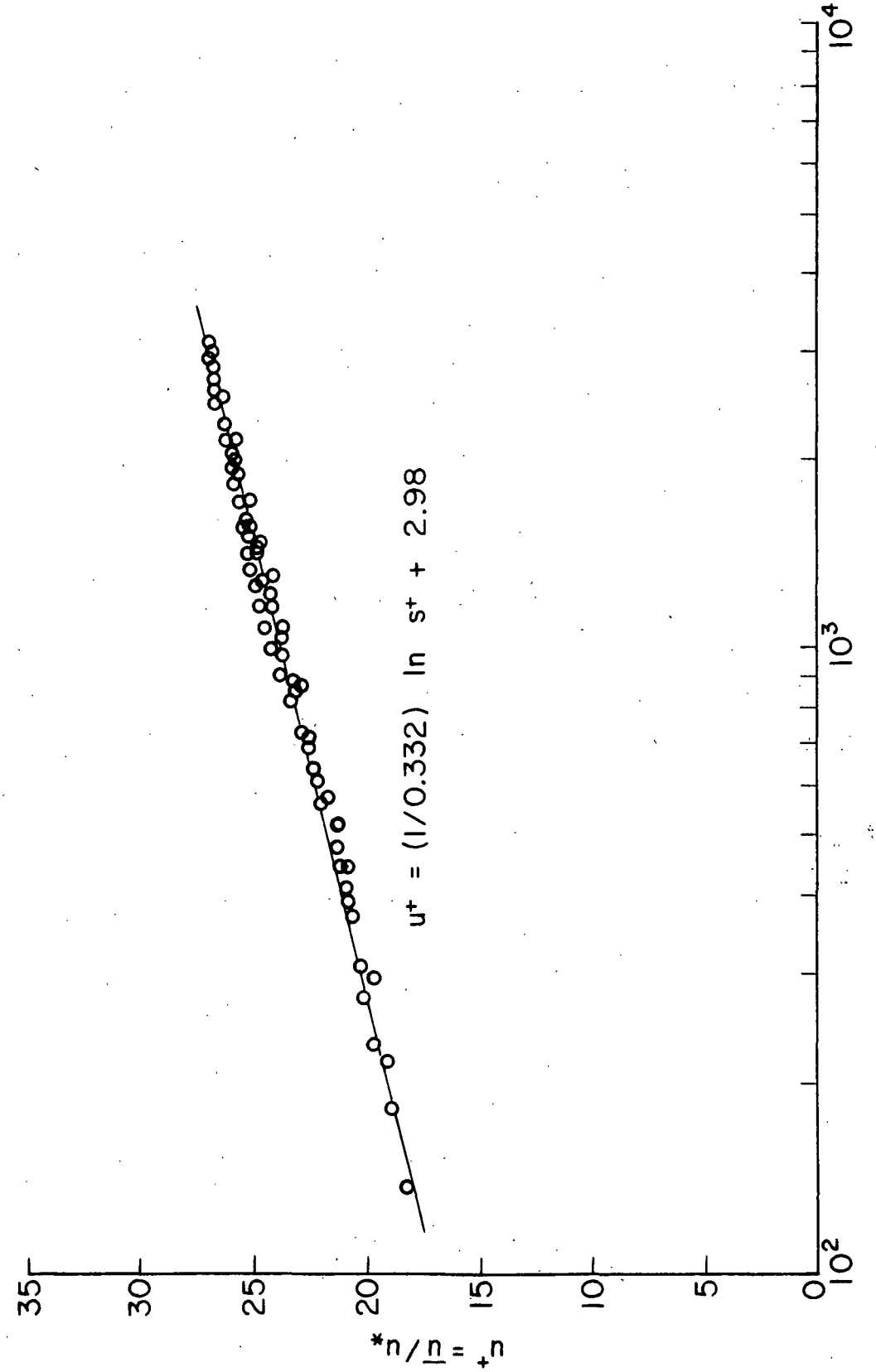

Figure 18. Dimensionless Velocity vs. Logarithm of Dimensionless Position, Water at 25°C

TABLE I

COMPARISON OF BULK FLOW RATES, $\underline{Q}$

Magnetic Flowmeter ($\underline{Q}_M$), ft^3/sec	Integrated Velocity Profiles ($\underline{Q}_I$), ft^3/sec	Difference $(1 - \underline{Q}_I/\underline{Q}_M) \times 100$
0.102	0.099	+2.9
0.113	0.114	-1.0
0.137	0.132	+3.5
0.156	0.156	0
0.158	0.159	-0.5
0.160	0.155	+3.0
0.183	0.176	+3.5
0.202	0.206	-1.9
0.228	0.223	+2.1
0.247	0.241	+2.4
0.245	0.252	-2.6

FIBER SUSPENSION FLOW STUDIES

Fibers

A bleached sulfite softwood pulp fiber first chosen for this study was found to undergo some refining in the system and fibrils were being brushed up from the fiber surface with time. Since this introduced another variable known to be of importance in fiber flocculation, other fiber types were investigated. A 1/4-inch × 3.0-denier rayon fiber was next considered and, although there was no problem with fiber degradation, the fibers were too long. They stapled over the diametrical support bar and any other protrusions and tended to form long threads.

A shorter rayon fiber was finally chosen for this study. Three-denier rayon cut to a uniform length of 1/8 inch was obtained from Cellusuede

Products, Incorporated. The fibers, although not circular in cross section, had an approximate diameter of 17 μm, yielding a length-to-diameter ratio of approximately 187. Photomicrographs of these fibers are shown in Fig. 19 and 20.

The fibers were washed prior to their first use and at the end of a run they were strained from the water, dried, and stored in plastic bags.

Pressure Drop-Flow Rate

To establish a working range of flow rate and consistency for the flocculation study, pressure drop and flow rate data were collected for suspensions of consistencies varying from 0.05 to about 0.45 g/100 ml. These data were collected in the same manner as the water data.

A sufficient amount of fiber to establish a specific system consistency was added to a premeasured volume of water in the stock tank. After the suspension had circulated a few minutes through the loop system, dip samples were taken from the tank and consistency checks were made by determining the weight of fibers in the volume of the suspension removed. In view of earlier work (27) this is a questionable procedure; therefore, a composite of several samples from various points within the tank was used to make a consistency determination. An average of at least three composite samples served as a consistency check.

The suspension was allowed to circulate one to two hours before any pressure measurements were taken. As with water, pressure drops between two pressure taps were measured by using liquid-liquid (H_2O-CCl_4 or H_2O-CB) differential manometers. The pressure taps were occasionally back-flushed, with water from the supply header, to keep the taps from becoming plugged

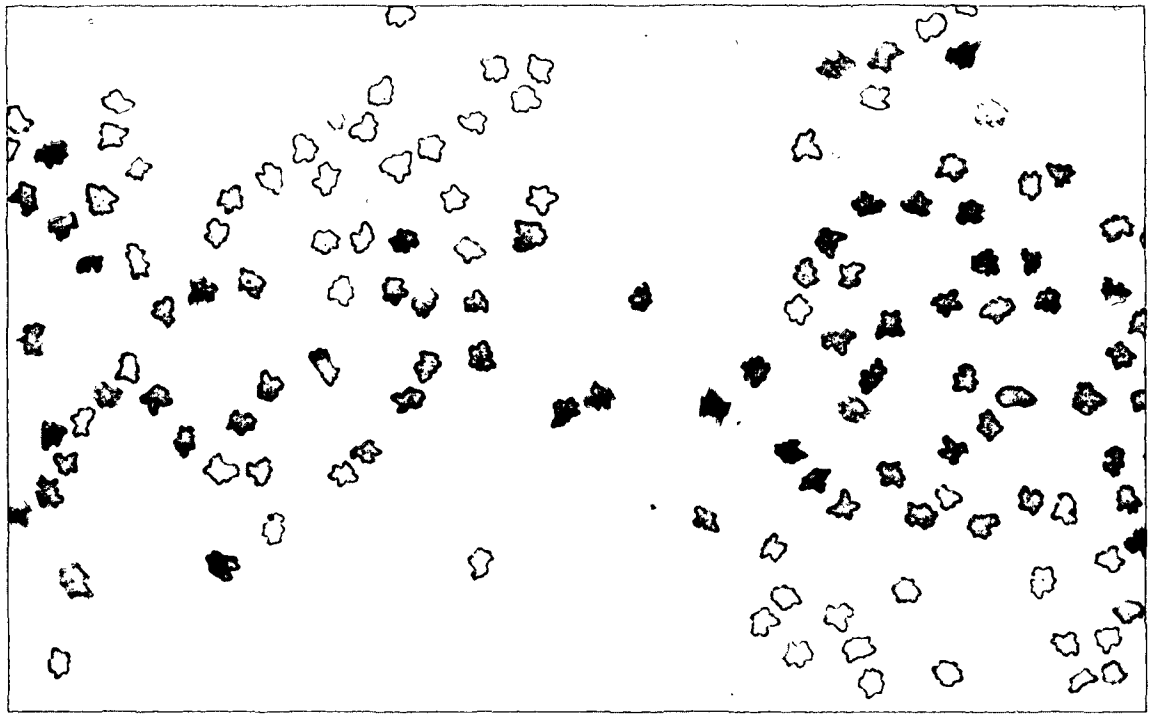

Figure 19. Cross Section View of 3.0-Denier Rayon — Stained Solvent Exchanged — Imbedded in Paraffin — Cleared with Xylene — Mounted in Canada Balsam. 185X

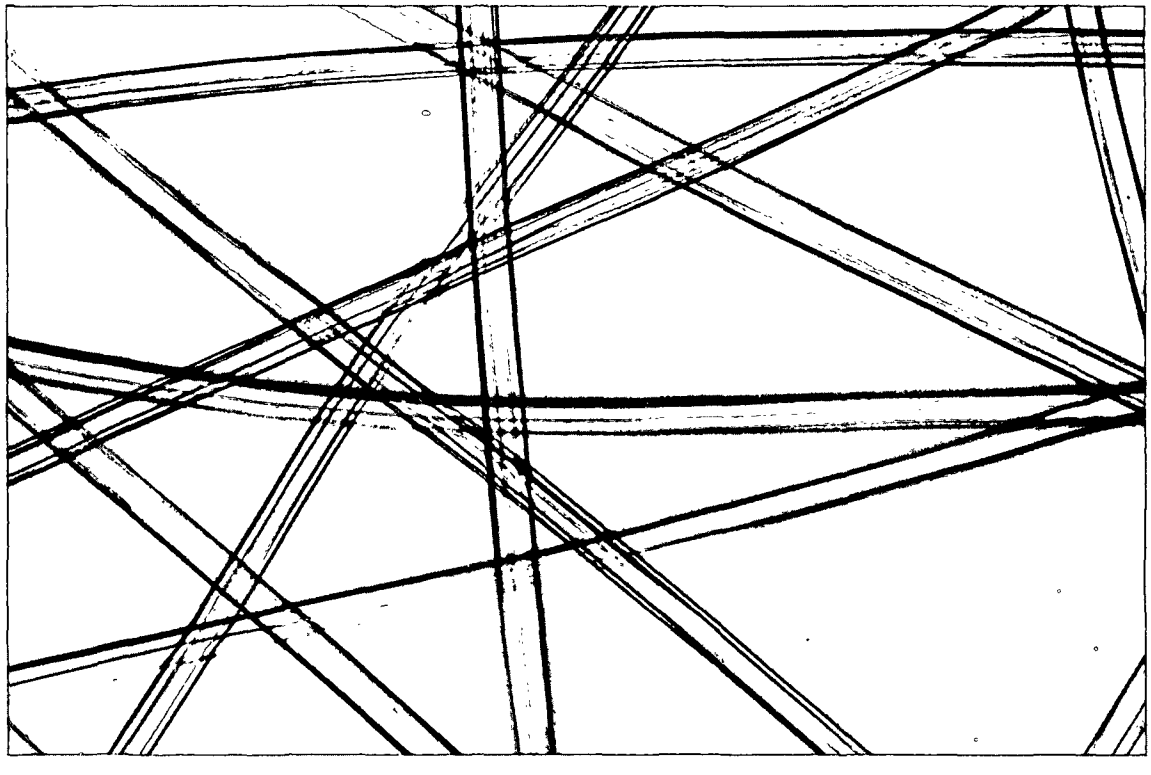

Figure 20. 3.0-Denier Rayon, Water Mount. 185X

with fibers. This was not a serious problem and was performed primarily as a precautionary measure.

There was a lower limit on the level to which the flow rate in the loop could be set and maintained. This was due to fibers accumulating in the flow control valve and causing flow to gradually decrease. The lowest operating level was a function of consistency and increased as the consistency increased.

At high consistencies another problem arose. The suspension could not be well dispersed in the tank at consistencies of approximately 0.30% and higher. This was apparent both from visual observations and from the scatter in the consistency checks at these levels.

The pressure drop-flow rate data are shown in Fig. 21 in the form of log f versus log Re plots.

Velocity Profiles

Velocity profiles for fiber suspension flow were made with the annular-purge impact probe. Procedures were similar to those used for the collection of water profile data. A water-carbon tetrachloride differential manometer was used to measure the difference between impact and static pressure.

There existed a plateau region of pressure differential from which velocity values could be calculated. Above a critical purge water flow rate, the pressure reading suddenly became negative. Below purge rates sufficient to give the plateau readings, the manometer readings were lower. Readings were observed at two different purge rates and then recorded to assure operation in the plateau region.

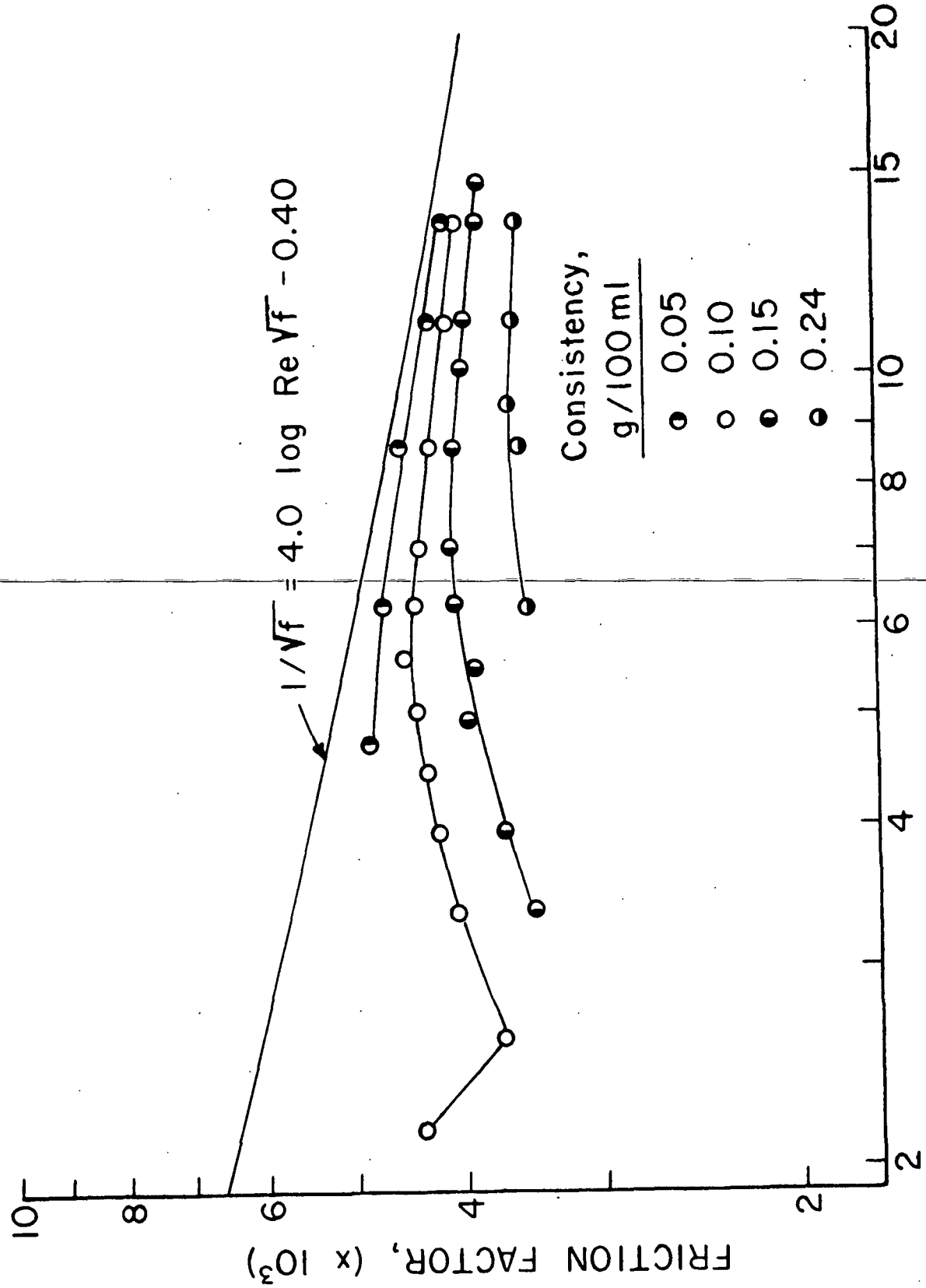

Figure 21. Friction-Factor vs. Reynolds Number for Suspension Flow

Velocity profiles were measured for suspensions having consistencies of 0.05, 0.10, 0.15, and 0.24 g/100 ml and Reynolds numbers of 6.25×10^4, 8.67×10^4, 1.12×10^5, and 1.36×10^5. Figures 22 through 26 show these profiles in dimensionless velocity versus the logarithm of dimensionless position plots. In Fig. 22 through 25 the Reynolds numbers were held constant as noted and consistency was a parameter. Figure 26 shows the effect of increasing Reynolds number at a constant suspension concentration.

LIGHT GUIDE PROBE STUDIES

These studies consisted essentially of two parts. In the first, the light guide probe response with respect to distance and angle using model systems was investigated. In the second part, the probe response to consistency, velocity, and purge rate was studied in a flowing suspension.

Sensing Volume Studies

Fiber optic light guides were used in this thesis study to measure fluctuating light signals caused by consistency variations in a small sensing volume at each probe tip. It is mainly speculation as to what actually occurs around the light guide probe tip in a dynamic situation such as in a flowing suspension stream, but in order to obtain an idea of how far the probe "sees" and to obtain an idea of what the sensing volume of the probe is, a few measurements were made using model systems. Similar studies have been performed by Wahren and coworkers (47) at the Swedish Forest Products Laboratories on a fiber optic light guide having a 1.5-mm tip diameter.

Wahren's group studied the intensity distribution in water of light from the light guide and found that the intensity along the center line decreased with the square of the distance from the probe tip and after 5 mm had decreased

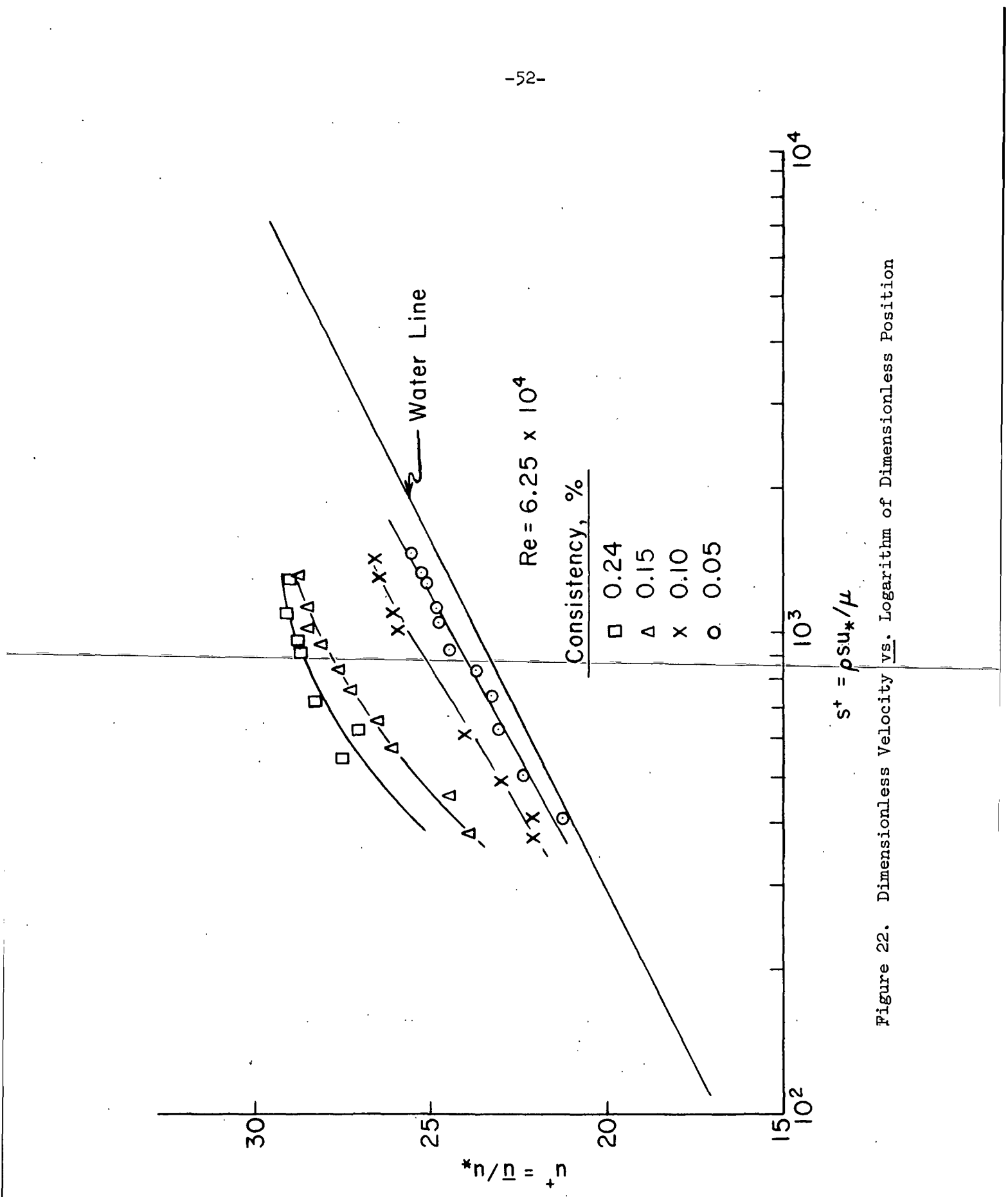

Figure 22. Dimensionless Velocity vs. Logarithm of Dimensionless Position

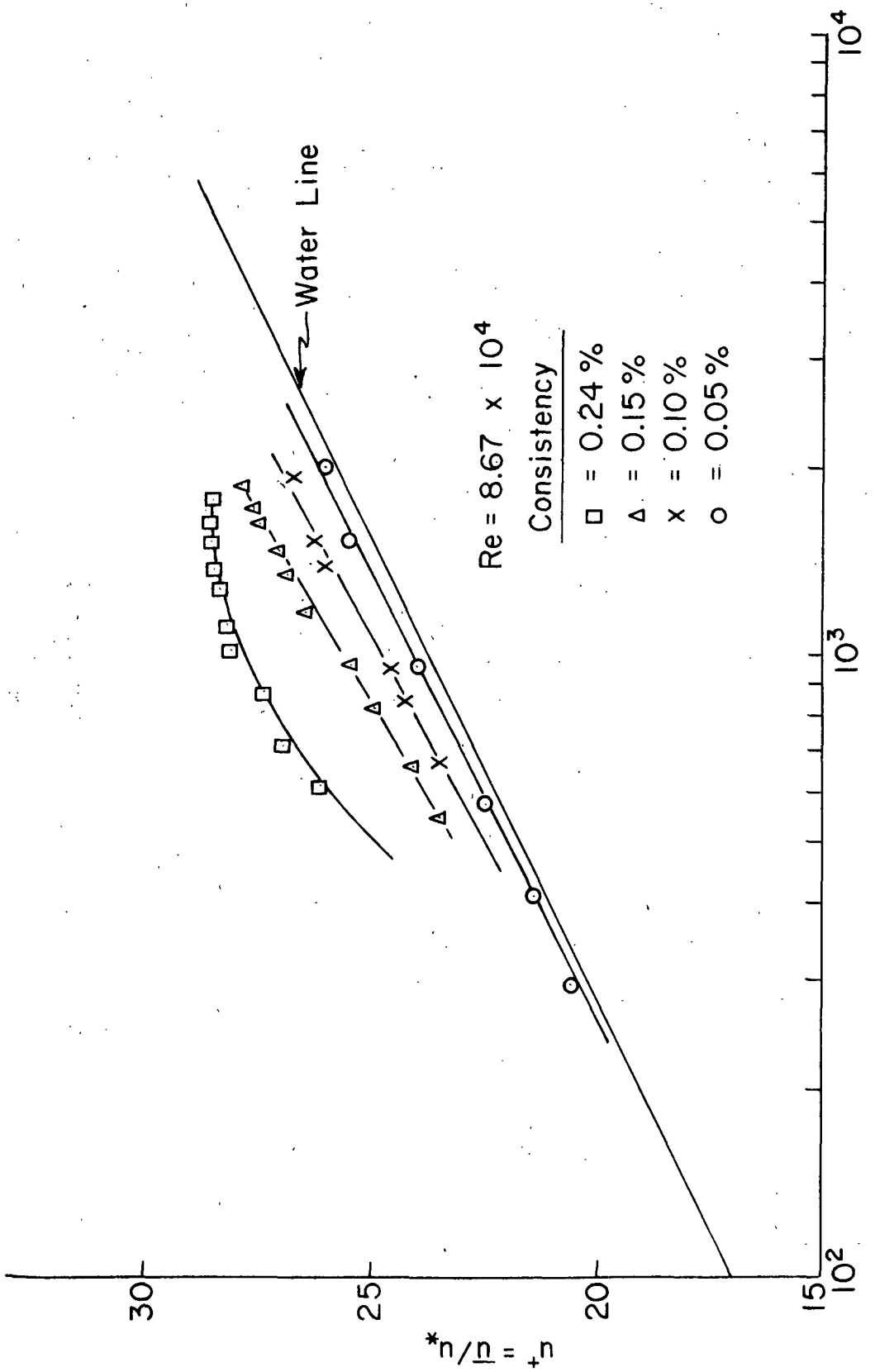

Figure 23. Dimensionless Velocity vs. Logarithm of Dimensionless Position

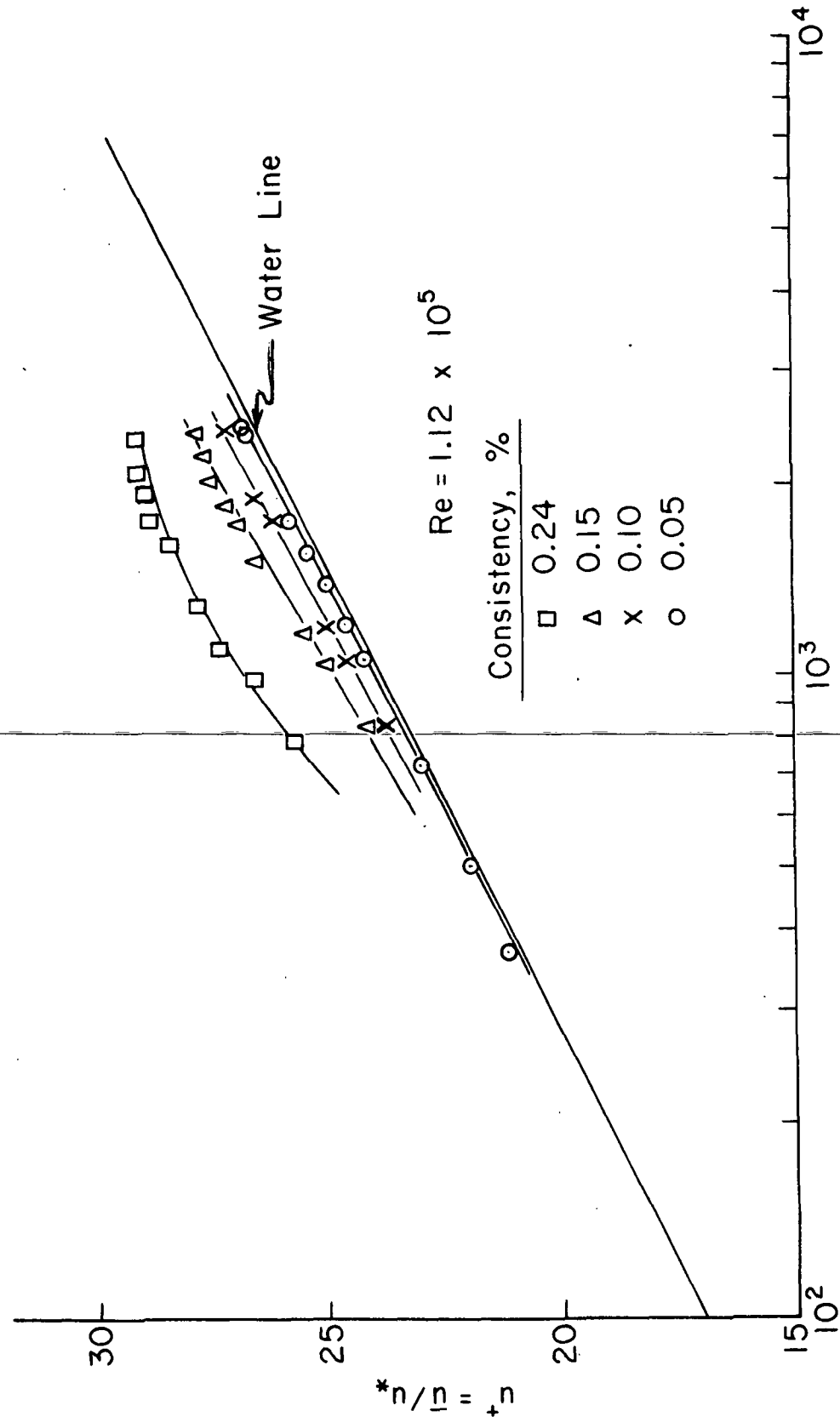

Figure 24. Dimensionless Velocity vs. Logarithm of Dimensionless Position

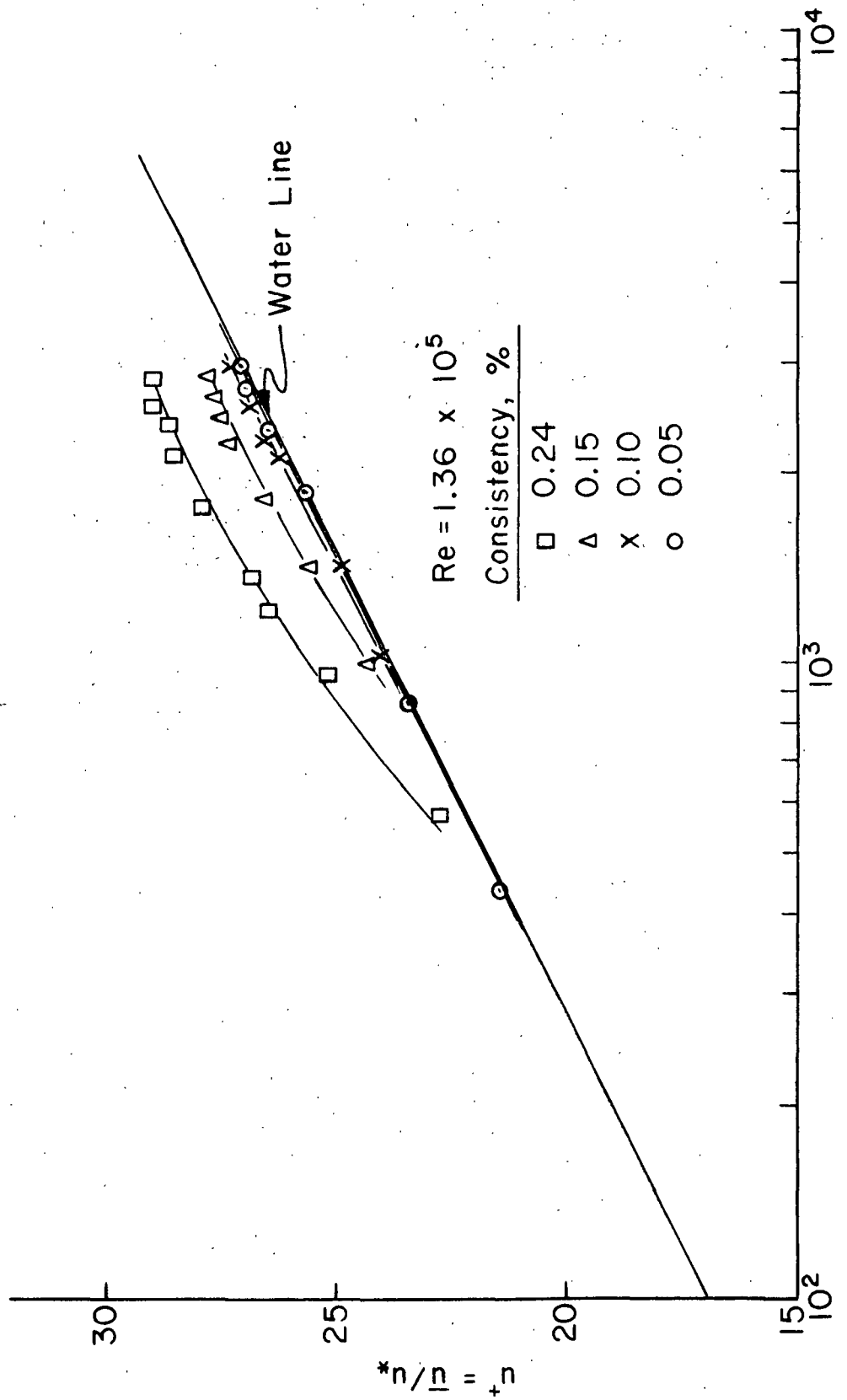

Figure 25. Dimensionless Velocity vs. Logarithm of Dimensionless Position

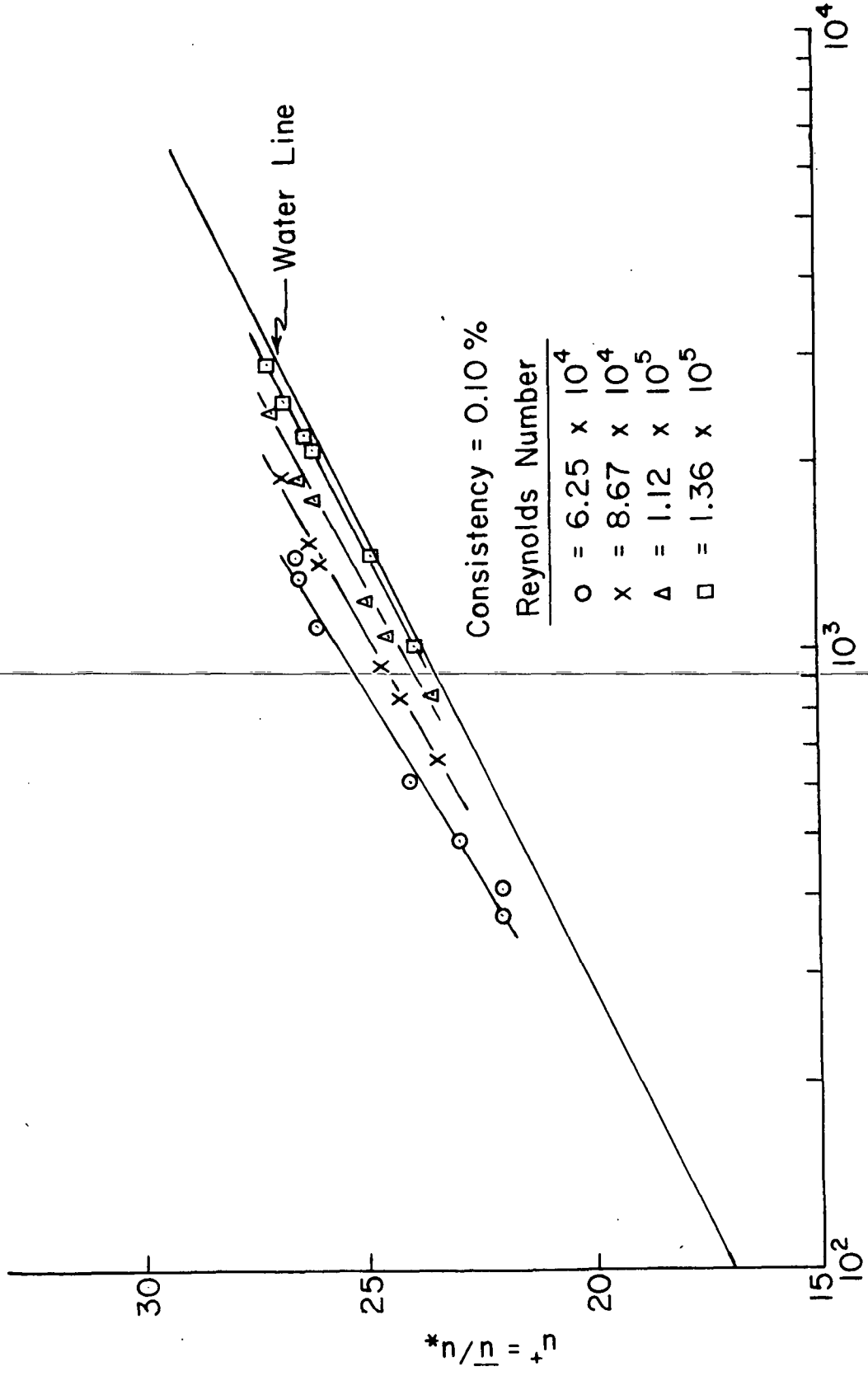

Figure 26. Dimensionless Velocity vs. Logarithm of Dimensionless Position

to 20% of the maximum intensity (intensity at the surface of the probe was equal to 100%). They also reported that the illuminated volume exhibited a pronounced intensity maximum at an angle of 8° from the probe center line, and that most of the light was within an angle of 25° of the center line. This angle may be calculated by use of the different indices of refraction by means of the following formula (48).

$$\sin \phi = (n_1^2 - n_2^2)^{1/2}/n_3. \qquad (14)$$

Here, n_1, n_2, and n_3 are the refractive indices of the core glass, plastic coating, and the surrounding medium, respectively. The angle ϕ is 25° when the surrounding medium is water and about 34° when air is the surrounding medium. This angle is the maximum angle at which total reflection occurs at the boundary between the core glass and the plastic coating (so that light beams reach the other end of the glass fiber with very small light losses). These angles of 25 or 34° suggest a transition regime and not a sharp limit, however, due to unevenness of the fiber surface, etc.

They also studied the reflection from steel balls at different positions in front of the probe tip in a water medium. Using balls of 1-, 2-, and 3-mm diameter, they found that the reflection intensity decreased with distance from the probe. For the 2- and 3-mm balls, the intensity was reported to have decreased to 1% of the maximum reflected light at a distance of 8 mm from the probe tip. It was also found that the sector between +10 and -10° of the probe center line had a dominating influence on reflectance measurements.

The light probe in their studies had the same type glass threads as did the probes in this present study, so the refractive indices of the core glass and the plastic coating were the same. This means that the shape of the

measuring volumes should be the same. No angle dependence measurements were performed in this present study, but based on the diameter of the light spot cast on a surface by light from the light guides at a known separation distance, ϕ was approximately 30°, or close to that calculated by formula.

Studies were performed, however, to measure the intensity of reflected light from both an opal glass surface and from small steel balls. Reflectances from the steel balls were taken with the balls located along the probe center line. The systems and the results obtained for each arrangement are shown in Fig. 27 to 29.

Figure 27 shows the magnitude of a reflected light signal from an opal glass surface for various separation distances, d. A sketch of the experimental setup is included as a part of Fig. 27. The light guide was clamped into a holder and the probe tip directed toward the opal glass surface. One of the two light guide leads went to a lamp and the other lead was connected to the instruments. The clamp holder and opal glass holder were mounted on a common base containing two guide rails upon which the probe holder could be moved toward or away from the glass surface. The separation distance between glass surface and probe tip was then measured. The entire system could be covered with several layers of black cloth, thereby excluding any outside light. This study was performed in an air medium.

Figure 28 presents the data, shown for the covered system of Fig. 27, with the signal on a relative intensity basis. One hundred percent was taken with essentially zero separation between probe tip and glass surface. As can be seen from either Fig. 27 or 28, the signal drops off rapidly with separation distance. The signal has decreased to 50% relative intensity for less than 1-mm separation, and is down to 10% between 2 to 3 mm. At a separation distance of

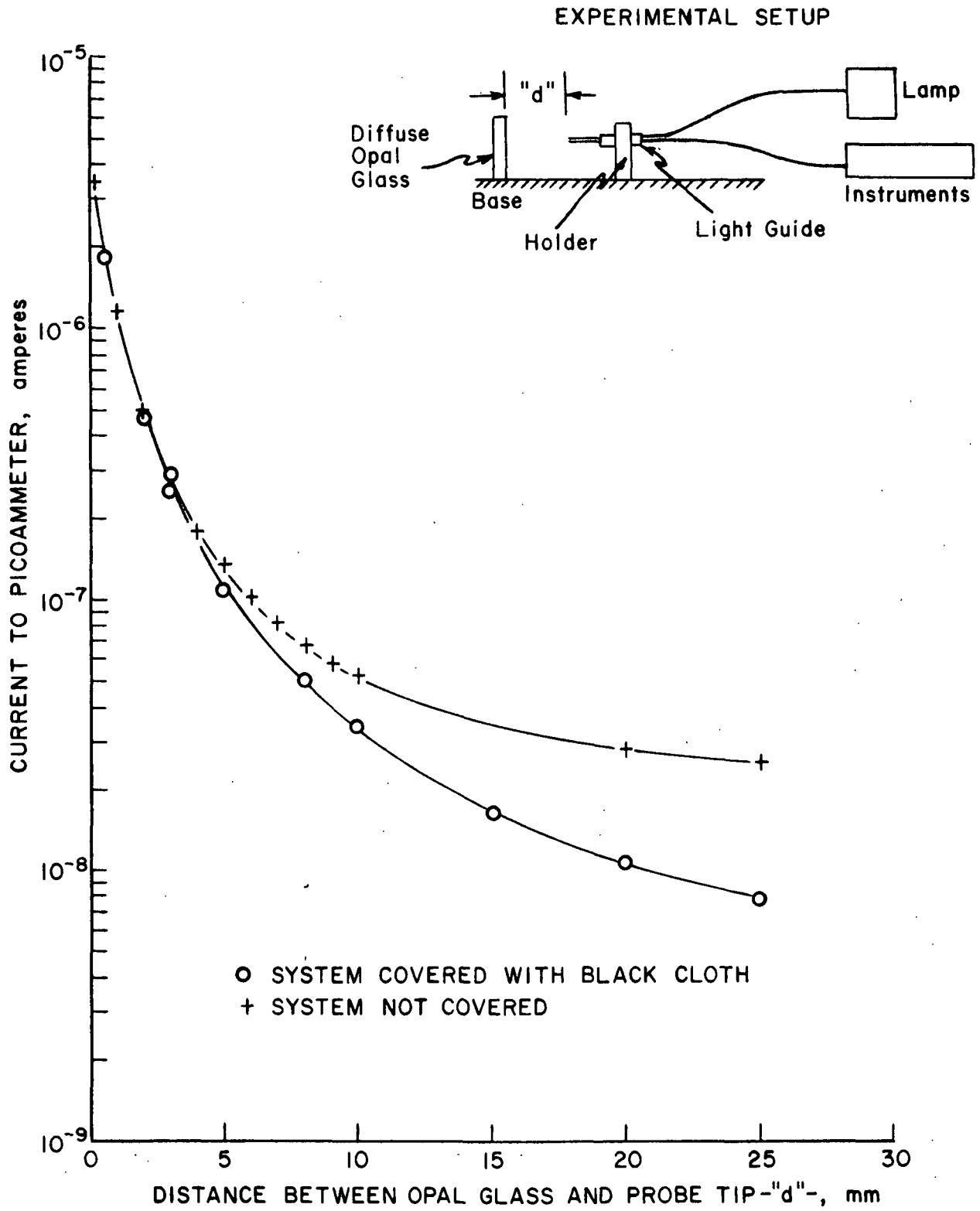

Figure 27. Reflected Light Signal from Opal Glass Surface

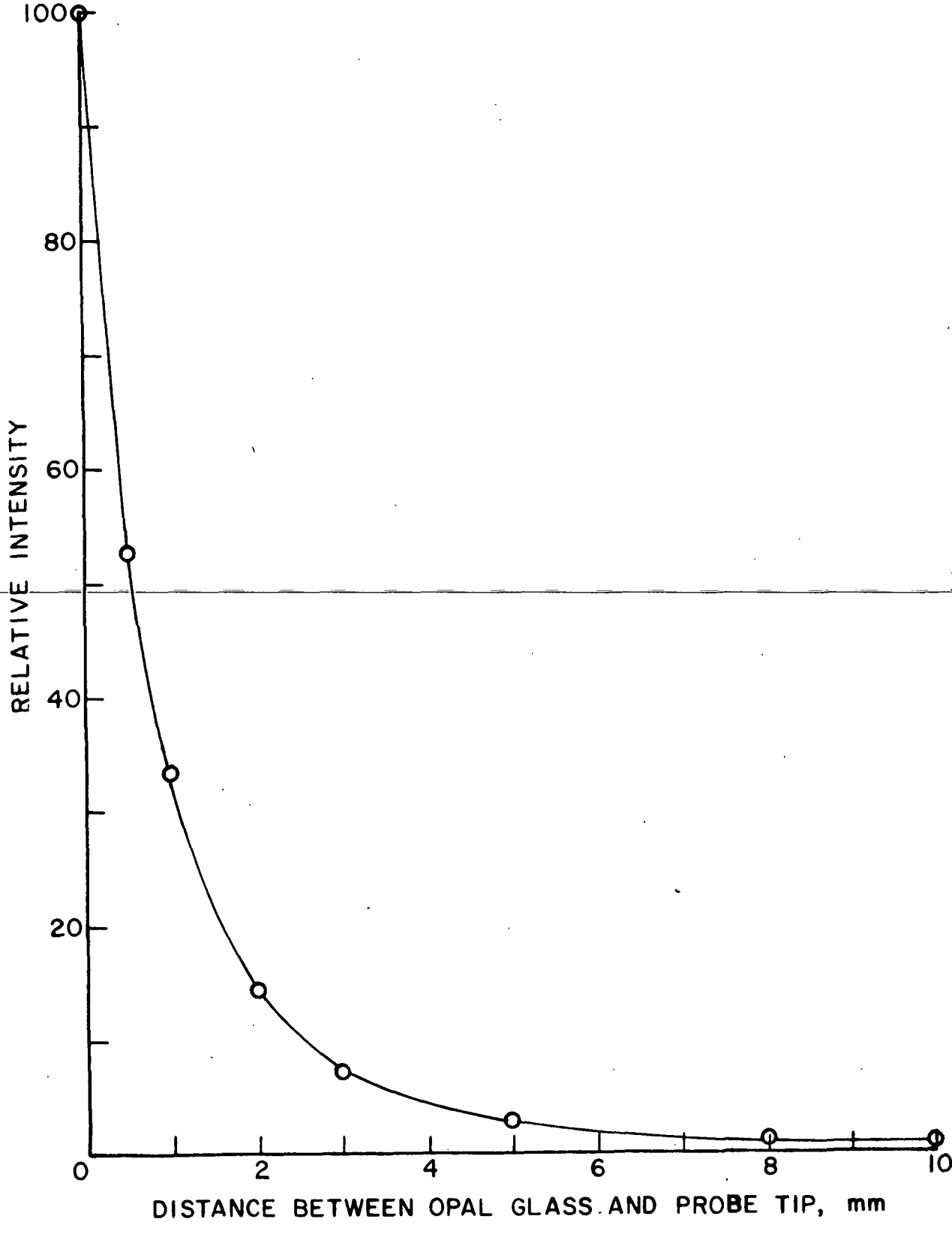

Figure 28. Relative Intensity of Signal vs. Distance (System Covered)

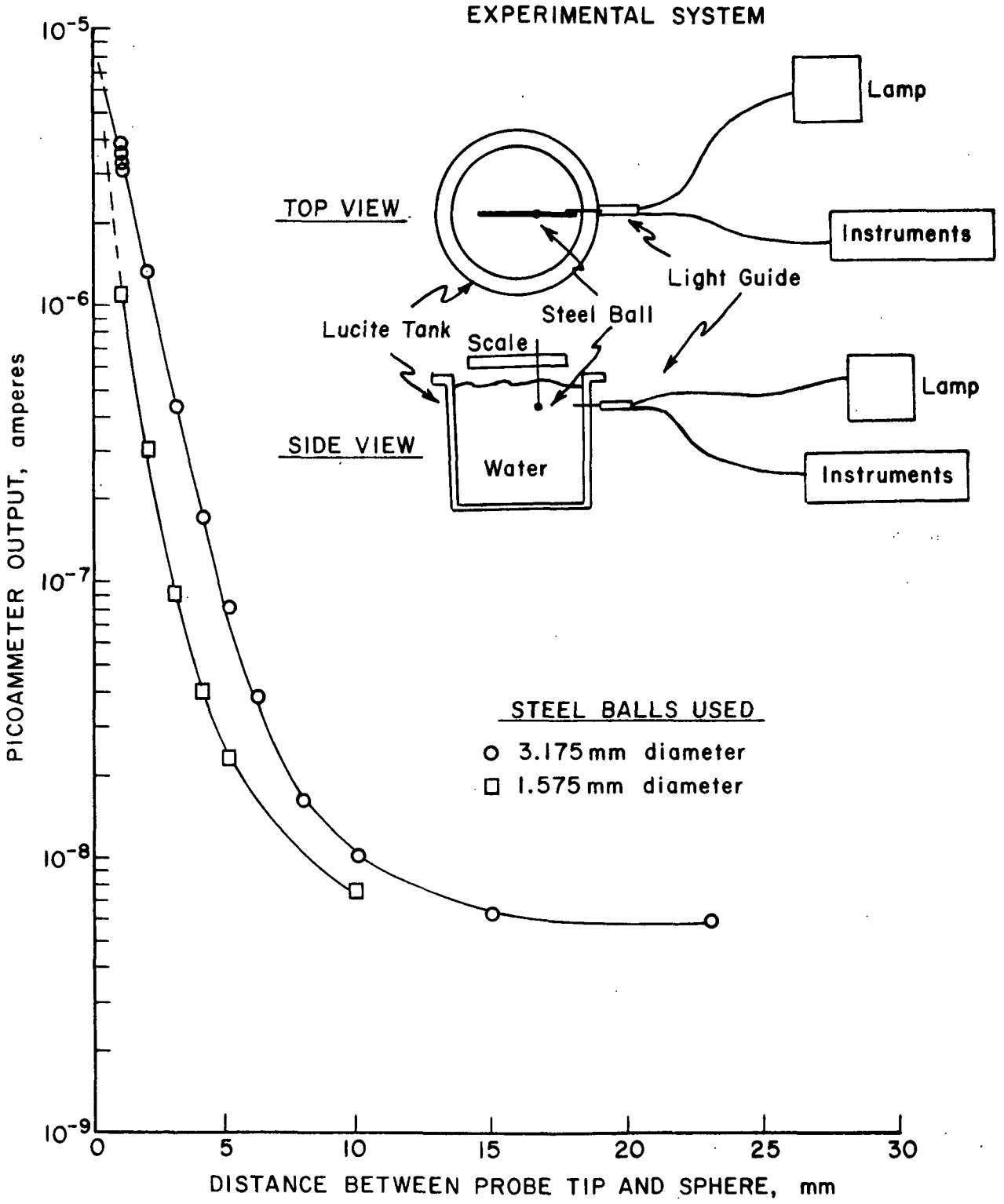

Figure 29. Light Signal-Reflected Light from Steel Balls in Water

10 mm the relative intensity is about 1%. It can also be seen that there is a difference whether the system is covered or not.

Figure 29 shows an experimental setup and the resulting data for the reflected light signal from small steel balls suspended in water. The light guide was mounted in the side of a small (approximately 5-liter capacity) Lucite tank. A sphere was suspended in front of the probe tip and the separation distance measured on a scale. Only reflectances along the probe center line were measured.

The data curves show the intensity of the light signal reflected from the two different size balls (3.175-mm diameter and 1.575-mm diameter) for various separation distances between probe tip and balls. These intensities decrease in a manner similar to those shown in Fig. 27. For the small ball, the intensity has decreased to about 10% of the maximum value at 3 mm whereas it takes 4 mm for the large ball to decrease to the same level.

These trends are quite similar to those reported by the Swedish workers (47). A shorter sensing distance is indicated for the slightly smaller diameter (approximately 1 mm) probe of this present study than for the 1.5-mm diameter probe of the Swedish workers. Based on the experimental results of both studies, a sensing volume of a few cubic millimeters (of the order of 10 mm^3) can be envisioned for the two light guides used here.

Studies of Alternatives to Using Purge Water

Prior to performing the second phase of the study, that is the probe calibration, several studies were undertaken to determine if the light guide probe could be operated without a purge system. The probe was first mounted by itself in the flow loop and observed under suspension flow conditions.

The probe became stapled over almost immediately. The term stapled over is used to denote that state when fibers are folding over the probe tip and resulting in a reflected light signal that is considerably higher than the time-average signal value.

In an attempt to make the probe tip more streamlined and thus possibly avoid stapling, two approaches were tried. The stainless steel casing surrounding the bundle of glass threads (encased in an epoxy matrix) was first beveled to a taper. This did not keep fibers from stapling over the tip. A second approach was to fit small streamlined Lucite lens caps over the probe tip. These also failed to keep the fibers from stapling over the probe tip. These two approaches are depicted in Fig. 30.

Consideration of having the probe electrically charged to repel fibers at the probe tip were abandoned when it was observed that a charged probe (using 12 volts) caused bubbles, probably from electrolysis, to form on the probe.

It was concluded from these studies that a purge water system was needed to operate the probe in a manner free from stapling.

Probe Calibration

The purpose of calibration of the light guides was to determine the relationship between fiber concentration in the sensing volume and the output voltage from the picoammeter. Of particular importance was the determination of the interaction of purge water rate and suspension flow rate, and the effect of purge tube shape on the recorded signal.

A small pipe loop calibration system was suggested by Meyer (49) and utilized in this study and also by Walseth (28). The system represents what

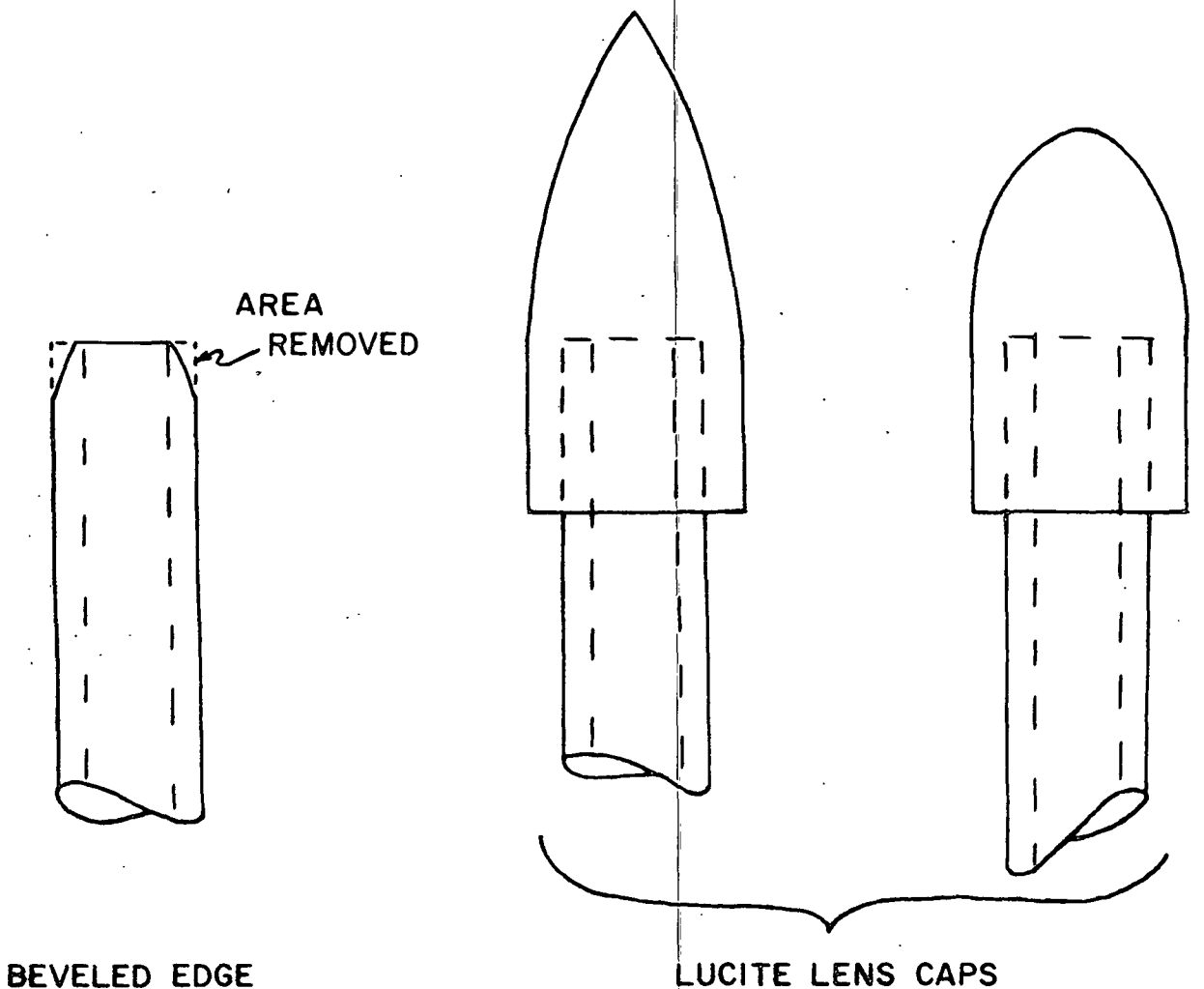

Figure 30. Two Approaches to Streamline Probes to Prevent Stapling

is felt to be a better approach to relating the output signal from an instrument setup to the consistency in the sensing volume of the light guide probe. The small total volume of the system allowed an easy formulation of suspensions of well-defined concentrations and the jet discharge afforded a location to measure reflected light signals from a suspension of uniform velocity and consistency.

Procedure

The light guide to be calibrated was mounted in the nozzle and probe support unit of the calibration loop downleg. The light guide leads were connected to the lamp and photomultiplier, the loop system was filled with water, and the circulation pump was started. While the water was circulating, the instruments were allowed to warm up and, after a period of at least two hours, calibration measurements were started.

A calibration run consisted of recording output signals from the picoammeter for various combinations of consistency, purge water flow rates, and bulk suspension flow rates. During all signal recording, the Lucite mix tank was covered with cloth to exclude ambient light. The zero consistency level was first obtained with water flow only and then the mean system consistency was increased in small increments by adding fiber to the mix tank. After the fibers were well mixed, the different variables were systematically changed and the resulting signal recorded on a strip chart recorder.

Figure 31 shows the effect of changing the flow rate of the suspension in the loop on the consistency signal. For low consistencies there was quite a large plateau extending over a wide range of flow rates. At low flow rates, the signals tended to tail off, however. Operation of the calibration loop at low flow rates was found difficult since the suspension became quite

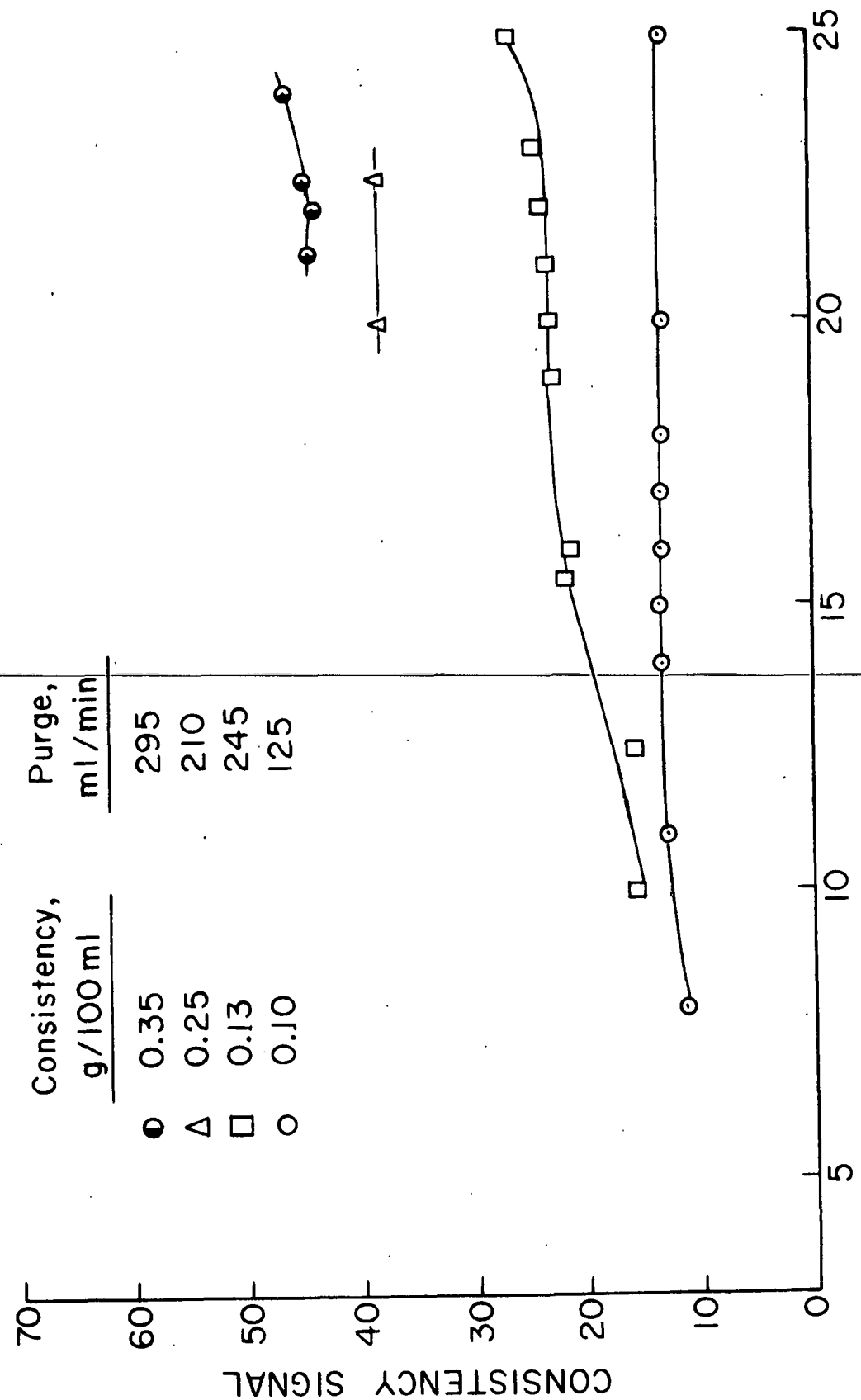

Figure 31. Effect of Flow Rate on Consistency Signal

flocculated and tended to plug the loop. As the consistency was increased, the plateau of constant consistency signal became narrower.

The effect of purge water rate is shown in Fig. 32. It shows the effect for four different suspensions ranging in concentration from 0.05 to 0.40 g/100 ml. For the 0.05 and 0.13 g/100-ml suspensions, there were two distinct plateau regions. For higher consistencies, the lower plateau (corresponding to high purge rates) was replaced by erratic behavior of the signal. It was observed that (for water flow in the flow loop) when dye was added to the purge water stream and an excessive amount of purge water was used, the purge stream danced around in an erratic manner in front of the probe tip. From this it is hypothesized that for lower consistencies this unstable purge pattern makes the distance to the light-reflecting fibers fluctuate whereas at higher consistencies the probe tip becomes stapled and then clears in an erratic sequence.

From these studies it appears that there is a purge water-main stream interaction. A precise description of the interaction is not possible, but it appears that the effect of changing purge rate is more pronounced than changing flow rate on the mean consistency signal. Since measurements in the large flow loop were not made close to the wall (i.e., the region where there is the greatest velocity change), there was not a great change in velocity as the probe was moved from the position closest to the wall to the tube center line. This means that in many cases the purge water rate did not need adjustment to maintain plateau readings. Figure 33 shows that as purge water rate is adjusted to compensate for lower suspension flow rates, a plateau reading of the same consistency level is obtained.

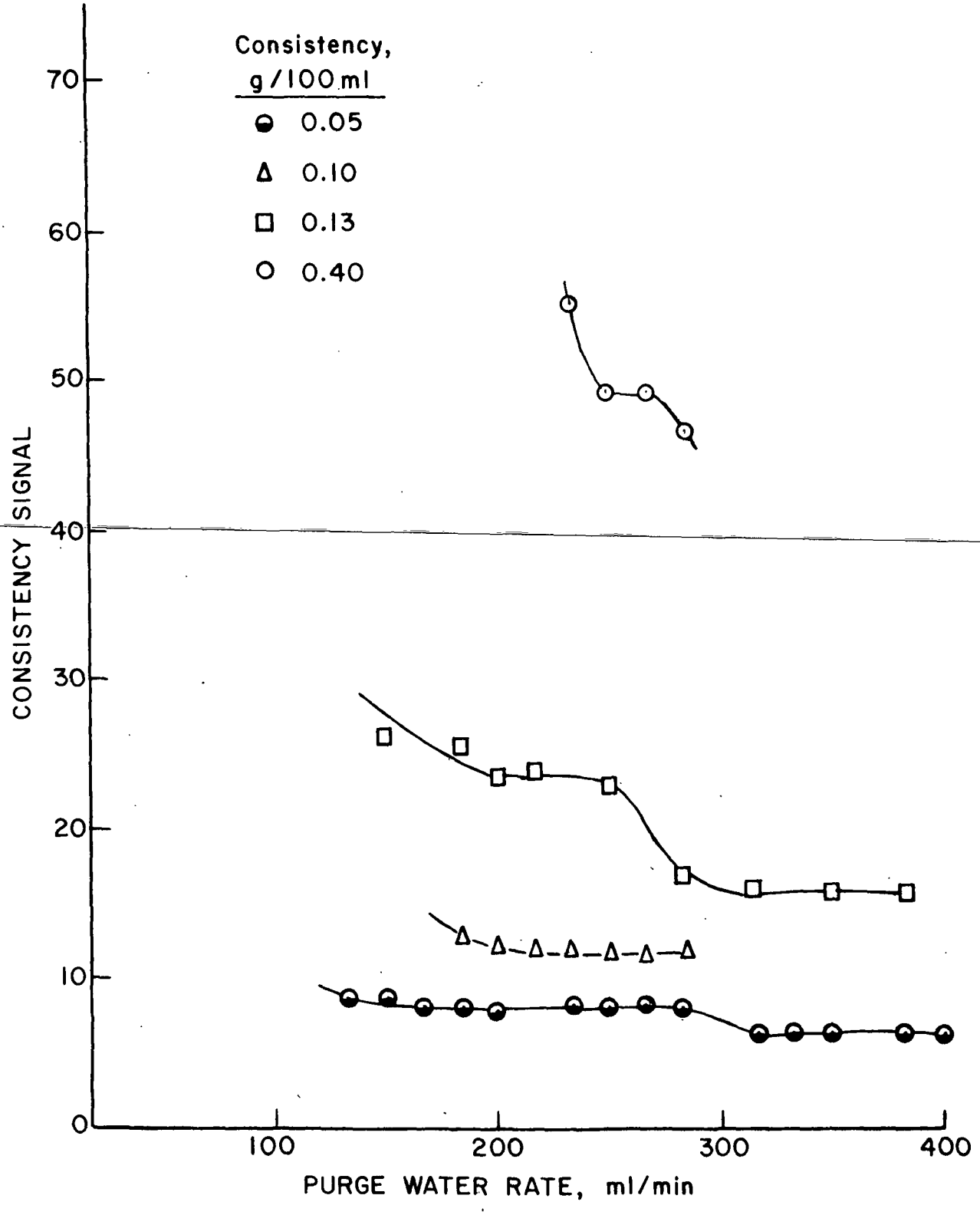

Figure 32. Effect of Purge Water Rate on Consistency Signal

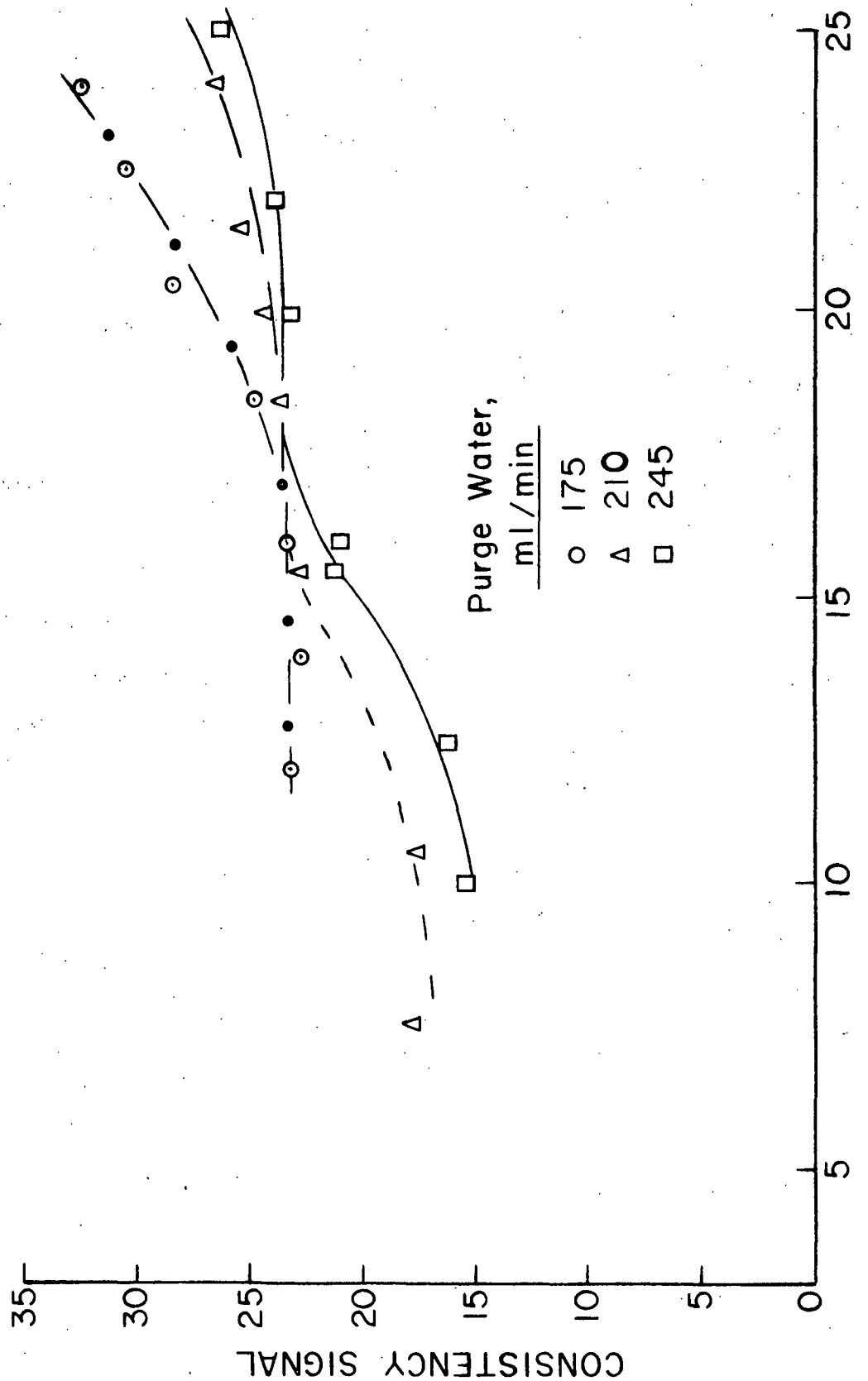

Figure 33. Purge Rate-Main Stream Interaction

Proper operation of the light guide probes required a good deal of operating experience in order to gain familiarity with the interaction between purge rate and main stream velocity. It is felt that the relatively sensitive dependence of the light probe to purge rate and stream velocity is mainly due to the crescent shape of the purge jacket used in this study.

Light guide leads to both the lamp and photomultiplier were positioned so that both the straight and the offset light guides produced signals that could be monitored entirely on the 1-μamp sensitivity scale of the picoammeters when the voltage to the photomultipliers was +710 volts. This geometry was maintained throughout the rest of the experimental work when the light guides were used.

Calibration runs were made with the straight light guide equipped with an annular purge arrangement as well as the crescent-shaped purge depicted in Fig. 8. There was no difference in the correlation between picoammeter output voltage and the mean consistency for the two purge systems.

Discussion

As the suspension was pumped from the mix tank through the loop, a non-uniform consistency distribution probably occurred in the pipe. The nozzle arrangement on the loop discharge was designed to destroy any such profiles by subjecting the flow to a sudden contraction in cross-sectional area.. In addition, the nozzle was sufficiently short to ensure that no developed flow would be attained over its length. Figure 34 shows the discharge of such a jet and velocity profiles that should exist at various points in the jet (50). Within a short distance of the discharge, the velocity distribution is uniform and the consistency distribution should also be uniform (49). The tip of the light guide to be calibrated was positioned within 1/4 inch of the plane of the nozzle discharge.

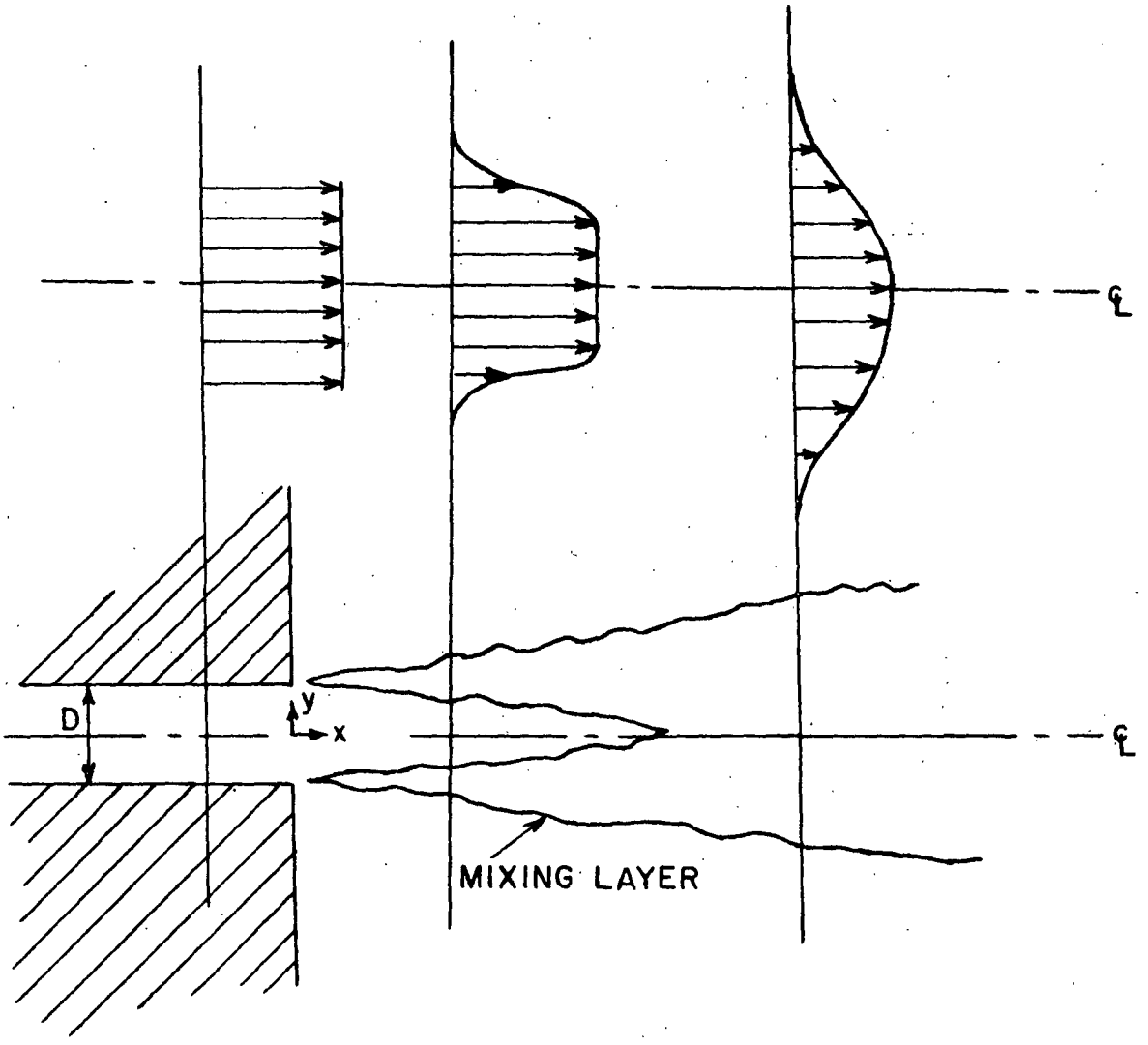

Figure 34. Velocity Profiles at Various Locations in a Plane Turbulent Jet (49)

Under turbulent flow conditions, the instantaneous consistency $\underline{c}$ of a suspension in a small sensing volume can be visualized as consisting of a temporal mean value $\underline{\bar{c}}$ and a fluctuation $\underline{c}'$ about $\underline{\bar{c}}$.

$$c = \bar{c} + c'. \tag{15}$$

The back-reflected light deflected by the light guides would also be fluctuating about a mean value.

The intensity of the reflected light incident on the photomultiplier cathode $\underline{I_c}$ depends on the light intensity at the lamp $\underline{I_l}$ transmission losses in the light guides, optical geometries of the apparatus, and light reflectance of the suspension in the sensing volume.

$$I_c = I_l \cdot \alpha \cdot \gamma. \tag{16}$$

The reflectance factor of the fiber suspension is represented by γ and depends on reflectance, concentration, color, etc., of the fibers. An apparatus factor α embodies all factors connected with the operation of the equipment. Included in α, other than transmission losses, are light guide lead-to-photomultiplier geometry, light guide lead-to-lamp geometry and choice of lead connected to lamp or photomultiplier. Both $\underline{I_l}$ and α were held constant, so that

$$I_c = k_1 \cdot \gamma, \tag{17}$$

where $\underline{k_1}$ is a constant.

A current $\underline{i}$ is produced by the photomultiplier as a result of the light incident on the cathode. This current is amplified by a picoammeter and results in a voltage output $\underline{e}$ from the picoammeter that is recorded on magnetic tape by an analog recorder. The steps are summarized by

$$i = k_2 \cdot \gamma, \tag{18}$$

$$e = k_3 \cdot \gamma, \tag{19}$$

where $\underline{k}_2$ and $\underline{k}_3$ are also proportionality constants. $\underline{I}_c$, $\underline{i}$, and $\underline{e}$ could also be written in a form similar to Equation (15) in terms of a mean and a fluctuating component. If γ is considered to be a function of concentration only (other factors being held constant), the voltage signal can be expressed as

$$e = k_3 \cdot \gamma (c) \tag{20}$$

or

$$e = \bar{e} + e' = k_3 \cdot \gamma (\bar{c} + c'). \tag{21}$$

The voltage signal from the picoammeter was proportional to the fiber consistency in a linear manner, as is shown in Fig. 35 and 36.

A low pass filter ahead of an Esterline Angus strip chart recorder was used to suppress the time-variable fluctuations so that only the time-mean signal was recorded.

FLOCCULATION STUDIES

General

The measurement, recording, and subsequent analysis of fluctuating consistency signals concluded the experimental program. The major change in the vertical pipe loop flow system was the replacement of the Lucite section housing the impact probe with the test section containing the two-branch light guides. The operating procedure for this work was similar to that previously described for the water and fiber flow studies.

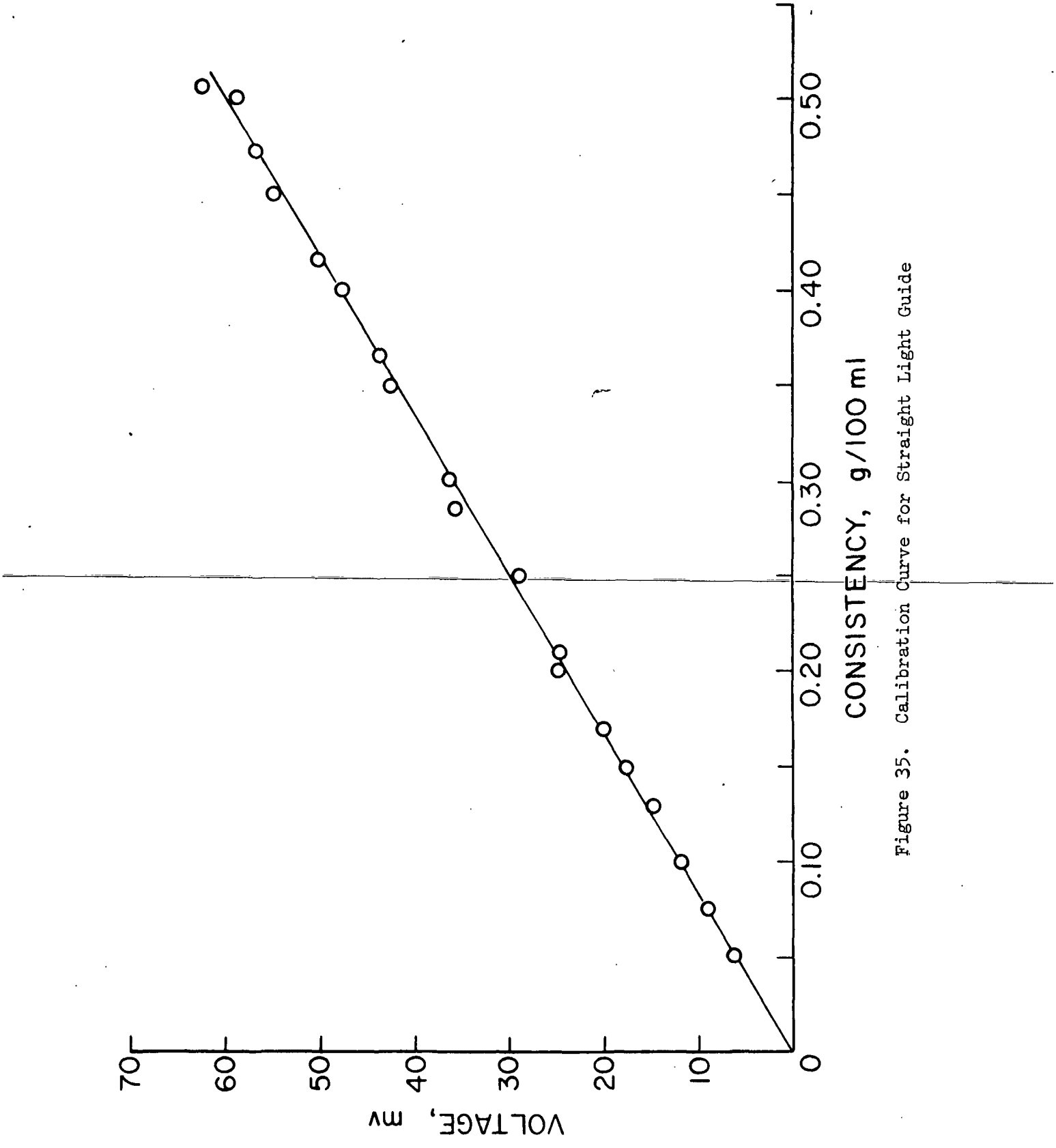

Figure 35. Calibration Curve for Straight Light Guide

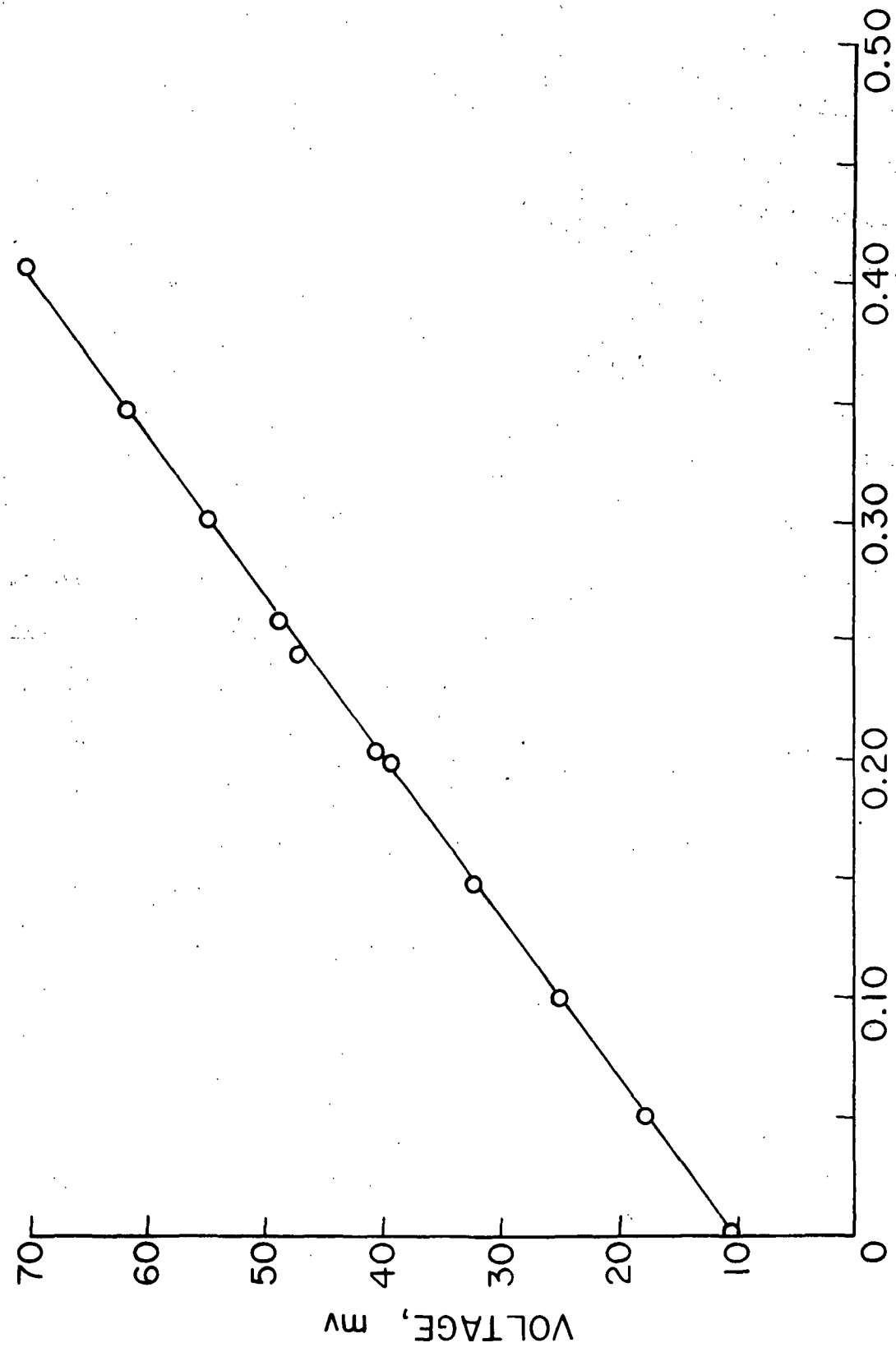

Figure 36. Calibration Curve for Offset Light Guide

The stock tank was filled with deionized-distilled water, heated to reduce the air content and allowed to cool. For starting the system, the loop was filled with water, the pump was started, and as the water circulated around the system, any entrained air was bled off through the air bleed valve at the top of the loop. Fiber was then added to the stock tank, the flow rate and temperatures were adjusted to the desired level, and the suspension was allowed to circulate at least two hours before any measurements were made.

Suspension consistencies were again checked from an average of at least three grab samples taken from the stock tank in the manner previously described. Water samples were also taken periodically and the pH and conductivity of these were determined using a Corning Model 12 pH meter and an Industrial Instruments Model RC-1 Conductivity Bridge in conjunction with a conductance cell (cell constant = 0.11 cm^{-1}). No attempt was made to control these two variables at any particular level. In general, however, pH remained fairly constant at about 7.5 and conductivity generally increased from initial values around 5×10^{-6} $ohm^{-1}cm^{-1}$ when the water was first added to the tank to values of around 5×10^{-5} $ohm^{-1}cm^{-1}$ near the end of a series of runs. Most of the increase occurred before the fibers were added to the water, indicating that the presence of several different materials (copper, brass, stainless steel, etc.) in contact with the water was probably the cause.

When fiber was added to increase the mean consistency to a higher value, the suspension was allowed to circulate for at least half an hour before measurements were again started.

Signal Collection

The light guide leads extending from the Lucite test section were connected to the instruments as shown in Fig. 11. The positions of the probes

inside the flow tube were indicated on metric scales attached to the lead screw assemblies.

While the suspension was circulating, the lamp and other instruments were turned on, set at the desired level and allowed to warm up. The Lucite flow section was wrapped with several layers of black cloth to exclude ambient light. The recording of the consistency signals in a systematic manner was then begun.

For each consistency-flow rate combination, the tube radius was traversed. The primary probe was located at the position closest to the tube wall and the secondary probe positioned adjacent to it (in contact). The fluctuating signals were then recorded for a period of 30 seconds. The secondary probe was then sequentially stepped off from the primary probe until a separation distance of 10 mm between the two probe tips was attained. A minimum of thirty seconds of the two signals was recorded for each step. The primary probe was then moved toward the center line to the next position and the above procedure repeated.

The tips of the light guide probes frequently became stapled over with fibers as evidenced by the needle on the picoammeter being driven up scale or off scale. The problem was most pronounced when the probes were brought close together or near the tube wall. Stapling frequency also increased as the consistency increased or as the flow rate was decreased. At 0.24 g/100-ml consistency and higher it was not possible to bring the two probes close to each other (within 2 to 4 mm) without having both staple over.

Signal Recording

Signals were recorded on a Hewlett-Packard instrumentation recorder at a tape speed of 3 3/4 inches per second (ips). The signals originating from the primary probe (straight light guide) were recorded on Channel 1 and those from the secondary probe (offset light guide) were recorded on Channel 2. An audio-oscillator was used to apply a 400 Hz signal to Channel 3 and a microphone connected to Channel 4 was used to log information regarding the signals on Channels 1 and 2.

Signal recording consisted of 1) connecting all signal sources to the recorder, 2) starting the tape drive, 3) applying the audio-oscillator signal to Channel 3 for 10 seconds, 4) continuing recording on Channels 1 and 2 for a total of at least 30 seconds, 5) letting the tape drive continue to operate for an additional 25 seconds, and 6) stopping the recorder. Each time the light guides were repositioned, Steps 2 through 6 were repeated. The additional 25 seconds of Step 5 were necessary to enable the digitizing of the signal to be performed at an increased rate.

Analog to Digital Conversion of the Data

After the data were recorded in the flow laboratory, the recorder and data tapes were taken to the University of Wisconsin's Data Acquisition and Simulation Laboratory (DASL) in Madison, Wisconsin. There the data were digitized on DASL's hybrid computer facilities consisting of an AD 256 (Applied Dynamic) analog computer interfaced with an XDS 930 (Scientific Data Systems) digital computer.

The data were processed through the converter at a tape recorder tape speed of 15 ips. This accelerated signal was sampled every 600 μm-seconds during a period of 7.2 seconds. This translated to 12,000 digital points

representing 28.8 seconds (real time) of analog data. These 12,000 point data sets were written on 1/2-inch wide computer tape in 7-track form by the XDS 930 at a packing of 200 characters per inch. The data had to be rewritten in 9-track form at a density of 800 characters per inch in order to be compatible with The Institute of Paper Chemistry's IBM 360 (IBM Corporation) digital computer. The rewriting was performed on the Madison Academic Computer Center's (MACC) Univac 1110 (Sperry Rand Corporation, Univac Division) computer and the data tapes were mailed to the Institute.

Each data set on the 9-track tape consisted of two 6004 word (24-bit words) records. Each record consisted of four 24-bit identification words at the beginning followed by 6000 pairs of 12-bit words representing the data from Channels 1 and 2 of the initially recorded data tapes.

Computer Analysis

The data were analyzed on the Institute's IBM 360 computer using a Biomedical Computer Program — BMD02T (51) from the University of California at Los Angeles. No filtering or prewhitening of the data was performed. Prior to analyzing the data with BMD02T, the data (in the form received from Madison) were rewritten to two separate tapes; one for Channel 1 data and the other for Channel 2 data. Program BMD02T, in a revised form, and the program to rewrite the data to the two tapes are included in Appendix IV.

Autocorrelation: $\underline{R}_{\underline{z}}$

As mentioned earlier, the probe tip underwent occasional fiber stapling. This could be detected by dividing the entire signal, measured for a particular set of conditions, into several intervals and calculating time-averages for each. Intervals with stapling were characterized by a much higher average than

those without. It was observed that the time-average over each interval was very close to the time-average for the entire signal for cases where no stapling occurred. For signals with periods of stapling, the same could be said if the higher average intervals were dismissed.

For conditions where only minor stapling occurred, sufficient time periods of the fluctuating signals were available to determine autocorrelation functions R_z. These functions could also be calculated over short time intervals, and it was observed that, as in the case of mean values, the autocorrelations for the various intervals were in good agreement. Representative autocorrelation curves are presented in Fig. 37-40.

The curves obtained for this study did not asymptotically approach zero as do theoretical autocorrelation functions (43). They decreased from $R_z = 1.0$ toward $R_z = 0$, but exhibited fluctuations about the time lag axis ($R_z = 0$). Negative values, however, were never greater than 0.1 in absolute value. It is not altogether clear why these curves deviate from theoretical ones. The deviation may arise from working with a system which is neither homogeneous nor isotropic or from noise or from both. Similar fluctuations have been noted for autocorrelation curves in other investigations (24,52-54).

In a study of sheet formation using autocorrelation techniques (54), similar fluctuations were attributed to wire marks. It was suggested (49) that the stock pump may have caused the fluctuations in this study by its pumping action.

For calculating values of the flocculation scales L_z, the positive area under the autocorrelation curve, from the origin to where R_z first crossed the time lag axis, was used. Areas for several curves were determined by three methods:

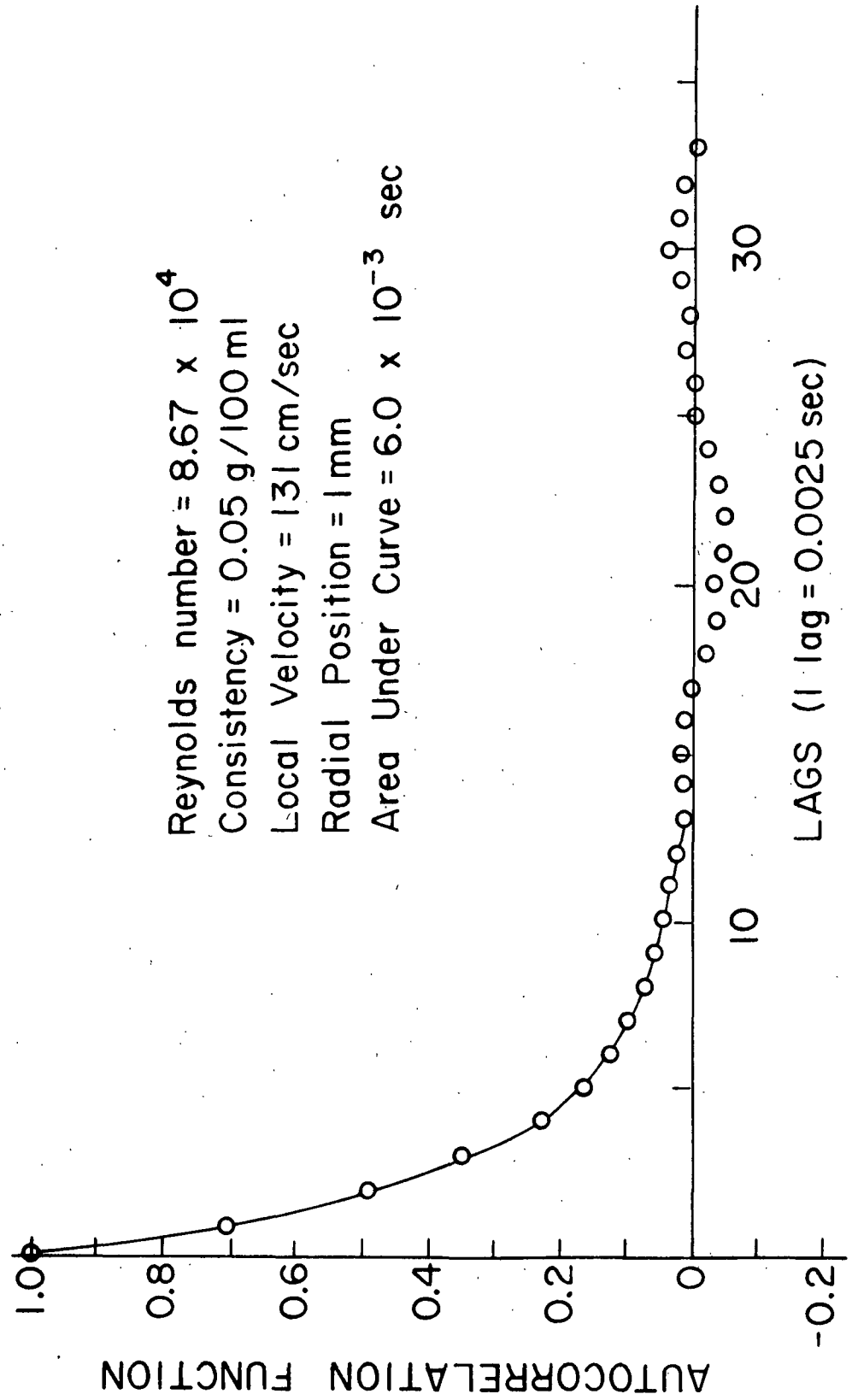

Figure 37. Autocorrelation Function vs. Time Lag

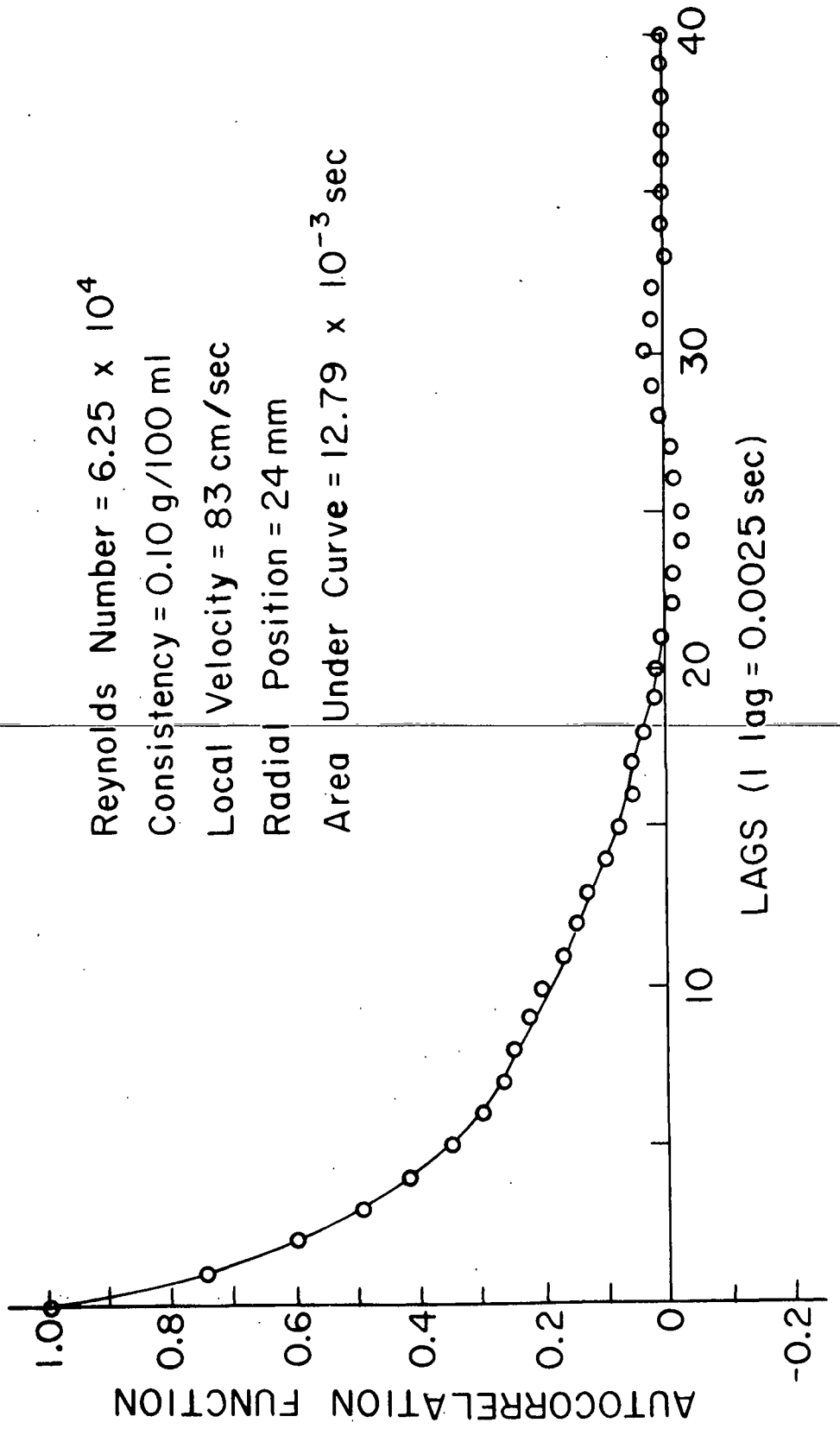

Figure 38. Autocorrelation Function vs. Time Lag

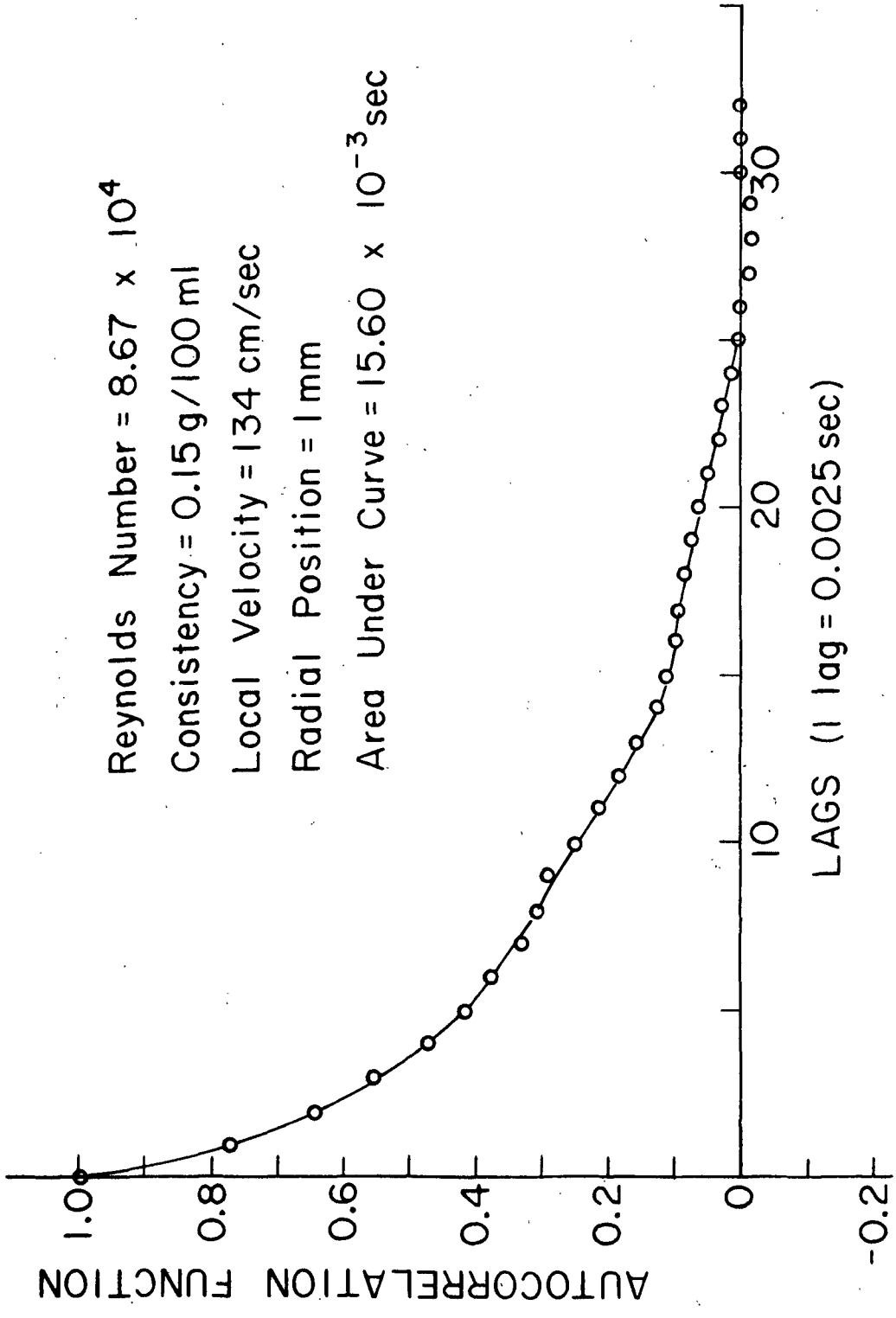

Figure 39. Autocorrelation Function vs. Time Lag

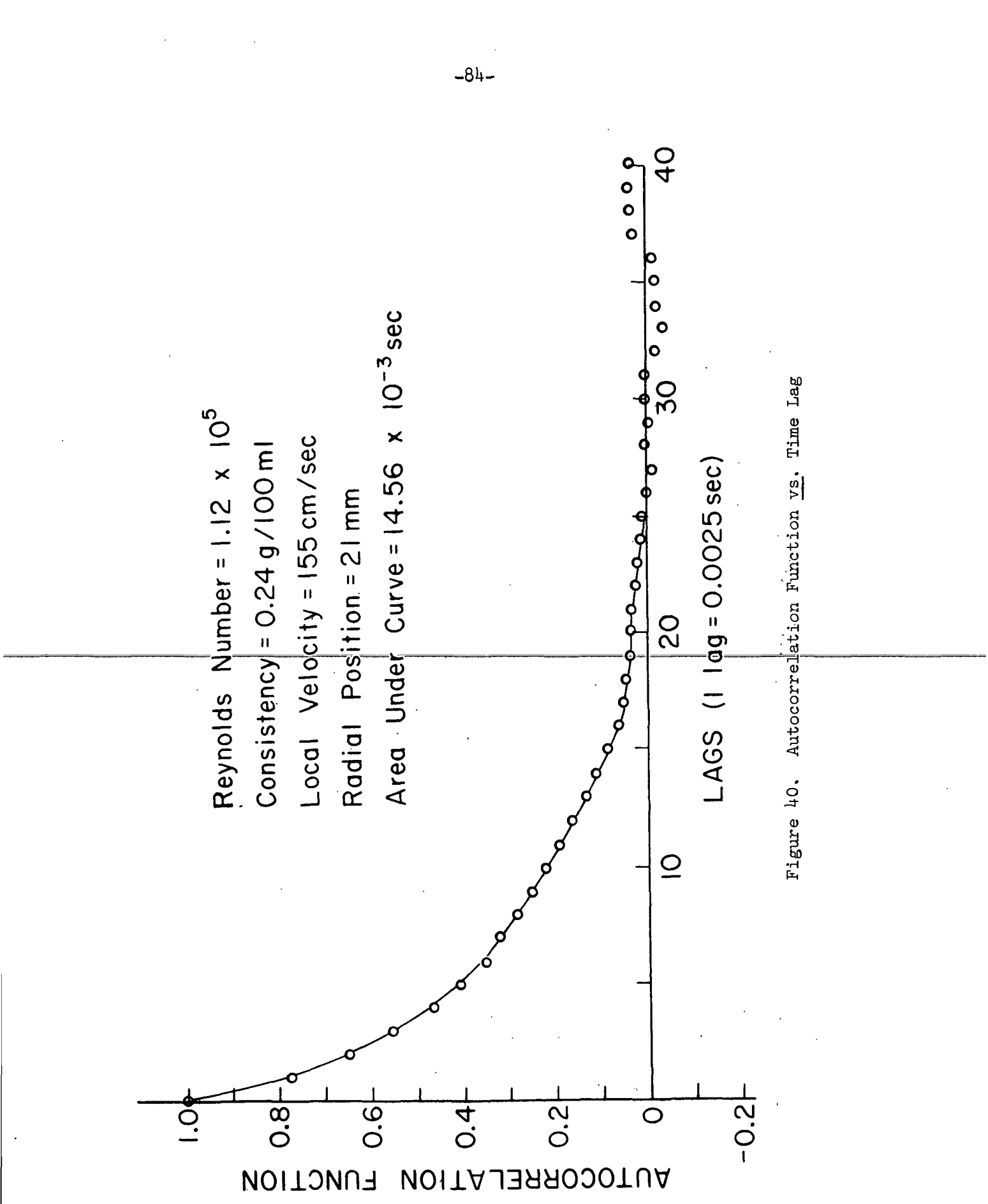

Figure 40. Autocorrelation Function vs. Time Lag

1. average of at least three planimeter traces over a smooth curve fit of the data,
2. average of at least three planimeter traces over actual point to point fit of the data, and
3. numerical integration (trapazoidal method) using a computer.

There was very good agreement among the three methods, so the computer was used to determine areas by numerical integration. In addition, integration of several of the curves up to the first zero crossing was compared to integration performed up to 200 time lags (over several fluctuations). A good agreement between the two integrations indicated that the positive and negative portions of the fluctuations tend to cancel over extended lag times.

Table II is a summary of the autocorrelation and longitudinal scale data. In addition to average values of $\underline{L}_{\underline{z}}$ and the areas from which they were calculated, values for average consistencies, Reynolds numbers, radial positions, and local velocities are included. Additional autocorrelation curves and data are presented in Appendix III.

Crosscorrelation: $\underline{R}_{\underline{r}}$

Studies involving crosscorrelation analyses of the signals from the two probes did, unfortunately, not produce results that could be translated into average radial floc dimensions. In general, the correlations were not reproducible so that no unique connection could be observed for any simultaneous pair of signals.

Although there were no typical forms of the crosscorrelations, the two shown in Fig. 41 may be used to illustrate the type of behavior observed.

TABLE II

SUMMARY OF LONGITUDINAL SCALE DATA

$\bar{c}$, g/100 ml	$\overline{Re}$, ($\times 10^{-4}$)	r, cm	$\bar{u}$, cm/sec	A, sec ($\times 10^{3}$)	L_z, mm
0.05	6.25	0.1	95	8.5	8.1
		0.9	94	7.8	7.3
		1.8	86	7.0	6.0
		2.6	79	6.9	5.4
	8.67	0.1	131	5.6	7.3
		0.9	129	5.0	6.5
		1.8	122	4.9	6.0
		2.6	111	4.0	4.5
	11.20	0.1	169	3.7	6.2
		0.9	165	3.5	5.6
		1.8	156	--	--
		2.6	145	3.3	4.8
	13.60	0.6	204	2.4	4.8
		1.1	200	2.0	4.0
		1.6	193	2.0	3.9
		2.1	184	2.0	3.6
		2.6	174	1.9	3.2
0.10	6.25	0.1	98	14.3	14.0
		0.9	97	12.9	13.0
		1.8	91	12.1	11.2
		2.4	83	12.5	10.6
	8.67	0.1	98	14.3	14.0
		0.9	97	12.9	13.0
		1.8	91	12.1	11.2
		2.4	83	12.5	10.6
	11.20	0.1	169	4.9	8.2
		0.9	168	4.7	7.9
		1.8	161	4.8	7.7
		2.6	143	4.8	5.9
	13.60	0.1	207	3.3	6.9
		0.9	202	2.9	5.8
		1.8	191	3.0	5.7
		2.6	174	3.0	5.2

TABLE II (Continued)

SUMMARY OF LONGITUDINAL SCALE DATA

$\bar{c}$, g/100 ml	$\overline{Re}$, ($\times 10^{-4}$)	r, cm	$\bar{u}$, cm/sec	A, sec ($\times 10^{3}$)	L_z, mm
0.15	8.67	0.1	134	15.2	20.4
		0.9	132	14.5	19.2
		1.8	123	14.2	17.4
		2.6	114	11.0	12.6
	11.20	0.1	171	--	--
		0.9	167	7.5	12.6
		1.8	157	7.6	12.0
		2.6	145	6.5	9.5
	13.60	0.1	206	5.5	11.3
		0.9	203	4.6	9.3
		1.8	194	4.7	9.1
		2.6	180	4.3	7.6
0.24	11.20	0.1	171	14.3	24.4
		0.6	170	12.9	22.0
		1.1	167	15.3	25.6
		1.6	163	13.8	23.6
		2.1	155	13.7	21.2
		2.6	145	10.6	15.4
	13.60	0.1	207	6.7	14.0
		0.6	205	6.1	12.5
		1.1	203	6.9	14.0
		1.6	198	7.1	14.0
		2.1	189	7.1	13.5
		2.6	176	8.8	15.3

Both curves are for the same flow rate, consistency, purge rates, and probe positions. The only difference between the two is that they were calculated over different intervals of the recorded signal. Correlations from other intervals produced different curves. The crosscorrelation curves exhibited fluctuations or oscillations from relatively high R_r values to relatively high (absolute value) negative values in a nonreproducible manner. The location of the first zero crossing ($R_r = 0$) was also not reproducible.

Typical for limited capacity digital equipm.

If not accurate, Fig 41 certainly is interesting and interpretable. If sampling lag = 2-5 ms and speed 137 cm/s only 1 sample/3-4 mm ! longitudinally ! Insufficient info.

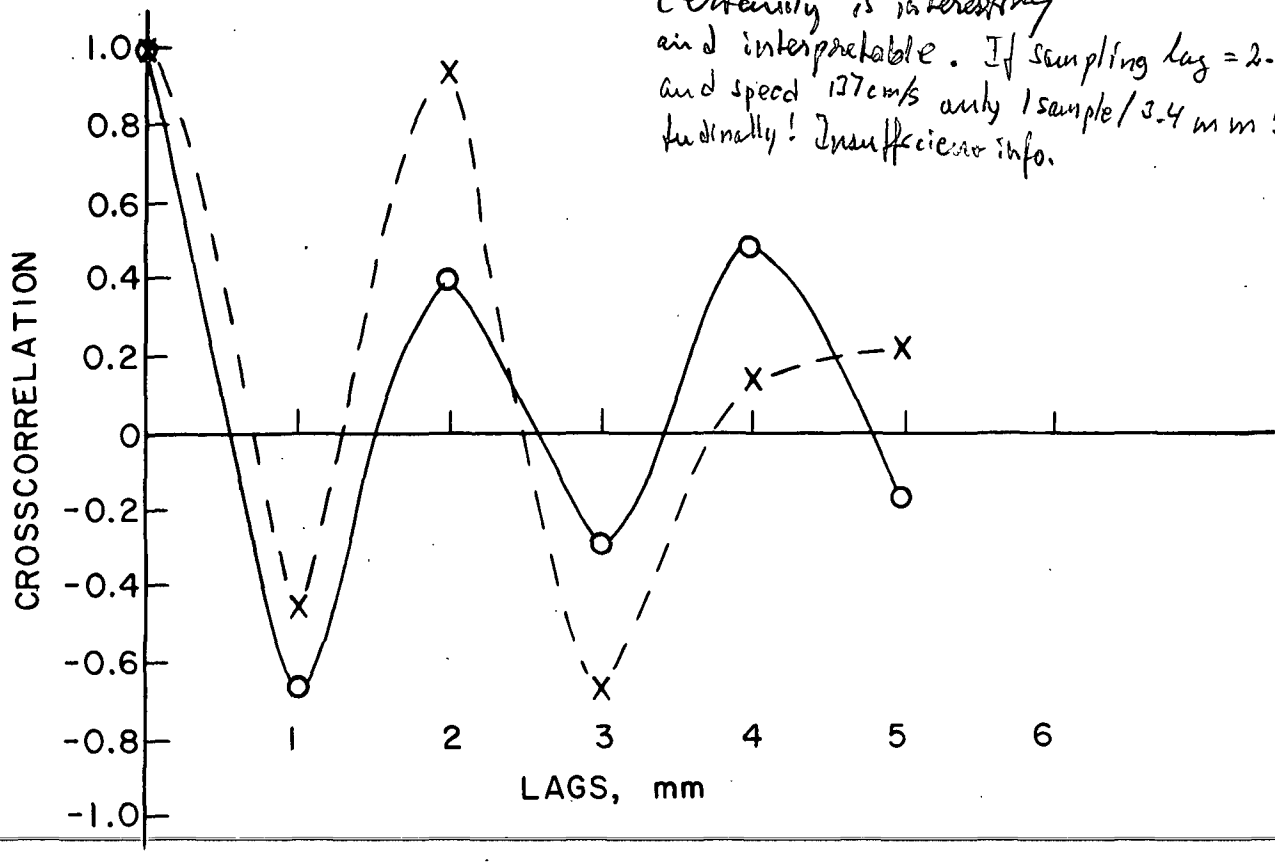

Figure 41. Crosscorrelation Curves

The above described behavior was intrinsic in all the crosscorrelation data that could be analyzed in this manner. As the consistency of the suspension was increased, fiber stapling became more frequent and it was thus harder to obtain pairs of signals to crosscorrelate at high consistencies. At 0.24 g/100 ml the stapling was so severe that the probes could not be brought closer together than 3 to 4 mm without complete stapling of both probes.

Consistency Distribution

Time-mean consistency information was calculated from the data by time-averaging the fluctuating signals. Periods including fiber stapling over the probe tips were treated as described earlier. The results are presented, in part, in Fig. 42 through 45.

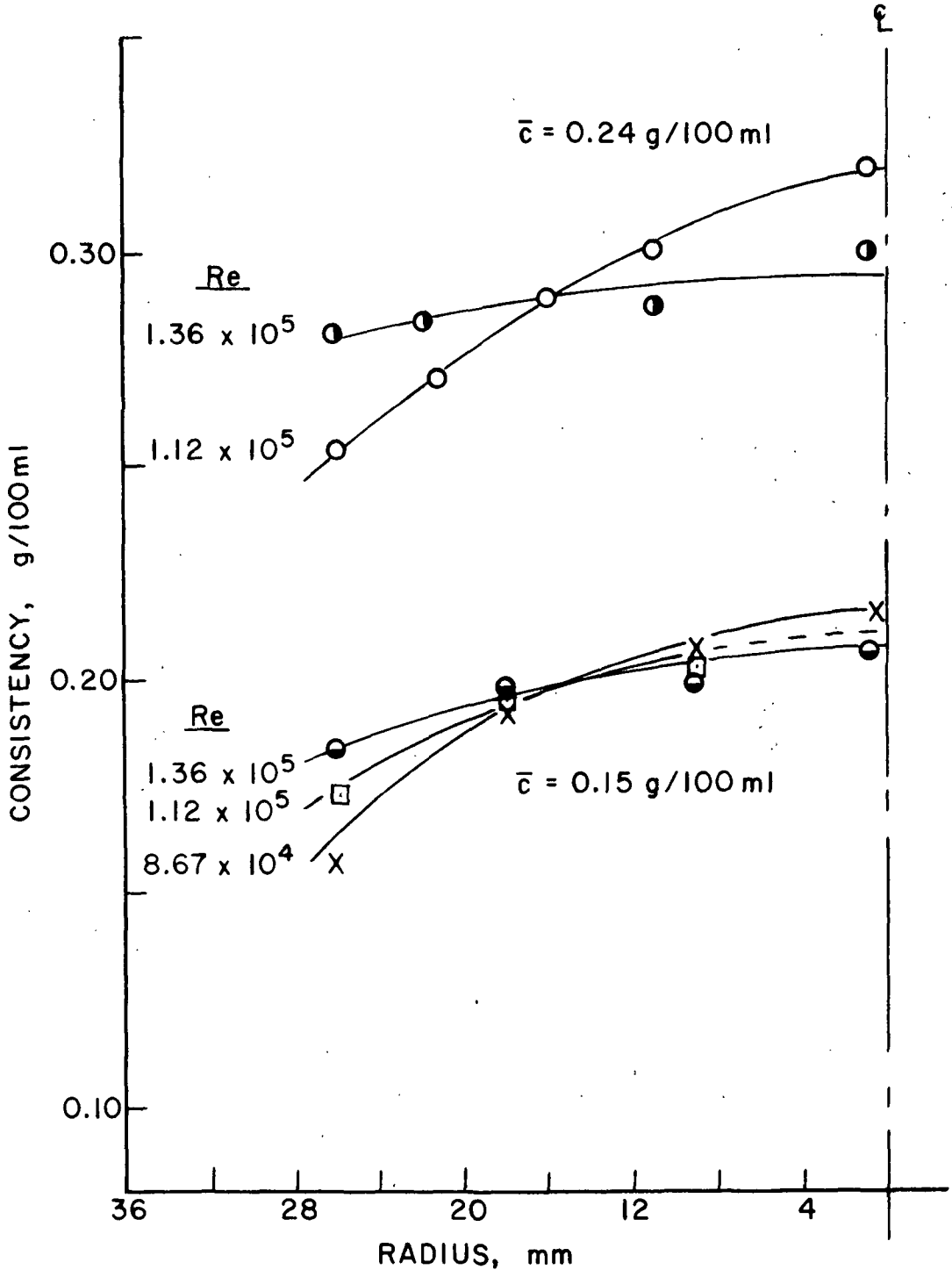

Figure 42. Representative Twice-Average Consistency Profiles

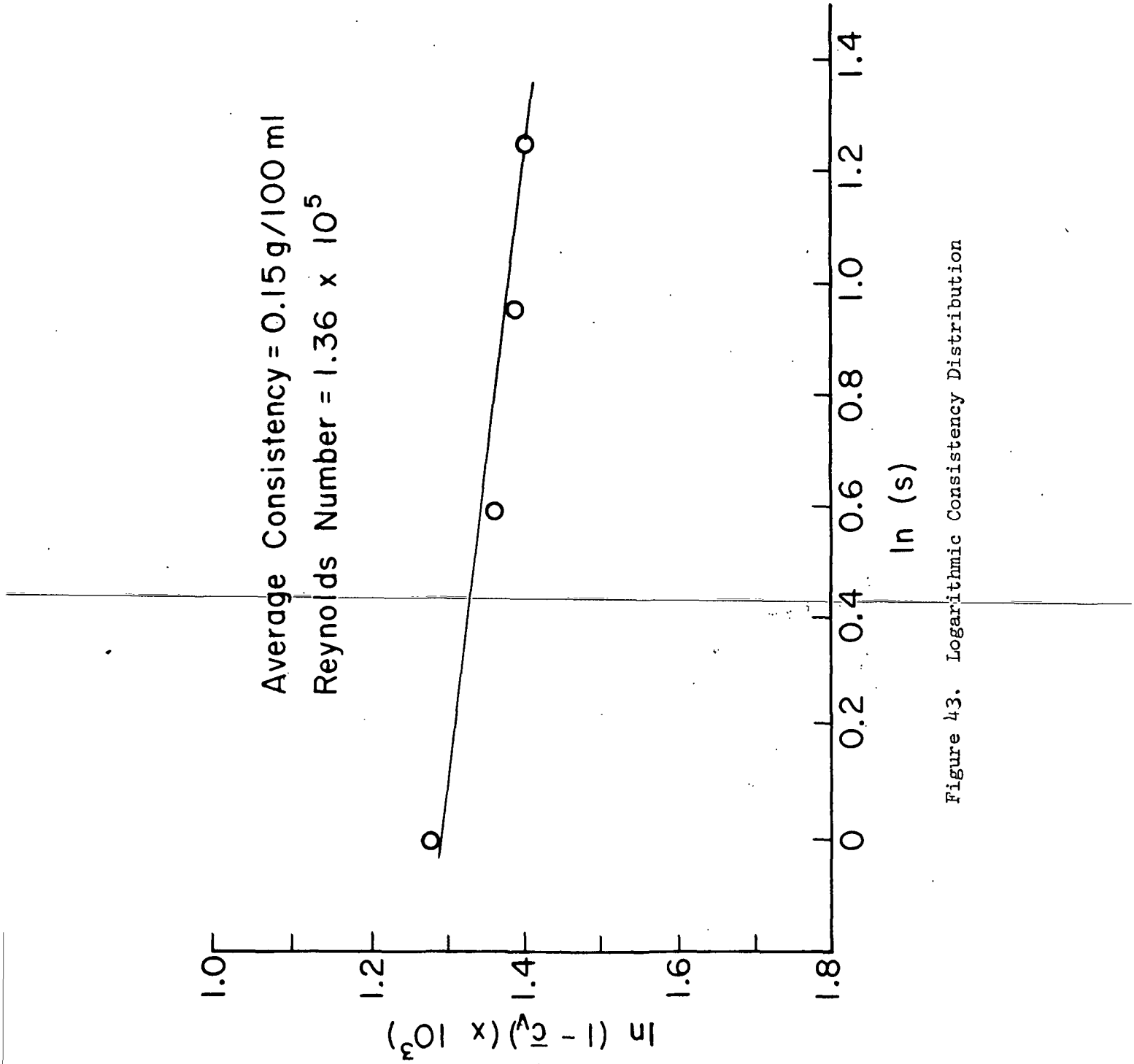

Figure 43. Logarithmic Consistency Distribution

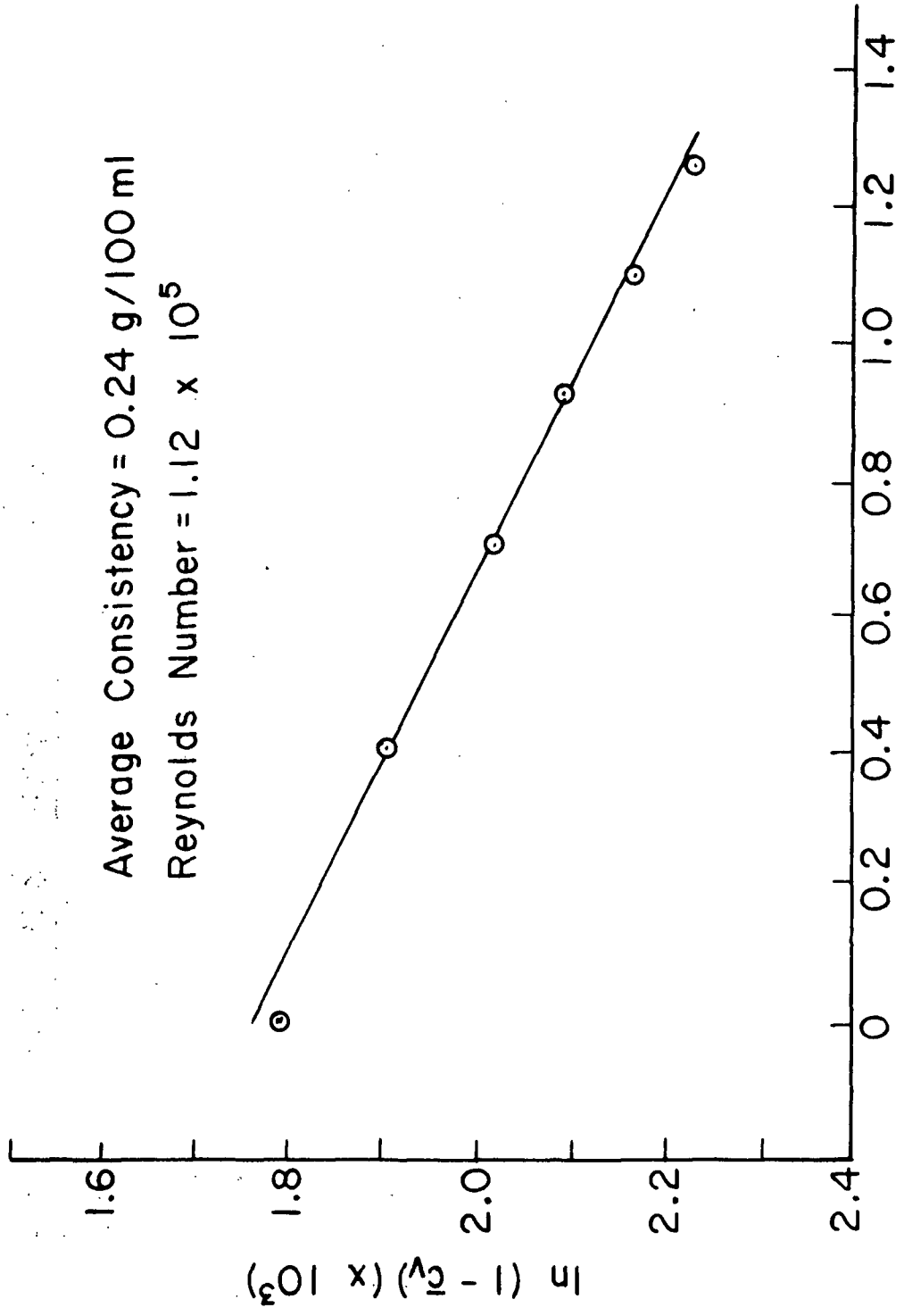

Figure 44. Logarithmic Consistency Distribution

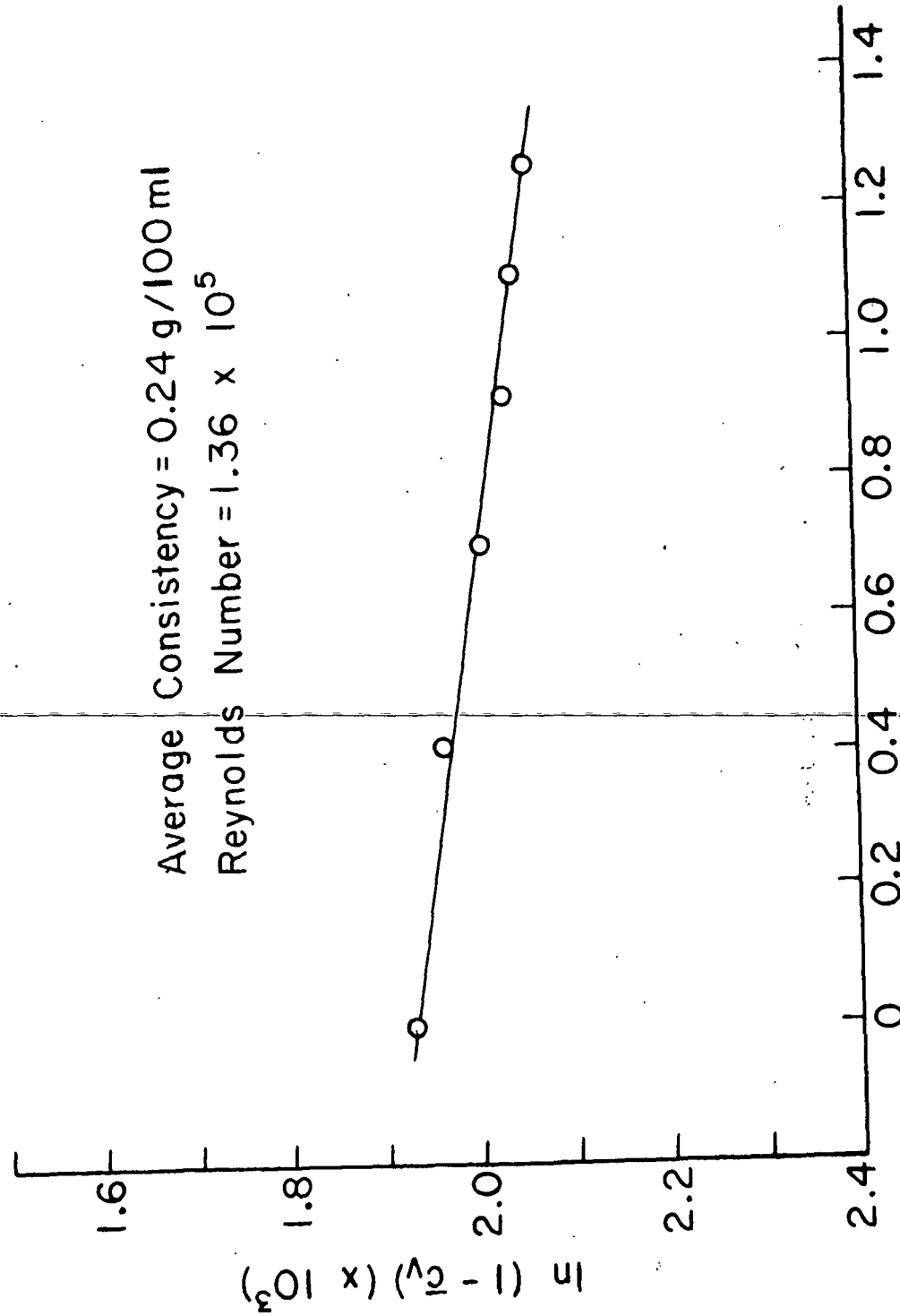

Figure 45. Logarithmic Consistency Distribution

Figure 42 shows consistency distribution profiles for 0.15 and 0.24 g/100-ml suspensions. The data are presented in the form of local time-mean consistency versus radial position. Suspensions of 0.05 and 0.10 g/100-ml consistency were more uniform and did not show as much dependence on flow rate as did the data shown in Fig. 42.

Figures 43 through 45 show three of the profiles of Fig. 42 plotted in the form of ln $(1 - \bar{c}_v)$ versus ln (s).

DISCUSSION OF RESULTS

Although the major goal of the program was to obtain scale factors of flocculation, certain preliminary steps were necessitated to establish a foundation for and ensure the validity of the final results. The flocculation data, in other words, were collected with calibrated light guides from defined fiber suspensions in a vertical flow loop that was functioning properly.

WATER STUDIES

Flow studies with water as the test fluid were conducted to establish that the flow loop was hydraulically smooth and that it and the associated equipment were functioning properly. Pressure drop and flow rate data plotted in log friction factor *versus* log Reynolds number form (Fig. 16) agreed well with Prandtl's universal resistance law for smooth tubes.

$$1/\sqrt{f} = 4.0 \log \left(Re\sqrt{f} \right) - 0.40. \qquad (2)$$

Velocity profiles taken both perpendicular to and in the plane of the loop crossover section were symmetrical about the tube center line, and indicated that fully developed turbulent flow existed at the measuring station. No residual secondary flow patterns were observed in this system. Good agreement between integrated velocity profiles and volumetric flow rates (Table I) added assurance that the annular-purge impact probe used to measure velocity data was functioning well.

When plotted in the form of dimensionless velocity *versus* logarithm of dimensionless position, all the profile data were correlated by a single straight-line function (Fig. 18) of the form of Equation (22).

$$u^+ = \frac{1}{\kappa} \ln s^+ + b. \qquad (22)$$

For this study, values of κ, the von Karman constant, and b, the additive term, were found to be 0.332 and 2.98, respectively. While being close to values obtained by Sanders (κ = 0.317 and b = 1.25) (27), these values differ from the κ and b values of 0.40 and 5.5, respectively, reported by Nikuradse (37) and 0.36 and 3.8, respectively, reported by Deissler (46).

Since the data agree well with Prandtl's resistance law [Equation (2)] but yield constants for the logarithmic distribution law [Equation (21)] different from those given by Nikuradse (37), there appears to be a discrepancy because the Prandtl's resistance law can be derived from the logarithmic distribution. Values for κ and b found in the study were used to derive the resistance law and yielded

$$1/\sqrt{f} = 4.89 \log\left(\mathrm{Re}\sqrt{f}\right) - 3.3. \qquad (2a)$$

This would require a little more forcing of the constants to fit the Prandtl form than would that found by using, for example, Deissler's constants.

$$1/\sqrt{f} = 4.52 \log\left(\mathrm{Re}\sqrt{f}\right) - 2.85. \qquad (2b)$$

As Tennakes and Lumley (50) point out, however, there is considerable scattering of the constants (κ and b) and the most commonly reported values represent averages over many experiments. They even attribute some of the scatter to the lack of experiments at large enough Reynolds numbers and state that the logarithmic slope ($1/\kappa$) is probably nearly 3.0 if the Reynolds number is large enough. The data from this study were not collected over wide enough Reynolds number range and were not taken across the entire width of the turbulent core. Limited pumping capacity was the reason for the former whereas the

reason for the latter was that the annular purge impact probe was too large to measure the region close to the wall. Deissler (46) reports an $\underline{s}^+$ value of 26 for the edge of the buffer zone, the lower point where the linear logarithmic relationship ends. As can be seen from Fig. 18 the lowest value of $\underline{s}^+$ attainable in the present study was around 200, or nearly an order of magnitude higher than that for the edge of the buffer zone.

It is felt that these factors, particularly the latter, account for the difference in the values of κ and $\underline{b}$ obtained in these experiments and thus the difference in the constants calculated for the Prandtl universal resistance law. The fact that the experimental pressure drop data fit the established correlation indicates that the loop was hydraulically smooth.

FIBER FLOW

For suspension flow, the friction factor-Reynolds number data were in general agreement with previous investigations in that for fully developed turbulent flow the friction factors for the various suspensions were lower than those for water only. The data, however, did not exhibit distinct transitions between flow regimes as observed, for example, by Seely (26) and Sanders (27) and depicted in Fig. 1. The transition from damped turbulence to plug turbulence (decreasing Reynolds number) for suspensions used in this study was characterized by a slight decrease in friction factor value (Fig. 21) before increasing. A similar trend was observed in other fiber suspension flow data reported in the literature (25,32). The shape of the log $\underline{f}$ versus log $\underline{Re}$ curves for suspensions, as well as the value where different flow regimes are encountered, depends in part on the type of fiber used, so this is not too surprising.

Fiber suspension velocity profiles were compared to water data by plotting them in the form of dimensionless velocity versus logarithm of dimensionless position (Fig. 22 through 26). As observed by previous investigators (25-27), the slope and position of the profile curves for suspensions differ from those for Newtonian fluids, the slopes indicating lower apparent von Karman constant, κ_*. The apparent von Karman constant for suspensions decreases with increasing consistency and as reported by Seely (26) and Sanders (27), κ_* increases with flow rate and tends to approach the water line at high flow rates. This latter point is shown in Fig. 26.

The presence of a central plug is indicated for higher consistency suspension flow, particularly at lower flow rates, by a change in the slope of the suspension profile curve. This can be seen best for the 0.24 g/100-ml suspension curves, especially at low flow rates (Fig. 23 and 24). These data correspond to the plug turbulent-damped turbulent transition region discussed earlier.

CONSISTENCY DISTRIBUTION

Time-mean consistency measurements made in this study were in agreement with Sanders' observations. The time-mean values were found to be dependent on both the average consistency and flow rate. In general, consistency increased from the wall to the tube center line and the distribution of consistency became more uniform with increasing flow rate and decreasing average consistency (Fig. 42).

The linear consistency profile equation [Equation (4)] was also found to correlate the time-mean consistency data satisfactorily (Fig. 43 through 45). Equation (4) is repeated here for convenience.

$$\ln\left(\frac{1 - \bar{c}_v}{1 - \bar{c}_{vo}}\right) = \frac{-C'_w \kappa_*}{\kappa_\varepsilon \kappa_w u_*} (\ln s - \ln s_o). \qquad (4)$$

The equation was simplified as suggested by Sanders (27) by assuming $\bar{c}_{vo}$ was small and thus reducing the numerator on the left-hand side of the equation to $\ln (1 - \bar{c}_v)$. This term was plotted versus $\ln s$ in Fig. 43 through 45.

In Sanders' work (27) it was suggested that the mass exchange term, $C'_w / \kappa_\varepsilon \kappa_w$, found in Equation (4) may be useful as an index of the overall scale of flocculation for turbulent suspension flow. From his data he found that the mass exchange term decreased with increasing flow rate and increased with increasing consistency and, for a given consistency, the term approached a fairly constant value at high flow rates.

Values of κ_* and u_* characteristic of the fiber suspension flow data of this study were used to determine relative values for the mass exchange term for the logarithmic consistency profiles shown in Fig. 43 through 45. These terms behaved in a manner similar to that reported by Sanders.

LONGITUDINAL SCALE: L_z

Flocculation data were collected over a Reynolds number range of 6.25×10^4 to 1.36×10^5 (based on density and viscosity of water) and a consistency range of 0.05 to 0.24 g/100 ml. Under these conditions most of the fiber suspension flow was in the damped turbulent regime, the exceptions occurring at the extremes of the consistency range. For the lowest consistency and high flow rates the flow was in or near Newtonian turbulence whereas at high consistency and low flow rates the flow was in the plug-turbulent regime.

Although the tips of the two-branch light guides underwent occasional fiber stapling, sufficient lengths of fluctuating signals were obtained to perform autocorrelation studies. It is felt that the crescent purge design probably accounted for more stapling and a narrower working consistency range than would have been encountered had probes with annular-purge systems been employed. Sanders (27) reported being able to measure consistency signals up to at least 0.80 g/100-ml consistency for suspensions of bleached softwood sulfite fiber and Walseth (28) obtained signals for 1.0 g/100-ml consistency suspensions of nylon fibers. Both used annular-purge type systems.

Time-mean scales for the longitudinal direction, henceforth referred to as $\underline{L}_{\underline{z}}$, flocs, or floc lengths, were calculated for radial tube positions by multiplying the area under the autocorrelation curve, as defined earlier, by the time-mean velocity, $\underline{\bar{u}}$, at that position. Average values of $\underline{L}_{\underline{z}}$ were tabulated in Table II. Over the consistency and Reynolds number range studied, time-average floc lengths ranging from 3 to 25 mm were obtained. For Reynolds numbers sufficiently great to preclude a central plug, there were distributions of time-average floc sizes across the tube as shown in Fig. 46 through 49.

The shapes of the profile curves are based on considerations of symmetry about the tube axis and also on the behavior of the normal stress for the $\underline{z}$-direction, $\rho\underline{\overline{u'^2}}$. Symmetry about the tube axis is suggested from velocity profile measurements made in this study and by others and also from time-mean consistency profiles determined by Sanders (27). In all cases, there was axis symmetry and there is no reason to expect otherwise for floc size distribution. This means that the slope of the profile curve should be zero at the tube center line.

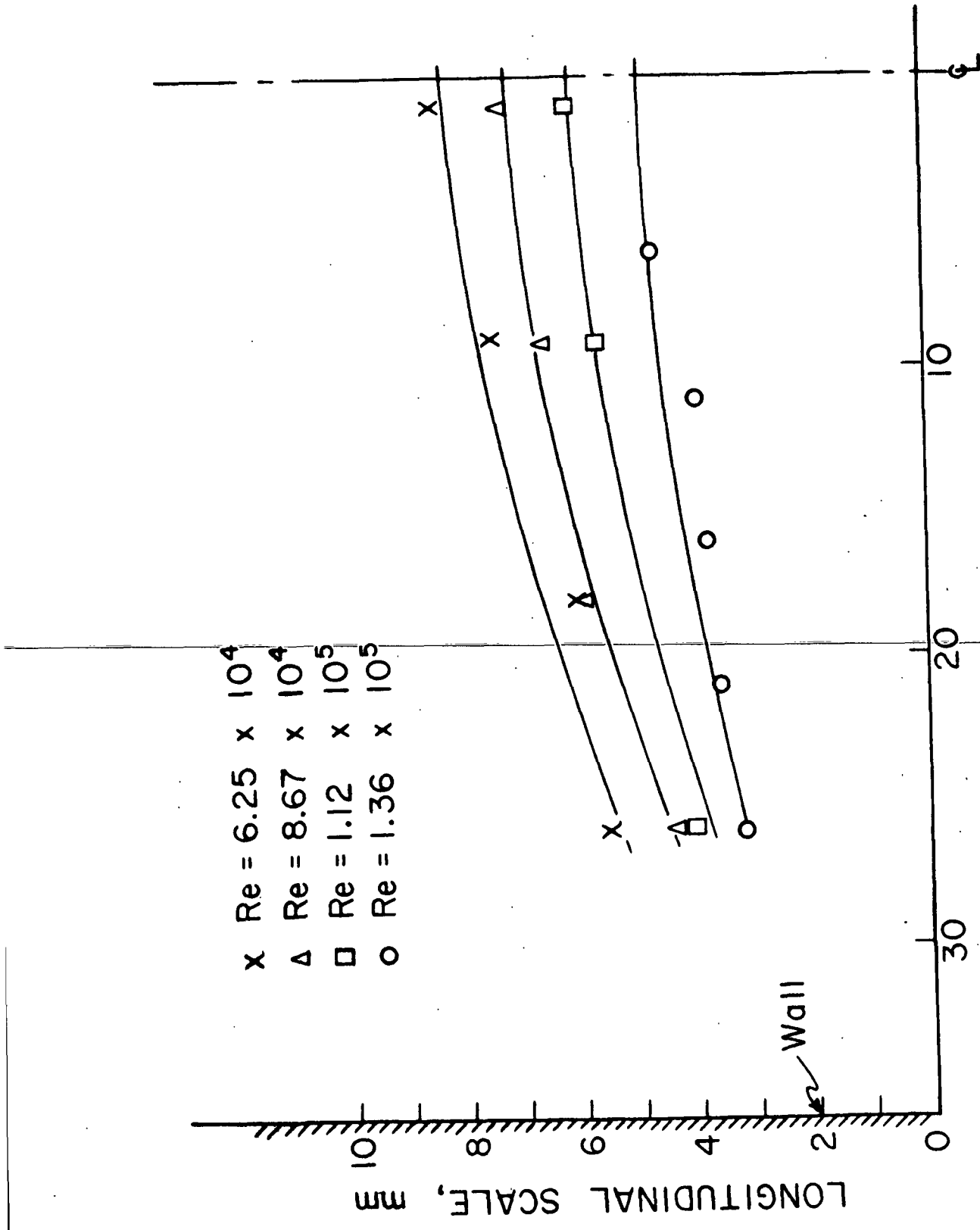

Figure 46. Longitudinal Scale Factor Distribution, Consistency = 0.05 g/100 ml

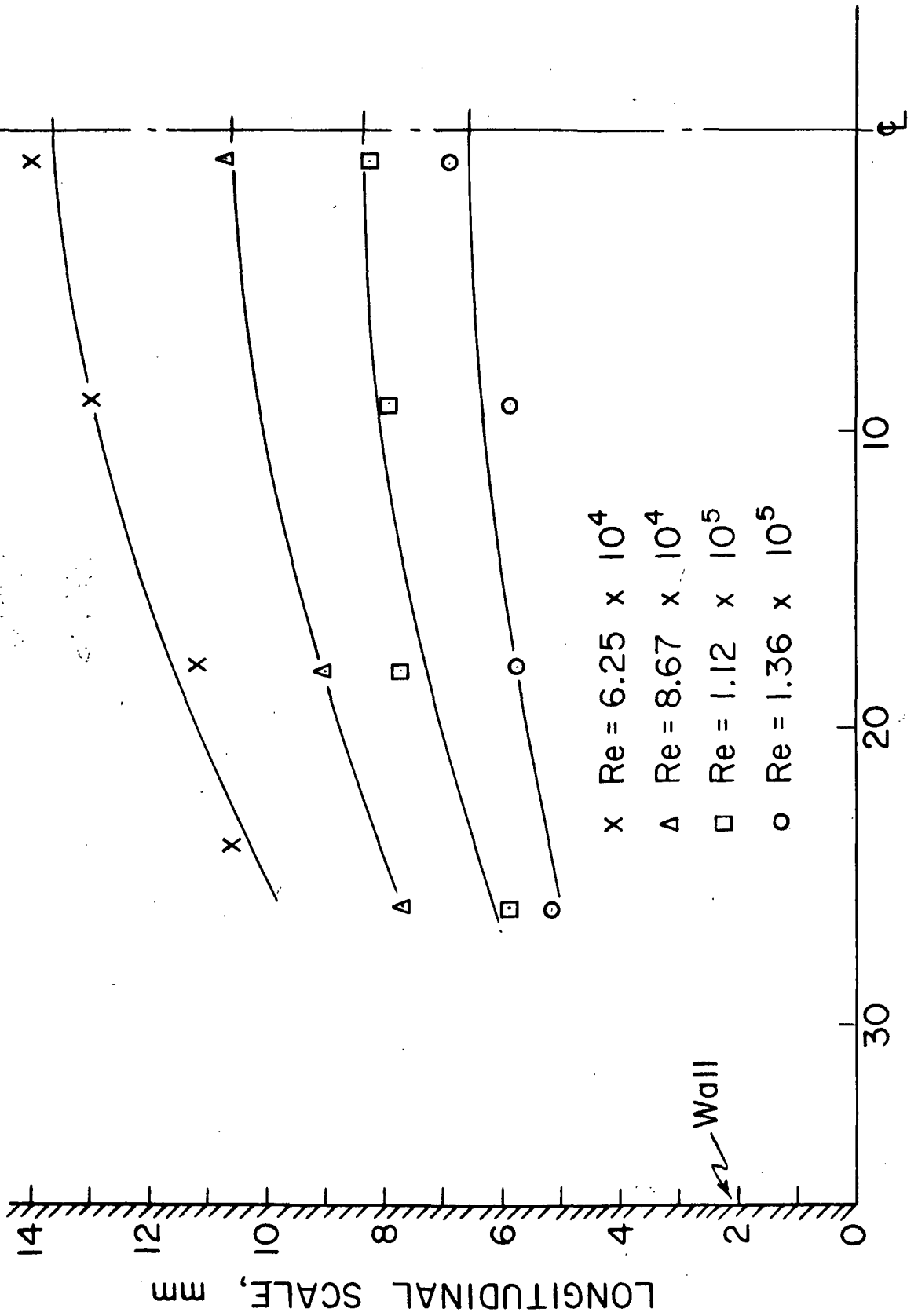

Figure 47. Longitudinal Scale Factor Distribution, Consistency = 0.10 g/100 ml

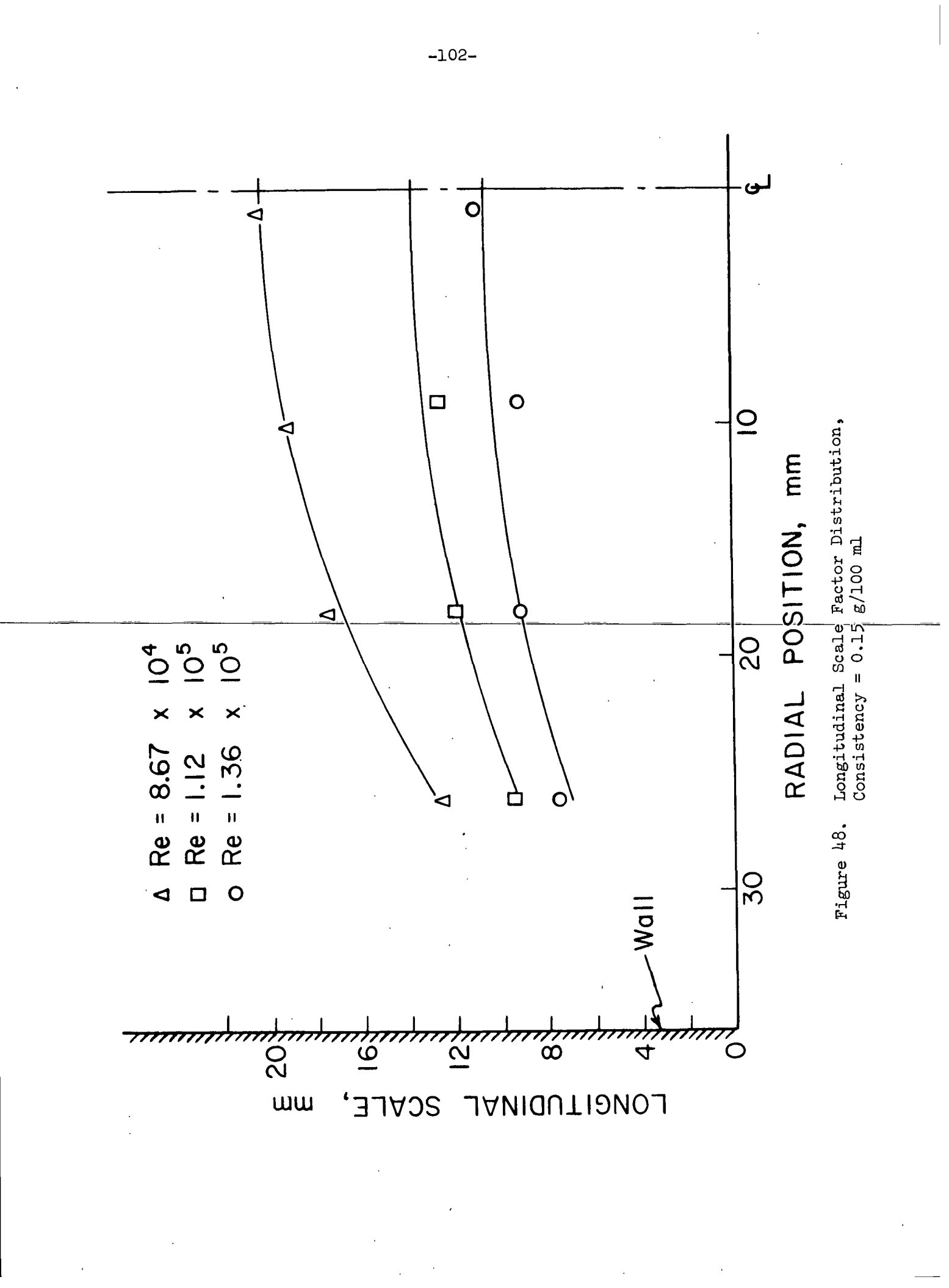

Figure 48. Longitudinal Scale Factor Distribution, Consistency = 0.15 g/100 ml

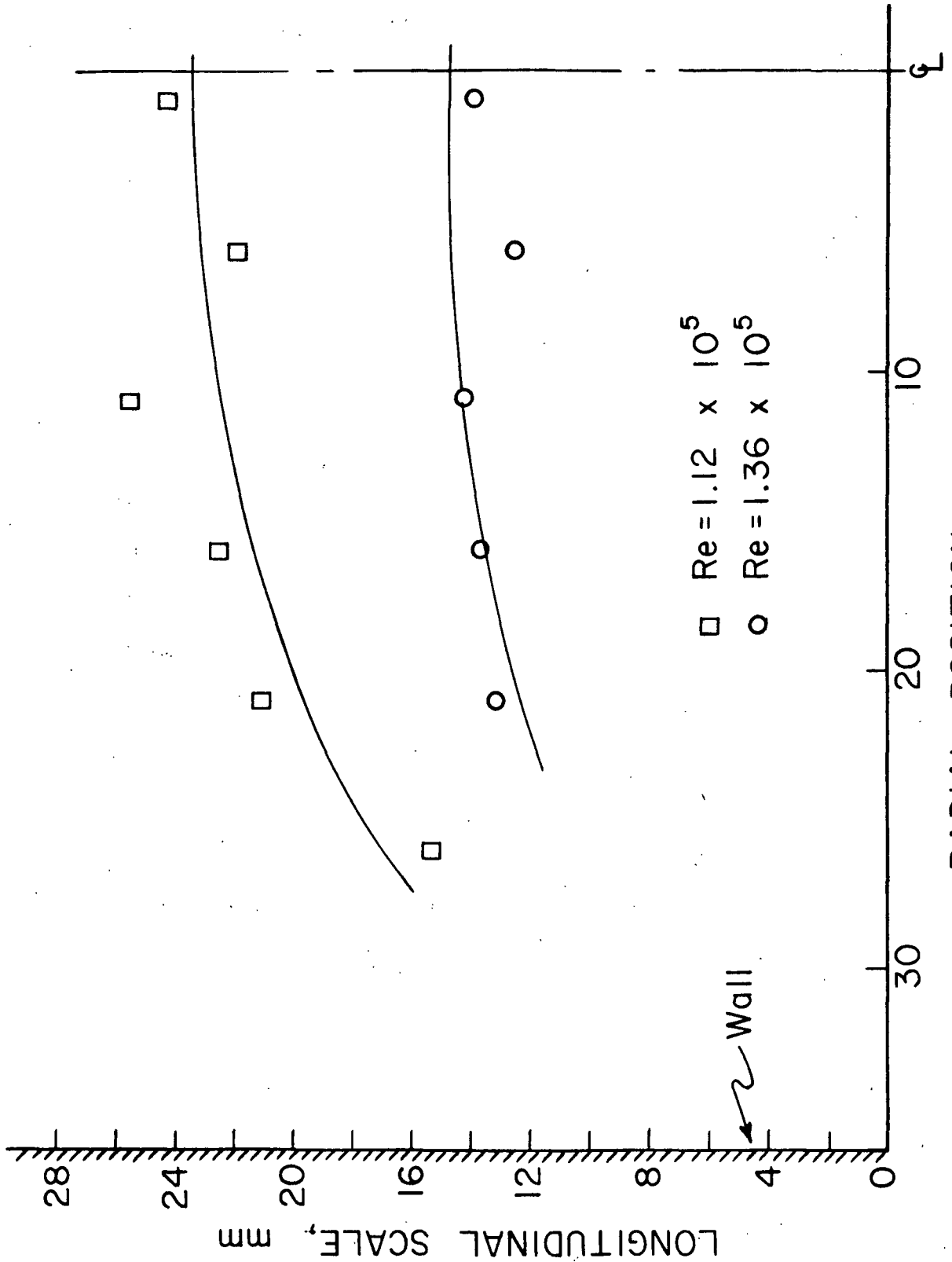

Figure 49. Longitudinal Scale Factor Distribution,
Consistency = 0.24 g/100 ml

It is known that there is a fiber-free water region near the tube wall (33) and for this reason L_z values must be zero somewhere close to the wall. In the turbulent core the fiber networks are subjected to turbulent disturbances which undoubtedly play an important role in network size distribution. The ratio $\sqrt{\overline{u'^2}}/\overline{U}_m$ is a measure of the magnitude of turbulent fluctuations for the z-direction.

This ratio is referred to as the intensity of turbulence in the z-direction and has, for tube flow, values ranging from about 4% at the center line to around 10% at the edge of the buffer zone. Although intensities were not determined in this study and values for fiber suspensions were not found in the literature, values for other fluid systems have been determined. Laufer (55) using hot wire anemometry determined values for air flow, Patterson and Zakin (56) using hot film anemometry did the same for toluene and Reiner and Wahren (57) using a piezoelectric probe determined values for water. All values were in good agreement. In addition, Laufer's data indicate very little difference in intensity between flow at Reynolds number of 5×10^4 and that of 5×10^5 for points well within the turbulent core. Laufer's data are represented in Fig. 50. For lack of specific data the assumption is made that Laufer's intensity profiles also apply to fibrous suspensions of the present low consistency range.

The nonlinear profiles presented in Fig. 46 through 49 for longitudinal scale distributions are suggested from the nonlinear intensity profiles of Fig. 50. Near the wall, there is a maximum in the z-direction turbulent intensity profile. From this maximum value, the intensity decreases in a nonlinear manner to lower values at the center line. If the turbulent fluctuations which give rise to the normal stress are considered to play a role in determining

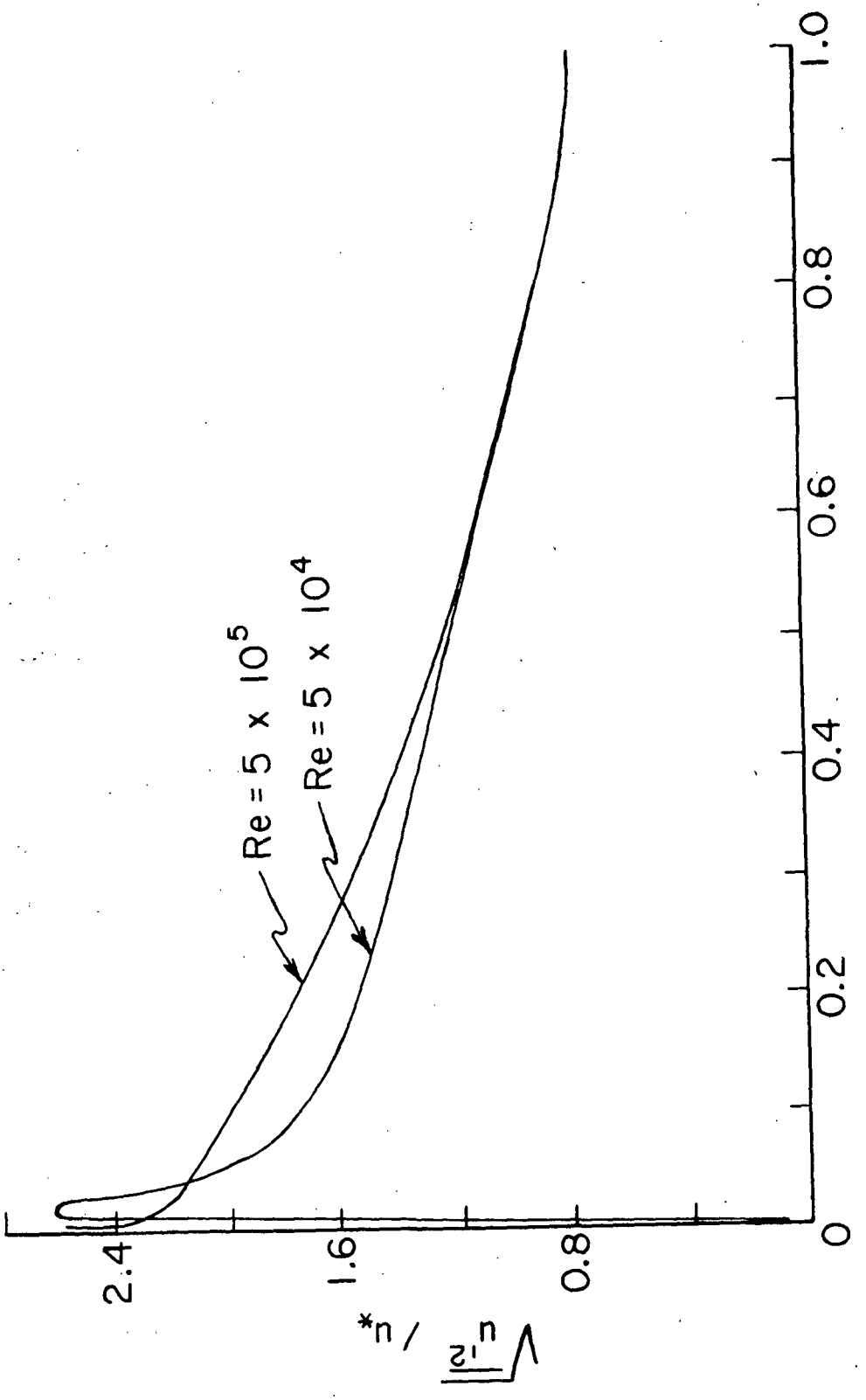

Figure 50. $\sqrt{\underline{u'^2}}/u_*$ Distribution After Laufer (55)

average fiber network sizes, then it is logical to consider smaller networks existing in regions of high intensities, and larger networks in regions of lower intensities.

In general, average floc lengths increased in going from the tube wall to the center line. For a particular suspension, floc sizes decreased with increased flow rate, an observation also made by Andersson (24) for pine kraft suspensions.

Considering that increasing the flow rate results in more energy input into the system, this observation is not surprising. The simultaneous increase in normal stress due to the turbulent fluctuation, u', acting in the z-direction would result, it is felt, in fiber networks being torn apart or degraded to smaller sizes. The time-mean square, $\overline{u'^2}$, is, of course, a measure of the normal stress ($\rho\overline{u'^2}$) acting in the z-direction.

Again, using Laufer's data (55) as a basis for calculation, assuming thus no significant change in the shape of the intensity distribution under suspension flow conditions, $\overline{u'^2}$ values for the various conditions were calculated. The time-average floc lengths for damped turbulent flow were then plotted versus the calculated $\overline{u'^2}$ values.

As shown in Fig. 51 the 11 profiles of Fig. 46 through 49 reduced to 3 curves, one for each consistency. At low mean square fluctuating velocity values, floc lengths for a particular consistency are large and, as more energy is added to the system, the normal stress is increased and floc size decreases. It appears that for a given consistency the value of the time-mean longitudinal scale approaches a constant value at high $\overline{u'^2}$ values (high flow rates).

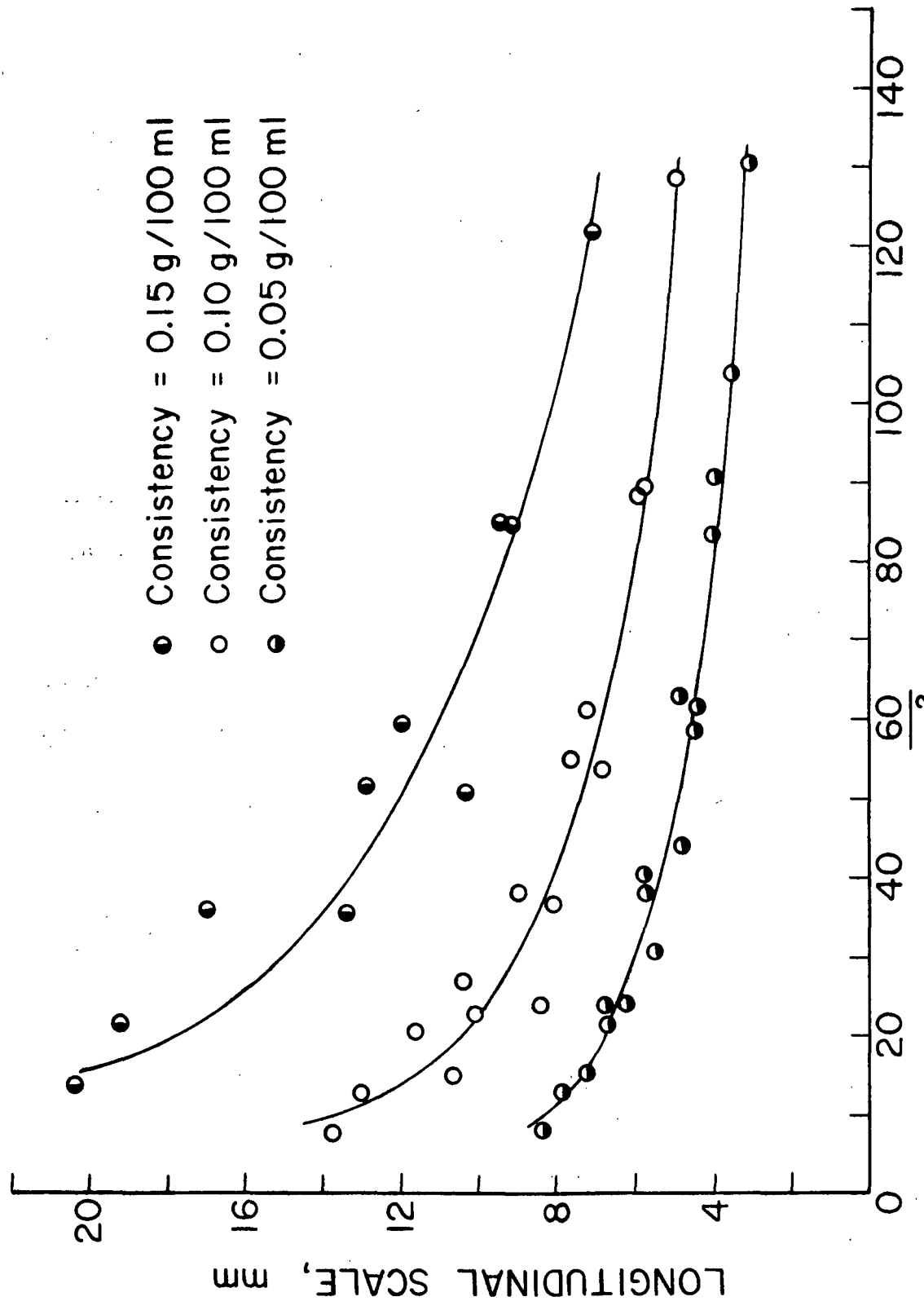

Figure 51. Longitudinal Scale Factor vs. $\overline{u'^2}$

Increasing the consistency at any value of $\overline{u'^2}$ results in an increase in floc length. This can also be seen in Fig. 52 where L_z profiles are plotted for an 0.10 g/100-ml suspension with Reynolds number as the parameter. The mass exchange term in Sanders' work (27), as mentioned earlier, behaved in a manner similar to the floc lengths determined in this study.

This trend would be expected when it is considered that the turbulent energy is not only expended by viscous dissipation, but also by the breakdown of fiber networks. The stronger the network, the greater the energy dissipated by the network degradation to any given average floc size (35). The stronger the network, on the other hand, the less breakdown that would occur for any given input of turbulent energy. Increasing the consistency of a suspension has the effect of increasing flocculation tendency and, through more entanglement, causing larger, stronger flocs.

Although it has been demonstrated that fiber networks do have a calculable tensile strength (20), nothing is inferred in this discussion as to the amount of energy that is required to degrade fiber networks.

The results of this part of the program indicate that the techniques of using autocorrelation analyses of fluctuating consistency signals, as obtained by using fiber optic light guide probes, to define indicators of local time-average flocculation scales is a valid approach. The magnitude of the lengths (3 to 25 mm) moreover, make more physical sense than do, for example, floc wavelengths of 100 mm or so obtained from frequency analysis (29). In addition to obtaining distributions of local floc lengths, it was also demonstrated that the technique can be used to study the effect of the variables that affect fiber flocculation.

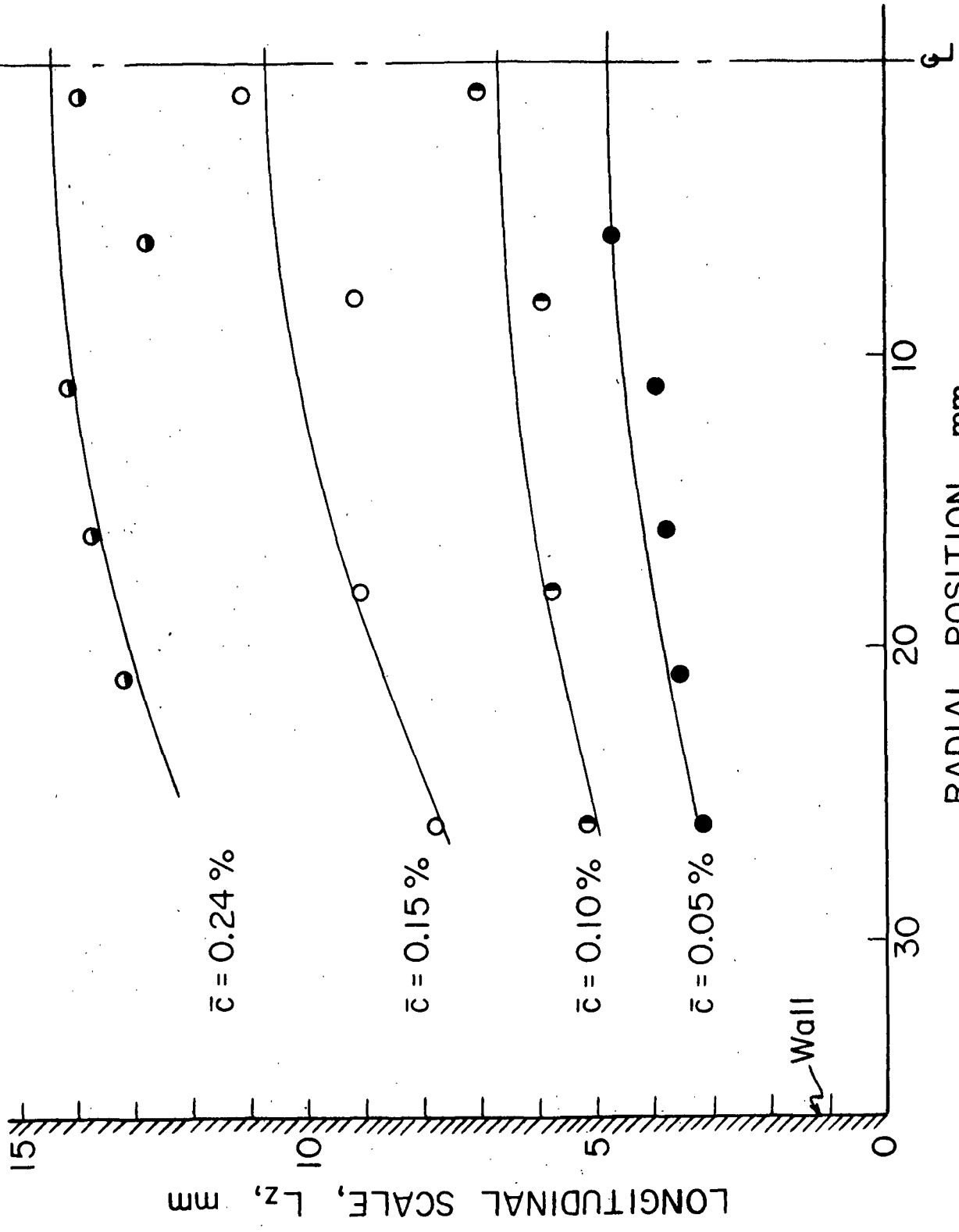

Figure 52. Effect of Consistency on $L_{\underline{z}}$ Distribution, $Re = 1.36 \times 10^5$

RADIAL SCALE: L_r

The results of the crosscorrelation studies of the signals from the two light guide probes did not lend themselves to straightforward interpretation in that there was no systematic trend apparent from the data. There appeared to be no distinctly reproducible crosscorrelation of any of the sets of consistency signals.

The only definite conclusion that can be made from this portion of the program is that for higher consistency flow (in the order of 0.25 g/100 ml for this type rayon fiber) the operation of the two probes in close proximity is not hydrodynamically favorable. Under these conditions, the two probes could not be brought closer together than 3 to 4 mm without both probes stapling over.

At lower consistency flow, there was still frequent stapling but it was possible to isolate signals to crosscorrelate. The crosscorrelations, however, were not reproducible and behaved in an erratic manner also in this range. Since the crosscorrelation is a measure of the coherence of the two signals (in this case one from each of the light guides) it is apparent that the two signals did not correlate with one another. This would indicate that the two probes are not seeing the same mass in their respective sensing volumes at any time and any separation.

Explanations as to why the signals are not correlated systematically are mainly speculative in nature. A possible reason for the oscillatory nonreproducible crosscorrelations is that the radial dimensions of fiber networks are smaller than that detectable by the present sensing system. In view of the shearing action present across the tube, increasing from zero at the tube center line to a maximum at the wall, it is not unreasonable to assume that

the average radial dimensions of networks are small. This is supported by Andersson's observations (24), using stereophotography, that flocs were irregular in shape and that they tended to be oblong or string shaped.

A few remarks concerning the optical geometry of the two probe system may be in order. Each light guide detects reflected light from the fibers in its sensing volume which then gives rise to an electrical signal which is subsequently used for crosscorrelation studies. When the two probes are in contact, the stainless steel casing of each light guide results in the glass fiber bundles still being separated by a distance of approximately 0.5 mm. Probe center line-to-center line distance is on the order of 1 mm. As discussed earlier, the light beam from each probe is in the shape of a cone of half angle around 25°. Each probe then detects fibers in its respective cone; however, the depth of field for viewing fiber suspensions has not been established. Figure 53A depicts the situation where the two probes are in contact. The shaded portion of the light beams is that volume seen by both probes. As the probes are stepped apart, Fig. 53B, the volume of vision common to both probes decreases and moves at the same time further upstream. Thus, the blind area, not seen by either probe, increases with separation distance.

To be registered by both probes, a mass of fibers or a part of it needs to pass through the viewing cone common to both probes, situated about the center line between the two probes. If a floc intercepts the probes on a line other than this center line, it will not register simultaneously with both probes. Since portions of neighboring flocs will pass through the sensing volume of the individual probe this will cause pairs of incoherent signals. It can be thus envisioned that narrow network structures can pass the probes and give rise to an erratic type crosscorrelation.

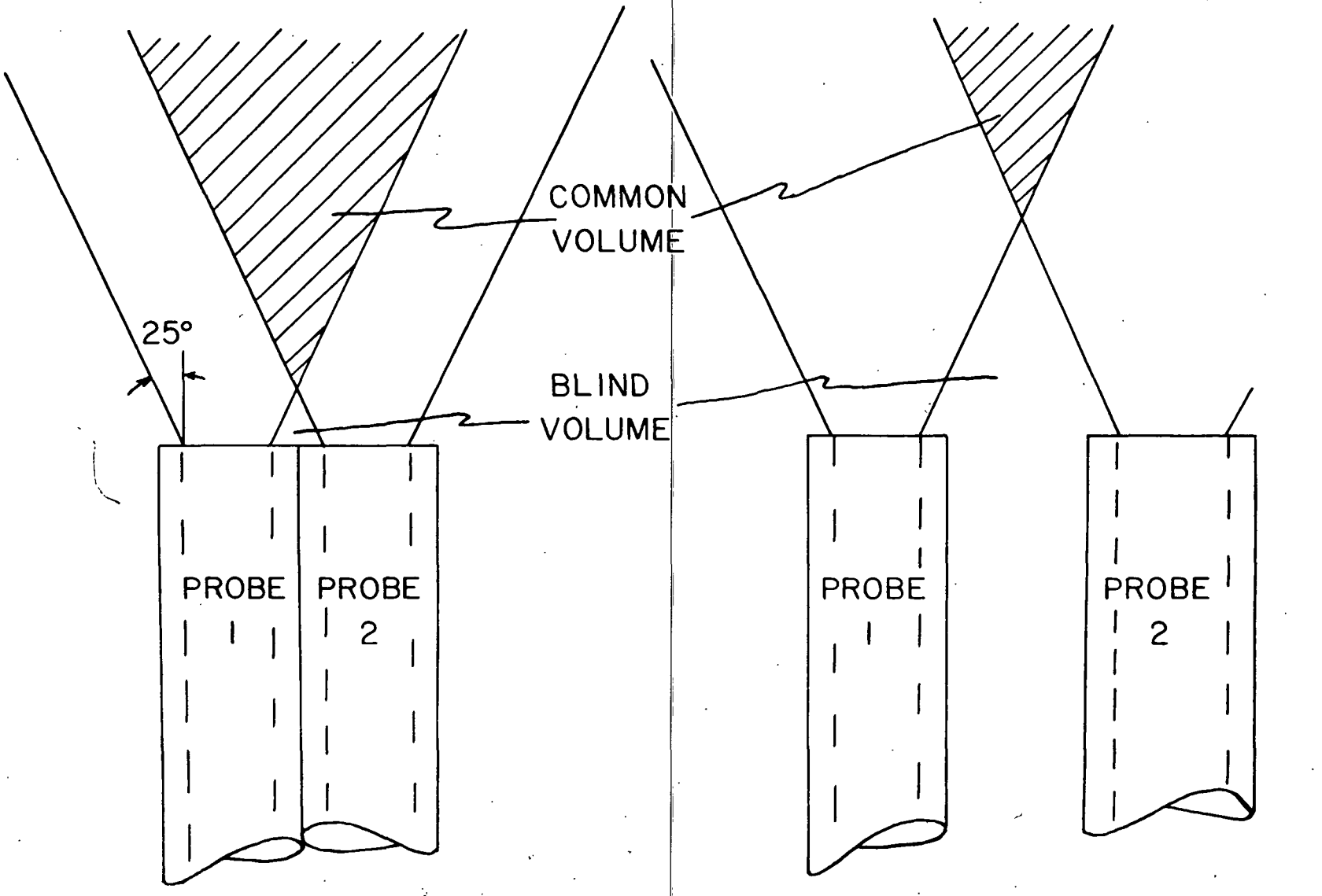

Figure 53. Geometry Around Probe Tips (not Including Purge)

In view of the results from this aspect of the program, there is certainly opportunity and need for more studies on radial dimensions of flocs. A different experimental approach may be in order since it appears that the system used in this study was not capable of resolving these dimensions.

CONCLUSIONS

An important aspect of this program was the development of a new experimental technique for measuring indicators of local time-average floc sizes and demonstrating that the technique can be used to observe the effect of changing flocculation variables on average floc sizes. The technique as used in this study was limited to consistencies of about 0.25 g/100 ml or less, but minor modifications such as using an annular-purge system should increase the useful range considerably. The technique should be useful in studying the various factors affecting flocculation since it affords a direct means of observing the changes in local floc sizes as flocculation variables are changed.

The experimental results of this investigation represent the first successful attempt to use fluctuating consistency signals and definitions common to turbulence research to define and measure indicators of time-average local floc sizes in turbulent tube flow of fiber suspensions. A nonuniform floc size distribution was observed with average floc lengths increasing in going from the tube wall to the tube center line. The distributions were found to be a function of both the Reynolds number and average consistency of the suspension. For a particular suspension, local time-average longitudinal floc sizes decreased with increased local velocity while at a constant local velocity the floc sizes increased with increased consistency.

Attempts to measure radial scales of flocculation were, in general, inconclusive in that no apparent correlation appeared to exist between the two fluctuating consistency signals. It was concluded that floc sizes in the radial direction were either too small to be detected by the sensing system or the capabilities of the measuring technique broke down when the two light guides were in close proximity.

Velocity distributions measured in this investigation were in general agreement with earlier investigations (26,27). They indicated that the apparent von Karman constant for turbulent fiber suspensions is a function of both flow rate and average consistency. The von Karman constant increased systematically with increasing flow rate and, depending on the consistency, tended to approach the value for water flow at particularly high flow rates. These flow rates were those at which the friction loss in suspension tube flow approached the Newtonian values.

Time-mean consistency distributions were in agreement with Sanders' work (27). They were a function of both flow rate and mean consistency and, in general, became more uniform with increasing flow rate and decreasing average consistency. The linear consistency distribution equation developed from the two-phase equation approach (27,31) was found to correlate the time-mean consistency data well and the mass exchange term in the equation was found to behave in a manner similar to Sanders' data.

SUGGESTIONS FOR FUTURE RESEARCH

Many unanswered questions afford considerable opportunity for additional studies on fiber suspension flow. Both Seely (26) and Sanders (27) have advanced several suggestions and insight gained during this study verifies the need for additional work on time-mean and time-dependent consistency measurements as well as velocity measurements.

There are many variables that can affect flocculation and thus many experiments can be envisioned. It is felt, however, that studies involving fluid and/or fiber variables would be most rewarding in rendering information of fiber network formation, network strength, and fiber network influence on turbulence damping. Extension of this program to include, for example, different fiber types, different l/d ratios, as well as different average consistencies seems reasonable. Considering fluid flow parameters, the effect of suspension temperature bears investigation. It might also be interesting to study flocculation in a different type of flow field, such as a submerged jet.

Different techniques for measuring time-average radial floc dimensions need to be explored.

The effect of chemical additives should be investigated to determine their role in fiber flocculation under turbulent flow conditions. Results could be quite beneficial, especially if they could be extrapolated to the sheet forming process. This might afford a means for evaluation of the effect of different additives on sheet formation quality.

ACKNOWLEDGMENTS

I wish to express a special note of gratitude to Mr. Heribert Meyer, Chairman of my thesis advisory committee, for his continual help and encouragement during the course of this work. The advice and critical discussions offered by the other members of my committee, Dr. G. A. Baum and Dr. R. W. Nelson, and those of Dr. D. G. Williams are also gratefully acknowledged.

There have been many people who have contributed toward the completion of this thesis. Among these are Mr. M. C. Filz, Jr. and Mr. P. F. Van Rossum, who constructed several items necessary for the experimental work. The continual help and advice of Mr. B. D. Andrews were certainly appreciated. I also thank Mr. J. O. Church who helped considerably in the establishment of the analog-to-digital conversion arrangements. In this vein, I also thank Dr. T. Linton of the University of Wisconsin staff for his assistance in the digitizing of the data.

The help of the following was greatly appreciated and is gratefully acknowledged: Mr. K. W. Hardacker for his assistance in selecting and setting up the associated electronics, Mr. J. D. Hankey for the photomicrographs, Mr. F. R. Sweeney and Mr. D. E. Beyer for their photographic work, and Mr. A. O. Johnson and Mr. S. J. Baumann for assembling the pipe loop.

Special thanks are extended to all other members of the Institute faculty and staff and to the students who have extended their knowledge and help in this work. I also wish to thank The Institute of Paper Chemistry for granting this opportunity to learn and for its financial support.

Last, but by no means least, my sincere thanks are extended to my wife Randa for her continual support and help in preparing and typing this manuscript, and to my son John who has hopes of seeing more of his Dad in the future.

NOMENCLATURE

a	viscous flow resistance coefficient
A	cross-sectional area of a pipe
b	a constant
$c, \bar{c}, c'$	instantaneous component of consistency, temporal mean of c, fluctuation of c about $\bar{c}$
c_L	center line
c_v	volume fraction of fibers
c_{vo}	volume fraction of fibers at boundary layer
C'_w	integration constant
d	fiber diameter; a measure of distance
D	tube diameter
$e, \bar{e}, e'$	instantaneous component of voltage, temporal mean of e, fluctuation of e about $\bar{e}$
f	friction factor, $2(u_*/\langle\bar{u}\rangle)^2$
G	flow rate
I	light intensity
I_c	light intensity incident on phototube cathode
$i, \bar{i}, i'$	instantaneous component of current, temporal mean of i, fluctuation of i about $\bar{i}$
I_l	light intensity at lamp
k_1, k_2, k_3, k_4	constants
l	fiber length; Taylor's scale of turbulence [Equation (9)]
L	length; scale
ln	natural logarithm
log	logarithm to base 10
L_r	radial scale of flocculation
L_z	longitudinal scale of flocculation
n	refractive index

p	pressure
$\Delta P/L$	pressure gradient
Q	volumetric flow rate
r	radial position in pipe flow
R	tube radius; correlation coefficient
Re	Reynolds number
R_r	radial correlation coefficient
r,θ,z	cylindrical coordinates
R_z	longitudinal correlation coefficient
s	wall distance, $R - r$
s^+	dimensionless wall distance, $s\rho u_*/\mu$
s_o	fiber-free boundary layer thickness
t	time
T	temperature; time
$\bar{u}$	bulk flow velocity
u^+	dimensionless velocity, u/u_*
u_*	friction velocity, $\sqrt{\tau/\rho}$
$\overline{u'^2}$	mean square turbulent fluctuation
u_f	velocity of fiber phase
$\bar{U}_m$	maximum velocity
u_{rz}	relative velocity between water and fiber phases, $\overline{u_w - U_f}$
$u,\bar{u},u'$	instantaneous component of velocity for the z-direction, temporal mean of u, fluctuation of u about $\bar{u}$
u_w	velocity of water phase
v	velocity component in the r-direction
V	volts
x,y,z	Cartesian coordinates
Y	a length

α	apparatus factor
$\varepsilon, \bar{\varepsilon}, \varepsilon'$	instantaneous component of volume fraction of water, temporal mean of ε, fluctuation of ε about $\bar{\varepsilon}$
γ	reflectance factor
κ	von Karman constant
κ_*	apparent von Karman constant
$\kappa_\varepsilon, \kappa_{\underline{w}}$	mixing length distribution parameters for water and fiber
μ	fluid viscosity; mean value
ϕ	angle
ρ	fluid density
σ	standard deviation; normal stress
τ	shear stress, time delay
τ_o	wall shear stress

LITERATURE CITED

1. Forrest, F., and Girlerson, G. A. H., Tech. Assoc. Papers 14(1):259(1931).

2. Bryant, E. O. A photographic method for hydrodynamic research and its application to the motion of fibers in flowing suspensions. Doctor's Dissertation. Appleton, Wis., The Institute of Paper Chemistry, 1937. 114 p.

3. Moss, L. A. A photographic study of the motion of fibers and water in flowing fiber suspensions. Doctor's Dissertation. Appleton, Wis., The Institute of Paper Chemistry, 1937. 159 p.

4. Van den Akker, J. A., Tappi 37(11):489-94(Nov., 1954).

5. Mardon, J., and Van der Meer, W., Pulp Paper Mag. Can. 55(11):107-27(Oct., 1954).

6. Baines, W. D., Svensk Papperstid. 62(22):823(1959).

7. Durst, R. E., Pulp Paper Mag. Can. 57(C):255-62(1956).

8. Durst, R. E., and Jenness, L. C., Tappi 39(5):277-83(May, 1956).

9. Brecht, W., and Heller, H., Tappi 33(9):14A(Sept., 1950).

10. Mason, S. G., Tappi 33(9):440-4(Sept., 1950).

11. Robertson, A. A., and Mason, S. G., Pulp Paper Mag. Can. 57:121-4(May, 1956).

12. Mason, S. G., Tappi 37(11):494-501(Nov., 1954).

13. Hubley, C. E., Robertson, A. A., and Mason, S. G., Can. J. Res. 28B(12): 770-87(1950).

14. Mason, S. G., Pulp Paper Mag. Can. 51(5):93-100(April, 1950).

15. Favis, D. V., Robertson, A. A., and Mason, S. G., Can. J. Technol. 30:280 (1952).

16. Beasley, D. E., Tappi 36(9):159-60A(Sept., 1953).

17. Gavelin, G., Pulp Paper Mag. Can. 55(3):191-200(March, 1954).

18. Robertson, A. A., and Mason, S. G., Pulp Paper Mag. Can. 55(C):263(1954).

19. Robertson, A. A., and Mason, S. G., Tappi 40(5):326-34(May, 1957).

20. Forgacs, O. L., Robertson, A. A., and Mason, S. G., Pulp Paper Mag. Can. 59(5):117-28(May, 1958).

21. Meyer, H., Tappi 47(2):78-84(Feb., 1964).

22. Balodia, V., Appita 18(5):184(1965).

23. Steenberg, B., and Wahren, D., Appita 18(5):180-3(1965).

24. Andersson, O., Svensk Papperstid. 69(2):23-31(Jan. 31, 1966).

25. Mih, W., and Parker, J., Tappi 50(5):237-46(May, 1967).

26. Seely, T. L. Turbulent tube flow of dilute fiber suspensions. Doctor's Dissertation. Appleton, Wis., The Institute of Paper Chemistry, 1968. 127 p.

27. Sanders, H. T., Jr. An investigation of fiber consistency distribution in turbulent tube flow. Doctor's Dissertation. Appleton, Wis., The Institute of Paper Chemistry, 1970. 123 p.

28. Walseth, D. S. Unpublished work, 1971-1973.

29. Nerelius, L., Norman, B., and Wahren, D., Tappi 55(4):574-80(April, 1972).

30. Reiner, L., and Wahren, D., Svensk Papperstid. 74(8):225-32(April 30, 1971).

31. Sanders, H. T., and Meyer, H., Tappi 54(5):722-30(May, 1971).

32. Daily, J., and Bugliarello, G., Tappi 44(7):497(July, 1961).

33. Bugliarello, G., and Daily, J., Tappi 44(12):881(Dec., 1961).

34. Ippen, A. T., Daily, J., and Bugliarello, G., Tappi 40(6):478-85(June, 1957).

35. Parker, J. D. The sheet forming process. STAP No. 9. New York, TAPPI, 1972.

36. Meyer, H., Tappi 54(9):1426-50(Sept., 1971).

37. Nikuradse, J. Gesetzmassigkeit der Turbulenten Stromung in glatten Rohren. Forschungshaft 356, 1932.

38. Bird, R. B., Stewart, W. E., and Lightfoot, E. N. Transport phenomena. New York, John Wiley and Sons, Inc., 1966. 780 p.

39. Swanson, J. W. A-235 Class Notes, 1970.

40. Wollwage, J. C. The flocculation of papermaking fibers. Doctor's Dissertation. Appleton, Wis., The Institute of Paper Chemistry, 1938. 177 p.

41. Erspamer, A. A study of the flocculation and dispersion of papermaking fibers. Doctor's Dissertation. Appleton, Wis., The Institute of Paper Chemistry, 1939. 143 p.

42. Hinze, J. O. Turbulence. New York, McGraw-Hill, 1959. 586 p.

43. Taylor, G. I., Proc. of the Royal Society of London, Series A, 51(873): 421-78(Sept. 2, 1935).

44. Dryden, H. L., Schubauer, G. B., Mock, W. C., and Skramstag, H. K., NACA Technical Report No. 581. Wash., D.C., Natl. Bur. Stds., 1937. 32 p.

45. Bandat, J. S., and Piersol, A. G. Random data: analysis and measurement procedures. New York, John Wiley and Sons, Inc.-Interscience, 1971. 407 p.

46. Deissler, R. G., NACA Technical Note 2138. Cleveland, Ohio, Lewis Flight Propulsion Lab., 1950. 41 p.

47. Nerelius, L., Norman, B., Wahren, D., Tappi 55(4):574-80(1972).

48. Siegmund, W. P. Fiber optics. Southbridge, Mass., American Optical Corp., 1972. 12 p.

49. Meyer, H. A-204 Class Notes and personal communication, 1971-1974.

50. Tennekes, H., and Lumley, J. L. A first course in turbulence. Cambridge, Mass., The MIT Press, 1972. 300 p.

51. Dixon, W. J. BMD Biomedical computer programs. Los Angeles, Calif., University of California Press, 1968. 600 p.

52. Martin, G. Q., and Johanson, L. N., AIChE J. 11(1):29-33(Jan., 1965).

53. Baldwin, L. V., and Walsh, T. J., AIChE J. 7(1):53-60(March, 1961).

54. Meyer, H. Unpublished work, 1973.

55. Laufer, J. NACA Technical Report 1174, 1954. 53 p.

56. Patterson, G. K., and Zakin, J. L., AIChE J. 13:513(1967).

57. Reiner, L., and Wahren, D., Svensk Papperstid. 71(21):767-73(Nov. 15, 1971).

APPENDIX I

ELECTRONIC EQUIPMENT SPECIFICATIONS

Item	Number Required	Specifications
Lamp	1	Quartz-iodide
Lamp power supply	1	Kepco Model PRM 6.3-8; modular power supply having multiple output regulated dc voltages
Photomultiplier (each unit consisting of a phototube and a housing)	2	
Phototube	2	EMI 9524B response (blue); 11 box and grid dynodes; cathode to anode voltage = 2 kv max.
Tube 1		Serial No. 61515; cathode sensitivity = 97 μamp/lumen; overall tube voltage necessary to give 200 amp/lumen sensitivity = 1240; dark current at 20°C for 200 amp/lumen sensitivity = 4 namp (dc)
Tube 2		Serial No. 61517; cathode sensitivity = 102 μamp/lumen; overall tube voltage necessary to give 200 amp/lumen sensitivity = 970; dark current at 20°C for 200 amp/lumen sensitivity = 5 namp (dc)
Phototube housing	2	EMI Type "T" (modified) with a potentiometer in series with the high voltage providing adjustment of approximately 300 v; 2 BNC connectors; Series 6 filter ring
Photomultiplier power supply	1	Brandenburg Model 472 R; 10-2100 v (bipolar); 0-5 ma max.; drift = 0.01%/day; ripple = 1 mv p-p

APPENDIX I (Continued)

ELECTRONIC EQUIPMENT SPECIFICATIONS

Item	Number Required	Specifications
Picoammeter	2	EMI Type 1012; input 10 μamp to 100 pamp (11 ranges); polarity — bipolar; resolution — 1 pamp; input impedance — to virtual ground; output noise — 3 mv p-p on 1 v output; output = 100 mv and 1 v
Analog recorder	1	Hewlett-Packard 3960B; 2 FM channels, No. 1 and 2; 2 direct channels, No. 3 and 4; tape speeds: 15, 3-3/4, 15/16 inch/sec; tape usage: 1/4-inch wide on 7-inch reels; reel revolution counter; voice interrupt capabilities on Channel 4; input level: FM = 1 v p-p to 30 v p-p 50 KΩ, 200 pF dc to 5000 Hz Direct: 0.1 v r.m.s. to 10 v r.m.s. 50 KΩ, 200 pF 50 Hz to 60 KHz
Audio oscillator	1	Hewlett-Packard Model 200 AB; 20 to 40,000 Hz (4 scales)
Strip chart recorder	1	Esterline Angus Model E 1101S; input ranges: 0-1,5,10,50,100,500 mv 0-1,5,10,50,100 v chart speed: 0.5,1,2,4,8 inches/hr, min. or sec.
Oscilliscope	1	DuMont Type 403 R; general application scope

APPENDIX II

WATER AND FIBER FLOW DATA

Presented in this appendix are data for pressure-drop flow rate and velocity profile runs for both water and suspension flow. The data are identified with a run number label as well as information on operating conditions: consistency, temperature, viscosity, and manometer fluids.

In general, the nomenclature in this appendix is the same as that given in the Nomenclature section. However, since the data are presented as computer printouts, the nomenclature that may cause confusion is summarized below:

RE	Reynolds number, $\underline{Re}$ in Nomenclature section
UAVG	Average velocity, $\bar{u}$ in Nomenclature section
DELTA HF	Static pressure drop as measured between the two pressure taps located on the loop downleg and indicated on a liquid/liquid differential manometer and listed in the tables as centimeters of manometer fluid
F	Fanning friction factor: $\underline{f}$ in Nomenclature section
S	Distance from the tube wall; $\underline{s}$ in Nomenclature section
DELTA HV	Pressure difference between impact and static pressure as sensed by an annular-purge impact probe and indicated on a liquid/liquid differential manometer as centimeters of CCl_4
UBAR	Time average velocity; $\bar{u}$ in Nomenclature section
SPLUS	s^+ in Nomenclature section
UPLUS	u^+ in Nomenclature section
POSITION	Scale reading indicated in centimeters; center line as noted
E FORMAT	The RE and F data are printed in this format representation. The following examples indicate how these numbers should be interpreted:

$$0.110E\ 05 = 0.110 \times 10^{5}$$

$$0.272E\text{-}02 = 0.272 \times 10^{-2}$$

RUN NO 052973W01

CONSISTENCY = 0.0 GR/100 ML
TEMPERATURE = 20.00 DEGREE C
VISCOSITY = 1.005 CENTIPOISE
MANOMETER FLUID-(MF) 1=CCL4 2=CB 3=HG

G GAL/MIN	Q CU FT/SEC	UAVG FT/SEC	DELTA HF CM (MF)	RE	F
42.0	0.094	2.1	2.95 (1)	0.462E 05	0.514E-02
66.5	0.148	3.3	37.15 (2)	0.732E 05	0.457E-02
66.5	0.148	3.3	6.75 (1)	0.732E 05	0.469E-02
73.8	0.164	3.7	45.65 (2)	0.812E 05	0.457E-02
73.8	0.164	3.7	8.30 (1)	0.812E 05	0.469E-02
78.0	0.174	3.9	49.00 (2)	0.859E 05	0.439E-02
78.0	0.174	3.9	8.90 (1)	0.859E 05	0.450E-02
101.5	0.226	5.1	79.90 (2)	0.112E 06	0.422E-02
101.5	0.226	5.1	14.30 (1)	0.112E 06	0.427E-02
117.0	0.261	5.9	106.00 (2)	0.129E 06	0.422E-02
117.0	0.261	5.9	19.25 (1)	0.129E 06	0.432E-02

RUN NO072273W1

CONSISTENCY = 0.0 GR/100 ML
TEMPERATURE = 25.00 DEGREE C
VISCOSITY = 0.894 CENTIPOISE
MANOMETER FLUID-(MF) 1=CCL4 2=CB 3=HG

G GAL/MIN	Q CU FT/SEC	UAVG FT/SEC	DELTA HF CM (MF)	RE	F
3.5	0.008	0.2	0.25 (2)	0.433E 04	0.111E-01
5.5	0.012	0.3	0.45 (2)	0.681E 04	0.810E-02
5.5	0.012	0.3	0.50 (2)	0.681E 04	0.900E-02
7.0	0.016	0.4	0.65 (2)	0.867E 04	0.722E-02
7.0	0.016	0.4	0.70 (2)	0.867E 04	0.778E-02
9.5	0.021	0.5	1.15 (2)	0.118E 05	0.694E-02
9.5	0.021	0.5	1.20 (2)	0.118E 05	0.724E-02
10.0	0.022	0.5	1.15 (2)	0.124E 05	0.626E-02
10.5	0.023	0.5	1.15 (2)	0.130E 05	0.568E-02
17.8	0.040	0.9	3.50 (2)	0.220E 05	0.605E-02
24.0	0.053	1.2	5.88 (2)	0.297E 05	0.555E-02
24.0	0.053	1.2	6.10 (2)	0.297E 05	0.577E-02
33.5	0.075	1.7	10.65 (2)	0.415E 05	0.517E-02
45.5	0.101	2.3	18.60 (2)	0.563E 05	0.489E-02
53.0	0.118	2.7	24.22 (2)	0.656E 05	0.470E-02
58.0	0.129	2.9	28.80 (2)	0.718E 05	0.466E-02
68.0	0.151	3.4	38.10 (2)	0.842E 05	0.449E-02
89.5	0.199	4.5	62.90 (2)	0.111E 06	0.428E-02
95.7	0.213	4.8	70.90 (2)	0.119E 06	0.422E-02
112.5	0.251	5.6	95.70 (2)	0.139E 06	0.412E-02
114.5	0.255	5.8	97.30 (2)	0.142E 06	0.404E-02
33.5	0.075	1.7	1.95 (1)	0.415E 05	0.534E-02
58.0	0.129	2.9	5.15 (1)	0.718E 05	0.471E-02
89.5	0.199	4.5	10.95 (1)	0.111E 06	0.420E-02
89.5	0.199	4.5	11.05 (1)	0.111E 06	0.424E-02
114.5	0.255	5.8	17.05 (1)	0.142E 06	0.400E-02

RUN NO 080373WFRE3

CONSISTENCY = 0.0 GR/100 ML
TEMPERATURE = 25.00 DEGREE C
VISCOSITY = 0.894 CENTIPOISE
MANOMETER FLUID-(MF) 1=CCL4 2=CB 3=HG

G GAL/MIN	Q CU FT/SEC	UAVG FT/SEC	DELTA HF CM (MF)	RE	F
13.5	0.030	0.7	2.25 (2)	0.167E 05	0.672E-02
28.5	0.063	1.4	8.70 (2)	0.353E 05	0.583E-02
39.0	0.087	2.0	14.90 (2)	0.483E 05	0.533E-02
50.5	0.113	2.5	23.25 (2)	0.625E 05	0.496E-02
70.0	0.156	3.5	41.20 (2)	0.867E 05	0.458E-02
90.5	0.202	4.5	65.50 (2)	0.112E 06	0.435E-02
110.0	0.245	5.5	93.00 (2)	0.136E 06	0.419E-02

RUN NO 081973FRE1

CONSISTENCY = 0.050 GR/100 ML
TEMPERATURE = 25.00 DEGREE C
VISCOSITY = 0.894 CENTIPOISE
MANOMETER FLUID-(MF) 1=CCL4 2=CB 3=HG

G GAL/MIN	Q CU FT/SEC	UAVG FT/SEC	DELTA HF CM (MF)	RE	F
50.5	0.113	2.5	21.85 (2)	0.625E 05	0.467E-02
70.0	0.156	3.5	40.60 (2)	0.867E 05	0.451E-02
90.5	0.202	4.5	63.25 (2)	0.112E 06	0.421E-02
110.0	0.245	5.5	91.10 (2)	0.136E 06	0.410E-02
38.5	0.086	1.9	13.10 (2)	0.477E 05	0.481E-02
110.0	0.245	5.5	89.60 (2)	0.136E 06	0.403E-02

RUN NO 081973FRE2

CONSISTENCY = 0.100 GR/100 ML
TEMPERATURE = 25.00 DEGREE C
VISCOSITY = 0.894 CENTIPOISE
MANOMETER FLUID-(MF) 1=CCL4 2=CB 3=HG

G GAL/MIN	Q CU FT/SEC	UAVG FT/SEC	DELTA HF CM (MF)	RE	F
50.5	0.113	2.5	20.65 (2)	0.625E 05	0.441E-02
70.0	0.156	3.5	38.25 (2)	0.867E 05	0.425E-02
90.5	0.202	4.5	61.80 (2)	0.112E 06	0.411E-02
110.0	0.245	5.5	89.60 (2)	0.136E 06	0.403E-02

RUN NO 081973FRE3

CONSISTENCY = 0.150 GR/100 ML
TEMPERATURE = 25.00 DEGREE C
VISCOSITY = 0.894 CENTIPOISE
MANOMETER FLUID-(MF) 1=CCL4 2=CB 3=HG

G GAL/MIN	Q CU FT/SEC	UAVG FT/SEC	DELTA HF CM (MF)	RE	F
44.5	0.099	2.2	14.10 (2)	0.551E 05	0.388E-02
50.5	0.113	2.5	17.90 (2)	0.625E 05	0.382E-02
70.0	0.156	3.5	36.35 (2)	0.867E 05	0.404E-02
83.0	0.185	4.2	50.20 (2)	0.103E 06	0.397E-02
90.5	0.202	4.5	59.25 (2)	0.112E 06	0.394E-02
110.0	0.245	5.5	85.20 (2)	0.136E 06	0.383E-02

RUN NO 072873F1

CONSISTENCY = 0.160 GR/100 ML
TEMPERATURE = 25.00 DEGREE C
VISCOSITY = 0.894 CENTIPOISE
MANOMETER FLUID-(MF) 1=CCL4 2=CB 3=HG

G GAL/MIN	Q CU FT/SEC	UAVG FT/SEC	DELTA HF CM	(MF)	RE	F
50.8	0.113	2.6	19.40	(2)	0.629E 05	0.409E-02
57.0	0.127	2.9	24.52	(2)	0.706E 05	0.411E-02
68.2	0.152	3.4	34.80	(2)	0.845E 05	0.407E-02
81.3	0.181	4.1	48.60	(2)	0.101E 06	0.400E-02
97.5	0.217	4.9	68.55	(2)	0.121E 06	0.393E-02
118.8	0.265	6.0	99.10	(2)	0.147E 06	0.382E-02
97.5	0.217	4.9	68.50	(2)	0.121E 06	0.392E-02
81.5	0.182	4.1	49.25	(2)	0.101E 06	0.404E-02
67.5	0.150	3.4	34.65	(2)	0.836E 05	0.414E-02
57.5	0.128	2.9	25.15	(2)	0.712E 05	0.414E-02
49.5	0.110	2.5	18.67	(2)	0.613E 05	0.415E-02
40.0	0.089	2.0	11.72	(2)	0.495E 05	0.399E-02
32.0	0.071	1.6	6.85	(2)	0.396E 05	0.364E-02
24.5	0.055	1.2	3.75	(2)	0.303E 05	0.340E-02
18.5	0.041	0.9	1.70	(2)	0.229E 05	0.270E-02
27.0	0.060	1.4	4.57	(2)	0.334E 05	0.342E-02
50.8	0.113	2.6	3.40	(1)	0.629E 05	0.405E-02
57.0	0.127	2.9	4.35	(1)	0.706E 05	0.411E-02
68.2	0.152	3.4	6.17	(1)	0.845E 05	0.408E-02
81.3	0.181	4.1	8.65	(1)	0.101E 06	0.402E-02
97.5	0.217	4.9	12.10	(1)	0.121E 06	0.391E-02
118.8	0.265	6.0	17.50	(1)	0.147E 06	0.381E-02
97.5	0.217	4.9	12.15	(1)	0.121E 06	0.393E-02
81.5	0.182	4.1	8.75	(1)	0.101E 06	0.405E-02
67.5	0.150	3.4	6.20	(1)	0.836E 05	0.418E-02
57.5	0.128	2.9	4.50	(1)	0.712E 05	0.418E-02
49.5	0.110	2.5	3.32	(1)	0.613E 05	0.417E-02
40.0	0.089	2.0	2.13	(1)	0.495E 05	0.408E-02

RUN NO 072373F1

CONSISTENCY = 0.162 GR/100 ML
TEMPERATURE = 25.00 DEGREE C
VISCOSITY = 0.894 CENTIPOISE
MANOMETER FLUID-(MF) 1=CCL4 2=CB 3=HG

G GAL/MIN	Q CU FT/SEC	UAVG FT/SEC	DELTA HF CM	(MF)	RE	F
23.5	0.052	1.2	2.60	(2)	0.291E 05	0.256E-02
26.7	0.059	1.3	3.90	(2)	0.331E 05	0.298E-02
35.5	0.079	1.8	8.15	(2)	0.440E 05	0.352E-02
42.0	0.094	2.1	12.70	(2)	0.520E 05	0.392E-02
44.7	0.100	2.2	14.30	(2)	0.554E 05	0.390E-02
51.5	0.115	2.6	19.90	(2)	0.638E 05	0.409E-02
53.0	0.118	2.7	20.00	(2)	0.656E 05	0.388E-02
62.0	0.138	3.1	28.15	(2)	0.768E 05	0.399E-02
67.5	0.150	3.4	33.65	(2)	0.836E 05	0.402E-02
77.3	0.172	3.9	43.30	(2)	0.957E 05	0.395E-02
94.5	0.211	4.7	64.60	(2)	0.117E 06	0.394E-02
116.7	0.260	5.9	95.70	(2)	0.145E 06	0.383E-02
26.7	0.059	1.3	0.70	(1)	0.331E 05	0.302E-02
35.5	0.079	1.8	1.40	(1)	0.440E 05	0.341E-02
53.0	0.118	2.7	3.54	(1)	0.656E 05	0.387E-02
62.0	0.138	3.1	4.95	(1)	0.768E 05	0.396E-02
67.5	0.150	3.4	5.92	(1)	0.836E 05	0.400E-02
77.3	0.172	3.9	7.60	(1)	0.957E 05	0.391E-02
94.5	0.211	4.7	11.35	(1)	0.117E 06	0.391E-02
116.7	0.260	5.9	16.80	(1)	0.145E 06	0.379E-02

RUN NO 081973FRE4

CONSISTENCY = 0.240 GR/100 ML
TEMPERATURE = 25.00 DEGREE C
VISCOSITY = 0.894 CENTIPOISE
MANOMETER FLUID-(MF) 1=CCL4 2=CB 3=HG

G GAL/MIN	Q CU FT/SEC	UAVG FT/SEC	DELTA HF CM (MF)	RE	F
50.5	0.113	2.5	16.40 (2)	0.625E 05	0.350E-02
70.0	0.156	3.5	31.80 (2)	0.867E 05	0.353E-02
76.0	0.169	3.8	38.15 (2)	0.941E 05	0.360E-02
90.5	0.202	4.5	53.75 (2)	0.112E 06	0.357E-02
110.0	0.245	5.5	79.55 (2)	0.136E 06	0.358E-02

RUN NO 072873F2

CONSISTENCY = 0.250 GR/100 ML
TEMPERATURE = 25.00 DEGREE C
VISCOSITY = 0.894 CENTIPOISE
MANOMETER FLUID-(MF) 1=CCL4 2=CB 3=HG

G GAL/MIN	Q CU FT/SEC	UAVG FT/SEC	DELTA HF CM (MF)	RE	F
31.5	0.070	1.6	5.11 (2)	0.390E 05	0.280E-02
40.5	0.090	2.0	9.63 (2)	0.502E 05	0.320E-02
50.5	0.113	2.5	15.65 (2)	0.625E 05	0.334E-02
57.0	0.127	2.9	20.15 (2)	0.706E 05	0.338E-02
66.8	0.149	3.4	29.22 (2)	0.827E 05	0.357E-02
81.3	0.181	4.1	42.35 (2)	0.101E 06	0.349E-02
97.5	0.217	4.9	61.35 (2)	0.121E 06	0.351E-02
120.0	0.267	6.0	91.40 (2)	0.149E 06	0.346E-02
120.5	0.268	6.1	92.50 (2)	0.149E 06	0.347E-02
130.0	0.290	6.5	106.80 (2)	0.161E 06	0.344E-02
40.5	0.090	2.0	1.67 (1)	0.502E 05	0.314E-02
50.5	0.113	2.5	2.78 (1)	0.625E 05	0.335E-02
57.0	0.127	2.9	3.65 (1)	0.706E 05	0.345E-02
66.8	0.149	3.4	5.17 (1)	0.827E 05	0.356E-02
81.3	0.181	4.1	7.50 (1)	0.101E 06	0.349E-02
97.5	0.217	4.9	10.80 (1)	0.121E 06	0.349E-02
120.0	0.267	6.0	16.00 (1)	0.149E 06	0.341E-02
120.5	0.268	6.1	16.20 (1)	0.149E 06	0.343E-02
130.0	0.290	6.5	18.85 (1)	0.161E 06	0.343E-02

RUN NO 072873F3

CONSISTENCY = 0.350 GR/100 ML
TEMPERATURE = 25.00 DEGREE C
VISCOSITY = 0.894 CENTIPOISE
MANOMETER FLUID-(MF) 1=CCL4 2=CB 3=HG

G GAL/MIN	Q CU FT/SEC	UAVG FT/SEC	DELTA HF CM (MF)	RE	F
66.5	0.148	3.3	27.10 (2)	0.824E 05	0.334E-02
57.5	0.128	2.9	20.20 (2)	0.712E 05	0.333E-02
50.5	0.113	2.5	15.80 (2)	0.625E 05	0.337E-02
40.5	0.090	2.0	10.15 (2)	0.502E 05	0.337E-02
37.5	0.084	1.9	8.57 (2)	0.464E 05	0.332E-02
30.0	0.067	1.5	4.70 (2)	0.372E 05	0.284E-02
33.5	0.075	1.7	6.20 (2)	0.415E 05	0.301E-02
45.0	0.100	2.3	12.55 (2)	0.557E 05	0.337E-02
80.5	0.179	4.0	39.10 (2)	0.997E 05	0.329E-02
97.5	0.217	4.9	57.00 (2)	0.121E 06	0.326E-02
118.8	0.265	6.0	84.00 (2)	0.147E 06	0.324E-02
131.0	0.292	6.6	100.90 (2)	0.162E 06	0.320E-02
66.5	0.148	3.3	4.80 (1)	0.824E 05	0.334E-02
57.5	0.128	2.9	3.60 (1)	0.712E 05	0.335E-02
50.5	0.113	2.5	2.80 (1)	0.625E 05	0.337E-02
40.5	0.090	2.0	1.88 (1)	0.502E 05	0.351E-02
80.5	0.179	4.0	6.82 (1)	0.997E 05	0.324E-02
97.5	0.217	4.9	9.95 (1)	0.121E 06	0.322E-02
118.8	0.265	6.0	14.65 (1)	0.147E 06	0.319E-02
131.0	0.292	6.6	17.70 (1)	0.162E 06	0.317E-02

CONSISTENCY = 0.0 GR/100 ML
TEMPERATURE = 25.00 DEGREE C
VISCOSITY = 0.894 CENTIPOISE
MANOMETER FLUID-(MF) 1=CCL4 2=CB 3=HG

RUN NO 080373WVP1

G GAL/MIN	Q CU FT/SEC	UAVG FT/SEC	DELTA HF CM (MF)	RE --	F --
50.5	0.113	2.5	23.25 (2)	0.625E 05	0.496E-02

VELOCITY PROFILE INFORMATION

CENTERLINE IS AT SCALE READING 8.10

POSITION SCALE RDG	RADIUS FT	S FT	DELTA HV CM CCL4	UBAR FT/SEC	SPLUS DIM	UPLUS DIM
8.20	0.0033	0.116	8.08	3.18	1514.8	25.18
11.00	0.0951	0.024	5.30	2.58	310.5	20.39
10.60	0.0820	0.037	5.85	2.71	482.6	21.42
10.20	0.0689	0.050	6.40	2.83	654.6	22.41
9.80	0.0558	0.063	6.95	2.95	826.7	23.35
9.40	0.0427	0.076	7.45	3.05	998.7	24.17
9.00	0.0295	0.089	7.78	3.12	1170.7	24.70
8.60	0.0164	0.102	8.00	3.17	1342.8	25.05
8.20	0.0033	0.116	8.10	3.18	1514.8	25.21
7.80	0.0098	0.109	8.10	3.18	1428.8	25.21
8.00	0.0033	0.116	8.15	3.19	1514.8	25.28
7.40	0.0230	0.096	7.93	3.15	1256.7	24.94
7.00	0.0361	0.083	7.65	3.09	1084.7	24.50
6.60	0.0492	0.070	7.20	3.00	912.7	23.76
6.20	0.0623	0.056	6.70	2.90	740.6	22.92
5.80	0.0755	0.043	6.28	2.80	568.6	22.19
5.40	0.0886	0.030	5.60	2.65	396.6	20.96
5.00	0.1017	0.017	4.70	2.43	224.5	19.20
6.00	0.0689	0.050	6.45	2.84	654.6	22.49
7.00	0.0361	0.083	7.58	3.08	1084.7	24.38
9.00	0.0295	0.089	7.85	3.14	1170.7	24.81
10.00	0.0623	0.056	6.93	2.95	740.6	23.31
11.40	0.1083	0.011	4.30	2.32	138.5	18.37
11.20	0.1017	0.017	4.70	2.43	224.5	19.20
8.10	0.0	0.119	8.15	3.19	1557.8	25.28

RUN NO 080373WVP2

G GAL/MIN	Q CU FT/SEC	UAVG FT/SEC	DELTA HF CM (MF)	RE --	F --
70.0	0.156	3.5	41.20 (2)	0.867E 05	0.458E-02

VELOCITY PROFILE INFORMATION

CENTERLINE IS AT SCALE READING 8.10

POSITION SCALE RDG	RADIUS FT	S FT	DELTA HV CM CCL4	UBAR FT/SEC	SPLUS DIM	UPLUS DIM
8.10	0.0	0.119	15.15	4.36	2073.7	25.90
5.00	0.1017	0.017	8.85	3.33	298.9	19.79
5.50	0.0853	0.034	10.65	3.65	585.1	21.71
6.00	0.0689	0.050	12.10	3.89	871.4	23.14
6.50	0.0525	0.066	13.20	4.07	1157.7	24.17

RUN NO 080373WVP2 CONT

POSITION SCALE RDG	RADIUS FT	S FT	DELTA HV CM CCL4	UBAR FT/SEC	SPLUS DIM	UPLUS DIM
7.00	0.0361	0.083	14.20	4.22	1443.9	25.07
7.50	0.0197	0.099	14.75	4.30	1730.2	25.55
8.00	0.0033	0.116	15.10	4.35	2016.5	25.85
8.50	0.0131	0.106	15.03	4.34	1844.7	25.79
9.00	0.0295	0.089	14.55	4.27	1558.5	25.38
9.50	0.0459	0.073	13.75	4.15	1272.2	24.67
10.00	0.0623	0.056	12.70	3.99	985.9	23.71
10.50	0.0787	0.040	11.45	3.79	699.7	22.51
11.00	0.0951	0.024	9.90	3.52	413.4	20.93
11.40	0.1083	0.011	8.10	3.18	184.4	18.94
11.20	0.1017	0.017	8.85	3.33	298.9	19.79
10.00	0.0623	0.056	12.50	3.96	985.9	23.52
8.30	0.0066	0.112	15.10	4.35	1959.2	25.85

RUN NO 080373WVP4

G GAL/MIN	Q CU FT/SEC	UAVG FT/SEC	DELTA HF CM (MF)	RE --	F --
90.5	0.202	4.5	65.50 (2)	0.112E 06	0.435E-02

VELOCITY PROFILE INFORMATION

CENTERLINE IS AT SCALE READING 8.10

POSITION SCALE RDG	RADIUS FT	S FT	DELTA HV CM CCL4	UBAR FT/SEC	SPLUS DIM	UPLUS DIM
8.30	0.0066	0.112	25.25	5.62	2470.3	26.51
11.40	0.1083	0.011	14.00	4.19	232.5	19.74
11.20	0.1017	0.017	15.30	4.38	376.9	20.64
11.00	0.0951	0.024	16.50	4.55	521.2	21.43
10.50	0.0787	0.040	19.37	4.92	882.2	23.22
10.00	0.0623	0.056	21.15	5.15	1243.1	24.27
9.50	0.0459	0.073	23.10	5.38	1604.1	25.36
9.00	0.0295	0.089	24.10	5.49	1965.0	25.90
8.50	0.0131	0.106	24.90	5.58	2326.0	26.33
8.00	0.0033	0.116	25.10	5.61	2542.5	26.44
7.50	0.0197	0.099	24.75	5.57	2181.6	26.25
7.00	0.0361	0.083	23.80	5.46	1820.6	25.74
6.50	0.0525	0.066	22.35	5.29	1459.7	24.95
6.00	0.0689	0.050	20.35	5.05	1098.7	23.80
5.50	0.0853	0.034	18.42	4.80	737.8	22.65
5.00	0.1017	0.017	15.20	4.36	376.9	20.57

RUN NO 080373WVP5

G GAL/MIN	Q CU FT/SEC	UAVG FT/SEC	DELTA HF CM (MF)	RE --	F --
110.0	0.245	5.5	93.00 (2)	0.136E 06	0.419E-02

VELOCITY PROFILE INFORMATION

CENTERLINE IS AT SCALE READING 8.10

POSITION SCALE RDG	RADIUS FT	S FT	DELTA HV CM CCL4	UBAR FT/SEC	SPLUS DIM	UPLUS DIM
5.00	0.1017	0.017	22.60	5.32	449.1	21.05
5.50	0.0853	0.034	26.50	5.76	879.1	22.80
6.00	0.0689	0.050	29.70	6.10	1309.2	24.13
6.50	0.0525	0.066	32.17	6.35	1739.3	25.12
7.00	0.0361	0.083	34.30	6.55	2169.4	25.93
7.50	0.0197	0.099	36.10	6.72	2599.5	26.61
8.00	0.0033	0.116	36.75	6.78	3029.6	26.85
8.50	0.0131	0.106	36.75	6.78	2771.5	26.85
7.90	0.0066	0.112	36.80	6.79	2943.6	26.86
9.00	0.0295	0.089	35.65	6.68	2341.5	26.44
9.50	0.0459	0.073	33.75	6.50	1911.4	25.73
10.00	0.0623	0.056	31.45	6.28	1481.3	24.83
10.50	0.0787	0.040	28.80	6.01	1051.2	23.76
11.00	0.0951	0.024	25.40	5.64	621.1	22.32
11.20	0.1017	0.017	22.85	5.35	449.1	21.17
11.40	0.1083	0.011	20.55	5.07	277.0	20.07
8.20	0.0033	0.116	36.82	6.79	3029.6	26.87
8.10	0.0	0.119	36.95	6.80	3115.6	26.92
7.80	0.0098	0.109	36.50	6.76	2857.6	26.75

CONSISTENCY = 0.050 GR/100 ML
TEMPERATURE = 25.00 DEGREE C
VISCOSITY = 0.894 CENTIPOISE
MANOMETER FLUID-(MF) 1=CCL4 2=CB 3=HG

RUN NO 081973FVP1

G GAL/MIN	Q CU FT/SEC	UAVG FT/SEC	DELTA HF CM (MF)	RE --	F --
50.5	0.113	2.5	21.85 (2)	0.625E 05	0.467E-02

VELOCITY PROFILE INFORMATION

CENTERLINE IS AT SCALE READING 8.10

POSITION SCALE RDG	RADIUS FT	S FT	DELTA HV CM CCL4	UBAR FT/SEC	SPLUS DIM	UPLUS DIM
8.00	0.0033	0.116	7.80	3.13	1468.5	25.52
7.00	0.0361	0.083	7.40	3.04	1051.5	24.85
6.00	0.0689	0.050	6.50	2.85	634.6	23.29
5.50	0.0853	0.034	5.35	2.59	426.1	21.13
5.00	0.1017	0.017	4.97	2.49	217.7	20.37
6.50	0.0525	0.066	6.77	2.91	843.1	23.77
7.50	0.0197	0.099	7.55	3.07	1260.0	25.10
8.50	0.0131	0.106	7.67	3.10	1343.4	25.30
9.50	0.0459	0.073	7.20	3.00	926.5	24.51
10.50	0.0787	0.040	6.00	2.74	509.5	22.38
11.00	0.0951	0.024	4.85	2.46	301.0	20.12
10.00	0.0623	0.056	6.50	2.85	718.0	23.29
9.00	0.0295	0.089	7.40	3.04	1134.9	24.85
8.00	0.0033	0.116	7.70	3.11	1468.5	25.35

RUN NO 081973FVP2

G GAL/MIN	Q CU FT/SEC	UAVG FT/SEC	DELTA HF CM (MF)	RE --	F --
70.0	0.156	3.5	40.60 (2)	0.867E 05	0.451E-02

VELOCITY PROFILE INFORMATION

CENTERLINE IS AT SCALE READING 8.10

POSITION SCALE RDG	RADIUS FT	S FT	DELTA HV CM CCL4	UBAR FT/SEC	SPLUS DIM	UPLUS DIM
8.00	0.0033	0.116	15.00	4.33	2001.7	25.96
9.00	0.0295	0.089	14.65	4.28	1547.1	25.65
10.00	0.0623	0.056	12.90	4.02	978.7	24.07
10.00	0.0623	0.056	12.70	3.99	978.7	23.88
11.00	0.0951	0.024	10.05	3.55	410.4	21.25
9.50	0.0459	0.073	13.35	4.09	1262.9	24.49
8.50	0.0131	0.106	14.75	4.30	1831.2	25.74
7.50	0.0197	0.099	14.75	4.30	1717.6	25.74
6.50	0.0525	0.066	13.30	4.08	1149.2	24.44
6.00	0.0689	0.050	12.30	3.92	865.0	23.51
5.50	0.0853	0.034	11.20	3.74	580.9	22.43
5.00	0.1017	0.017	9.60	3.47	296.7	20.77
7.00	0.0361	0.083	13.90	4.17	1433.4	24.99
8.20	0.0033	0.116	14.80	4.30	2001.7	25.78

RUN NO 081973FVP3

G GAL/MIN	Q CU FT/SEC	UAVG FT/SEC	DELTA HF CM (MF)	RE --	F --
90.5	0.202	4.5	63.25 (2)	0.112E 06	0.421E-02

VELOCITY PROFILE INFORMATION

CENTERLINE IS AT SCALE READING 8.10

POSITION SCALE RDG	RADIUS FT	S FT	DELTA HV CM CCL4	UBAR FT/SEC	SPLUS DIM	UPLUS DIM
8.10	0.0	0.119	24.70	5.56	2569.4	26.69
8.00	0.0033	0.116	24.75	5.57	2498.5	26.71
7.00	0.0361	0.083	23.25	5.40	1789.1	25.89
6.00	0.0689	0.050	20.35	5.05	1079.7	24.22
5.00	0.1017	0.017	15.55	4.41	370.3	21.17
5.50	0.0853	0.034	18.10	4.76	725.0	22.84
6.50	0.0525	0.066	21.70	5.21	1434.4	25.01
7.50	0.0197	0.099	23.92	5.47	2143.8	26.26
8.00	0.0033	0.116	24.55	5.54	2498.5	26.61
8.50	0.0131	0.106	24.55	5.54	2285.7	26.61
9.00	0.0295	0.089	23.85	5.46	1931.0	26.22
10.00	0.0623	0.056	21.05	5.13	1221.6	24.64
11.00	0.0951	0.024	16.50	4.55	512.2	21.81
10.50	0.0787	0.040	18.60	4.83	866.9	23.16
9.50	0.0459	0.073	22.40	5.30	1576.3	25.41
8.00	0.0033	0.116	24.45	5.53	2498.5	26.55

RUN NO 081973FVP4

G GAL/MIN	Q CU FT/SEC	UAVG FT/SEC	DELTA HF CM (MF)	RE --	F --
110.0	0.245	5.5	91.10 (2)	0.136E 06	0.410E-02

VELOCITY PROFILE INFORMATION

CENTERLINE IS AT SCALE READING 8.10

POSITION SCALE RDG	RADIUS FT	S FT	DELTA HV CM CCL4	UBAR FT/SEC	SPLUS DIM	UPLUS DIM
8.00	0.0033	0.116	36.25	6.74	2998.5	26.94
8.50	0.0131	0.106	36.30	6.74	2743.1	26.96
9.00	0.0295	0.089	35.05	6.62	2317.4	26.49
9.50	0.0459	0.073	33.25	6.45	1891.7	25.80
10.00	0.0623	0.056	30.70	6.20	1466.1	24.79
10.50	0.0787	0.040	27.80	5.90	1040.4	23.59
11.00	0.0951	0.024	24.40	5.53	614.7	22.10
11.40	0.1083	0.011	19.90	4.99	274.2	19.96
9.15	0.0344	0.084	35.25	6.64	2189.7	26.56
7.50	0.0197	0.099	35.85	6.70	2572.8	26.79
7.00	0.0361	0.083	34.60	6.58	2147.1	26.32
6.50	0.0525	0.066	32.50	6.38	1721.5	25.51
6.00	0.0689	0.050	30.15	6.14	1295.8	24.57
5.50	0.0853	0.034	27.10	5.83	870.1	23.29
5.00	0.1017	0.017	23.10	5.38	444.4	21.50
8.20	0.0033	0.116	36.55	6.77	2998.5	27.05

CONSISTENCY = 0.100 GR/100 ML
TEMPERATURE = 25.00 DEGREE C
VISCOSITY = 0.894 CENTIPOISE
MANOMETER FLUID-(MF) 1=CCL4 2=CB 3=HG

RUN NO 081973FVP5

G GAL/MIN	Q CU FT/SEC	UAVG FT/SEC	DELTA HF CM (MF)	RE	F
50.5	0.113	2.5	20.65 (2)	0.625E 05	0.441E-02

VELOCITY PROFILE INFORMATION

CENTERLINE IS AT SCALE READING 8.10

POSITION SCALE RDG	RADIUS FT	S FT	DELTA HV CM CCL4	UBAR FT/SEC	SPLUS DIM	UPLUS DIM
8.20	0.0033	0.116	8.03	3.17	1427.6	26.63
8.50	0.0131	0.106	7.97	3.16	1306.0	26.53
9.00	0.0295	0.089	7.75	3.12	1103.3	26.16
9.50	0.0459	0.073	6.83	2.92	900.7	24.56
10.00	0.0623	0.056	0.0	0.0	698.0	0.0
10.50	0.0787	0.040	6.00	2.74	495.3	23.02
10.80	0.0886	0.030	5.53	2.63	373.7	22.10
8.00	0.0033	0.116	7.87	3.14	1427.6	26.36
7.00	0.0361	0.083	7.60	3.08	1022.3	25.91
6.00	0.0689	0.050	6.55	2.86	616.9	24.05
5.50	0.0853	0.034	5.50	2.62	414.3	22.04

RUN NO 081973FVP6

G GAL/MIN	Q CU FT/SEC	UAVG FT/SEC	DELTA HF CM (MF)	RE	F
70.0	0.156	3.5	38.25 (2)	0.867E 05	0.425E-02

VELOCITY PROFILE INFORMATION

CENTERLINE IS AT SCALE READING 8.10

POSITION SCALE RDG	RADIUS FT	S FT	DELTA HV CM CCL4	UBAR FT/SEC	SPLUS DIM	UPLUS DIM
8.00	0.0033	0.116	15.05	4.34	1942.9	26.79
9.00	0.0295	0.089	14.55	4.27	1501.6	26.34
10.00	0.0623	0.056	12.80	4.00	950.0	24.70
10.50	0.0787	0.040	11.65	3.82	674.1	23.57
7.00	0.0361	0.083	14.30	4.23	1391.3	26.11
6.00	0.0689	0.050	12.40	3.94	839.6	24.31

RUN NO 081973FVP7

G GAL/MIN	Q CU FT/SEC	UAVG FT/SEC	DELTA HF CM (MF)	RE --	F --
90.5	0.202	4.5	61.80 (2)	0.112E 06	0.411E-02

VELOCITY PROFILE INFORMATION

CENTERLINE IS AT SCALE READING 8.10

POSITION SCALE RDG	RADIUS FT	S FT	DELTA HV CM CCL4	UBAR FT/SEC	SPLUS DIM	UPLUS DIM
6.00	0.0689	0.050	20.40	5.05	1067.3	24.54
7.00	0.0361	0.083	23.30	5.40	1768.5	26.22
8.00	0.0033	0.116	24.90	5.58	2469.7	27.11
9.00	0.0295	0.089	24.10	5.49	1908.7	26.67
10.00	0.0623	0.056	21.10	5.14	1207.5	24.95
10.50	0.0787	0.040	19.30	4.92	856.9	23.87

RUN NO 081973FVP8

G GAL/MIN	Q CU FT/SEC	UAVG FT/SEC	DELTA HF CM (MF)	RE --	F --
110.0	0.245	5.5	89.60 (2)	0.136E 06	0.403E-02

VELOCITY PROFILE INFORMATION

CENTERLINE IS AT SCALE READING 8.10

POSITION SCALE RDG	RADIUS FT	S FT	DELTA HV CM CCL4	UBAR FT/SEC	SPLUS DIM	UPLUS DIM
10.50	0.0787	0.040	28.15	5.94	1031.8	23.94
10.00	0.0623	0.056	30.30	6.16	1453.9	24.83
9.00	0.0295	0.089	34.90	6.61	2298.3	26.65
8.00	0.0033	0.116	36.25	6.74	2973.7	27.16
8.50	0.0131	0.106	36.05	6.72	2720.4	27.09
7.50	0.0197	0.099	35.60	6.68	2551.6	26.92
7.00	0.0361	0.083	34.35	6.56	2129.4	26.44

CONSISTENCY = 0.150 GR/100 ML
TEMPERATURE = 25.00 DEGREE C
VISCOSITY = 0.894 CENTIPOISE
MANOMETER FLUID-(MF) 1=CCL4 2=CB 3=HG

RUN NO 081973FVP9

G GAL/MIN	Q CU FT/SEC	UAVG FT/SEC	DELTA HF CM (MF)	RE	F
50.5	0.113	2.5	17.90 (2)	0.625E 05	0.382E-02

VELOCITY PROFILE INFORMATION

CENTERLINE IS AT SCALE READING 8.10

POSITION SCALE RDG	RADIUS FT	S FT	DELTA HV CM CCL4	UBAR FT/SEC	SPLUS DIM	UPLUS DIM
7.00	0.0361	0.083	7.80	3.13	951.8	28.19
6.50	0.0525	0.066	7.35	3.03	763.1	27.36
6.00	0.0689	0.050	6.70	2.90	574.4	26.13
5.50	0.0853	0.034	5.55	2.64	385.7	23.78
7.50	0.0197	0.099	8.00	3.17	1140.5	28.55
8.00	0.0033	0.116	8.10	3.18	1329.1	28.73
8.20	0.0033	0.116	8.17	3.20	1329.1	28.85
8.50	0.0131	0.106	8.09	3.18	1215.9	28.71
9.00	0.0295	0.089	8.00	3.17	1027.2	28.55
9.50	0.0459	0.073	7.50	3.06	838.5	27.64
10.00	0.0623	0.056	6.90	2.94	649.9	26.51
10.50	0.0787	0.040	5.90	2.72	461.2	24.52

RUN NO 081973FVP10

G GAL/MIN	Q CU FT/SEC	UAVG FT/SEC	DELTA HF CM (MF)	RE	F
70.0	0.156	3.5	36.35 (2)	0.867E 05	0.404E-02

VELOCITY PROFILE INFORMATION

CENTERLINE IS AT SCALE READING 8.10

POSITION SCALE RDG	RADIUS FT	S FT	DELTA HV CM CCL4	UBAR FT/SEC	SPLUS DIM	UPLUS DIM
10.50	0.0787	0.040	11.50	3.79	657.2	24.02
10.00	0.0623	0.056	13.05	4.04	926.1	25.59
9.50	0.0459	0.073	14.05	4.19	1195.0	26.55
9.00	0.0295	0.089	14.75	4.30	1463.9	27.20
8.50	0.0131	0.106	15.40	4.39	1732.7	27.80
8.00	0.0033	0.116	15.40	4.39	1894.1	27.80
7.50	0.0197	0.099	15.25	4.37	1625.2	27.66
7.00	0.0361	0.083	14.50	4.26	1356.3	26.97
6.00	0.0689	0.050	12.40	3.94	818.5	24.94
5.50	0.0853	0.034	11.00	3.71	549.6	23.49

RUN NO 081973FVP11

G GAL/MIN	Q CU FT/SEC	UAVG FT/SEC	DELTA HF CM (MF)	RE --	F --
90.5	0.202	4.5	59.25 (2)	0.112E 06	0.394E-02

VELOCITY PROFILE INFORMATION

CENTERLINE IS AT SCALE READING 8.10

POSITION SCALE RDG	RADIUS FT	S FT	DELTA HV CM CCL4	UBAR FT/SEC	SPLUS DIM	UPLUS DIM
6.00	0.0689	0.050	20.10	5.02	1045.0	24.87
7.00	0.0361	0.083	23.40	5.41	1731.6	26.84
7.50	0.0197	0.099	24.40	5.53	2074.9	27.40
8.00	0.0033	0.116	24.95	5.59	2418.2	27.71
8.50	0.0131	0.106	24.85	5.58	2212.2	27.66
9.00	0.0295	0.089	24.05	5.49	1868.9	27.21
9.50	0.0459	0.073	22.90	5.35	1525.6	26.55
10.00	0.0623	0.056	21.15	5.15	1182.3	25.51
10.50	0.0787	0.040	19.20	4.90	839.0	24.31

RUN NO 081973 FVP12

G GAL/MIN	Q CU FT/SEC	UAVG FT/SEC	DELTA HF CM (MF)	RE --	F --
110.0	0.245	5.5	85.20 (2)	0.136E 06	0.383E-02

VELOCITY PROFILE INFORMATION

CENTERLINE IS AT SCALE READING 8.10

POSITION SCALE RDG	RADIUS FT	S FT	DELTA HV CM CCL4	UBAR FT/SEC	SPLUS DIM	UPLUS DIM
10.50	0.0787	0.040	27.50	5.87	1006.1	24.26
10.00	0.0623	0.056	30.70	6.20	1417.8	25.63
9.50	0.0459	0.073	32.80	6.41	1829.5	26.50
9.00	0.0295	0.089	34.50	6.57	2241.1	27.17
8.50	0.0131	0.106	35.85	6.70	2652.8	27.70
8.00	0.0033	0.116	36.10	6.72	2899.8	27.80
7.50	0.0197	0.099	35.70	6.69	2488.1	27.64
7.00	0.0361	0.083	34.50	6.57	2076.5	27.17
6.50	0.0525	0.066	32.40	6.37	1664.8	26.33
6.00	0.0689	0.050	30.20	6.15	1253.1	25.43
5.50	0.0853	0.034	26.95	5.81	841.5	24.02

CONSISTENCY = 0.240 GR/100 ML
TEMPERATURE = 25.00 DEGREE C
VISCOSITY = 0.894 CENTIPOISE
MANOMETER FLUID-(MF) 1=CCL4 2=CB 3=HG

RUN NO 081973FVP13

G GAL/MIN	Q CU FT/SEC	UAVG FT/SEC	DELTA HF CM (MF)	RE	F
50.5	0.113	2.5	16.40 (2)	0.625E 05	0.350E-02

VELOCITY PROFILE INFORMATION

CENTERLINE IS AT SCALE READING 8.10

POSITION SCALE RDG	RADIUS FT	S FT	DELTA HV CM CCL4	UBAR FT/SEC	SPLUS DIM	UPLUS DIM
6.00	0.0689	0.050	6.80	2.92	549.8	27.50
6.50	0.0525	0.066	7.20	3.00	730.4	28.30
7.00	0.0361	0.083	7.40	3.04	911.0	28.69
7.50	0.0197	0.099	7.60	3.08	1091.6	29.07
8.00	0.0033	0.116	7.50	3.06	1272.2	28.88
9.00	0.0295	0.089	7.40	3.04	983.3	28.69
9.50	0.0459	0.073	6.90	2.94	802.6	27.70
10.00	0.0623	0.056	6.52	2.86	622.0	26.93

RUN NO 081973FVP14

G GAL/MIN	Q CU FT/SEC	UAVG FT/SEC	DELTA HF CM (MF)	RE	F
70.0	0.156	3.5	31.80 (2)	0.867E 05	0.353E-02

VELOCITY PROFILE INFORMATION

CENTERLINE IS AT SCALE READING 8.10

POSITION SCALE RDG	RADIUS FT	S FT	DELTA HV CM CCL4	UBAR FT/SEC	SPLUS DIM	UPLUS DIM
10.00	0.0623	0.056	13.15	4.06	866.2	27.46
10.50	0.0787	0.040	11.85	3.85	614.7	26.07
9.50	0.0459	0.073	13.90	4.17	1117.7	28.23
9.00	0.0295	0.089	14.25	4.22	1369.2	28.59
8.50	0.0131	0.106	14.35	4.24	1620.7	28.69
8.00	0.0033	0.116	14.25	4.22	1771.6	28.59
7.50	0.0197	0.099	14.15	4.21	1520.1	28.49
7.00	0.0361	0.083	14.05	4.19	1268.6	28.39
6.50	0.0525	0.066	13.83	4.16	1017.1	28.16
5.90	0.0722	0.047	12.70	3.99	715.3	26.99

RUN NO 081973FVP15

G GAL/MIN	Q CU FT/SEC	UAVG FT/SEC	DELTA HF CM (MF)		RE --	F --
90.5	0.202	4.5	53.75	(2)	0.112E 06	0.357E-02

VELOCITY PROFILE INFORMATION

CENTERLINE IS AT SCALE READING 8.10

POSITION SCALE RDG	RADIUS FT	S FT	DELTA HV CM CCL4	UBAR FT/SEC	SPLUS DIM	UPLUS DIM
6.00	0.0689	0.050	20.80	5.10	995.3	26.57
6.50	0.0525	0.066	22.83	5.35	1322.3	27.83
7.00	0.0361	0.083	23.65	5.44	1649.3	28.33
7.50	0.0197	0.099	24.55	5.54	1976.2	28.86
8.10	0.0	0.119	24.80	5.57	2368.6	29.01
8.50	0.0131	0.106	24.93	5.59	2107.0	29.08
9.00	0.0295	0.089	24.75	5.57	1780.1	28.98
10.00	0.0623	0.056	22.00	5.25	1126.1	27.32
10.50	0.0787	0.040	19.50	4.94	799.1	25.72

RUN NO 081973FVP16

G GAL/MIN	Q CU FT/SEC	UAVG FT/SEC	DELTA HF CM (MF)		RE --	F --
110.0	0.245	5.5	79.55	(2)	0.136E 06	0.358E-02

VELOCITY PROFILE INFORMATION

CENTERLINE IS AT SCALE READING 8.10

POSITION SCALE RDG	RADIUS FT	S FT	DELTA HV CM CCL4	UBAR FT/SEC	SPLUS DIM	UPLUS DIM
11.00	0.0951	0.024	24.35	5.52	574.4	23.63
10.50	0.0787	0.040	27.90	5.91	972.2	25.29
10.00	0.0623	0.056	31.60	6.29	1370.0	26.92
9.50	0.0459	0.073	34.25	6.55	1767.8	28.02
9.00	0.0295	0.089	35.85	6.70	2165.5	28.67
8.50	0.0131	0.106	36.65	6.77	2563.3	28.99
8.00	0.0033	0.116	36.60	6.77	2802.0	28.97
7.50	0.0197	0.099	36.45	6.76	2404.2	28.91
7.00	0.0361	0.083	35.75	6.69	2006.4	28.63
6.00	0.0689	0.050	30.70	6.20	1210.9	26.53

APPENDIX III

AUTOCORRELATION DATA

Autocorrelation data used to determine longitudinal scale factors presented in the text are presented in this Appendix. Several representative plots of the autocorrelation function versus time lag are presented first (Fig. 54-57) with Tables III and IV presenting the bulk of the data.

Table III lists representative autocorrelation versus time lag points for different consistencies, Reynolds numbers, and positions in the flow tube. Also listed in Table III is the local velocity and the area under each of the curves represented by the data points. Additional areas under the autocorrelation function are presented in Table IV.

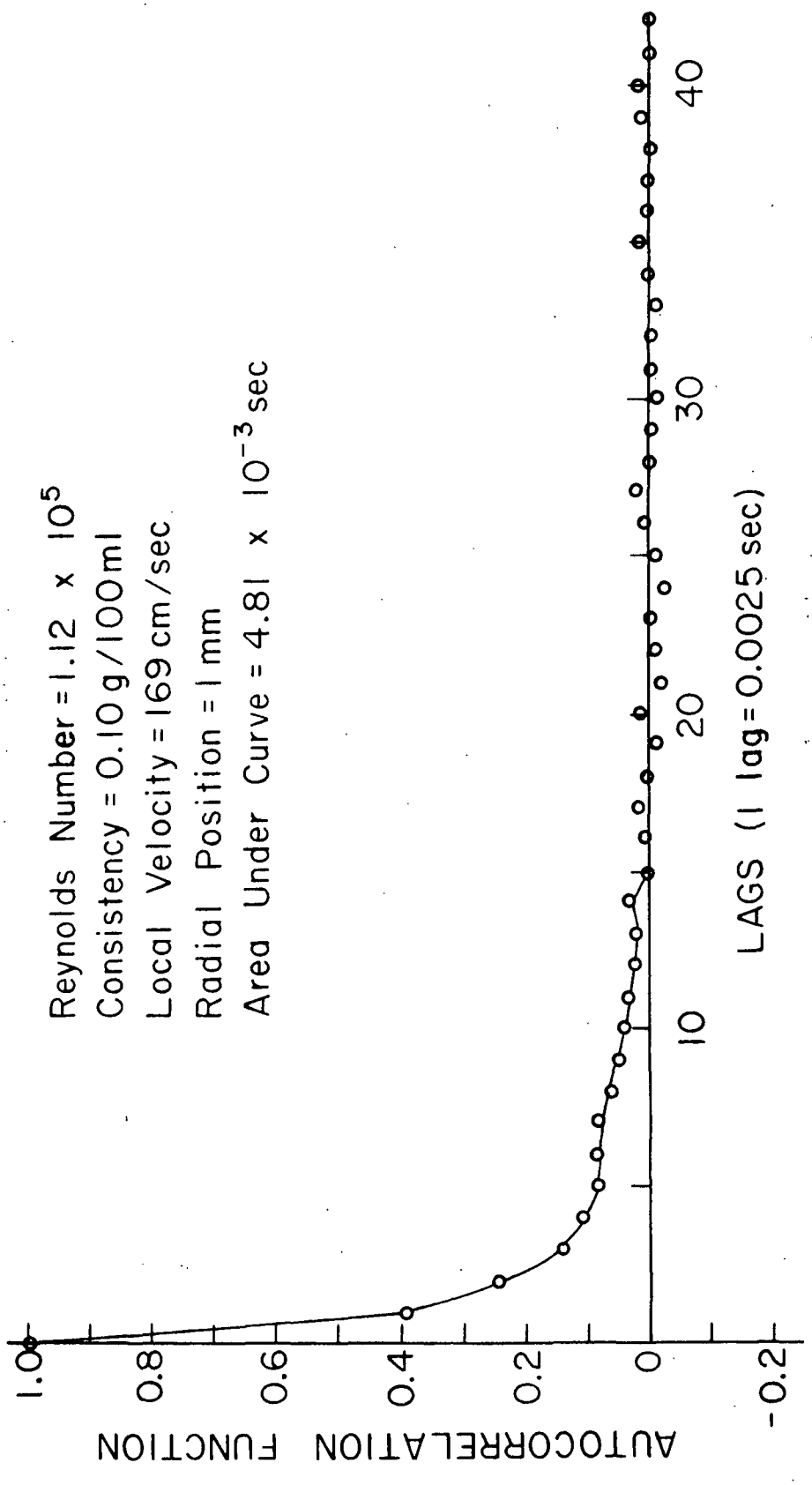

Figure 54. Autocorrelation Function vs. Time Lag

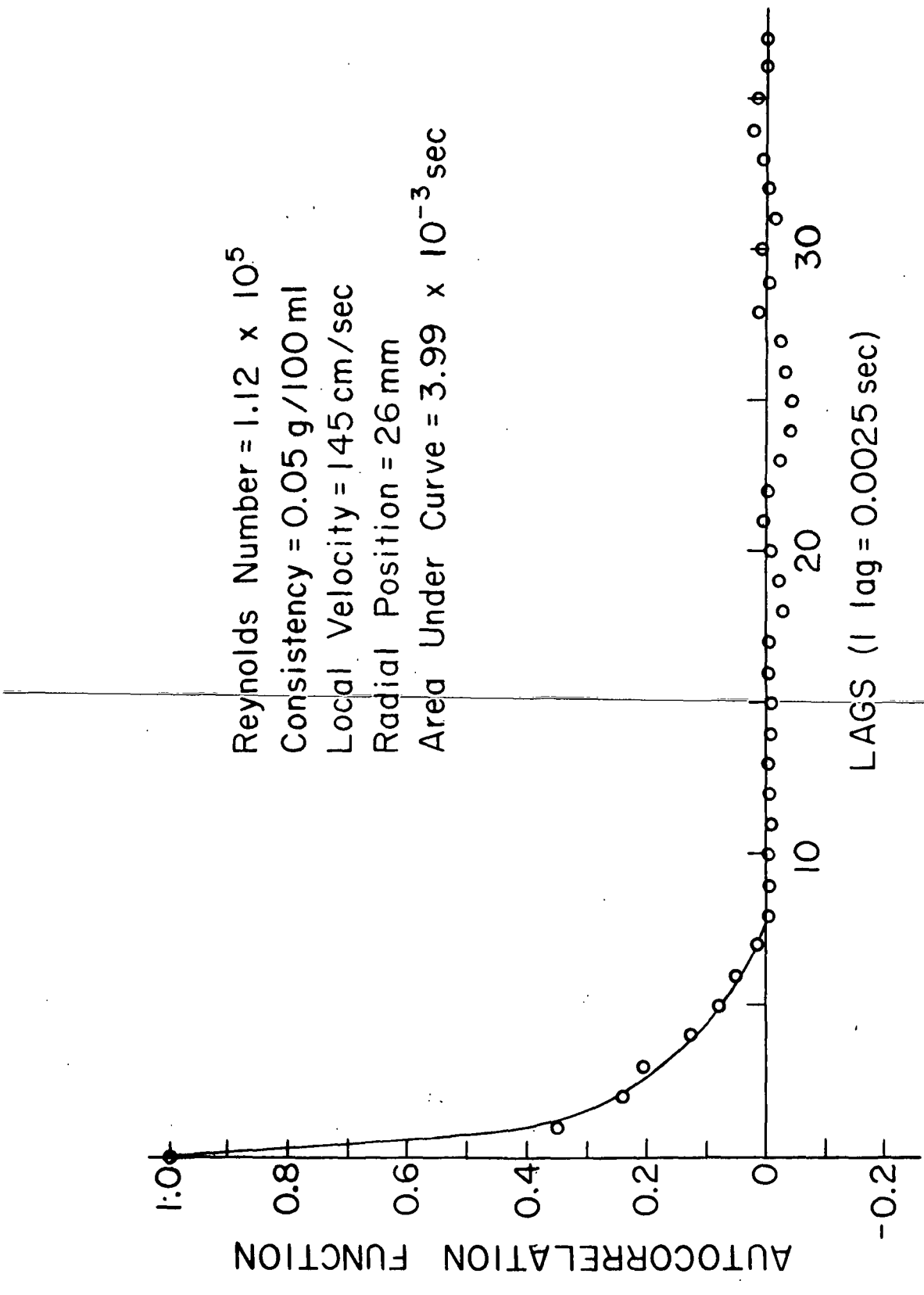

Figure 55. Autocorrelation Function vs. Time Lag

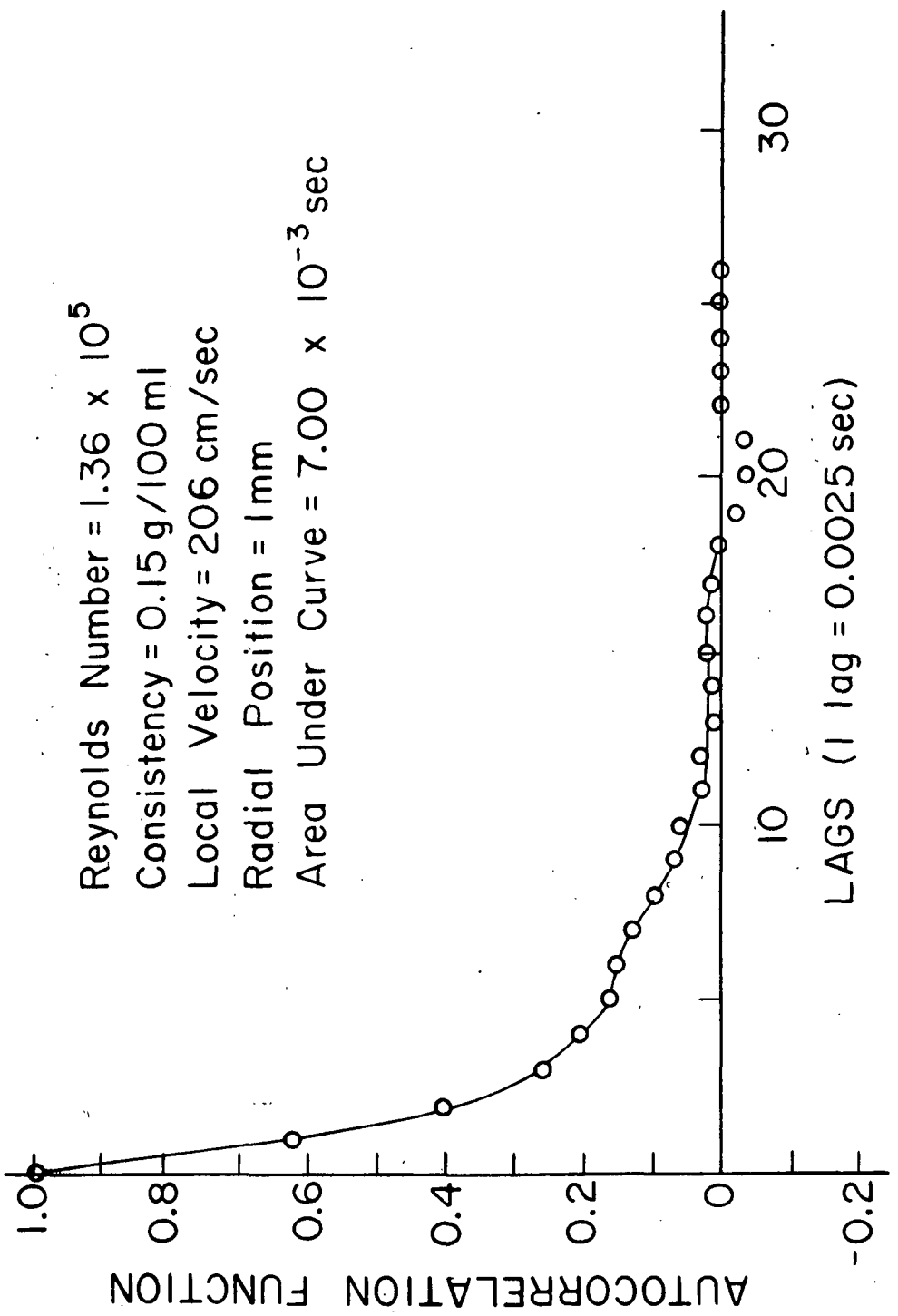

Figure 56. Autocorrelation Function vs. Time Lag

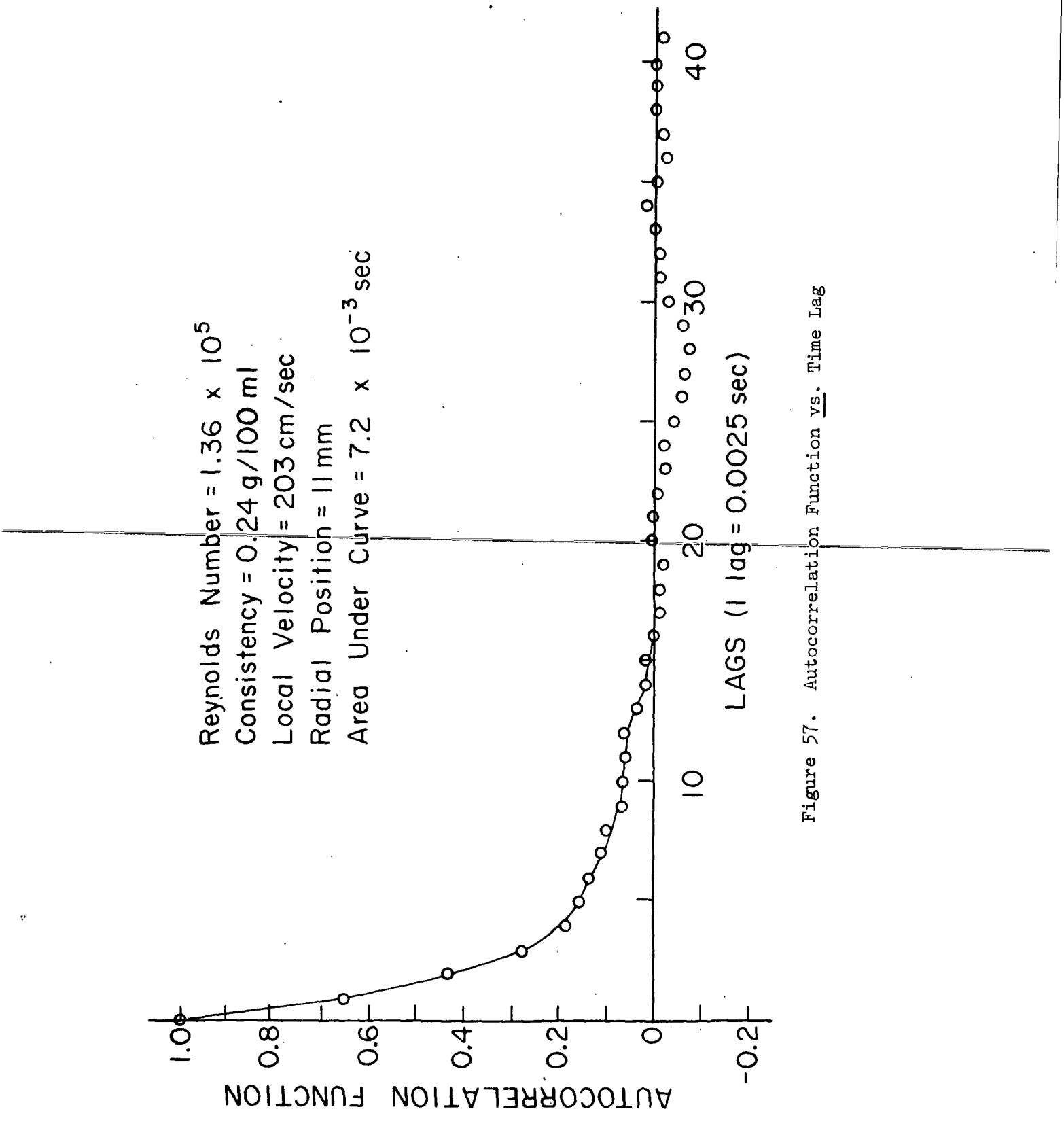

Figure 57. Autocorrelation Function vs. Time Lag

TABLE III

REPRESENTATIVE AUTOCORRELATION DATA

Consistency, g/100 ml	0.05						
Reynolds Number × 10^{-4}	8.67		11.20	13.60			
Radial Position, mm	1	18	26	6	11	16	21
Local Velocity, cm/sec	131	122	145	204	200	193	184
Lag in Seconds							
0.0	1.000	1.000	1.000	1.000	1.000	1.000	1.000
0.0025	0.712	0.597	0.353	0.103	0.069	0.063	0.089
0.0050	0.494	0.385	0.243	0.071	0.033	0.035	0.061
0.0075	0.350	0.246	0.214	0.052	0.037	0.092	0.048
0.0100	0.230	0.124	0.128	0.049	0.022	0.027	0.025
0.0125	0.169	0.068	0.084	0.038	0.034	0.023	0.024
0.0150	0.127	0.017	0.054	0.029	0.085	0.021	0.016
0.0175	0.093	0.006	0.019	0.030	0.011	0.026	0.004
0.0200	0.072	-0.018	0.003	0.028	-0.002	0.022	-0.003
0.0225	0.063	-0.027	-0.007	0.024	-0.004	0.020	-0.000
0.0250	0.042	-0.048	-0.008	0.021	0.011	0.021	0.007
0.0275	0.034	-0.060	-0.005	0.012	0.003	0.012	-0.010
0.0300	0.025	-0.046	0.004	-0.004	0.002	0.019	0.001
0.0325	0.010	-0.039	0.005	-0.003	-0.002	0.018	-0.012
0.0350	0.019	-0.035	-0.001	-0.003	-0.018	0.014	-0.015
0.0375	0.028	-0.014	-0.007	0.006	-0.008	0.009	-0.024
0.0400	0.019	-0.018	-0.009	0.024	0.010	-0.003	-0.022
0.0425	-0.007	0.008	-0.022	-0.012	0.000	-0.003	-0.012
0.0450	-0.028	-0.003	-0.014	-0.005	-0.005	-0.000	-0.007
0.0475	-0.040	-0.009	0.008	-0.007	-0.003	-0.016	-0.013
0.0500	-0.039	0.001	0.010	-0.016	-0.019	-0.008	0.001
0.0525	-0.045	-0.018	0.005	-0.009	0.007	0.065	-0.011
0.0550	-0.051	-0.029	-0.018	0.001	0.010	-0.008	-0.006
0.0575	-0.039	-0.026	-0.028	-0.007	0.132	-0.001	-0.002
0.0600	-0.017	-0.019	-0.035	0.004	-0.014	-0.001	-0.000
0.0625	-0.003	0.001	-0.024	0.010	-0.015	-0.004	0.012
0.0650	0.007	0.007	-0.015	-0.006	-0.003	-0.002	0.023
0.0675	0.012	0.030	0.013	-0.015	-0.016	-0.016	0.006
0.0700	0.013	0.035	-0.010	-0.000	-0.003	-0.007	-0.005
0.0725	0.035	0.037	0.012	-0.007	-0.004	-0.013	0.002
0.0750	0.042	0.046	-0.013	-0.003	-0.005	-0.006	0.003
0.0775	0.037	0.019	0.003	-0.003	0.003	-0.010	0.016
0.0800	0.020	0.011	0.013	-0.009	0.020	0.005	0.021
0.0825	0.004	-0.023	0.029	-0.010	0.014	-0.002	0.009
0.0850	-0.033	-0.048	0.025	-0.010	-0.002	-0.013	0.009
0.0875	-0.044	-0.073	0.008	-0.014	0.001	0.002	0.009
0.0900	-0.047	-0.077	-0.006	-0.007	-0.007	-0.003	0.013
0.0925	-0.037	-0.067	-0.030	0.091	-0.015	-0.005	-0.007
0.0950	-0.038	-0.052	-0.005	-0.010	-0.014	-0.011	-0.010
0.0975	-0.044	-0.044	0.011	-0.009	-0.015	-0.002	-0.007
0.1000	-0.026	-0.044	-0.025	-0.020	-0.006	-0.003	-0.002
Area under curve[a]	6.0	4.84	3.99	2.39	1.98	2.28	1.91

[a] To first zero crossing; × 10^3 sec.

TABLE III (Continued)

REPRESENTATIVE AUTOCORRELATION DATA

Consistency, g/100 ml	0.05	0.10					
Reynolds Number × 10^{-4}	13.6	6.25				8.67	
Radial Position, mm	26	1	9	18	24	1	9
Local Velocity, cm/sec	174	98	97	91	83	134	131
Lag in Seconds							
0.0	1.000	1.000	1.000	1.000	1.000	1.000	1.000
0.0025	0.103	0.735	0.702	0.714	0.743	0.627	0.605
0.0050	0.052	0.574	0.539	0.528	0.599	0.401	0.377
0.0075	0.046	0.473	0.412	0.388	0.495	0.291	0.243
0.0100	0.029	0.414	0.342	0.324	0.414	0.220	0.121
0.0125	0.014	0.345	0.276	0.265	0.351	0.185	0.071
0.0150	0.004	0.300	0.215	0.209	0.294	0.177	0.084
0.0175	0.004	0.260	0.170	0.146	0.268	0.189	0.133
0.0200	0.016	0.231	0.141	0.114	0.246	0.175	0.172
0.0225	0.006	0.210	0.125	0.110	0.223	0.141	0.173
0.0250	0.003	0.215	0.110	0.106	0.202	0.096	0.172
0.0275	-0.006	0.218	0.101	0.096	0.169	0.061	0.130
0.0300	-0.012	0.214	0.086	0.093	0.147	0.017	0.082
0.0325	-0.014	0.208	0.095	0.080	0.124	0.013	0.083
0.0350	-0.021	0.191	0.098	0.086	0.095	0.017	0.071
0.0375	-0.010	0.169	0.097	0.090	0.068	0.027	0.059
0.0400	-0.009	0.160	0.114	0.071	0.051	0.024	0.078
0.0425	-0.026	0.156	0.085	0.058	0.055	0.029	0.059
0.0450	-0.012	0.151	0.079	0.047	0.037	0.001	0.046
0.0475	-0.020	0.129	0.090	0.039	0.019	-0.006	0.040
0.0500	-0.014	0.107	0.104	0.030	0.014	-0.018	0.017
0.0525	-0.011	0.091	0.089	0.019	0.001	-0.022	0.033
0.0550	0.000	0.063	0.066	0.022	-0.018	-0.018	0.048
0.0575	-0.013	0.043	0.063	0.033	-0.018	-0.017	0.038
0.0600	-0.018	0.028	0.075	0.043	-0.032	-0.009	0.020
0.0625	-0.022	0.002	0.076	0.023	-0.019	0.003	-0.018
0.0650	-0.022	0.002	0.076	0.023	-0.019	0.003	-0.032
0.0675	-0.005	0.002	0.082	0.028	-0.017	-0.005	-0.036
0.0700	-0.004	0.006	0.008	0.032	0.007	0.012	-0.040
0.0725	-0.002	0.029	0.085	0.010	0.019	0.013	-0.010
0.0750	0.004	0.017	0.066	0.016	0.028	-0.000	0.001
0.0775	0.018	0.030	0.051	0.008	0.015	0.023	0.013
0.0800	0.014	0.029	0.049	0.003	0.018	0.013	0.019
0.0825	0.013	0.027	0.032	-0.006	0.008	0.012	-0.015
0.0850	-0.010	0.020	0.007	-0.006	0.003	0.009	-0.025
0.0875	-0.004	0.010	-0.008	-0.031	0.004	0.017	-0.052
0.0900	0.001	0.019	-0.013	-0.062	0.008	0.001	-0.031
0.0925	0.019	0.022	-0.011	-0.072	-0.002	0.002	-0.005
0.0950	0.029	0.017	-0.023	-0.082	-0.003	-0.006	-0.008
0.0975	0.006	0.015	-0.047	-0.065	0.005	-0.019	-0.001
0.1000	0.016	0.013	-0.049	-0.069	0.000	-0.007	-0.023
Area under curve[a]	1.86	15.51	13.39	10.87	12.79	7.98	8.6

[a] To first zero crossing; × 10^3 sec.

TABLE III (Continued)

REPRESENTATIVE AUTOCORRELATION DATA

Consistency, g/100 ml	0.10						
Reynolds Number × 10^{-4}	8.67		11.20				13.60
Radial Position, mm	18	26	1	9	18	26	1
Local Velocity, cm/sec	124	111	169	168	161	143	207
Lag in Seconds							
0.0	1.000	1.000	1.000	1.000	1.000	1.000	1.000
0.0025	0.724	0.607	0.499	0.391	0.362	0.452	0.284
0.0050	0.568	0.363	0.262	0.242	0.251	0.307	0.162
0.0075	0.434	0.256	0.095	0.177	0.194	0.202	0.095
0.0100	0.329	0.189	0.060	0.105	0.155	0.154	0.062
0.0125	0.262	0.153	0.066	0.073	0.121	0.112	0.049
0.0150	0.201	0.144	0.028	0.041	0.081	0.080	0.056
0.0175	0.179	0.131	0.061	0.064	0.074	0.045	0.053
0.0200	0.140	0.107	0.070	0.053	0.067	0.031	-0.006
0.0225	0.104	0.073	0.057	0.054	0.062	0.027	-0.017
0.0250	0.078	0.043	0.054	0.050	0.033	-0.003	0.064
0.0275	0.052	0.010	0.056	0.045	0.031	0.005	0.030
0.0300	0.008	-0.020	0.066	0.032	0.020	-0.006	0.019
0.0325	-0.002	-0.037	0.058	0.021	-0.002	-0.011	-0.004
0.0350	0.014	-0.050	0.051	-0.013	-0.007	0.005	-0.028
0.0375	-0.007	-0.048	0.041	-0.018	-0.001	0.001	-0.023
0.0400	-0.016	-0.029	0.028	-0.009	0.009	-0.026	0.029
0.0425	-0.027	-0.015	0.010	-0.015	-0.008	-0.026	-0.040
0.0450	-0.032	-0.009	0.012	0.000	-0.016	-0.012	-0.009
0.0475	-0.019	-0.006	0.007	0.002	-0.021	0.007	-0.020
0.0500	-0.006	-0.007	0.004	0.011	-0.018	-0.019	-0.022
0.0525	0.007	-0.010	-0.010	0.003	-0.011	-0.018	-0.015
0.0550	0.022	-0.008	0.009	-0.009	-0.003	-0.033	0.001
0.0575	0.042	-0.023	0.024	-0.006	0.036	-0.023	0.004
0.0600	0.050	-0.021	0.005	-0.004	0.048	-0.029	0.014
0.0625	0.038	-0.013	0.012	-0.016	0.036	-0.031	0.007
0.0650	0.034	-0.027	-0.000	-0.016	0.015	-0.042	0.010
0.0675	0.013	-0.028	0.017	-0.007	0.010	-0.039	-0.010
0.0700	0.014	-0.025	0.019	-0.010	0.036	-0.042	-0.019
0.0725	0.033	-0.026	0.010	-0.003	0.029	-0.045	-0.009
0.0750	0.046	-0.037	0.016	0.010	0.017	-0.051	0.003
0.0775	0.059	-0.061	0.009	0.003	0.022	-0.039	0.037
0.0800	0.042	-0.075	-0.003	0.020	0.044	0.001	0.047
0.0825	0.046	-0.083	-0.009	0.001	0.032	0.031	0.017
0.0850	0.042	-0.078	-0.002	0.011	0.015	0.042	0.006
0.0875	0.040	-0.073	0.015	0.029	0.003	0.051	-0.016
0.0900	0.036	-0.091	0.031	0.018	-0.013	0.019	-0.015
0.0925	0.037	-0.084	0.025	0.006	-0.005	0.018	-0.028
0.0950	0.029	-0.046	0.006	-0.013	-0.011	0.045	-0.039
0.0975	0.003	-0.039	0.013	0.007	0.002	0.046	-0.034
0.1000	0.009	-0.050	0.002	0.000	-0.010	0.022	-0.025
Area under curve[a]	8.93	6.44	5.18	4.62	4.88	4.77	3.16

[a] To first zero crossing; × 10^3 sec.

TABLE III (Continued)

REPRESENTATIVE AUTOCORRELATION DATA

Consistency, g/100 ml	0.10			0.15			
Reynolds Number × 10^{-4}	13.60			8.67			
Radial Position, mm	9	18	26	1	26	18	9
Local Velocity, cm/sec	202	191	174	134	132	123	114
Lag in Seconds							
0.0	1.000	1.000	1.000	1.000	1.000	1.000	1.000
0.0025	0.240	0.293	0.241	0.774	0.734	0.773	0.780
0.0050	0.131	0.135	0.099	0.641	0.543	0.636	0.607
0.0075	0.082	0.059	0.042	0.553	0.401	0.548	0.497
0.0100	0.069	0.053	0.034	0.474	0.315	0.474	0.405
0.0125	0.057	0.070	0.049	0.413	0.267	0.400	0.343
0.0150	0.034	0.040	0.053	0.372	0.241	0.356	0.304
0.0175	0.033	0.051	0.026	0.335	0.198	0.328	0.268
0.0200	0.021	0.021	0.010	0.304	0.188	0.293	0.231
0.0225	0.013	0.047	0.004	0.282	0.159	0.256	0.200
0.0250	-0.002	0.023	-0.004	0.249	0.148	0.237	0.194
0.0275	0.000	0.012	0.009	0.214	0.132	0.224	0.188
0.0300	-0.005	0.001	0.012	0.186	0.131	0.202	0.162
0.0325	-0.010	-0.030	0.022	0.159	0.121	0.191	0.134
0.0350	0.026	0.002	0.019	0.130	0.111	0.186	0.116
0.0375	-0.019	-0.028	0.042	0.115	0.100	0.173	0.097
0.0400	-0.019	-0.026	-0.010	0.095	0.082	0.157	0.086
0.0425	-0.029	-0.019	-0.003	0.097	0.074	0.127	0.071
0.0450	-0.027	-0.010	-0.002	0.085	0.076	0.110	0.065
0.0475	-0.026	0.019	-0.005	0.076	0.070	0.094	0.069
0.0500	-0.020	0.027	-0.003	0.068	0.058	0.081	0.070
0.0525	-0.028	0.027	0.009	0.049	0.036	0.068	0.061
0.0550	-0.038	0.026	0.001	0.034	0.001	0.059	0.056
0.0575	-0.018	0.051	0.016	0.030	-0.022	0.045	0.059
0.0600	-0.008	0.028	0.012	0.018	-0.014	0.031	0.048
0.0625	-0.009	-0.018	0.032	0.003	-0.009	0.021	0.036
0.0650	-0.013	-0.027	0.029	-0.003	0.013	0.027	0.033
0.0675	0.008	-0.038	0.005	-0.012	0.032	0.045	0.019
0.0700	0.014	-0.028	-0.002	-0.019	0.017	0.061	0.010
0.0725	0.035	-0.035	0.024	-0.016	0.016	0.076	0.024
0.0750	0.047	-0.019	0.292	-0.000	0.009	0.086	0.043
0.0775	0.021	0.003	0.001	0.004	0.003	0.076	0.043
0.0800	0.013	0.002	0.009	-0.001	0.009	0.073	0.027
0.0825	0.026	0.001	-0.010	-0.016	0.012	0.062	0.019
0.8500	0.020	-0.009	-0.026	-0.023	0.034	0.055	0.022
0.0875	-0.000	0.000	-0.007	-0.038	0.076	0.044	0.011
0.0900	-0.009	-0.006	0.010	-0.039	0.103	0.034	0.015
0.0925	-0.005	-0.005	-0.001	-0.039	0.101	0.023	0.015
0.0950	0.006	-0.008	0.038	-0.027	0.134	0.013	0.026
0.0975	-0.010	-0.019	0.019	-0.032	0.154	0.003	0.035
0.1000	-0.019	-0.026	-0.007	-0.033	0.169	-0.002	0.049
Area under curve[a]	2.95	3.26	2.63	15.64	11.71	18.12	14.25

[a] To first zero crossing; × 10^3 sec.

TABLE III (Continued)

REPRESENTATIVE AUTOCORRELATION DATA

Consistency, g/100 ml	0.15						
Reynolds Number × 10^{-4}	11.20			13.60			
Radial Position, mm	9	18	26	26	18	9	1
Local Velocity, cm/sec	167	157	145	180	194	203	206
Lag in Seconds							
0.0	1.000	1.000	1.000	1.000	1.000	1.000	1.000
0.0025	0.350	0.668	0.408	0.394	0.564	0.570	0.543
0.0050	0.239	0.443	0.279	0.222	0.336	0.319	0.323
0.0075	0.162	0.287	0.192	0.133	0.215	0.181	0.198
0.0100	0.125	0.182	0.149	0.092	0.138	0.098	0.147
0.0125	0.097	0.131	0.130	0.333	0.076	0.062	0.117
0.0150	0.106	0.105	0.121	0.029	0.064	0.054	0.101
0.0175	0.121	0.094	0.095	0.074	0.081	0.017	0.066
0.0200	0.095	0.088	0.073	0.059	0.089	-0.005	0.047
0.0225	0.077	0.088	0.068	0.058	0.080	-0.014	0.041
0.0250	0.078	0.087	0.060	0.032	0.033	-0.007	0.043
0.0275	0.104	0.083	0.059	0.013	0.015	-0.003	0.015
0.0300	0.068	0.072	0.063	0.023	-0.004	0.014	0.012
0.0325	0.065	0.073	0.046	0.018	-0.010	0.015	-0.005
0.0350	0.042	0.068	0.072	0.014	-0.005	0.006	0.006
0.0375	0.041	0.049	0.035	0.021	0.019	-0.014	0.007
0.0400	0.016	0.022	0.020	0.026	0.023	-0.023	-0.019
0.0425	0.015	-0.005	0.017	0.004	-0.002	-0.025	-0.024
0.0450	0.029	-0.019	0.010	0.035	0.006	-0.016	-0.009
0.0475	0.048	-0.032	0.025	0.030	0.016	-0.002	-0.022
0.0500	0.034	-0.042	0.029	0.016	0.001	-0.000	-0.031
0.0525	0.036	-0.039	0.024	0.033	0.001	-0.012	-0.025
0.0550	0.063	-0.044	0.028	0.005	0.023	-0.040	-0.012
0.0575	0.017	-0.043	0.045	0.026	0.032	-0.051	-0.020
0.0600	0.049	-0.051	0.060	0.044	0.030	-0.044	-0.016
0.0625	0.058	-0.033	0.045	0.094	0.024	-0.047	-0.031
0.0650	0.060	-0.013	0.051	0.104	0.018	-0.021	-0.018
0.0675	0.064	0.001	0.056	0.052	0.050	-0.029	-0.015
0.0700	0.076	0.009	0.088	0.046	0.037	-0.035	-0.012
0.0725	0.063	0.003	0.094	0.065	0.033	-0.044	0.013
0.0750	0.059	0.023	0.073	0.038	0.043	-0.018	0.041
0.0775	0.035	0.016	0.081	0.050	0.047	0.005	0.035
0.0800	0.009	0.031	0.078	0.017	0.024	-0.021	0.051
0.0825	0.006	0.029	0.054	0.010	0.025	-0.033	0.045
0.0850	-0.004	0.024	0.046	0.008	0.033	-0.062	0.044
0.0875	0.008	0.003	0.055	0.003	0.028	-0.043	0.072
0.0900	0.007	-0.024	0.074	-0.013	0.012	-0.038	0.083
0.0925	-0.004	-0.034	0.088	-0.003	0.014	-0.037	0.060
0.0950	-0.007	-0.025	0.082	0.007	0.006	-0.035	0.039
0.0975	-0.002	-0.005	0.075	0.005	0.012	-0.025	0.047
0.1000	-0.005	0.013	0.079	-0.008	0.005	-0.025	0.040
Area under curve[a]	7.48	7.63	5.97	4.35	5.48	4.50	5.38

[a] To first zero crossing; × 10^3 sec.

TABLE III (Continued)

REPRESENTATIVE AUTOCORRELATION DATA

Consistency, g/100 ml	0.24						
Reynolds Number × 10^{-4}	11.20						13.60
Radial Position, mm	1	6	11	16	21	26	26
Local Velocity, cm/sec	171	170	167	163	155	145	176
Lag in Seconds							
0.0	1.000	1.000	1.000	1.000	1.000	1.000	1.000
0.0025	0.638	0.730	0.700	0.797	0.764	0.768	0.665
0.0050	0.495	0.551	0.508	0.640	0.612	0.627	0.458
0.0075	0.405	0.420	0.388	0.522	0.515	0.499	0.337
0.0100	0.348	0.331	0.313	0.435	0.433	0.389	0.249
0.0125	0.321	0.263	0.250	0.373	0.357	0.293	0.184
0.0150	0.281	0.237	0.214	0.326	0.302	0.201	0.158
0.0175	0.228	0.210	0.202	0.290	0.260	0.158	0.145
0.0200	0.198	0.205	0.186	0.261	0.228	0.128	0.143
0.0225	0.189	0.202	0.196	0.218	0.214	0.113	0.123
0.0250	0.173	0.211	0.182	0.163	0.191	0.108	0.109
0.0275	0.156	0.176	0.163	0.109	0.170	0.114	0.089
0.0300	0.140	0.141	0.130	0.072	0.147	0.104	0.091
0.0325	0.147	0.103	0.098	0.053	0.129	0.096	0.072
0.0350	0.169	0.082	0.086	0.037	0.095	0.081	0.048
0.0375	0.142	0.079	0.044	0.042	0.061	0.044	0.052
0.0400	0.116	0.084	0.041	0.035	0.034	0.011	0.050
0.0425	0.091	0.091	0.053	0.025	0.012	-0.009	0.035
0.0450	0.080	0.098	0.056	0.029	-0.015	-0.019	0.024
0.0475	0.083	0.107	0.059	0.028	-0.033	-0.058	0.020
0.0500	0.086	0.093	0.054	0.026	-0.034	-0.074	-0.002
0.0525	0.083	0.077	0.055	0.013	-0.029	-0.086	-0.008
0.0550	0.073	0.057	0.044	0.015	-0.033	-0.083	-0.008
0.0575	0.068	0.044	0.042	0.025	-0.027	-0.065	-0.008
0.0600	0.084	0.031	0.047	0.040	-0.002	-0.065	0.003
0.0625	0.073	0.017	0.060	0.037	-0.005	-0.060	0.026
0.0650	0.034	0.024	0.067	0.049	-0.014	-0.051	0.013
0.0675	0.032	0.038	0.073	0.052	-0.019	-0.058	0.021
0.0700	0.022	0.044	0.093	0.066	-0.012	-0.061	0.019
0.0725	0.006	0.031	0.071	0.073	-0.011	-0.072	0.012
0.0750	0.001	0.029	0.075	0.065	0.003	-0.085	0.001
0.0775	-0.003	0.030	0.077	0.056	0.012	-0.088	0.007
0.0800	-0.025	0.042	0.074	0.051	0.022	-0.097	0.003
0.0825	-0.037	0.046	0.072	0.039	0.020	-0.088	-0.013
0.0850	-0.039	0.054	0.062	0.040	0.007	-0.080	0.005
0.0875	-0.054	0.049	0.054	0.037	0.001	-0.072	0.015
0.0900	-0.040	0.041	0.030	0.029	-0.013	-0.062	0.019
0.0925	-0.056	0.019	0.024	0.026	-0.012	-0.051	0.038
0.0950	-0.047	0.020	0.033	0.011	0.002	-0.027	0.046
0.0975	-0.074	0.032	0.042	0.015	0.021	-0.024	0.044
0.1000	-0.079	0.049	0.039	0.025	0.033	-0.025	0.043
Area under curve[a]	13.64	14.42	15.28	14.52	12.56	10.59	8.88

[a]To first zero crossing; × 10^3 sec.

TABLE III (Continued)

REPRESENTATIVE AUTOCORRELATION DATA

Consistency, g/100 ml	0.24				
Reynolds Number × 10^{-4}	13.60				
Radial Position, mm	1	6	11	16	21
Local Velocity, cm/sec	207	205	203	198	189
Lag in Seconds					
0.0	1.000	1.000	1.000	1.000	1.000
0.0025	0.554	0.626	0.530	0.488	0.575
0.0050	0.278	0.403	0.321	0.341	0.338
0.0075	0.138	0.268	0.210	0.234	0.229
0.0100	0.103	0.204	0.191	0.169	0.171
0.0125	0.120	0.161	0.179	0.122	0.145
0.0150	0.150	0.125	0.167	0.126	0.126
0.0175	0.148	0.122	0.153	0.105	0.094
0.0200	0.157	0.108	0.092	0.079	0.085
0.0225	0.109	0.080	0.054	0.069	0.092
0.0250	0.090	0.074	0.061	0.044	0.067
0.0275	0.056	0.037	0.081	0.050	0.063
0.0300	0.071	0.042	0.084	0.024	0.056
0.0325	0.070	0.042	0.072	0.019	0.026
0.0350	0.054	0.038	0.040	0.049	0.012
0.0375	0.035	0.025	0.028	0.040	0.024
0.0400	0.042	0.057	0.007	0.018	0.049
0.0425	0.012	0.044	-0.009	0.037	0.070
0.0450	-0.021	0.001	-0.006	0.035	0.057
0.0475	-0.025	0.004	0.008	0.034	0.036
0.0500	-0.005	0.041	0.026	0.053	0.003
0.0525	0.006	0.079	0.032	0.051	-0.001
0.0550	0.013	0.070	0.035	0.053	-0.022
0.0575	-0.024	0.081	0.008	0.062	-0.043
0.0600	-0.011	0.085	-0.016	0.022	-0.037
0.0625	0.011	0.081	0.011	0.009	-0.021
0.0650	0.011	0.071	0.022	0.008	-0.033
0.0675	0.034	0.072	0.058	0.030	-0.026
0.0700	0.034	0.066	0.030	0.018	-0.035
0.0725	0.031	0.062	0.018	0.014	-0.051
0.0750	0.051	0.058	-0.011	0.039	-0.043
0.0775	-0.005	0.048	-0.010	0.021	-0.018
0.0800	-0.057	0.035	0.020	0.004	-0.031
0.0825	-0.028	0.013	0.041	-0.015	-0.010
0.0850	-0.011	-0.025	0.055	-0.036	0.001
0.0875	-0.016	-0.032	0.008	-0.033	0.009
0.0900	-0.033	-0.021	-0.027	-0.014	0.026
0.0925	-0.048	-0.034	-0.055	-0.050	0.041
0.0950	-0.028	-0.054	-0.034	-0.037	0.025
0.0975	-0.018	-0.047	-0.024	-0.034	0.015
0.1000	-0.044	-0.036	-0.007	-0.026	0.007
Area under curve[a]	6.72	6.5	6.91	7.06	7.04

[a] To first zero crossing; × 10^3 sec.

TABLE IV

REPRESENTATIVE AREAS[a] UNDER AUTOCORRELATION CURVES

Consistency																	
0.05 g/100 ml					0.10 g/100 ml				0.15 g/100 ml				0.24 g/100 ml					
Reynolds Number																		
1.36 × 10⁵					6.25 × 10⁴				1.36 × 10⁵				1.36 × 10⁵					
Local Velocity, cm/sec																		
174	184	193	200	204	83	91	97	98	180	194	203	206	176	189	198	203	205	207
Radial Position, mm																		
26	21	16	11	6	24	18	9	1	26	18	9	1	26	21	16	11	6	1
1.60	1.68	1.97	1.94	2.30	12.36	9.70	13.39	15.20	4.35	5.38	4.50	5.48	8.88	7.04	7.06	6.91	7.39	6.72
1.85	1.96	1.98	2.08	2.02	12.28	11.92	11.96	16.90	4.00	4.79	4.93	6.30	9.44	7.42	6.84	5.83	6.06	8.53
1.58	2.10	2.00	1.98	2.09	12.11	12.19	14.54	10.40	4.60	4.39	5.26	4.90	8.71	7.13	6.64	7.71	5.70	5.66
1.84	1.97	2.09	1.95	2.12	12.04	12.23	13.10	17.33	4.01	4.10	4.60	7.01	8.66	8.14	6.90	6.69	5.44	6.39
1.78	1.95	2.13	2.12	2.13	11.83	12.29	11.16	10.63	3.80	4.81	4.70	4.47	8.35	7.29	9.02	6.72	5.85	6.39
1.61	1.82	2.06	2.20	3.00	12.97	13.41	11.15	13.58	4.88	5.37	4.59	4.71	8.39	7.04	5.77	7.05	6.20	6.32
1.62	2.30	2.07	1.99	2.37	12.82	13.15	13.90	15.61		4.88	4.26			7.19	8.41	6.75	6.09	6.79
1.64	1.99	2.04	2.03	2.41	12.61	12.71	13.33	14.48		4.42	4.40			6.89	8.17	7.11	6.16	6.95
1.57	1.90	1.99	2.16	2.27	12.32	10.87	13.21	13.55		4.17				6.56	7.35	7.04		
1.70	1.85	1.94	1.98	2.30	12.19			15.51		3.80				6.62	7.58			
1.73	1.97	2.11	2.01	2.22	12.15										7.01			
1.87	1.98	1.91	2.00	2.39											6.22			
1.98	1.92		2.00	2.80											6.39			
2.99	1.68		2.05	2.73											8.09			
2.16	1.73		2.07	2.07											6.22			
1.86	2.39		2.07												6.54			
1.85			2.12															
			2.11															
			2.12															
			1.60															
Mean																		
1.86	1.95	2.02	2.03	2.35	12.48	12.05	12.86	14.32	4.27	4.61	4.66	5.48	8.77	7.13	7.14	6.87	6.11	6.72
Standard Deviation																		
0.33	0.19	0.07	0.12	0.29	0.59	1.15	1.18	2.35	0.41	0.53	0.32	0.99	0.40	0.44	0.90	0.50	0.58	0.83

[a] Areas shown × 10^3 sec.

APPENDIX IV

COMPUTER PROGRAMS

Most of the lengthy calculations involved in analyzing the pressure drop, flow, and autocorrelation data were performed using the Institute's IBM 360 computer. The programs used are included in this appendix. Comment statements are included throughout the various programs to assist in program usage.

FLOW DATA

Pressure drop and flow data were analyzed using the 360 RAX mode of operation and the first program listed. "VELPR" is a subroutine called by the main program. Appendix II includes data output from this program.

DIGITIZED DATA ANALYSIS

The digitized data received from DASL were analyzed using the 360 OS mode of operation. Program "TPRP" was used to prepare two separate data tapes from the tape received from DASL to then be used with program "BMD02T." The two subroutines, "GET" and "SBSTR" used in "TPRP" were contained in the computer library.

Auto- and crosscorrelation studies were performed using a revised version of "BMD02T," a Biomedical Computer Program from the University of California in Los Angeles (50). Since the study involved record lengths generally greater than the program was designed to accommodate, several of the subroutines were short-circuited, if not needed, to allow more data points to be analyzed. Comment cards are included in various places of the program to explain other modifications.

The program in its original form was designed to compute the autocovariance, power spectrum, crosscovariance, crossspectrum, transfer function, and coherence function of time series. A plotting subroutine, "PLOTR," is called to plot the various functions. The program also allows transformation of the input data, detrending of the input series, and simple prewhitening transformation in the form of a moving linear combination. These options were not used in the study. Job deck setup and special cards used were as follows.

JOB DECK SETUP

1. System job control cards (JCL)
2. Program cards (source or object deck form)
3. JCL cards for tape input
4. Special cards
   - a. PROBLEM cards
   - b. FORMAT cards
   - c. SELECT cards

   } Repeated as necessary

   d. FINISH card

PROBLEM CARD

Column	Contents
1-6	PROBLEM (mandatory)
7-12	Alphanumeric job code
13-27	Blank
28-29	Number of time series ($1<S\leq 2$)
30-33	Number of points in each series ($1<n\leq 6000$)
34-36	Number of lags ($1<m\leq 199$)
37-38	Number of selection cards
39-40	Blank
41-47	Constant time internal (punch decimal, e.g., 0.01 sec)
48-53	Time unit, e.g., second, minute
54-66	Blank
67-68	00
69-70	-1
71-72	-1

SELECT CARD

Column	Contents
1-6	SELECT
7	Blank
8-10	YES if autocorrelation is to be calculated; otherwise leave blank
11	Blank
12-14	YES if crosscorrelation is to be computed; otherwise leave blank
15-19	Blank
20-21	Number designation of base series (01)
22	A if autocorrelation is to be plotted; otherwise leave blank
23-24	Blank
25-26	Number of series to be crossed with base series (should be 01 if only a single series is being processed)
27	Blank
28-29	Number designation of 1st series to cross with the base series
30	A if autocorrelation is to be plotted; otherwise leave blank

```
C
C     ******************************************************************
C     ANALYSIS  OF PRESSURE AND VELOCITY PROFILE DATA
C
C     ******************************************************************
C
      DIMENSION POS(25),DLHV(25),S(25),SPLUS(25),VBAR(25)
      DIMENSION VPLUS(25),RUN(5),RF(25),DLHSP(30)
      DIMENSION Q(30),TMF(30),RE(30),DPF(30),VAVG(30)
      DIMENSION F(30),TAUO(30),G(30),TPIRV(25),NMF(25)
33    READ(5,1000) RUN
1000  FORMAT(8A4)
      READ(5,2000) T,CONS,VNPT,NPT,NPTF
2000  FORMAT(F5.2,F7.3,F5.1,I4,I4)
C
C     VNPT TELLS IF THERE IS ANY VEL DATA  1.0=YES 0.0=NO
C     NPTF TELLS HOW MANY  F-RE    POINTS THERE ARE
C     NPT TELLS HOW MANY VEL. POINTS THERE ARE
C
      PI=3.14159
      RHOHG=13.5939
      RHOCT=1.585
      RHOCB=1.102
      RHOW=0.998
      DENSW=62.3
      GC=32.174
      DI=2.852
      DF=2.852/12.
      CR=DF/2.
      AL23=9.5
      A=PI*CR**2
      VISC=1./(2.1482*((T-8.435)+SQRT(8078.4+(T-8.435)**2))-120.)*100.
      EVISC=VISC*0.000672
      ANU=EVISC/DENSW
C
C     VISC IS VISCOSITY IN CENTIPOISE & EVISC IS IN LBM/FT*SEC
C     ANU IS IN FT**2/SEC
C
      DO 5 K=1,NPTF
      READ(5,2500) G(K),DLHSP(K),TMF(K)
C
C     TMF TELLS WHAT THE MANOMETER FLUID,(MF), IS
C     TMF=1.0,2.0,3.0   MF=CCL4,CB,HG RESPT.
C
2500  FORMAT(F7.2,F7.3,F5.1)
      Q(K)=G(K)/(7.481*60.)
      VAVG(K)=Q(K)/A
      RE(K)=(DF*VAVG(K))/ANU
      IF(TMF(K)-2.) 10,20,30
10    RHOMF=RHOCT
      GO TO 40
20    RHOMF=RHOCB
      GO TO 40
30    RHOMF=RHOHG
40    DPF(K)=DLHSP(K)*((DENSW*(RHOMF-RHOW))/(2.54*12.))
      TAUO(K)=(DPF(K)*CR)/(2.*AL23)
C
C     TAUO HAS UNITS (LB/FT**2)
C
5     F(K)=(TAUO(K)*GC)/((DENSW/2.)*VAVG(K)**2)
      VSTAR=SQRT((TAUO(1)*GC)/DENSW)
      WRITE(6,1500) RUN
1500  FORMAT(1H1,8A4)
      WRITE(6,3000) CONS
3000  FORMAT(1HO,'CONSISTENCY = ',F5.3,' GR/100 ML')
      WRITE(6,3001) T
3001  FORMAT(1H ,'TEMPERATURE = ',F5.2,' DEGREE C')
      WRITE(6,3002) VISC
3002  FORMAT(1H ,'VISCOSITY = ',F5.3,'   CENTIPOISE')
      WRITE(6,3003)
3003  FORMAT(1H ,'MANOMETER FLUID-(MF)  1=CCL4  2=CB  3=HG')
      WRITE(6,4000)
4000  FORMAT(1HO,4X'G'9X'Q'8X'UAVG'9X'DELTA HF '7X'RE'12X'F')
      WRITE(6,4300)
```

```
4300  FORMAT(1H ,1X'GAL/MIN'2X'CU FT/SEC   FT/SEC'8X'CM  (MF)'8X'--'12X'
     1--')
      WRITE(6,4400)
4400  FORMAT(1HO)
      DO 6 L=1,NPTF
      NMF(L)=TMF(L)
6     WRITE(6,4500) G(L),Q(L),VAVG(L),DLHSP(L),NMF(L),RE(L),F(L)
4500  FORMAT(1H ,F7.1,F11.3,F9.1,F12.2,3H  (,I2,2H ),E12.3,E13.3)
      IF(VNPT-0.0) 50,50,60
50    GO TO 70
60    CALL VELPR(S,SPLUS,VBAR,VPLUS,VSTAR,POS,DLHV,NPT,RF,ANU,CL)
C
C     SUBROUTINE VELPR ANALYZES VELOCITY PROFILE DATA
C
      WRITE(6,6000)
6000  FORMAT(1HO,'VELOCITY PROFILE INFORMATION')
      WRITE(6,6100) CL
6100  FORMAT(1HO,'CENTERLINE IS AT SCALE READING',F6.2)
      WRITE(6,7000)
7000  FORMAT(1HO,'POSITION'4X'RADIUS'5X'S'5X'DELTA HV'4X'UBAR'4X'SPLUS'5
     2X'UPLUS')
      WRITE(6,7100)
7100  FORMAT(1H ,'SCALE RDG'5X'FT'7X'FT'5X'CM CCL4  FT/SEC'5X'DIM'6X'DIM
     2')
      WRITE(6,4400)
      DO 80 L=1,NPT
80    WRITE(6,8000) POS(L),RF(L),S(L),DLHV(L),VBAR(L),SPLUS(L),VPLUS(L)
8000  FORMAT(1H ,F7.2,F11.4,F9.3,F9.2,F8.2,F10.1,F9.2)
      GO TO 90
70    WRITE(6,9000)
9000  FORMAT(1HO,'THERE IS NO VELOCITY PROFILE DATA')
90    CONTINUE
      GO TO 33
      END
C
C
C
C     ******************************************************************
C
      SUBROUTINE VELPR(S,SPLUS,VBAR,VPLUS,VSTAR,POS,DLHV,NPT,RF,ANU,CL)
C
C     ******************************************************************
C
      DIMENSION S(25),SPLUS(25),VBAR(25),VPLUS(25),POS(25),DLHV(25)
      DIMENSION RF(25)
      READ(5,100) CL
100   FORMAT(F6.3)
      READ(5,200)(POS(I),I=1,NPT)
200   FORMAT(5F6.3)
      READ(5,300)(DLHV(J),J=1,NPT)
300   FORMAT(5F7.2)
      CR=(2.852/24.)
      DO 1 K=1,NPT
      T=POS(K)-CL
      RF(K)=ABS(T)/30.48
      S(K)=CR-RF(K)
      VBAR(K)=1.119*SQRT(DLHV(K))
C
C     VBAR HAS UNITS (FT/SEC)
C
      VPLUS(K)=VBAR(K)/VSTAR
1     SPLUS(K)=(S(K)*VSTAR)/ANU
      RETURN
      END
C
```

```
C
C     ******************************************************************
C
C     PROGRAM TPRP   TO PREPARE DATA TAPES FOR BMD02T
C
C     ******************************************************************
C
C
C
C
C     NF HAS TO BE LESS THAN OR EQUAL TO 10 OR WILL GET AN 80A
C      SUBROUTINES 'GET' AND 'SBSTR' ARE IN THE COMPUTER LIBRARY
C     NF HAS TO BE EVEN FOR SKIPPING RECORDS WITHIN STATEMENT 1
C     NN ALLOWS RECORDS TO BE SKIPPED AND HAS TO BE DEFINED
C     FIRST 10 RECORDS WILL BE SKIPPED FOR EXAMPLE
C
      DIMENSION NOS(4505),CH1(10),CH2(10)
      K=0
      NF=10
      NN=10
      DO 100 I=1,NN
100   CALL GET (NOS,91,1,18018)
1     CALL GET (NOS,91,1,18018)
      IB=1
      N1=0
      N2=0
      CALL SBSTR (NOS,1,N1,2,3)
      CALL SBSTR (NOS,4,N2,2,3)
      CALL SBSTR (NOS,7,N1,2,3)
      WRITE(6,9002) N1
9002  FORMAT(1H ,12HRECORD ID IS,I4)
      CALL SBSTR (NOS,10,N2,2,3)
      WRITE(6,9003) N2
9003  FORMAT(1H ,14HDATA SET ID IS,I4)
      IB=13
      I=1
      J=0
2     NUM=0
      N1=0
      N2=0
      CALL SBSTR (NOS,IB,NUM,2,3)
      N1=NUM/4096
      N2=NUM-4096*N1
      J=J+1
      CH1(J)=N1
      CH2(J)=N2
      IF(J-10) 6,5,5
5     WRITE(2,9001) CH1
      WRITE(3,9001) CH2
9001  FORMAT(10F8.0)
      J=0
6     IB=IB+3
      I=I+1
      IF(I-6000) 2,2,3
3     IF(J) 7,7,4
4     WRITE(2,9001) (CH1(I),I=1,J)
      WRITE(3,9001) (CH2(I),I=1,J)
7     END FILE 2
      END FILE 3
300   K=K+1
      IF(K-NF) 1,8,8
8     CALL EXIT
      END
C
```

```
C      ******************************************************************
C
CID                          BMD02T
C
C      ******************************************************************
C
CBMD02T  AUTOCOVARIANCE AND POWER SPECTRAL ANALYSIS  AUGUST 13, 1966
C      THIS PROGRAM WAS MODIFIED BY W.H. PERSINGER TO DO THE VARIOUS
C      AUTO-CORRELATION CALCULATIONS NECESSARY FOR THESIS WORK
C      MODIFICATIONS WERE PRIMARILY THOSE NECESSARY TO READ IN LONGER
C        RECORDS AND TO READ THEM FROM TAPE
C
       DIMENSION Z(05C00),DUMB(20),FMT(180),NSELL(20),RX(200),PX(200),
      1 LISA(20),ADDXY(200),SUBXY(200),CXY(200),QXY(200),SCXY(200),
      2 SQXY(200),AMXY(200),PHASXY(200),RXY(200),RYX(200),YP( 4),
      3 CRC(4C0),COXYSQ(200),IPRNT1(20),IPRNT2(20)
       DIMENSION X(10C0),Y(1000),SPX(200),SPY(200),IPRNT3(20)
       REAL*8 IPROB
       REAL*8 PROBLM/6HPROBLM/,SEL/6HSELECT/,END/6HFINISH/,JOB,PROB,UNIT
       INTEGER*2 SYM(4)
       COMMON UNIT
       COMMON  RXY     , RYX     , RX      , SUBXY
       COMMON  Z       , DUMB    , FMT     , NSELL   , LISA    , SCXY
       COMMON  SQXY    , YP                , CRC     , COXYSQ  , IORDAT
       COMMON  IPLOAT  , IDETRN  , IPREWT  , THETA   , KSER    , NPOINT
       COMMON  LAG     , NSEL    , IPLOT   , DELTAT              , INFORM
       COMMON  KVR     , IPRNT1  , IPRNT2  , IPRNT3  , IPOW    , ICCS
       COMMON  ICOH    , PI      , FNPT    , CONST   , PMO     , FLAG
       COMMON  FLLAG   , LLAG    , KIT     , KDUM    , MISTAK  , MX
       COMMON  KX      , Q       , KPOINT
       COMMON SYM
C
       EQUIVALENCE (RXY,CXY,AMXY),(RYX,QXY,PHASXY),(RX,ADDXY),(PX,SUBXY),
      1(YES,IYES),(END,IEND),(PROBLM,IPROB),(SEL,ISEL)
C
 9002 FORMAT(1H1/77H BMD02T-AUTOCOVARIANCE AND POWER SPECTRAL ANALYSIS -
      1VERSION OF APR. 20, 1966/
      22X40HHEALTH SCIENCES COMPUTING FACILITY, UCLA//)
C
C        THIS PROGRAM CAN BE CHANGED IN SEVERAL PLACES IF NECESSARY
C        IF DIMENSION OF Z IS INCREASED TO ACCOMODATE MORE POINTS
C      IT IS NECESSARY TO CUT BACK IN OTHER PLACES SO AS NOT TO USE TOO
C      MUCH CORE.  SOME SUBROUTINES CAN BE SHORT CIRCUITED.
C      THE PLOTER AND SCALE SUBROUTINES CAN BE S.C. ALSO.
C
       DATA IYES/3HYES/
       IPLOAT=0
C
       PI=3.141593
       INFORM=5
C
  999  READ (5,5001) JOB,PROB,IORDAT,IDETRN,IPREWT,THETA,KSER,NPOINT,LAG,
      1NSEL,IPLOT,DELTAT,UNIT,IOLD,NCD,NTAPE,KVR
 5001 FORMAT(2A6,3A3,F6.3,I2,I4,I3,2I2,F7.0,A6,A3,10X,3I2)
       IF( END .NE. JOB) GO TO 10
       WRITE (6,887)
  887 FORMAT(1H0 / / / 'OFINISH CARD ENCOUNTERED.' )
  888 IF (INFORM .EQ. 5) GO TO 890
  889 REWIND INFORM
  890 STOP
   10 IF (IPROB .NE. JOB) GO TO 740
  150  WRITE (6,9002)
       WRITE (6,9003)PROB
 9003 FORMAT(1H ///4CX,26HP R O B L E M  N U M B E R,4X,A6/40X,26(1H*)//
      1/)
       WRITE (6,9005)IORDAT,IPLOAT,IDETRN,IPREWT,THETA,KSER, NPOINT,LAG,N
      1SEL,IOLD
 9005 FORMAT(20X,31HINPUT DATA TO BE PRINTED OUT---A3//20X,33HINPUT SERI
      1ES TO BE PLOTTED OUT---A3//20X,13HDETRENDING---A3//20X,15HPREWHITE
      2NING---A3//20X,81HVALUE OF CONSTANT C USED IN THE PREWHITENING TRA
      3NSFORMATION Z(T)=X(T+1)-CX(T) ---F10.5//20X19HNUMBER OF SERIES = I
      42//20X,23HNUMBER OF DATA POINTS =I5//20X,24HNUMBER OF LAGS CHOSEN
      5= I3//20X,28HNUMBER OF SELECTION CARDS = I2//20X,20HUSE PREVIOUS D
      6ATA---A3//)
```

```
      IF(KSER*(KSER-21))904,750,750
  904 WRITE (6,9013)DELTAT,UNIT
 9013 FORMAT(20X,25HCONSTANT TIME INTERVAL = F10.5,1X,A6//)
      IF(NPOINT*(NPOINT-1001))909,760,760
  909 WRITE (6,9021)KVR
 9021 FORMAT(20X,34HNUMBER OF VARIABLE FORMAT CARDS = I3//)
      KPOINT=NPOINT
      CTHETA=ABS(THETA)
      IF(LAG-199)8,8,730
    8 IF((NPOINT*KSER)-17000)9,9,720
    9 IF(CTHETA-1.0) 99,99,99
   99 IF(IGLD-IYES)11,30,11
   11 ASSIGN 75 TO NSKIP
   12 IF(KVR)40,705,20
   40 IF(KVR+1)42,45,42
   42 L=1
      ASSIGN 74 TO NSKIP
      GO TO 46
   45 L=2
   46 KVR=1
      GO TO (25,20),L
   20 CALL VFCHCK(KVR)
      KVR=KVR*18
      READ (5,1002)(FMT(I),I=1,KVR)
 1002 FORMAT (18A4)
      WRITE (6,1003) (FMT(I),I= 1, KVR)
 1003 FORMAT( '0VARIABLE FORMAT IS' / (20X,18A4))
   25 ASSIGN 80 TO KSKIP
      ASSIGN 30 TO LSKIP
      IF ( NTAPE) 71,72,73
   71 KADD=-NPOINT
        DO 84 K=1,KSER
      KADD=KADD+NPOINT
      GO TO NSKIP,(74,75,715)
  715 READ (INFORM)(X(I),I=1,NPOINT)
      GO TO 755
C
   74 READ (5,1002)(FMT(J),J=1,18)
      WRITE (6,1003) (FMT(I),I= 1, KVR)
   75 IF(NCD)2000,2000,2001
 2001 READ(5,FMT)(X(I),I=1,NPOINT)
      GO TO 755
C
C     TO BE ABLE TO READ DIFFERENT LENGTH RECORDS
C
 2000 READ(2,FMT)(X(I),I=1,NPOINT)
 5000 READ(2,FMT,END=6000) DUMMY
      GO TO 5000
 6000 CONTINUE
  755 DO 84 I=1,NPOINT
      ND=I+KADD
   84 Z(ND)=X(I)
      GO TO 825
C
   73 ASSIGN 83 TO LSKIP
      IF(70- NTAPE)735,735,738
  735 NTAPE=NTAPE-70
      ASSIGN 715 TO NSKIP
      CALL TPWD(NTAPE,INFORM)
      GO TO 71
C
  738 CALL TPWD(NTAPE,INFORM)
      ASSIGN 81 TO KSKIP
   72 DO 82 I=1,NPOINT
      KADD=0
      GO TO KSKIP,(80,81)
   80 READ (5,FMT)(DUMB(J),J=1,KSER)
      GO TO 815
C
   81 READ (INFORM)(DUMB(J),J=1,KSER)
  815 DO 82 J=1,KSER
      L=KADD+I
      KADD=KADD+NPOINT
   82 Z(L)=DUMB(J)
  825 GO TO LSKIP,(30,83)
```

```
 83    REWIND INFORM
   30 LLAG=LAG+1
      FLLAG=LLAG
      FLAG=LAG
      FNPT=NPOINT
      Q=PI/FLAG
      CONST=2.0*DELTAT/PI
      PMU=0.5/(FLAG*DELTAT)
      IF(-NSEL)95,770,770
   95 DO 9000 KOUM=1,NSEL
      KIT=0
      DO 98 I=1,20
      NSELL(I)=0
      IPRNT1(I)=0
      IPRNT2(I)=0
      IPRNT3(I)=0
      LISA(I)=0
 98   CONTINUE
      READ (5,5003)JOB,IPOW,ICCS,ICOH,NNX,IPRNT1(1),LISA(1),NNS,(NSELL(I
     1),IPRNT1(I+1),IPRNT2(I+1),IPRNT3(I+1),LISA(I+1),I=1,NNS)
 5003 FORMAT(A6,1X,3A4,I2,A1,2I2,1X,6(I2,3A1,I2)/6X,9(I2,3A1,I2)/6X,
     14(I2,3A1,I2))
      IF (JOB .NE. SEL) GO TO 745
 101  CALL SMEAN (NNX,X,XBAR,XALPHA)
 102  IF (MISTAK) 9000,100,9000
 100  ASSIGN 145 TO KPOWR
      IF(IPOW-IYES)105,110,105
 110  ASSIGN 135 TO KPOWR
      CALL POWER (NNX,X,XBAR,XALPHA,SPX)
  105 DO 8000 I=1,NNS
      KIT=I
      NNY=NSELL(I)
      IF(NNX-NNY)120,9000,120
  120 CALL SMEAN (NNY,Y,YBAR,YALPHA)
      IF(MISTAK-17)122,740,122
 122  IF(MISTAK) 9000,125,9000
 125  GO TO KPOWR,(135,145)
  135 CALL POWER (NNY,Y,YBAR,YALPHA,SPY)
      IF(ICCS-IYES)8000,140,8000
 140  IF(IPREWT-IYES)145,130,145
  145 CALL CROSS (NNX,NNY,X,Y,SPX,SPY,XBAR,YBAR,XALPHA,YALPHA)
      GO TO 8000
  130 WRITE (6,1051)
 1051 FORMAT(1H1,10X,77HSINCE PREWHITENING IS DONE IN THE INPUT DATA , C
     1ROSS-SPECTRUM IS NOT COMPUTED/ 10X,66HPROGRAM WILL PROCEED TO NEXT
     2 SERIES IN THE SELECTION CARD (IF ANY)/ 10X,39H OR TO THE NEXT SEL
     3ECTION CARD (IF ANY))
 8000 CONTINUE
 9000 CONTINUE
      GO TO 999
C
  705 IF(INFORM)20,20,73
C
  710  WRITE (6,9200)THETA
       GO TO 751
C
  720  WRITE (6,9300)
       GO TO 751
C
  730  WRITE (6,9400)LAG
       GO TO 751
C
  740 CONTINUE
      WRITE (6,9501)
 9501 FORMAT('0PROGRAM EXPECTS A ''PROBLM'' CARD.')
      WRITE (6,9500) JOB,PROB,IORDAT,IPLDAT,IDETRN,IPREWT,THETA,KSER,
     1 NPOINT,LAG,NSEL,IPLOT,DELTAT,UNIT,IOLD,NTAPE,KVR
      GO TO 751
C
  745 CONTINUE
      WRITE (6,9551)
      WRITE (6,9550) JOB,IPOW,ICCS,ICOH,NNX,IPRNT1(1),LISA(1),NNS
      GO TO 751
```

```
  750 WRITE (6,9600)
  751 WRITE (6,9800)
      GO TO 888
C
  760 WRITE (6,9700)
      GO TO 751
C
  770 WRITE (6,9900)
      NSEL =1
      GO TO 95
C
 9200 FORMAT(1HO,20X,47HCONSTANT USED IN PREWHITENING TRANSFORMATION IS,
     1F7.5,23H,A VALUE NOT PERMITTED.)
 9300 FORMAT(1HO,37X,22HDATA STORAGE EXCEEDED.)
 9400 FORMAT(1HO,37X,29HNUMBER OF LAGS IS TOO LARGE =,I5)
 9500 FORMAT( '0CONTROL CARD OUT OF ORDER OR MISPUNCHED. CARD IS PRINTED
     1 BELOW. ' / 1X,2A6,4A3,F5.0,I2,I4,I3,2I2,F5.0,A6,A3,12X,2I2)
 9550 FORMAT('0CONTROL CARD OUT OF ORDER OR MISPUNCHED. CARD IS PRINTED
     1BELOW.' / 1X,A6,1X,3A4,I2,A1,2I2)
 9551 FORMAT('0PROGRAM EXPECTS A ''SELECT'' CARD.')
 9600 FORMAT(1HO,37X,43HNUMBER OF SERIES IS OUTSIDE PROGRAM LIMITS.)
 9700 FORMAT(1HO,37X,43HNUMBER OF POINTS IS OUTSIDE PROGRAM LIMITS.)
 9800 FORMAT(1HO,37X,23HPROGRAM CANNOT PROCEED.)
 9900 FORMAT(1HO,37X,44HNO SELECTION CARD SPECIFIED. ONE IS ASSUMED.)
C
      END
C
C
C
C     ******************************************************************
CSMEAN    SUBROUTINE SMEAN FOR BMD02I                    APRIL 20, 1966
      SUBROUTINE SMEAN (NNX,X,XBAR,XALPHA)
C
      DIMENSION Z(05C00),DUMB(20),FMT(180),NSELL(20),RX(200),PX(200),
     1 LISA(20),ADDXY(200),SUBXY(200),CXY(200),QXY(200),SCXY(200),
     2 SQXY(200),AMXY(200),PHASXY(200),RXY(200),RYX(200),YP( 4),
     3 CRO(400),COXYSQ(200),IPRNT1(20),IPRNT2(20)
      DIMENSION X(00C1),IPRNT3(20)
      INTEGER*2  SYM(4), Q001CT
      REAL*8  UNIT, ACUMX(2)
      COMMON UNIT
      COMMON  RXY    , RYX    , RX     , SUBXY
      COMMON  Z      , DUMB   , FMT    , NSELL  , LISA   , SCXY
      COMMON  SQXY   , YP                , CRO    , CCXYSQ , IGRDAT
      COMMON  IPLDAT , IDETRN , IPREWT , THETA  , KSER   , NPOINT
      COMMON  LAG    , NSEL   , IPLOT  , DELTAT           , INFORM
      COMMON  KVR    , IPRNT1 , IPRNT2 , IPRNT3 , IPOW   , ICCS
      COMMON  ICOH   , PI     , FNPT   , CONST  , PMD    , FLAG
      COMMON  FLLAG  , LLAG   , KIT    , KDUM   , MISTAK , MX
      COMMON  KX     , Q      , KPOINT
      COMMON SYM
      EQUIVALENCE (RXY,CXY,AMXY),(RYX,QXY,PHASXY),(RX,ADDXY),(PX,SUBXY),
     1(YES,IYES)
C
      DATA IYES/3HYES/
      DATA Q001CT/2H*0/
      SYM(1)=Q001CT
C
      NPOINT=KPOINT
      IF (INFORM) 100,105,105
  100  DO 110 I=1,NPOINT
      ND=I+(NNX-1)*NPOINT
  110  X(I) = Z(ND)
      GO TO 135
  105 ISX=NPOINT*(NNX-1)
      DO 115 I=1,NPOINT
      K=I+ISX
  115 X(I)=Z(K)
  135  IF(IORDAT-IYES)140,130,140
  130  WRITE (6,1102)NNX
 1102 FORMAT(1H1,5X,24HORIGINAL DATA OF SERIES I3//)
      WRITE (6,1104)(X(I),I=1,NPOINT)
 1104 FORMAT(10F11.5)
  140  IF(IPLDAT-IYES)141,200,141
  200 HU=-10**10
```

```
      SM=10**10
      DO 210 I=1,NPOINT
      HU=AMAX1(HU,X(I))
  210 SM=AMIN1(SM,X(I))
      WRITE (6,2001)NNX
 2001 FORMAT(1H1,10X,22HGRAPH OF INPUT SERIES I3///)
      FI=0.0
      DO 215 I=1,NPOINT
      FI=FI+1.0
      YP(1)=X(I)
      CALL PLOTR (FI,1.0,FNPT,YP,SYM,SM,HU,1,-1)
  215 CONTINUE
      CALL PLOTR (FI,1.0,FNPT,YP,SYM,SM,HU,-1,-1)
  141 MISTAK=0
  150 LL=KIT+1
      IF(NNX-LISA(LL)) 145,155,145
  155 CALL TRANS(NNX,X)
      IF (MISTAK) 160,145,160
  145 IF(IPREWT-IYES) 305,340,305
  340 NT = NPOINT-48
      DO 350 I=1,NT
  350 X(I) = -.0625*(X(I)+X(I+48))-.25*(X(I+8)+X(I+40))
     1 -.50*(X(I+16)+X(I+32)) + THETA*X(I+24)
      NPOINT=NT
  305 FNPT=NPOINT
      ACUMX(1) = 0.
      ACUMX(2) = 0.
      DO 330 I1=1,NPOINT
  330 ACUMX(1) = ACUMX(1) + X(I1)
      XBAR = ACUMX(1) / FNPT
      IF(IDETRN-IYES) 360,300,360
  300 ACUMX(1) = 0.
      ACUMX(2) = 0.
      TBAR = NPOINT - 1
      TBAR = TBAR / 2.
      DENOM = (FNPT-1.) * FNPT * (FNPT+1.) / 6.
      DO 310 I1=1,NPOINT
      ACUMX(2) = 2 * I1 - NPOINT + 1
      ACUMX(2) = (X(I1) - XBAR) * ACUMX(2)
  310 ACUMX(1) = ACUMX(1) + ACUMX(2)
      XALPHA = ACUMX(1) / DENOM
      XBETA = XBAR - XALPHA * TBAR
      DO 320 I1=1,NPOINT
      FI1 = I1 - 1
  320 X(I1) = X(I1) - FI1 * XALPHA - XBETA
      GO TO 160
  360 DO 370 I1=1,NPOINT
  370 X(I1) = X(I1) - XBAR
      FNPT=NPOINT
  160 RETURN
C
      END
C
C
C
C
  470 RETURN
C
      END
C
C
C     ***************************************************************************
CPOWER          SUBROUTINE POWER FOR BMD02T                  APRIL 20, 1966
C
C
C       THIS SUBROUTINE CAN BE CHANGED TO CALCULATE THE AUTO-
C     CORRELATION FUNCTION FOR DIFFERENT INTERVAL SIZES
C       THE STARTING POINT CAN ALSO BE VARIED
C     THE AREA UNDER RX WAS CALCULATED USING  TRAPAZOIDAL METHOD
C
      SUBROUTINE POWER (NNX,X,XBAR,XALPHA,SPX)
```

```
      DIMENSION Z(105C00),DUMB(20),FMT(180),NSELL(20),RX(200),PX(200),
     1 LISA(20),ADDXY(200),SUBXY(200),CXY(200),QXY(200),SCXY(200),
     2 SQXY(200),AMXY(200),PHASXY(200),RXY(200),RYX(200),YP( 4),
     3 CRO(400),COXYSQ(200),IPRNT1(20),IPRNT2(20)
      INTEGER*2 SYM(4)
      REAL*8 UNIT
      DIMENSION X(0001),SPX(C01),IPRNT3(20)
      COMMON UNIT
      COMMON  RXY     , RYX     , RX      , SUBXY
      COMMON  Z       , DUMB    , FMT     , NSELL   , LISA    , SCXY
      COMMON  SQXY    , YP                , CRO     , CCXYSQ  , IORDAT
      COMMON  IPLDAT  , IDETRN  , IPREWT  , THETA   , KSER    , NPOINT
      COMMON  LAG     , NSEL    , IPLOT   , DELTAT              , INFORM
      COMMON  KVR     , IPRNT1  , IPRNT2  , IPRNT3  , IPOW    , ICCS
      COMMON  ICOH    , PI      , FNPT    , CONST   , PMD     , FLAG
      COMMON  FLLAG   , LLAG    , KIT     , KDUM    , MISTAK  , MX
      COMMON  KX      , Q       , KPOINT
      COMMON SYM
C
C
      EQUIVALENCE (RXY,CXY,AMXY),(RYX,QXY,PHASXY),(RX,ADDXY),(PX,SUBXY),
     1(YES,IYES),(IA,A),(IB,B),(IP,P)
C
      DATA A,B,BLANK,P,STAR,YES/1HA,1HB,1H ,1HP,1H*,3HYES/
      INTEGER*2 ICOSCT
      DATA ICOSCT/2H*0/
      SYM(1)=ICOSCT
C
      DO 301 I=1,LLAG
      SX=0.0
      M=I-1
      NX=NPOINT-M
      FNX=NX
      DO 305 J=1,NX
      K=M+J
  305 SX=SX+X(J)*X(K)
  301 RX(I)=SX/FNX
      DO 302 K=2,LLAG
      RX(K)=RX(K)/RX(1)
      RX(1)=1.0
302   CONTINUE
  303 WRITE (6,1301)UNIT,NNX
 1301 FORMAT(1H1,21X,3HLAG,30X,14HAUTOCOVARIANCE/20X,1H(,A6,1H),28X,9HOF
     1 SERIES,I3//)
      TIME=-DELTAT
      DO 320 I=1,LLAG
      TIME=TIME+DELTAT
  320 WRITE (6,1302)TIME,RX(I)
 1302 FORMAT(19X,F9.4,26X,F13.6)
      TIME1=TIME
      IF(IPRNT1(KIT+1)-IB)321,325,321
  321 IF(IPRNT1(KIT+1)-IA)615,325,615
  325 RXMIN=10**10
      RXMAX=-10**10
      WRITE (6,1303)NNX,TIME1,UNIT
 1303 FORMAT(1H1,9X,42HGRAPH OF AUTOCOVARIANCE FUNCTION OF SERIES,I3,37H
     1 PLOTTED AGAINST TIME UP TO A LAG OF F9.4,1X,A6//)
      DO 335 I=1,LLAG
      RXMIN=AMIN1(RXMIN,RX(I))
  335 RXMAX=AMAX1(RXMAX,RX(I))
      ANY=-DELTAT
      IF(LLAG-50) 600,605,605
  600 K1=0
      K2=1
      GO TO 606
C
  605 K1=-1
      K2=K1
  606 DO 610 I=1,LLAG
      ANY=ANY+DELTAT
      YP(1)=RX(I)
  610 CALL PLOTR(ANY,0.0,TIME1,YP,SYM,RXMIN,RXMAX,1,K2)
      CALL PLOTR(ANY,0.0,TIME1,YP,SYM,RXMIN,RXMAX,K1,K2)
  615 SX=RX(1)
      RETURN
      END
```

```
      ************************************************************************
CTPWD           SUBROUTINE TPWD FOR BMDXXX SERIES
C
C
C
      SUBROUTINE TPWD(NT1,NT2)
      IF(NT1)40,10,12
 10   NT1=5
 12   IF(NT1-NT2)14,19,14
 14   IF(NT2-5)15,19,17
   15 REWIND NT2
      GO TO 19
   17 REWIND NT2
   19 IF(NT1-5)18,24,18
 18   IF(NT1-6)22,40,22
 22   REWIND NT1
 24   NT2=NT1
 28   RETURN
 40   WRITE (6,49)
      STOP
 49   FORMAT(25H ERROR ON TAPE ASSIGNMENT)
      END
C
C
C
C     ************************************************************************
C             SUBROUTINE PLOTR (IBM 360)                    AUGUST 13, 1966
C
C     'PLOTR' IS A UTILITY SUBPROGRAM FOR THE BMD... PROGRAMS WHICH
C     PLOTS EITHER SINGLE-LINE OR WHOLE-PAGE GRAPHS AND SETS UP
C     APPROPRIATE SCALING.  THE CALLING PARAMETERS ARE AS FOLLOWS -
C
C     X - THE VALUE OF THE INDEPENDENT VARIABLE
C     ZMIN - THE MINIMUM VALUE OF X FOR THIS PLOT
C     ZMAX - THE MAXIMUM VALUE OF X FOR THIS PLOT
C     Y - THE ARRAY CONTAINING THE VALUES OF UP TO 15 DEPENDENT VAR.'S
C     SYM - THE ARRAY CONTAINING THE SYMBOLS TO BE PLOTTED
C     WMIN - THE MINIMUM VALUE OF ALL Y'S FOR THIS PLOT
C     WMAX - THE MAXIMUM VALUE OF ALL Y'S FOR THIS PLOT
C     NC - THE NUMBER OF DEPENDENT VARIABLES
C               NC=-1 CLOSES A SINGLE-LINE PLOT
C               NC=0 PRINTS AND CLOSES A WHOLE-PAGE PLOT
C     NP - THE CONTROL VARIABLE
C               NP=-1 PRINTS A SINGLE LINE
C               NP=0 OR NP=1 SETS UP A WHOLE-PAGE PLOT
C
C     THE PLOTTING ROUTINE MUST BE CALLED ONCE FOR EACH VALUE OF THE
C     INDEPENDENT VARIABLE THAT IS TO BE PLOTTED NO MATTER WHETHER IN
C     THE SINGLE-LINE OR WHOLE-PAGE MODE
C
      SUBROUTINE PLOTR(X,ZMIN,ZMAX,Y,SYM,WMIN,WMAX,NC,NP)
C
      DIMENSION Y(15),CLAB(12),GF(10),FMT(12),XY(51,101),SYM(15)
      INTEGER*2 XY,BLANKS,SYM,SYMB
      DATA TC,TP,BLANKS/1H.,1H+,1H /
      DATA GF/          4H 1X,,4H 2X,,4H 3X,,4H 4X,,4H 5X,,4H 6X,,
     14H 7X,,4H 8X,,4H 9X,,4H 10X/
      DATA FMT/'(17X',',  ',',5(F1',',2.3,',',8X)/',',7X, ',',  ',',4(F1',',2.3,',
     1',8X),',',F12.',',3)  '/
C
  100   FORMAT(1H 6X5(F12.3,8X),F12.3/17X,5(F12.3,8X))
  101  FORMAT(1H F12.3,1X,103A1,F12.3)
  102 FORMAT (1H 13X,103A1)
 1000 FORMAT(1H  14X,101A1)
 1001 FORMAT(15X,20(5H+....),1H+)
C
      DATA NCC/2/
C     'NCC' ON THE INITIAL ENTRY TO PLOTR IS NON-ZERO BECAUSE OF THE DATA
C     STATEMENT ABOVE.
C
C     'NCC' IS 0 WHILE A PLOT IS BEING MADE.  IT IS 1 OR 2 AT OTHER TIMES
C
      IF(NCC) 50,48,50
```

```
C     THE VARIABLE 'KL' CONTROLS THE FUNCTIONING OF THE OPENING AND
C     CLOSING  SECTIONS OF PLOTR.  KL=0 INDICATES OPENING OF THE GRAPH,
C     KL=1 INDICATES CLOSING.
C
   50 KL=0
      CALL SCALE(WMIN,WMAX,100.0,JY,YMIN,YMAX,YIJ)
      YR=YMAX-YMIN
  230 J=JY
      IF(J*(J-10))204,201,201
C
C     THE FOLLOWING SECTION OPENS OR CLOSES A PLOT IN FIXED FORMAT
C     UNDER CONTROL OF KL
C
  201 IF(KL)220,220,231
C
  231 WRITE (6,1001)
      IF(KL)250,250,220
C
  220 CLAB(1)= YMIN
      DO 222 I=2,11
  222 CLAB(I)=CLAB(I-1)+YIJ
      WRITE (6,100)(CLAB(I),I=1,11,2),(CLAB(J),J=2,10,2)
      IF(KL)231,231,14
C
C     THE FOLLOWING SECTION OPENS OR CLOSES A PLOT IN A VARIABLE
C     FORMAT UNDER CONTROL OF KL AND JY FROM 'SCALE'
C
  204 IF(J-5)205,221,207
  207 J=J-5
  205 JYT=5-J
  221 CONTINUE
  226 FMT(2)=GF(JY)
      IF (KL) 225,225,227
C
  225 FMT(7)=GF(JY)
      TT=JY
      TT=TT*YIJ/10.0
      CLAB(1)= YMIN+TT
      DO 223 I=2,10
  223 CLAB(I)=CLAB(I-1) +YIJ
      WRITE (6,FMT)(CLAB(I),I=2,10,2),(CLAB(I),I=1,9 ,2)
      IF(KL)227,227,14
C
  227 IF(JY-5)208,209,208
  208 WRITE(6,1000)(TC,I=1,J     ),(TP,(TC,I=1,4),K=1,19),TP,(TC,I=1,JYT)
      IF (KL) 250,250,225
C
  209 WRITE (6,1001)
      IF (KL) 250,250,225
C
  250 CONTINUE
      NCC=0
      IC=0
      IF(NP)80,11,11
C
C     THIS SECTION PREPARES FOR A FULL PAGE PLOT BY FILLING IN XY WITH
C     BLANKS AND SETTING UP SCALING FOR THE INDEPENDENT VARIABLE 'X'
C
   11 DO 1 I=1,51
        DO 1 J=1,101
    1 XY(I,J)=BLANKS
      CALL SCALE (ZMIN,ZMAX,50.0,JX,XMIN,XMAX,XIJ)
      XR=XMAX-XMIN
      GO TO 48
C
C
C     ENTRY TO PLOTS CAN BE USED ONLY AFTER THE CALLING PARAMETERS
C     HAVE BEEN TRANSFERRED BY A CALL ON PLOTR.  THE CALL ON PLOTS
C     IS IDENTICAL WITH ENTRY TO PLOTR BUT IT ALLOWS THE PROGRAMMER TO
C     CALL THE PLOTTING ROUTINE WITHOUT HAVING TO INCLUDE THE PARAMETERS
C
      ENTRY PLOTS
   48 IF(NC)52,13,49
   49 IF(NP)80,10,10
C     THE FOLLOWING SECTION SETS UP A FULL PAGE BUT DOES NO PRINTING.
C     THIS SECTION IS REACHED BY SPECIFYING NC POSITIVE AND NP POSITIVE.
```

```
   10 DO 9 N=1,NC
      SYMB=SYM(N)
      XDIFFR=XMAX-X
      IF(XDIFFR)105,106,106
  105 XDIFFR=0.0
  106 YDIFFR=YMAX-Y(N)
      IF(YDIFFR)107,108,108
  107 YDIFFR=0.0
  108 L=51.0-(50.0*XDIFFR)/XR+.5
      K=101.0-(100.0*YDIFFR)/YR+.5
      CALL FORM2(SYMB,XY(L,K))
    9  CONTINUE
      GO TO 15
C
CC    THE FOLLOWING SECTION CONSTRUCTS AND PLOTS ONE LINE OF A MULTILINE
CC    GRAPH.  LOCATION ALONG THE AXIS OF THE PAPER IS PRINTED AT EVERY
CC    STEP.  THIS SECTION IS ACCESSIBLE BY SPECIFYING NC POSITIVE AND
CC    NP NEGATIVE.
C
   80 DO 86 I=1,101
   86 XY(1,I)=BLANKS
       L=1
      DO 95 N=1,NC
      SYMB=SYM(N)
      YDIFFR=YMAX-Y(N)
      IF(YDIFFR)860,865,865
  860 YDIFFR=0.0
  865 K=101.0-(100.0*YDIFFR)/YR+.5
   95 CALL FORM2(SYMB,XY(L,K))
      IF(MOD(IC,5))97,96,97
   96 W=TP
      GO TO 98
   97 W=TC
   98 WRITE (6,101)X,W,(XY(1,N),N=1,101),W,X
      IC=IC+1
      GO TO 15
C
CC    THIS SECTION PLOTS OUT THE PREVIOUSLY PREPARED WHOLE PAGE GRAPH.
CC    IT PRINTS LOCATION ALONG THE PAPER'S AXIS EVERY FIFTH STEP.  THIS
CC    SECTION IS ACCESSED BY SPECIFYING NC=0.
C
   13 M=6-JX
      LL=50+M
      T=JX
      IF(5-JX)131,131,135
  131 T=0.0
  135 RLAB=XMAX-(T*XIJ)/5.0
      W=TC
      K=52
      DO 31 L=M,LL
      K=K-1
      I=MOD(L,5)
      IF(I-1)2,3,2
    3 W=TP
      WRITE (6,101)RLAB,W,(XY(K,N),N=1,101),W,RLAB
      RLAB=RLAB-XIJ
      W=TC
      GO TO 31
    2 WRITE (6,102)W,(XY(K,N),N=1,101),W
   31 CONTINUE
C
   52 KL=1
      GO TO 230
C
   14 NCC=1
   15 RETURN
      END
C
CC
CC    ***************************************************************
CC             SUBROUTINE SCALE FOR PLOTR                JUNE 21, 1966
C
CC    SUBROUTINE 'SCALE' CALCULATES THE SCALING FOR 'PLOTR'
C
      SUBROUTINE SCALE(YMIN,YMAX,YINT,JY,TYMIN,TYMAX,YIJ)
      DIMENSION C(10)
```

```
      DATA C             /1.0,1.5,2.0,3.0,4.0,5.0,7.5,10.0,15.0,20.0/
        DATA TEST / C.7629394E-05/
   50 YR=YMAX-YMIN
      TT=YR/YINT
      J = ALOG10(TT)+TEST
      E=10.0**J
      TT=TT/E
      I=0
      IF(TT-1.0+TEST)205,201,201
  205 TT=TT*10.0
      E=E/10.0
  201 I=I+1
      IF(9-I)1,2,2
    1 E=E*10.0
      I=1
    2 IF(TT-C(I))233,202,201
  233 YIJ=C(I)*E
      GO TO 203
  202 Y=YMIN/C(I)
      J=Y
      T=J
      IF(0.0001-ABS(T-Y))204,233,233
  204 YIJ=C(I+1)*E
  203 X=((YMAX+YMIN)/YIJ-YINT )/2.0+.00001
      K=X
      IF(K)235,240,240
  235 Y=K
      IF(X-Y)236,240,236
  236 K=K-1
  240 TYMIN=K
      TYMIN=YIJ*TYMIN
      TYMAX=TYMIN+YINT*YIJ
      IF (YMAX-TYMAX-TEST)11,11,201
   11 YIJJ=C(I)*E
      XT=((YMAX+YMIN)/YIJJ-YINT)/2.0+.00001
      KT=XT
      IF (KT) 1235,1240,1240
 1235 YT=KT
      IF (XT.NE.YT) KT=KT-1
 1240 TYMINT=KT
      TYMINT=YIJJ*TYMINT
      TYMAXT=TYMINT+YINT*YIJJ
      IF (YMAX-TYMAXT.GT.TEST) GO TO 10
      TYMIN=TYMINT
      TYMAX=TYMAXT
      YIJ=YIJJ
      K=KT
   10 TT=YINT/10.0
      JY=TT+.000001
      YIJ=YINT*(YIJ/10.0)
      J=TYMIN/ YIJ
      IF (K)242,241,241
  242 J=J-1
  241 J=J*JY+JY-K
      JY=J
      RETURN
      END
      SUBROUTINE FORM2(SYMB,XY)
C         SUBROUTINE FORM2 FOR PLOTR (IBM 360)          JUNE 21, 1966
      INTEGER*2 XY,SYMB,BLANK/' '/,TEST(18)/'2 ','3 ','4 ','5 ','6 ',
     1'7 ','8 ','9 ','A ','B ','C ','D ','E ','F ','G ','H ','I ','/ '/
      IF(XY.EQ.BLANK)GO TO 50
      DO 30 I=1,17
      IF(XY.NE.TEST(I))GO TO 30
C         PUT IN NEXT SYMBOL OF ARRAY FOR MULTIPLE POINTS
      XY=TEST(I+1)
      GO TO 100
   30 CONTINUE
      IF(XY.EQ.TEST(18))GO TO 100
C         IF OTHER THAN CHARACTERS IN ARRAY TEST PUT IN CHARACTER 2.
      XY=TEST(1)
      GO TO 100
C         IF BLANK, PUT IN SYMBOL
   50 XY=SYMB
  100 RETURN
      END
```

```
C
C
C
C     ******************************************************************
CTRANS          SUBROUTINE TRANS FOR BMD02T
C
C
      RETURN
      END
C
C
C
C     ******************************************************************
CCROSS          SUBROUTINE CROSS FOR BMD02T
C
  777 RETURN
C
      END
C
C
C
C     ******************************************************************
CHONG     SUBROUTINE HONG FOR BMD02T
C
      RETURN
C
      END
C
C
C
C     ******************************************************************
CKONG     SUBROUTINE KONG FOR BMD02T
C
      RETURN
C
      END
C
C
C
C     ******************************************************************
CPLUG           SUBROUTINE PLUG FOR BMD02T
C
      RETURN
C
      END
C
C
C
```